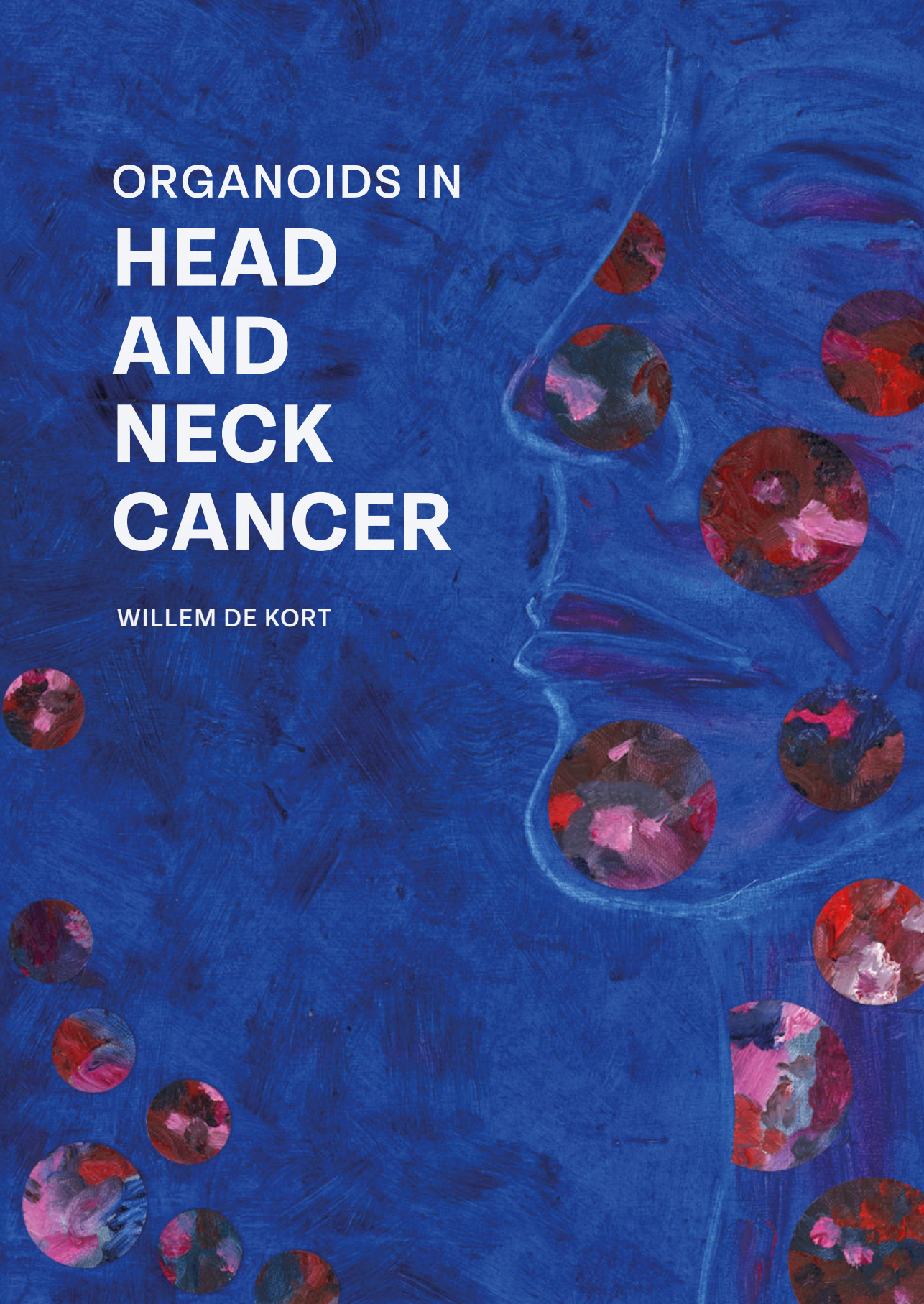


ORGANOIDS IN HEAD AND NECK CANCER

WILLEM DE KORT



ORGANOIDS IN HEAD AND NECK CANCER

Willem Walter Benjamin de Kort

Colofon

Copyright 2025 © Willem de Kort

All rights reserved. No parts of this thesis may be reproduced, stored in a retrieval system or transmitted in any form or by any means without permission of the author.

ISBN: 978-94-6522-931-7

DOI: <https://doi.org/10.33540/2946>

Cover image: Erna de Kort

Cover design: Indah Hijmans

Layout and design: Indah Hijmans, persoonlijkproefschrift.nl

Provided by thesis specialist Ridderprint, ridderprint.nl

Printing: Ridderprint

Financial support for the printing and distribution of this thesis was kindly supported by:

Utrechtse Stichting tot bevordering der mondziekten, kaak- en aangezichtschirurgie

Nederlandse Vereniging voor Mondziekten, Kaak- en Aangezichtschirurgie (NVMKA)

Koninklijke Nederlandse Maatschappij tot bevordering der Tandheelkunde (KNMT)

Nederlandse Vereniging voor DentoMaxilloFaciale Radiologie

MKA groep

BAP Medical

DAM Medical

ExamVision

Organoids in Head and Neck Cancer

Organoïden in hoofd-halskanker
(met een samenvatting in het Nederlands)

Proefschrift

ter verkrijging van de graad van doctor aan de
Universiteit Utrecht
op gezag van de
rector magnificus, prof. dr. ir. W. Hazeleger,
ingevolge het besluit van het College voor Promoties
in het openbaar te verdedigen op

vrijdag 19 december 2025 des middags te 2.15 uur

door

Willem Walter Benjamin de Kort

geboren op 24 maart 1994
te Tilburg

Promotoren:

Prof. dr. J.C. Clevers
Prof. dr. S.M. Willems

Copromotoren:

Dr. R.J.J. van Es
Dr. L.A. Devriese

Beoordelingscommissie:

Prof. dr. R.P. Coppes
Prof. dr. P.J. van Diest
Prof. dr. M. Koopman (voorzitter)
Dr. M. de Ridder
Prof. dr. M.J.H. Witjes

Paranimfen:

Dhr. W.B. Hurkens

Dr. G.J.M. Hassing

CONTENTS

Chapter 1	General introduction	9
Chapter 2	Predictive value of EGFR-PI3K-AKT-mTOR-pathway inhibitor biomarkers for head and neck squamous cell carcinoma - a systematic review	19
Chapter 3	Patient-derived head and neck cancer organoids allow treatment stratification and serve as a tool for biomarker validation and identification	57
Chapter 4	p-mTOR, p-ERK and PTEN expression in tumor biopsies and organoids as predictive biomarkers for patients with HPV negative head and neck cancer	103
Chapter 5	Jaw bone invasion of oral squamous cell carcinoma is associated with osteoclast count and expression of its regulating proteins in patients and organoids	131
Chapter 6	Clinicopathological factors as predictors for establishment of patient derived head and neck squamous cell carcinoma organoids	157
Chapter 7	Summary and general discussion	179
Appendices	Nederlandse samenvatting	190
	Dankwoord	197
	Curriculum Vitae	201
	List of publications	202



CHAPTER 1

General introduction

HEAD AND NECK CANCER

Head and neck cancer (HNC) is a collective term for all tumors arising from the upper aerodigestive tract, i.e. the oral cavity, pharynx, larynx, nasal cavity, paranasal sinuses and the salivary glands. Head and neck cancer is the 7th most common type of cancer worldwide with around 1.000.000 new cases and 465.000 deaths in 2020¹. Over 95% of these cancers are squamous cell carcinomas (HNSCC) that develop from epithelium²⁻⁴. Common risk factors for developing HNSCC are tobacco use, excessive alcohol consumption or both with a synergistic effect⁵. Apart from this, infection with high-risk Human Papillomavirus (hrHPV), is associated with an increased risk of oropharyngeal cancer^{6,7}. HPV-positive oropharyngeal cancers have a better prognosis and occur in a younger population compared to HPV-negative oropharyngeal cancers caused by alcohol and/or tobacco use⁸⁻¹⁰. The incidence of HPV-negative HNSCC slowly declines, partly due to a decline in the prevalence of smoking¹¹. Contrarily, the incidence of HPV-positive HNSCC is increasing¹². The distinction of HPV-negative and HPV-positive HNSCC's has resulted in a different approach for staging and treatment of these tumors¹³.

The staging of HNC provides prognostic information and guides treatment decisions. The TNM system is the staging system commonly used, which stands for Tumor, Nodes, and Metastasis¹⁴. This system classifies the extent of the cancer based on the size of the primary tumor (T), the involvement of regional lymph nodes (N), and the presence of distant metastasis (M). Since 2017, HPV-negative - and HPV-positive oropharyngeal cancer have their own TNM staging^{14,15}.

Treatment modalities for HNC are usually surgery, radiotherapy and systemic therapy. The choice of treatment depends on the location and extent of the disease. Small primary cancers without or limited lymph node involvement can be treated with surgery or radiotherapy only, with 3-year overall survival rates of over 80%^{16,17}. However, many patients present with advanced-stage disease containing large invasive tumors and/or the presence of extensive lymph nodal spread and sometimes distant metastases^{18,19}. Oral cancer is treated with curative intent preferably with surgical resection including elective neck dissection or sentinel node biopsy and adjuvant (chemo)radiotherapy on indication. Pharyngeal and laryngeal cancers often undergo primary (chemo)radiation for functional reasons. Chemoradiotherapy often consist of a platinum-based chemotherapy with concurrent radiotherapy.

Apart from conventional therapies like surgery and/or (chemo)radiation, targeted therapy also plays a role in the treatment of HNSCC. Cetuximab is an epidermal growth factor receptor (EGFR) inhibitor, which was approved by the European Medicines Agency (EMA) for the treatment of recurrent or metastatic disease^{20,21}. Cetuximab can be administered as radiosensitizer to patients with contraindications for cisplatin. However, its efficacy is under debate especially in HPV-positive oropharyngeal cancer, as several phase 3 trials showed

inferior survival for HPV-positive oropharyngeal cancer patients that received cetuximab and radiotherapy as compared to cisplatin and radiotherapy²²⁻²⁴.

Besides focusing on the properties of cancer cells solely, it is known that the tumor micro-environment and immunosuppression influences the aggressiveness of cancer and its therapy resistance²⁵. Therefore immunotherapy, enhancing the immune system, was introduced. The immune checkpoint inhibitors pembrolizumab and nivolumab are approved by the European Medicines Agency (EMA) and the US Food and Drug Administration (FDA) for the treatment of recurrent and/or metastatic HNSCC²⁶⁻²⁸. Pembrolizumab alone or in combination with chemotherapy yields better overall survival compared with cetuximab and chemotherapy with similar toxicity results in a subset of patients²⁷. Also, nivolumab and pembrolizumab monotherapy for patients with cisplatin-refractory cancer improves survival compared with chemotherapy^{28,29}.

Despite different treatment options and the advances in development of targeted therapy, the 5-year HNC survival has only modestly improved over the last three decades to around 66% for all subsites and stages combined³⁰. Therefore many biomarkers have been investigated to predict survival outcome and help with treatment decisions preventing unnecessary side effects and costs³¹⁻³³. Nonetheless, robust biomarkers are lacking and few biomarkers have been confirmed in clinical trials. Furthermore, biomarkers are difficult to test in traditional *in vitro* models as the *in vivo* tumor structure and 3D morphology is missing. Accordingly, better models mirroring a more accurate tumor heterogeneity, are needed. Organoids may fill this void.

ORGANOIDS

Patient derived organoids are three-dimensional structures grown from pluripotent or adult stem cells (PSCs or ASCs)³⁴. In 2008, Eiraku et al described the development of self-organizing three-dimensional cortical neural formations grown from PSCs³⁵. After this, in 2009, Sato et al. described the culture of intestinal epithelium organoids grown from mice ASCs³⁶. The neural organoids were functional, transplantable and could form connections *in vitro* and *in vivo*. The intestinal epithelium organoids showed villus like structures where all types of cells normally present in mouse intestines were present.

The three dimensional structure of organoids allows for better mimicking of the *in vivo* microenvironment. In addition, organoids can consist of multiple cell types and have some level of self-organization with cells organizing themselves into structures that resemble the architecture of the actual organ. This property is a result of the intrinsic developmental program of the cells. Furthermore, organoids can exhibit some level of organ-specific functionality and have the ability to recapitulate *in vivo* functional and structural characteristics of the tissue of origin³⁷.

PSC derived organoids have been cultured for amongst others: lung, liver, intestine, brain, stomach and kidney^{35,38-42}. The culture of PSC derived organoids depends on differentiation with specific growth factors, cytokines and signaling molecules for differentiation and maturation. PSC organoid models can contain different cell types like mesenchymal, endothelial and epithelial cells and have the possibility to form complex structures⁴³. PSC derived organoids are mainly used to study development, infectious – and hereditary disease^{44,45}.

ASCs are undifferentiated stem cells present in most adult tissues. Organoids derived from ASCs can only contain the epithelial part of the organ where it is derived from; vasculature, nerves and stroma are absent. Compared to PSC derived organoid cultures, culture protocols for ASC derived organoids are simpler, shorter and more mature⁴⁶. ASC derived organoids have been developed for amongst others: oral mucosa, taste buds, salivary gland, breast, stomach, intestine, pancreas, liver, kidney, prostate, bladder and ovary^{36,37,47-55}. The possibility to grow patient-specific tissue in 3D make organoids suitable to study the physiology of organs and pathophysiology of related diseases.

Besides establishing organoids from healthy tissue, it is also possible to grow organoids from cancerous tissue. Over the past decade, tumor organoids, mainly ASC-derived, were established for many tumor types⁴⁶. Tumor organoids can be used for two important areas in cancer research: Cancer biology research and Personalized medicine. For cancer biology research, tumor organoids can be used to improve the understanding of the development of cancer, enhance the understanding of tumor heterogeneity, expand tissues of rare cancers, investigate mechanisms of drug resistance, contribute to drug discovery and development and support biomarker research. For personalized medicine, tumor organoids can predict treatment response and can contribute to personalized drug screening for treatment optimisation.

The potential of organoids is underscored in several clinical applications. In patients with radiotherapy induced xerostomia, salivary gland stem cells show the ability to self-renew in vitro and functionally restore saliva production after xenotransplantation⁵⁶. In patients with cystic fibrosis, organoid drug response correlates with drug response in patients⁵⁷. Also in the field of oncology, multiple studies show correlations between drug response in cancer organoids and drug response in the patients where the organoids are derived from⁵⁸⁻⁶². For HNC, the study of Driehuis et al. introduced the first biobank of HNSCC organoids³⁷. These organoids are established from ASCs residing in the HNSCCs. These HNSCC organoids recapitulate molecular characteristics known for HNSCC and respond differential to cisplatin, carboplatin, cetuximab and radiotherapy which is used for the treatment of HNSCC. This study opened the door for a new study establishing a more extensive biobank for HNC organoids which is described in this thesis.

In this thesis, the potential use of organoids in the HNC field is elaborated. Towards personalized medicine, HNC organoids allow profound understanding of the underlying biology of these cancers, may help in treatment stratification and serve as a tool for biomarker identification and validation.

OUTLINE AND AIM OF THIS THESIS

1

First, a systematic review of the literature will be executed with the aim to discover biomarkers for targeted therapy in HNSCC. For HNSCC, targeted therapy targeting EGFR has been explored extensively and EGFR is overexpressed in 50-90% of the cases, therefore we solely focus on biomarkers in the EGFR-PI3K-AKT-mTOR pathway and investigate which biomarkers are confirmed in clinical trials, with the idea to investigate these biomarkers in HNSCC organoid models.

Next, we expand our existing HNSCC organoid biobank and determine whether HNSCC organoids hold potential to stratify treatment for patients with HNSCC. Organoid response to either radiotherapy or chemotherapy will be measured and compared with the response of patients diagnosed with HNSCC.

Successively, immunohistochemical p-mTOR, PTEN and p-ERK expression will be assessed for the applicability as prognostic biomarkers in a prospective cohort of HPV-negative HNSCC patients. Additionally, these biomarkers will be analyzed in a small set of HNSCC organoids and correlated to response of mTOR inhibitor everolimus in organoids to investigate if immunohistochemistry in organoids could predict targeted therapy response.

Subsequently, a retrospective cohort study is conducted to determine factors that could clarify the mechanism of jaw bone invasion in patients with oral cancer. The protein expression of factors related to osteoclast maturation (RANKL, RANKL and OPG) will be investigated in oral cancer patients and the protein and mRNA expression of these factors will be compared in a small set of HNSCC organoids to see whether organoids can play a role in elucidating these factors.

Finally, the described HNSCC organoid biobank will be used to investigate if patient-, tumor- or sampling-factors may influence organoid establishment, which could help future organoid studies to maximize organoid success rates.

REFERENCES

1. Sung H, Ferlay J, Siegel RL, et al. Global Cancer Statistics 2020: GLOBOCAN Estimates of Incidence and Mortality Worldwide for 36 Cancers in 185 Countries. *CA Cancer J Clin.* 2021;71(3):209-249. doi:10.3322/CAAC.21660
2. Carvalho AL, Nishimoto IN, Califano JA, Kowalski LP. Trends in incidence and prognosis for head and neck cancer in the United States: A site-specific analysis of the SEER database. *Int J Cancer.* 2005;114(5):806-816. doi:10.1002/ijc.20740
3. Ostman J, Anneroth G, Gustafsson H, Tavelin B. Malignant oral tumours in Sweden 1960-1989--an epidemiological study. *Eur J Cancer B Oral Oncol.* 1995;31B(2):106-112. doi:10.1016/0964-1955(94)00018-y
4. Muir C, Weiland L. Upper aerodigestive tract cancers. *Cancer.* 1995;75(1 S):147-153. doi:10.1002/1097-0142(19950101)75:1+<147::AID-CNCR2820751304>3.0.CO;2-U
5. Mello FW, Melo G, Pasetto JJ, Silva CAB, Warnakulasuriya S, Rivero ERC. The synergistic effect of tobacco and alcohol consumption on oral squamous cell carcinoma: a systematic review and meta-analysis. *Clin Oral Investig.* 2019;23(7):2849-2859. doi:10.1007/s00784-019-02958-1
6. Isayeva T, Li Y, Maswahu D, Brandwein-Gensler M. Human Papillomavirus in Non-Oropharyngeal Head and Neck Cancers: A Systematic Literature Review. *Head Neck Pathol.* 2012;6(SUPPL. 1):104-120. doi:10.1007/s12105-012-0368-1
7. Gillison ML, Alemany L, Snijders PJF, et al. Human papillomavirus and diseases of the upper airway: Head and neck cancer and respiratory papillomatosis. *Vaccine.* 2012;30(SUPPL.5). doi:10.1016/j.vaccine.2012.05.070
8. Ang KK, Harris J, Wheeler R, et al. Human Papillomavirus and Survival of Patients with Oropharyngeal Cancer. *N Engl J Med.* 2010;363(1):24-35. doi:10.1056/nejmoa0912217
9. Marur S, D'Souza G, Westra WH, Forastiere AA. HPV-associated head and neck cancer: A virus-related cancer epidemic. *Lancet Oncol.* 2010;11(8):781-789. doi:10.1016/S1470-2045(10)70017-6
10. Wang MB, Liu IY, Gornbein JA, Nguyen CT. HPV-Positive Oropharyngeal Carcinoma: A Systematic Review of Treatment and Prognosis. *Otolaryngol - Head Neck Surg (United States).* 2015;153(5):758-769. doi:10.1177/0194599815592157
11. Sturgis EM, Cinciripini PM. Trends in head and neck cancer incidence in relation to smoking prevalence: An emerging epidemic of human papillomavirus-associated cancers? *Cancer.* 2007;110(7):1429-1435. doi:10.1002/cncr.22963
12. Stein AP, Saha S, Kraninger JL, et al. Prevalence of human papillomavirus in oropharyngeal cancer. *Cancer J (United States).* 2015;21(3):138-146. doi:10.1097/PPO.0000000000000115
13. Badoual C. Update from the 5th Edition of the World Health Organization Classification of Head and Neck Tumors: Oropharynx and Nasopharynx. *Head Neck Pathol.* 2022;16(1):19-30. doi:10.1007/s12105-022-01449-2
14. Amin MB, Greene FL, Edge SB, et al. The Eighth Edition AJCC Cancer Staging Manual: Continuing to build a bridge from a population-based to a more "personalized" approach to cancer staging. *CA Cancer J Clin.* 2017;67(2):93-99. doi:10.3322/caac.21388
15. Lydiatt WM, Patel SG, O'Sullivan B, et al. Head and neck cancers—major changes in the American Joint Committee on cancer eighth edition cancer staging manual. *CA Cancer J Clin.* 2017;67(2):122-137. doi:10.3322/caac.21389
16. Pfister DG, Spencer S, Brizel DM, et al. Head and neck cancers, version 2.2014. *JNCCN J Natl Compr Cancer Netw.* 2014;12(10):1454-1487. doi:10.6004/jnccn.2014.0142

17. Lee NCJ, Kelly JR, Park HS, et al. Patterns of failure in high-metastatic node number human papillomavirus-positive oropharyngeal carcinoma. *Oral Oncol.* 2018;85:35-39. doi:10.1016/j.oraloncology.2018.08.001
18. Chow LQM. Head and neck cancer. *N Engl J Med.* 2020;382(1):60-72. doi:10.1056/NEJMra1715715
19. Johnson DE, Burtneess B, Leemans CR, Lui VVY, Bauman JE, Grandis JR. Head and neck squamous cell carcinoma. *Nat Rev Dis Prim.* 2020;6(1). doi:10.1038/s41572-020-00224-3
20. James A. Bonner, Paul M. Harari, Jordi Giral, et al. Radiotherapy plus Cetuximab for Squamous Cell Carcinoma of the Head and Neck. *N Engl J Med.* 2006;354:567-578. doi:10.1056/NEJMoa053422
21. Vermorken JB, Mesia R, Rivera F, et al. Platinum-Based Chemotherapy plus Cetuximab in Head and Neck Cancer. *N Engl J Med.* 2008;359(11):1116-1127. doi:10.1056/nejmoa0802656
22. Mehanna H, Robinson M, Hartley A, et al. Radiotherapy plus cisplatin or cetuximab in low-risk human papillomavirus-positive oropharyngeal cancer (De-ESCALaTE HPV): an open-label randomised controlled phase 3 trial. *Lancet.* 2019;393(10166):51-60. doi:10.1016/S0140-6736(18)32752-1
23. Gillison ML, Trotti AM, Harris J, et al. Radiotherapy plus cetuximab or cisplatin in human papillomavirus-positive oropharyngeal cancer (NRG Oncology RTOG 1016): a randomised, multicentre, non-inferiority trial. *Lancet.* 2019;393(10166):40-50. doi:10.1016/S0140-6736(18)32779-X
24. Rischin D, King M, Kenny L, et al. Randomized Trial of Radiation Therapy With Weekly Cisplatin or Cetuximab in Low-Risk HPV-Associated Oropharyngeal Cancer (TROG 12.01) – A Trans-Tasman Radiation Oncology Group Study. *Int J Radiat Oncol Biol Phys.* 2021;111(4):876-886. doi:10.1016/j.ijrobp.2021.04.015
25. Chen SMY, Krinsky AL, Woolaver RA, Wang X, Chen Z, Wang JH. Tumor immune microenvironment in head and neck cancers. *Mol Carcinog.* 2020;59(7):766-774. doi:10.1002/mc.23162
26. Seiwert TY, Burtneess B, Mehra R, et al. Safety and clinical activity of pembrolizumab for treatment of recurrent or metastatic squamous cell carcinoma of the head and neck (KEYNOTE-012): an open-label, multicentre, phase 1b trial. *Lancet Oncol.* 2016;17(7):956-965. doi:10.1016/S1470-2045(16)30066-3
27. Burtneess B, Harrington KJ, Greil R, et al. Pembrolizumab alone or with chemotherapy versus cetuximab with chemotherapy for recurrent or metastatic squamous cell carcinoma of the head and neck (KEYNOTE-048): a randomised, open-label, phase 3 study. *Lancet.* 2019;394(10212):1915-1928. doi:10.1016/S0140-6736(19)32591-7
28. Ferris RL, Blumenschein G, Fayette J, et al. Nivolumab for Recurrent Squamous-Cell Carcinoma of the Head and Neck. *N Engl J Med.* 2016;375(19):1856-1867. doi:10.1056/nejmoa1602252
29. Cohen EEW, Soulières D, Le Tourneau C, et al. Pembrolizumab versus methotrexate, docetaxel, or cetuximab for recurrent or metastatic head-and-neck squamous cell carcinoma (KEYNOTE-040): a randomised, open-label, phase 3 study. *Lancet.* 2019;393(10167):156-167. doi:10.1016/S0140-6736(18)31999-8
30. Pulte D, Brenner H. Changes in Survival in Head and Neck Cancers in the Late 20th and Early 21st Century: A Period Analysis. *Oncologist.* 2010;15(9):994-1001. doi:10.1634/theoncologist.2009-0289
31. Gavrielatou N, Dumas S, Economopoulou P, Foukas PG, Psyrri A. Biomarkers for immunotherapy response in head and neck cancer. *Cancer Treat Rev.* 2020;84. doi:10.1016/j.ctrv.2020.101977
32. Hsieh JCH, Wang HM, Wu MH, et al. Review of emerging biomarkers in head and neck squamous cell carcinoma in the era of immunotherapy and targeted therapy. *Head Neck.* 2019;41(S1):19-45. doi:10.1002/hed.25932
33. de Kort WWB, Spelier S, Devriese LA, van Es RJJ, Willems SM. Predictive Value of EGFR-PI3K-AKT-mTOR-Pathway Inhibitor Biomarkers for Head and Neck Squamous Cell Carcinoma: A Systematic Review. *Mol Diagnosis Ther.* 2021;25(2):123-136. doi:10.1007/s40291-021-00518-6

34. Kretschmar K, Clevers H. Organoids: Modeling Development and the Stem Cell Niche in a Dish. *Dev Cell*. 2016;38(6):590-600. doi:10.1016/j.devcel.2016.08.014
35. Eiraku M, Watanabe K, Matsuo-Takasaki M, et al. Self-Organized Formation of Polarized Cortical Tissues from ESCs and Its Active Manipulation by Extrinsic Signals. *Cell Stem Cell*. 2008;3(5):519-532. doi:10.1016/j.stem.2008.09.002
36. Sato T, Vries RG, Snippert HJ, et al. Single Lgr5 stem cells build crypt-villus structures in vitro without a mesenchymal niche. *Nature*. 2009;459(7244):262-265. doi:10.1038/nature07935
37. Driehuis E, Kolders S, Spelier S, et al. Oral mucosal organoids as a potential platform for personalized cancer therapy. *Cancer Discov*. 2019;9(7):852-871. doi:10.1158/2159-8290.CD-18-1522
38. Dye BR, Hill DR, Ferguson MA, et al. In vitro generation of human pluripotent stem cell derived lung organoids. *Elife*. 2015;2015(4):1-25. doi:10.7554/eLife.05098
39. McCracken KW, Catá EM, Crawford CM, et al. Modelling human development and disease in pluripotent stem-cell-derived gastric organoids. *Nature*. 2014;516(7531):400-404. doi:10.1038/nature13863
40. Spence JR, Mayhew CN, Rankin SA, et al. Directed differentiation of human pluripotent stem cells into intestinal tissue in vitro. *Nature*. 2011;470(7332):105-110. doi:10.1038/nature09691
41. Takasato M, Er PX, Becroft M, et al. Directing human embryonic stem cell differentiation towards a renal lineage generates a self-organizing kidney. *Nat Cell Biol*. 2014;16(1):118-126. doi:10.1038/ncb2894
42. Takebe T, Zhang RR, Koike H, et al. Generation of a vascularized and functional human liver from an iPSC-derived organ bud transplant. *Nat Protoc*. 2014;9(2):396-409. doi:10.1038/nprot.2014.020
43. Brassard JA, Lutolf MP. Engineering Stem Cell Self-organization to Build Better Organoids. *Cell Stem Cell*. 2019;24(6):860-876. doi:10.1016/j.stem.2019.05.005
44. Clevers H. Modeling Development and Disease with Organoids. *Cell*. 2016;165(7):1586-1597. doi:10.1016/j.cell.2016.05.082
45. Drost J, Clevers H. Organoids in cancer research. *Nat Rev Cancer*. 2018;18(7):407-418. doi:10.1038/s41568-018-0007-6
46. Yang S, Hu H, Kung H, et al. Organoids: The current status and biomedical applications. *MedComm*. 2023;4(3). doi:10.1002/mco2.274
47. Boj SF, Hwang C II, Baker LA, et al. Organoid models of human and mouse ductal pancreatic cancer. *Cell*. 2015;160(1-2):324-338. doi:10.1016/j.cell.2014.12.021
48. Ren W, Lewandowski BC, Watson J, et al. Single Lgr5- or Lgr6-expressing taste stem/progenitor cells generate taste bud cells ex vivo. *Proc Natl Acad Sci U S A*. 2014;111(46):16401-16406. doi:10.1073/pnas.1409064111
49. Huch M, Gehart H, Van Boxtel R, et al. Long-term culture of genome-stable bipotent stem cells from adult human liver. *Cell*. 2015;160(1-2):299-312. doi:10.1016/j.cell.2014.11.050
50. Schutgens F, Rookmaaker MB, Margaritis T, et al. Tubuloids derived from human adult kidney and urine for personalized disease modeling. *Nat Biotechnol*. 2019;37(3):303-313. doi:10.1038/s41587-019-0048-8
51. Karthaus WR, Iaquinta PJ, Drost J, et al. Identification of multipotent luminal progenitor cells in human prostate organoid cultures. *Cell*. 2014;159(1):163-175. doi:10.1016/j.cell.2014.08.017
52. Mullenders J, de Jongh E, Brousalı A, et al. Mouse and human urothelial cancer organoids: A tool for bladder cancer research. *Proc Natl Acad Sci U S A*. 2019;116(10):4567-4574. doi:10.1073/pnas.1803595116

53. Kopper O, de Witte CJ, Löhmußaar K, et al. An organoid platform for ovarian cancer captures intra- and interpatient heterogeneity. *Nat Med*. 2019;25(5):838-849. doi:10.1038/s41591-019-0422-6
54. Sachs N, de Ligt J, Kopper O, et al. A Living Biobank of Breast Cancer Organoids Captures Disease Heterogeneity. *Cell*. 2018;172(1-2):373-386.e10. doi:10.1016/j.cell.2017.11.010
55. Bartfeld S, Bayram T, Van De Wetering M, et al. In vitro expansion of human gastric epithelial stem cells and their responses to bacterial infection. *Gastroenterology*. 2015;148(1):126-136.e6. doi:10.1053/j.gastro.2014.09.042
56. Pringle S, Maimets M, Van Der Zwaag M, et al. Human salivary gland stem cells functionally restore radiation damaged salivary glands. *Stem Cells*. 2016;34(3):640-652. doi:10.1002/stem.2278
57. Berkers G, van Mourik P, Vonk AM, et al. Rectal Organoids Enable Personalized Treatment of Cystic Fibrosis. *Cell Rep*. 2019;26(7):1701-1708.e3. doi:10.1016/j.celrep.2019.01.068
58. Tiriach H, Belleau P, Engle DD, et al. Organoid profiling identifies common responders to chemotherapy in pancreatic cancer. *Cancer Discov*. 2018;8(9):1112-1129. doi:10.1158/2159-8290.CD-18-0349
59. Vlachogiannis G, Hedayat S, Vatsiou A, et al. Patient-derived organoids model treatment response of metastatic gastrointestinal cancers. *Science (80-)*. 2018;359(6378):920-926. doi:10.1126/science.aao2774
60. Wensink GE, Elias SG, Mullenders J, et al. Patient-derived organoids as a predictive biomarker for treatment response in cancer patients. *npj Precis Oncol*. 2021;5(1). doi:10.1038/s41698-021-00168-1
61. Ooft SN, Weeber F, Dijkstra KK, et al. Patient-derived organoids can predict response to chemotherapy in metastatic colorectal cancer patients. *Sci Transl Med*. 2019;11(513). doi:10.1126/scitranslmed.aay2574
62. Yao Y, Xu X, Yang L, et al. Patient-Derived Organoids Predict Chemoradiation Responses of Locally Advanced Rectal Cancer. *Cell Stem Cell*. 2020;26(1):17-26.e6. doi:10.1016/j.stem.2019.10.010



CHAPTER 2

Predictive value of EGFR-PI3K-AKT-mTOR-pathway inhibitor biomarkers for head and neck squamous cell carcinoma - a systematic review

W.W. B. de Kort[^], S. Spelier[^], L.A. Devriese, R.J.J. van Es, S.M. Willems

[^]These authors contributed equally to this work

ABSTRACT

Background

Understanding of molecular pathogenesis of head and neck squamous cell carcinomas (HNSCC) has considerably improved in the last decades. As a result, novel therapeutic strategies evolved, amongst which are epidermal growth factor receptor (EGFR) targeted therapies. With the exception of cetuximab, targeted therapies for HNSCC are not yet introduced in the clinical practice. One important aspect of new treatment regimes in clinical practice is presence of robust biomarkers predictive for therapy response.

Methods

We performed a systematic search in PubMed, Embase and the Cochrane library. Articles were included if they investigated a biomarker for targeted therapy in the EGFR-AKT-mTOR-pathway.

Results

Of 83 included articles, 52 were preclinical and 33 were clinical studies (two studies contained both a preclinical and a clinical part). We classified EGFR pathway inhibitor types and investigated the type of biomarker (biomarker on epigenetic, DNA, mRNA or protein level).

Conclusion

Several EGFR-PI3K-AKT-mTOR-pathway inhibitor biomarkers have been researched for HNSCC but few of the investigated biomarkers have been adequately confirmed in clinical trials. A more systematic approach is needed to discover proper biomarkers as stratifying patients is essential to prevent unnecessary costs and side effects.

INTRODUCTION

Squamous cell carcinoma of the head and neck (HNSCC) is the 6th most common type of cancer, representing 6% of all cancer cases globally¹. HNSCCs are challenging to treat, not only due to their anatomical location that complicates surgery, but also due to their highly variable biological behavior and treatment response. Robust factors predicting patient response to a specific treatment are lacking. HNSCC is primarily treated with surgery, and (chemo) radiotherapy ((Ch)RT), or a combination of these modalities. Recently the application of immunotherapy, especially PD-L1 inhibitors, was introduced^{2,3}. Although some patients benefit from this treatment regime, relapse rates of over 50% are observed⁴. Moreover, treatment with chemo and radiotherapy can result in significant morbidity and oropharyngeal discomfort such as mucositis and dermatitis, xerostomia, dysphagia, loss of taste, hoarseness, fibrosis, osteoradionecrosis, peripheral neuropathy, nephrotoxicity and ototoxicity, which affect the patient's quality of life^{5,6}. Once HNSCC recurs after surgery and (Ch)RT or if metastatic disease is present and also immunotherapy is ineffective, only limited palliative treatment options are available.

The understanding of the molecular pathogenesis of HNSCC has considerably improved in the last decade, resulting in the development of several targeted therapies for HNSCC⁷. In particular therapies targeting the Epidermal Growth Factor Receptor (EGFR) have been explored extensively. For the clinician treating patients with HNSCC, knowledge concerning EGFR-inhibiting therapies is therefore relevant. EGFR is overexpressed in 50-90% of HNSCC cases⁸. EGFR, also known as ErbB1 or HER, is part of the ErbB family of cell surface receptors. ErbB signaling is involved in pivotal cellular processes including proliferation, anti-apoptotic signaling and differentiation via, among others, the phosphoinositide 3-kinase / protein kinase B, also known as oncogene Thymoma in Ak-mouse / mammalian target of rapamycin (PI3K/AKT/mTOR) pathway, the most mutated pathway in HNSCC^{9,10}. Overexpression of EGFR or proteins downstream the EGFR signaling pathway can drive malignant behavior of a tumor^{11,12}.

Several types of EGFR pathway inhibitors have been described in the EGFR-PI3K-AKT-mTOR-pathway. Monoclonal antibodies (mABs) and tyrosine kinase inhibitors (TKIs) constitute the largest categories. PI3K-inhibitors and mTOR-inhibitors make up a smaller group. Currently, cetuximab is the only EGFR-targeting agent approved by the European Medicines Agency (EMA) for the treatment of HNSCC. Cetuximab can be administered concomitantly with radiotherapy in the curative setting to patients who have a contraindication for cisplatin. In recurrent and/or metastatic HNSCC, single agent cetuximab can be administered as a palliative therapy. However, in the curative setting, two recent randomized controlled trials demonstrated that human papillomavirus (HPV)-positive patients with oropharyngeal carcinoma showed inferior overall survival if treated with cetuximab + RT compared to cisplatin+RT^{13,14}. This led

to concerns about efficacy or development of resistance. Another mAB is panitumumab, which like cetuximab binds the ectopic domain of EGFR¹⁵.

Despite the development of many new targeting agents, both primary and acquired resistance to these agents has unfortunately resulted in low response rates when tested in patients. Additionally, albeit side effects of chemotherapy and radiotherapy are in general more severe, side effects of targeted therapy can still be serious^{16–19}. For HNSCC, the only biomarker for a targeted therapy used in the clinic today, is presence and severity of cetuximab-induced skin rash, which is predictive for response²⁰. However, it is preferable that biomarkers can be used to predict effective patient response prior to treatment in order to circumvent unnecessary side effects and costs. We therefore solely focus on such biomarkers in this review. The aim of this study was to systematically review predictive biomarkers that are currently explored in HNSCC to predict the response of targeting therapies in the EGFR-PI3K-AKT-mTOR pathway. We also raise questions that need to be addressed in the future to guide patient treatment with EGFR inhibitors in the clinic.

MATERIALS AND METHODS

A systematic search of PubMed, Embase database and the Cochrane library was performed on January 25th, 2021. Articles were included if they were original articles and investigated a biomarker for targeted therapies interfering with the EGFR-PI3K-AKT-mTOR-pathway, in patients with any type of HNSCC. PI3K and mTOR inhibitors were included in this review as the PI3K-AKT-mTOR pathway harbored the highest percentage of mutations in HNSCC^{9,10}. Reviews, commentaries and studies in another language than English were excluded. This review is written in accordance to the PRISMA guidelines²¹. The search was set up in DDO-format (Domain, Determinant, Outcome). PubMed and Embase search syntaxes are displayed in **Appendix 1**. The Cochrane library was searched with similar search terms. Two authors (WWBDK and SS) screened all articles on title and abstract. Conflicts were resolved by discussion. To prevent missing articles cross-reference screening was performed (**Figure 1**). As various papers discussed several EGFR pathway inhibitors and reported preclinical and clinical data, the total number of studies is lower than the number of studies depicted in **Figure 2**. Pre-clinical data is defined as data obtained using in vitro cell lines and xenograft models both with cell lines and patient-derived cells. The following data was extracted from the studies: study title, first authors name, date of publication, administered EGFR pathway inhibitor type, biomarker potentially correlated to response, analyzing techniques, sample size and additional treatment. Due to extensive variance in the studied biomarkers, data could not be quantitatively pooled and thus a meta-analysis was not performed.

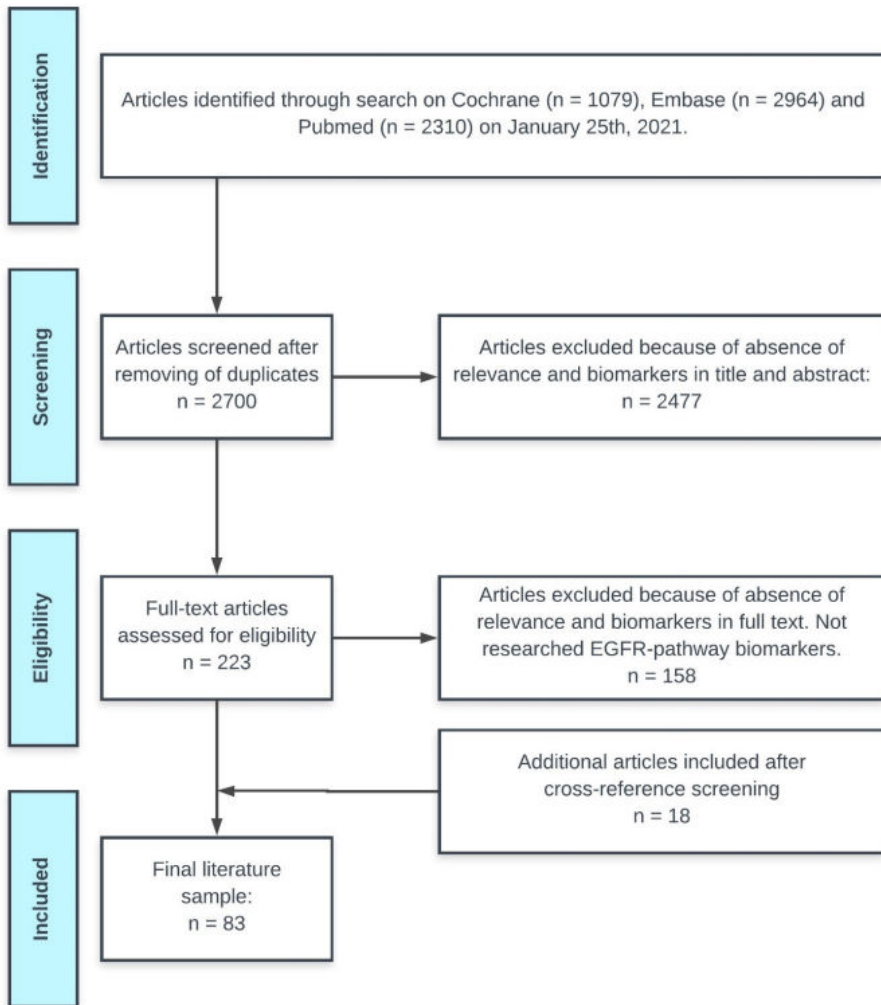


Figure 1. Flowchart of search, date of search 25th January 2021. After screening 2700 abstracts, 223 papers were full text screened. After adding cross-references, a total number of 83 articles were included.

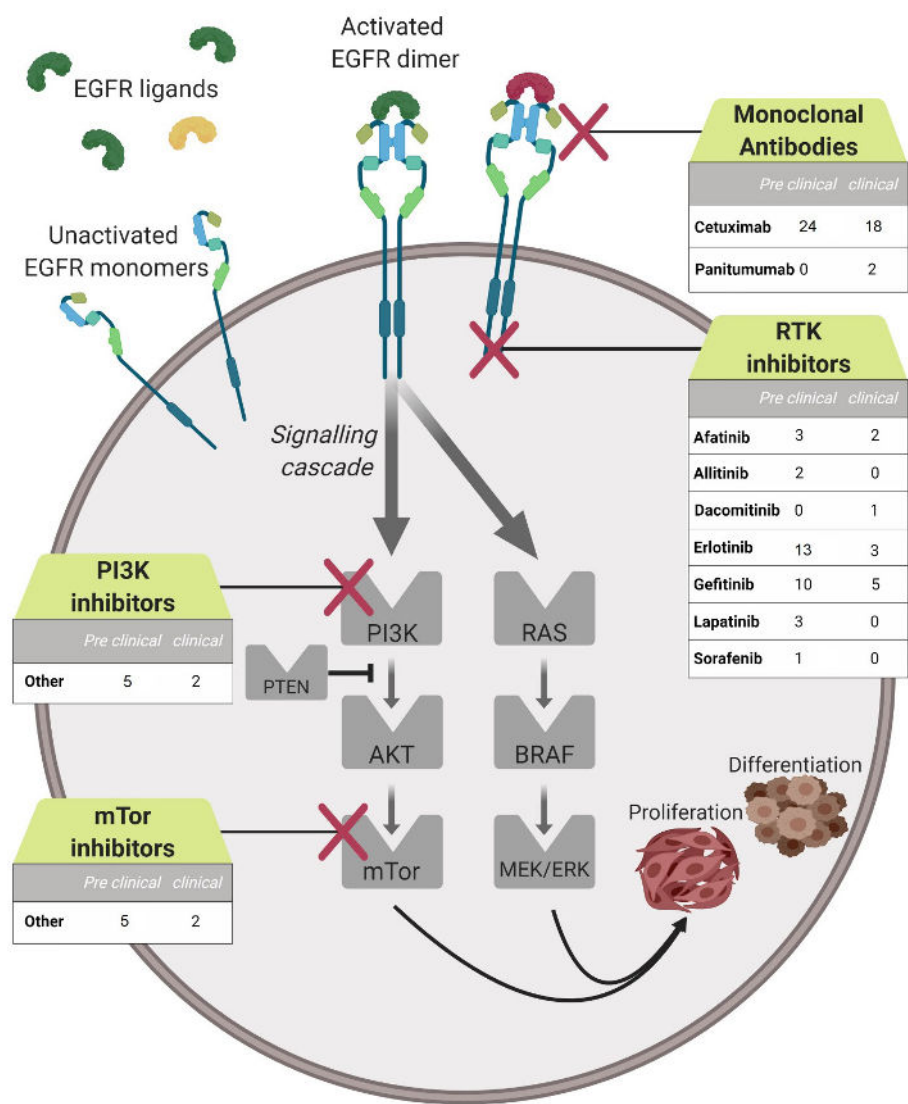


Figure 2. Simplified overview of EGFR pathway, with numbers of studies included per EGFR pathway inhibitor target. Important note: several studies investigated more than 1 inhibitor; the total number of studies depicted in this figure exceeds the total number of inclusions. EGFR can be bound by natural ligands such as EGF, leading to dimerization of two EGFR monomers and subsequent activation of the intracellular tyrosine kinase domain of EGFR. This results in activation of the downstream signaling cascade via PI3K/AKT/mTOR or KRAS/BRAF/MEK/ERK, signaling resulting in cellular processes such as cell proliferation or differentiation. *Illustration made with BioRender®*

RESULTS

Of the 83 included articles, 52 articles were preclinical and discussed *in vitro* experiments and 33 articles discussed the results of clinical trials performed in patients (**Figure 1**). Some studies were placed in both categories. Of the clinical studies, fifteen were cohort studies, five phase-II studies, one phase-II/III study and five phase-III studies. Within these two subgroups distinctions are made between 1) the different EGFR pathway inhibitors and 2) the type of biomarker (biomarker on epigenetic, DNA, mRNA or protein level). A schematic overview of the EGFR pathway with numbers of included studies per agent is shown in **Figure 2**. The number of biomarkers researched per EGFR pathway inhibitor and biomarker-level are displayed in **Table 1**. Note that one biomarker researched by two studies is counted as two researched biomarkers in table 1. For a detailed description of all biomarkers, we refer to **supplemental table 1A-D** (pre-clinical) and **supplemental table 2A-D** (clinical).

Biomarkers predicting response to mABs (supplemental table 1A and 2A)

Cetuximab and panitumumab bind the extracellular domain of EGFR with higher affinity than natural ligands thus inhibiting EGFR activation²². Cetuximab additionally stimulates internalization of EGFR²³. Moreover, being an immunoglobulin G molecule, cetuximab stimulates antibody dependent cell cytotoxicity^{24,25}.

EGFR overexpression (cetuximab)

It has been hypothesized that EGFR overexpression correlates with response to cetuximab. The increase in expression of EGFR molecules could result in increased binding of cetuximab resulting in a stronger inhibitory effect. Six studies showed a positive correlation between EGFR overexpression and cetuximab response²⁶⁻³¹. Other studies obtained conflicting results, one mentioned that about half of the preclinical tumour models did benefit from cetuximab while lacking EGFR amplification²⁶ and two studies were based on only two and three cell lines respectively^{27,30}. Moreover, the fact that five clinical studies³²⁻³⁷ and six preclinical studies^{28,29,38-41} failed to show any correlation between EGFR overexpression and cetuximab response implies that EGFR expression is not suitable as single biomarker.

Table 1: Number of biomarkers

Biomarker Level											
		Epigenetic		DNA		RNA		Protein		Other	
		Pre-clinical	Clinical	Pre-clinical	Clinical	Pre-clinical	Clinical	Pre-clinical	Clinical	Pre-clinical	Clinical
Monoclonal Antibodies											
Cetuximab	2	-	-	8	9	11	12	31	15	1	-
Panitumumab	-	-	-	-	-	-	4	-	1	-	-
RTK-inhibitors											
Gefitinib	-	-	-	5	3	2	1	22	4	-	-
Erlotinib	-	-	-	7	5	1	1	6	2	2	-
Afatinib	-	-	-	2	1	-	1	2	8	-	-
Lapatinib	-	-	-	1	-	-	-	2	-	-	-
Allitinib	-	-	-	2	-	-	-	-	-	-	-
Sorafenib	-	-	-	-	-	-	-	1	-	-	-
Dacomitinib	-	-	-	-	1	-	-	-	-	-	-
PI3K-inhibitors	-	-	-	12	2	-	-	-	1	-	2
mTOR-inhibitors	-	-	-	2	1	5	-	3	-	2	1

Table 1: Numbers of biomarkers researched per EGFR pathway inhibitor type and per biomarker-level. Important note: All the studies were added separately. For example: EGFR-expression investigated for Gefitinib response in three studies is displayed in the table as 3, not as 1. Several studies researched multiple biomarkers, because of this the total number of biomarkers exceeds the number of included studies.

ErbB family member overexpression and activation (cetuximab)

The ErbB family of proteins contains four RTKs, Her1 (EGFR, ErbB1), Her2 (Neu, ErbB2), Her3 (ErbB3) and HER4 (erbB4). Apart from HER1 (EGFR) It has been hypothesized that the expression/activation-level HER2, HER3 and HER4 correlates with cetuximab response. Preclinical studies showed that HER3 expression⁴⁰ and phosphorylated HER2/HER3⁴² correlated negatively with cetuximab response. In one preclinical study, expression levels of HER4 on tumor, were found to correlate positively with patient response to cetuximab³⁰. However, the authors investigated only two cell lines. Two other preclinical studies reported no correlation between expression or activation of ErbB family members and cetuximab response^{28,38}. Clinical studies in HNSCC elaborating on these preclinical results are lacking. Investigating the potential of the ErbB family members as biomarkers for HNSCC in clinical trials is recommended.

EGFR ligand overexpression (cetuximab)

Apart by EGF, EGFR can be activated by other EGFR-ligands like heparin-binding EGF (HB-EGF), transforming growth factor- α (TGF- α), epiregulin (ERE) and amphiregulin (AREG). Expression of the EGFR ligands AREG⁴³ and EREG^{39,43} correlated positively with cetuximab response. Interestingly, mRNA levels of yes-associated-protein 1 (YAP1) correlated negatively with cetuximab response⁴⁴. YAP1 is an activating transcription factor of among others AREG, explains an indirect negative correlation. However, YAP1 also is a transcriptional co-activator for several genes involved in anti-apoptosis and proliferation, resulting in a potential bias when drawing conclusion about the correlation between AREG and cetuximab response per se. Ansell et al. could not correlate EREG and AREG expression to cetuximab response in a preclinical study on tongue cancer⁴⁵. In clinical studies, contradicting results are demonstrated as well: Kogashiwa et al. described a positive correlation between EREG and AREG mRNA expression and cetuximab response⁴⁶ whereas AREG protein levels correlated negatively with cetuximab response in the study of Tinhofer et al.³⁵ Tinhofer et al. base their conclusions on immunohistochemistry, which is more conclusive than RNA levels determined on qPCR⁴⁶.

Three preclinical studies investigated EGFR-ligands HB-EGF^{47,48} and EGF⁴⁵ as biomarker for cetuximab response. Ligand expression correlated negatively with cetuximab response in all three studies. No clinical studies elaborate on these findings. EGFR ligands seem potential biomarkers for cetuximab response in HNSCC patients, although contradictory results warrant further clinical studies using larger cohorts of patients.

Epithelial to mesenchymal transition (cetuximab)

Epithelial to mesenchymal transition (EMT) is a process pivotal in (early) developmental processes as well as for metastasis of tumour cells. EMT is characterized by loss of epithelial cell characteristics like E-cadherin expression and gain of mesenchymal characteristics like vimentin and fibronectin expression. EMT can result in cell detachment from adjacent

epithelial cells and subsequent cell migration⁴⁹. E-cadherin/vimentin expression did not correlate with cetuximab response in one preclinical study⁴⁰.

Four preclinical studies reported a positive correlation between cetuximab response and the absence/presence of EMT-like features. Expression of epithelial markers as keratin(KRT)13/14⁴⁸ and possession of a basal epithelial gene expression signature⁵⁰ correlated positively with cetuximab response. Accordingly, expression of EMT markers correlated negatively with cetuximab response in HNSCC cell lines⁴⁸. Keck et al. discovered five subtypes of HNSCC using gene expression-based consensus clustering, copy number profiling and HPV status⁵¹. The 'basal' subtype was characterized as; HPV negative with strong hypoxic differentiation (enrichment for hypoxia signaling) and prominent EGFR/HER signaling. HNSCC patients with this basal expression profile were more responsive to cetuximab⁵². On the contrary, expression of matrix metalloproteinase 9 (MMP9), known to be expressed during EMT⁵³, correlated positively to cetuximab response in a clinical study³². This correlation is supported by the fact that MMPs can liberate EGFR ligands from the extracellular matrix, thereby potentially promoting EGFR signaling leading to tumour cells becoming extra sensitive to EGFR inhibition³². This correlation does therefore not immediately interfere with previous discussed results on EMT as predictive biomarker for mAB resistance.

To summarize, it is hard to draw conclusions due to the limited number of clinical inclusions; yet we see the potential of EMT markers like e-cadherin expression, to serve as potential biomarkers of response to EGFR mABs.

Other biomarkers (cetuximab)

Several biomarkers were investigated by only a small number of studies. The rapid development of sequencing technologies and microarrays enables high throughput genomic, expression or proteomic profiling of tumor material. This has led to the introduction of gene signatures: specific expression profiles correlated to a cancer subtype, or even to therapy response⁵⁴. MammaPrint® (Agendia, The Netherlands) highlights the potential of such expression profiles. By investigating the expression of 70 genes it aids in stratification of breast cancer patients into low and high-risk groups, advising on treatment strategies⁵⁵. In HNSCC cell lines, a specific RNA expression profile correlated with an increased response to cetuximab + RT²⁶. Similarly, a specific miRNA expression profile correlated positively to cetuximab + CT response in a clinical trial⁵⁶. The potential of expression profiles as biomarkers is not very surprising, as a profile in fact is a combination of multiple biomarkers. Therefore, studies on expression profiles as biomarker deserve more confirmation in prognostic clinical trials.

Various other preclinical studies describe biomarkers that correlate negatively to cetuximab response, like possession of EGFR-K single-nucleotide polymorphism on DNA level⁵⁷, which was

validated in patients⁵⁸. Two preclinical studies demonstrated that growth factor receptor (c) MET expression correlated negatively with cetuximab response^{40,42} whereas two clinical studies could not verify this correlation^{32,59}. Several additional biomarkers correlating to cetuximab resistance were identified: mutations downstream the EGFR signaling cascade (PI3KCA, KRAS, HRAS, BRAF)^{37,41}, Chemokine ligand(CXC)L14 expression⁶⁰, tyrosine kinase receptor AXL expression⁶¹, Fibroblast growth factor(FGF) receptor-3 expression⁴³ and pAKT expression^{29,62}.

Four biomarkers were described in clinical studies that correlate positively with cetuximab response: 1) the possession of a germline mutation in a microRNA-binding site in KRAS⁶³, 2) phosphatase and tensin homolog (PTEN) protein expression^{36,59,64} supported by a study where PTEN knock down correlates with cetuximab resistance⁶⁵, although, no correlation was found in two studies^{37,66}; 3) Vascular endothelial growth factor (VEGF) protein/Interleukin(IL)-6 expression⁶⁷ and 4) Expression of IL-1 ligands⁶⁸. Four clinical studies describe biomarkers that correlate negatively with cetuximab response; 1) KRAS/HRAS mutations⁵⁷, 2) presence of the EGFR-variant EGFRvIII³⁵, 3) phosphorylated AKT levels⁶⁹ and 4) the presence of a long noncoding RNA transcript fusion⁷⁰.

KRAS mutations occur in <5%of HNSCC cases.⁷¹ Braig et al.^{57,58} underline the potential of this biomarker, albeit its relevance for a relatively small subgroup of the HNSCC patients^{57,58}. H-RAS mutations occur slightly more frequent than KRAS mutations (11%)⁷². Few studies describe the role of KRAS or HRAS mutations in HNSCC treatment with EGFR inhibitors and prospective clinical studies lack.

Biomarkers for panitumumab

Panitumumab, like cetuximab binds the ectopic domain of EGFR¹⁵. In this review, no studies were included on the relation between RAS status and panitumumab response in HNSCC patients. Two clinical studies investigated prognostic biomarkers for panitumumab response in HNSCC. Cluster3 gene signature (a hypoxia signature with miRNA-gene expression of ARRDC4, CRCT1, IL36G, KLK10 and PLA2G4E) or the individual expression of seven different miRNAs¹⁵ and a negative P16 status⁷³ correlate with improved panitumumab response in clinical trials. It is impossible to draw conclusions because only few biomarkers were studied.

Receptor tyrosine kinase (RTK) inhibitors

EGFR-targeting TKIs are small molecules that cross the cell membrane and intracellularly inhibit the receptor tyrosine kinase (RTK) of EGFR by binding and blocking the adenosine triphosphate(ATP) binding site, thereby inhibiting downstream EGFR phosphorylation essential for downstream signaling⁷⁴. Downstream of EGFR, HNSCCs often show oncogenic alterations in the PI3K/AKT/mTOR pathway.

Biomarkers for gefitinib

Gefitinib is a TKI targeting EGFR²⁸. For gefitinib, seven biomarkers have been identified that successfully predict patient response. EGFR amplification correlated with gefitinib response in three preclinical studies^{28,75,76}. This positive correlation between EGFR amplification and gefitinib response was not found in two other preclinical^{77,78} and two clinical studies^{79,80}. As for cetuximab, the results are heterogeneous and further studies are warranted.

Several other biomarkers that correlated with response to gefitinib were; a specific RNA signature⁷⁵, MET/AREG expression⁷⁶, ANO1 (a calcium-activated chloride channel that interacts with EGFR) expression⁸¹ and protein kinase C- ϵ (PKC ϵ) expression⁸². Two clinical studies described biomarkers on protein level that correlated positively with response to gefitinib; IGF1R expression⁸³ and MMP11 expression⁷⁹.

Eleven biomarkers correlated negatively with gefitinib response in the preclinical studies, all on protein level; HER3 and phosphorylated HER2 expression²⁸, expression of AREG/Hepatocyte growth factor(HGF)/IGF1/ FGF1/FGF2/IGFR/EGFR/MET⁷⁸, EMT associated protein expression alterations (increased vimentin and decreased e-cadherin)⁸⁴, cortactin protein levels⁸⁵ and a protein signature (Granulocyte-macrophage colony-stimulating factor(GM-CSF), IL-8, metalloproteinase inhibitor-1 (TIMP-1), VEGF)⁸⁶. One clinical study reports that the possession of a stable EGFR-AS1 long noncoding RNA variant is associated with gefitinib resistance⁸⁷.

Biomarkers in two clinical studies did not correlate to gefitinib response: The protein signature as described above (GM-CSF, IL-8, TIMP-1, VEGF)⁸⁶ and EGFR amplification/EGFR kinase-domain mutations⁸⁰

Biomarkers for erlotinib

Erlotinib is a TKI targeting EGFR. Five preclinical studies showed a positive correlation of biomarkers with erlotinib response. ANO1 protein expression⁸¹, pEGFR expression³¹, presence of Mitogen-activated protein kinase(MAPK)1p.D321N mutation⁸⁸ or MAPK1 E322K mutation⁸⁹ and EREG expression^{90,81}. Also preclinically, six biomarkers correlated negatively with erlotinib response. Whereof three can be linked to EMT characteristics similarly as described for cetuximab; SNAIL (an e-cadherin inhibitor) overexpression correlates negatively with erlotinib response⁹¹; a combination of low EGFR & negative e-cadherin protein expression correlates negatively with erlotinib response⁹²; EMT characteristics demonstrated in a functional assay correlate negatively with erlotinib response⁹³. Although these results are promising, the influence of EMT related biomarkers on erlotinib response is not validated in clinical trials.

Three other biomarkers correlated negatively with erlotinib response; PTEN knockout⁶⁵, HMG-box transcription factor 1 (HBP1) knockout⁹⁴ and a protein signature of GM-CSF, IL-8, TIMP-1

and VEGF⁸⁶. However, this signature could not be correlated to patient resistance clinically due to small cohort size. In the clinical studies, none of the biomarkers correlated significantly with erlotinib response^{80,95,96}

Biomarkers for afatinib

Afatinib is a TKI targeting both EGFR, HER2 and HER4⁹⁷. In preclinical studies, AKT expression⁹⁸ and EGFR amplification⁹⁹ correlated positively to afatinib response and one clinical trial confirmed that EGFR amplification correlated positively with afatinib response¹⁰⁰. A specific protein signature correlated negatively to afatinib response in a preclinical study⁸⁶.

Possession of a Tumor protein(P53) wildtype and a specific cluster3 hypoxia profile correlated positively with afatinib response⁹⁷. In another clinical study, PTEN expression on protein level correlated positively with afatinib response¹⁰⁰. Contradictory, two clinical studies elaborated on the absence of a correlation between PTEN expression and afatinib response^{97,99}. Machiels et al. however emphasize that the number of patients in their study was quite low (30) and that the clinical background of their treated patients was different (palliative versus curative intent)⁹⁷.

Biomarkers for Lapatinib / Allitinib / Sorafenib / Dacomitinib

Lapatinib and allitinib are dual kinase inhibitors targeting both EGFR and HER2^{98,101}. Sorafenib is a multi-kinase inhibitor also targeting EGFR¹⁰² and dacomitinib, a pan-HER inhibitor¹⁰³. Lapatinib, allitinib and sorafenib were only studied in preclinical studies. On DNA level, a specific gene expression profile of nine distinct genetic loci including gains of HER2 and EGFR and loss of CDKN2A correlated positively with lapatinib response¹⁰¹. On a protein level ANO1 expression correlated positively lapatinib response⁸¹, while PKCε expression correlated with worse response⁸². AKT expression correlated positively with allitinib response⁹⁸. In contrast, KRAS mutations correlated negatively with allitinib response¹⁰⁴.

MET expression was investigated as biomarker for sorafenib, but did not correlate to response¹⁰². A clinical trial on dacomitinib showed that REV3L mutations correlated positively with dacomitinib response¹⁰³.

PI3K inhibitors

PI3Ks are a family of related intracellular signal transducer enzymes that include the oncogene PIK3CA and tumour suppressor gene PTEN. PI3K-inhibitors inhibit one or more signal transducer enzymes. HNSCCs are known to contain activating mutations in PIK3CA^{9,10}. As a result, PI3K-targeting agents resulting in PI3K inhibition and subsequent tumour suppression have consequently gained interest as emerging therapeutics for HNSCC¹⁰⁵. Constitutive activation of the PI3K pathway has been described as a potential of resistance to EGFR

inhibitors. Therefore, therapeutic agents targeting PI3K/AKT/mTOR pathway have become an important focus in HNSCC research^{41,62}.

Biomarkers for PI3K-inhibitors

Based on in vitro studies, cancers carrying PIK3CA mutations are thought to be more responsive to specific PI3K α inhibitors¹⁰⁵. Presence of oncogene PIK3CA mutations correlated with improved response to PI3K-inhibitors in three preclinical studies^{77,106,107} and in the preclinical and clinical part of Lui et al.⁹ Two other preclinical studies could not confirm this correlation^{105,108}.

Also in preclinical studies, presence of Notch1 mutations¹⁰⁷, PI3KCA amplification⁷⁷, EGFR/AKT1 amplification and CUB and Sushi multiple domains 1 (CSMD1) deletion¹⁰⁵ correlated to improved response. However, PIK3CA amplification did not correlate with response in another preclinical study¹⁰⁶.

In a clinical study, HPV-negative tumor status, the presence of TP53 mutations and an increase in tumor infiltration of CD8⁺ T-cells correlated with improved response to buparlisib, a PIK3CA inhibitor¹⁰⁹. Because the number of studies investigating biomarkers for PI3K inhibitors is low, drawing firm conclusions on clinical implementation is not yet possible.

mTOR inhibitors

Additional to the development of PI3K inhibitors, inhibitors of mTOR have been explored to treat HNSCC¹⁰⁵. mTOR inhibitor inhibit the mechanistic target of rapamycin (mTOR).

Biomarkers for mTOR-inhibitors

For mTOR inhibitors, similar biomarkers as for PI3K inhibitors have been suggested to be relevant. Presence of PIK3CA mutations correlated with improved response to mTOR inhibitors in three preclinical studies^{106,107,110}, like presence of Notch1 mutations in one study¹⁰⁷. PI3KCA amplification, Loss of PTEN and TP53 mutations did not correlate with improved response to mTOR inhibitors^{106,111}. Niehr et al. describe improved mTOR inhibitor response in patients with cisplatin resistance, and worse mTOR inhibitor response with EGFR protein expression and cetuximab resistance¹¹¹. Response to the mTOR-inhibitor temsirolimus did not correlate with mRNA expression of the mTOR pathway members: Akt1, mTOR, RPS6KB1, FKBP1B and TSC1 expression in another preclinical study¹¹².

Clinically, baseline caspase-3 activity correlated negatively with temsirolimus response in one study¹¹³. Also PIK3CA mutations and HPV status did not correlate to mTOR response¹¹⁴.

Due to the limited number of clinical inclusions, it is impossible to draw conclusion about predictive biomarkers for response to mTOR inhibitors.

DISCUSSION

The majority of HNSCC tumors depend on EGFR pathway activation for processes like cell proliferation, anti-apoptotic signaling, angiogenesis and even metastasis. Consequently, EGFR pathway inhibitors have received attention as potential therapeutic agents. However, primary and acquired resistance to EGFR targeting agents often occurs, resulting in low response rates and tumor recurrence. There are many mechanisms of resistance to EGFR targeting agents. Tumor cells resistant to cetuximab can re-activate pro-angiogenic factors via alternative pathways increasing VEGF leading to neovascularisation¹¹⁵. Cetuximab treatment can induce EGFR internalization and degradation and HER-family members can be upregulated to bypass EGFR blockade by cetuximab¹¹⁶. For other TKI's activation of alternative pathways also leads to resistance¹¹⁷. This underscores the need for biomarkers predictive for response to EGFR pathway inhibitors prior to treatment. The only biomarker used at present-day is not molecular but a clinical, i.e. presence and severity of skin rash, which is predictive for cetuximab response²⁰. Apart from the EGFR-PI3K-AKT-mTOR pathway, the immune environment of the tumor is also interesting regarding targeted therapy response. Here biomarkers for immunotherapy were not included, although immunotherapy in HNSCC might be promising¹¹⁸. In this review studies investigating a range of biomarkers for the response to different EGFR-targeting agents have shown conflicting results. This review aimed giving an overview and analysis of these studies published until January 25th 2021.

We encountered several hurdles that impaired us from drawing firm conclusions on the applicability of the biomarkers included in this review. First, the number of clinical studies investigating biomarkers in general is low, with cetuximab as an exception. Second, a lot of studies contained a very small sample size, which makes it hard to draw conclusions about the effect of the correlations found. Most biomarkers have been investigated in only a limited number of studies and subsequently have not been followed up by clinical trials, thus confirmation of their relevance is lacking. Exceptions are EGFR amplification and biomarkers relating to EMT. Also, the discrepancies between exact treatments in clinical trials as well as the differences in the clinical background in patients (recurrent versus metastatic, or palliative versus curative) limit the possibility to draw firm conclusions. Moreover, head and neck cancers comprise of a heterogenic group of tumors both HPV-positive and -negative in different sub-sites of oral cavity, pharynx and larynx

Albeit such differences are hard to avoid, it is challenging to compare clinical studies. Concerning additional treatments, all the discussed targeted therapies were given concurrent with a form of traditional chemotherapy and/or radiotherapy, which limits drawing conclusions about the predictive value of that biomarker for the EGFR pathway inhibitor of interest. All these limitations are applicable for the whole predictive biomarker field. We therefore underline the need for a

more systematic approach tackling these problems. This could be by adding two mandatory components in clinical trials; 1) the assessment of potential biomarkers for the specific EGFR pathway inhibitor studies in that clinical trial, by preferably an independent expert (panel) prior to submitting a proposal for a clinical trial and 2) including these potential biomarker assays in the clinical trial. On the other hand, it should be questioned whether the classic approach via clinical trials should be continued. Clearly the development of biomarkers through clinical trials has not resulted in any relevant biomarker. As every tumor is genetically unique it is hard to set up a decent biomarker trial with high numbers of comparable tumors. Biankin et al. therefore advocate other types of studies in personalized medicine towards more patient-centered trials¹¹⁹. Although this would ask for a big effort in the field, this review underlines the need for increased attention to biomarkers for targeted therapies. Patients themselves will benefit from pre-treatment stratification as this will prevent unnecessary side-effects in non-responders. Also, despite that screening all patients before treatment is expensive, we believe that the advantages will outweigh time and costs. For example, Cetuximab costs approximately €8000 per HNSCC patient, excluding hospital administration and follow-up. For screening every patient targeted Next Generation Sequencing (NGS) is most commonly used. Targeted NGS panels are panels of approximately 70 cancer-related genes which are read using next generation targeted sequencing. Using NGS, point mutations and small indels can be detected, although larger, more complex chromosomal alterations (including large deletions, gene fusions or large CNV) cannot be detected using this approach. On average, performing NGS for one patient, costs approximately €600 (including material and analysis). Screening 13 patients with NGS is equally expensive as treating 1 patient with Cetuximab. Screening-techniques will become cheaper resulting in more patients who can be screened for the costs of 1 cetuximab-treatment. In case of a reliable biomarker all patients will be screened and only the patients where the drug is effective will be treated, which in the end is cheaper.

This review emphasizes the lack of clinically validated biomarkers with high predictive value. EGFR expression is studied in many papers, but the results are too heterogeneous to consider any of the proposed biomarkers suitable for clinical response prediction in general. We think the application of a single biomarker is not adequate in predicting patient response. Studies integrating expression or mutation status of multiple genes and/or proteins have more potential to predict therapy response as they contain a combination of single biomarkers. A DNA/RNA/protein profile is a barcode of many biomarkers combined. In this review several papers found predictive value of such profiles on DNA^{48,101}, RNA^{15,26,50,52,56,75,97} and protein level^{84,86}. Based on these papers, as well as promising advances in other similar fields (as the previously mentioned example of the MammaPrint) DNA/RNA/protein profiles deserve further validation as biomarkers for EGFR targeted therapies for HNSCC patients. Although such an expression profile for the prediction of nodal metastasis in HNSCC was created previously, its applicability in daily clinical practice did not work out yet.¹²⁰

We additionally want to highlight a specific type of biomarker relatively new in the personalized medicine field, being patient-derived organoids. Organoids are 3D structures that are adult stem cell derived, that to some degree resemble the tissue or tumor they are derived of. Organoids derived from tumors from patients recapitulate the original tumors in tissues such as the colon, small intestine, pancreas and prostate¹²¹⁻¹²³. This enables correlating in vitro organoid drug response to the response of patients in the clinic, as shown in a clinical study for organoids derived from gastrointestinal cancer¹²⁴. Recently, HNSCC-derived organoids have been established and several targeted therapies were tested on patient-derived HNSCC organoids⁴¹. Differences between HNSCC organoid lines in response to cetuximab were demonstrated, and initial comparisons to clinical data of the corresponding patients showed the potential of organoid technology in the predictive biomarker field.

In conclusion, several EGFR-PI3K-AKT-mTOR-pathway inhibitor biomarkers are researched for HNSCC but few of the investigated biomarkers are adequately confirmed in clinical trials. A more systematic approach is needed to discover proper biomarkers as stratifying patients is essential to prevent unnecessary costs and side-effects.

REFERENCES

1. Fitzmaurice C, Allen C, Barber RM, et al. Global, regional, and national cancer incidence, mortality, years of life lost, years lived with disability, and disability-adjusted life-years for 32 cancer groups, 1990 to 2015: A Systematic Analysis for the Global Burden of Disease Study Global Burden of Disease Cancer Collaboration. *JAMA Oncol.* 2017;3(4):524-548. doi:10.1001/jamaoncol.2016.5688
2. Cramer JD, Burtneß B, Le QT, Ferris RL. The changing therapeutic landscape of head and neck cancer. *Nat Rev Clin Oncol.* 2019;16(11):669-683. doi:10.1038/s41571-019-0227-z
3. Chow LQM. Head and neck cancer. *N Engl J Med.* 2020;382(1):60-72. doi:10.1056/NEJMra1715715
4. Argiris, AthanassiosView Profile; Karamouzis, Michalis V; Raben, DavidView Profile; Ferris RL. Head and neck cancer - ProQuest. 2008. doi:10.1016/S0140-6736(08)60728-X
5. Trotti A, Bellm LA, Epstein JB, et al. Mucositis incidence, severity and associated outcomes in patients with head and neck cancer receiving radiotherapy with or without chemotherapy: A systematic literature review. *Radiother Oncol.* 2003;66(3):253-262. doi:10.1016/S0167-8140(02)00404-8
6. Rosenthal DI, Lewin JS, Eisbruch A. Prevention and treatment of dysphagia and aspiration after chemoradiation for head and neck cancer. *J Clin Oncol.* 2006;24(17):2636-2643. doi:10.1200/JCO.2006.06.0079
7. Gougis P, Moreau Bachelard C, Kamal M, et al. Clinical Development of Molecular Targeted Therapy in Head and Neck Squamous Cell Carcinoma. *JNCI Cancer Spectr.* 2019;3(4):1-12. doi:10.1093/jncics/pkz055
8. Bossi P, Resteghini C, Paielli N, Licitra L, Pilotti S, Perrone F. Prognostic and predictive value of EGFR in head and neck squamous cell carcinoma. *Oncotarget.* 2016;7(45):74362-74379. doi:10.18632/oncotarget.11413
9. Lui VWY, Hedberg ML, Li H, et al. Frequent mutation of the PI3K pathway in head and neck cancer defines predictive biomarkers. *Cancer Discov.* 2013;3(7):761-769. doi:10.1158/2159-8290.CD-13-0103
10. Iglesias-Bartolome R, Martin D, Silvio Gutkind J. Exploiting the head and neck cancer oncogenome: Widespread PI3K-mTOR pathway alterations and novel molecular targets. *Cancer Discov.* 2013;3(7):722-725. doi:10.1158/2159-8290.CD-13-0239
11. Normanno N, De Luca A, Bianco C, et al. Epidermal growth factor receptor (EGFR) signaling in cancer. *Gene.* 2006;366(1):2-16. doi:10.1016/j.gene.2005.10.018
12. Glazer CA, Chang SS, Ha PK, Califano JA. Applying the molecular biology and epigenetics of head and neck cancer in everyday clinical practice. *Oral Oncol.* 2009;45(4-5):440-446. doi:10.1016/j.oraloncology.2008.05.013
13. Mehanna H, Robinson M, Hartley A, et al. Radiotherapy plus cisplatin or cetuximab in low-risk human papillomavirus-positive oropharyngeal cancer (De-ESCALaTE HPV): an open-label randomised controlled phase 3 trial. *Lancet.* 2019;393(10166):51-60. doi:10.1016/S0140-6736(18)32752-1
14. Gillison ML, Trotti AM, Harris J, et al. Radiotherapy plus cetuximab or cisplatin in human papillomavirus-positive oropharyngeal cancer (NRG Oncology RTOG 1016): a randomised, multicentre, non-inferiority trial. *Lancet.* 2019;393(10166):40-50. doi:10.1016/S0140-6736(18)32779-X
15. Siano M, Espeli V, Mach N, et al. Gene signatures and expression of miRNAs associated with efficacy of panitumumab in a head and neck cancer phase II trial. *Oral Oncol.* 2018;82(May):144-151. doi:10.1016/j.oraloncology.2018.05.013
16. Fabbrocini G, Panariello L, Caro G, Cacciapuoti S. Acneiform Rash Induced by EGFR Inhibitors: Review of the Literature and New Insights. *Ski Appendage Disord.* 2015;1(1):31-37. doi:10.1159/000371821

17. Mittmann N, Seung SJ. Rash rates with EGFR inhibitors: Meta-analysis. *Curr Oncol*. 2011;18(2):e54. doi:10.3747/co.v18i2.605
18. Kubo A, Hashimoto H, Takahashi N, Yamada Y. Biomarkers of skin toxicity induced by anti-epidermal growth factor receptor antibody treatment in colorectal cancer. *World J Gastroenterol*. 2016;22(2):887-894. doi:10.3748/wjg.v22.i2.887
19. Takahashi N, Yamada Y, Furuta K, et al. Association between serum ligands and the skin toxicity of anti-epidermal growth factor receptor antibody in metastatic colorectal cancer. *Cancer Sci*. 2015;106(5):604-610. doi:10.1111/cas.12642
20. Burtneess B, Goldwasser MA, Flood W, Mattar B, Forastiere AA. Phase III randomized trial of cisplatin plus placebo compared with cisplatin plus cetuximab in metastatic/recurrent head and neck cancer: An Eastern Cooperative Oncology Group Study. *J Clin Oncol*. 2005;23(34):8646-8654. doi:10.1200/JCO.2005.02.4646
21. Moher D, Shamseer L, Clarke M, et al. Preferred reporting items for systematic review and meta-analysis protocols (PRISMA-P) 2015 statement. *Rev Esp Nutr Humana y Diet*. 2016;20(2):148-160. doi:10.1186/2046-4053-4-1
22. Goldstein NI, Prewett M, Zuklys K, Rockwell P, Mendelsohn J. Biological Efficacy of a Chimeric Antibody to the Epidermal Growth Factor Receptor in a Human Tumor Xenograft Model. *Clin Cancer Res*. 1995;1(11):1311-1318.
23. Ciardiello F, Tortora G. EGFR Antagonists in Cancer Treatment. *N Engl J Med*. 2008;358(11):1160-1174. doi:10.1056/NEJMra0707704
24. Kimura H, Sakai K, Arai T, Shimoyama T, Tamura T, Nishio K. Antibody-dependent cellular cytotoxicity of cetuximab against tumor cells with wild-type or mutant epidermal growth factor receptor. *Cancer Sci*. 2007;98(8):1275-1280. doi:10.1111/j.1349-7006.2007.00510.x
25. Patel D, Guo X, Ng S, et al. IgG isotype, glycosylation, and EGFR expression determine the induction of antibody-dependent cellular cytotoxicity in vitro by cetuximab. *Hum Antibodies*. 2010;19(4):89-99. doi:10.3233/HAB-2010-0232
26. Koi L, Löck S, Linde A, et al. EGFR-amplification plus gene expression profiling predicts response to combined radiotherapy with EGFR-inhibition: a preclinical trial in 10 HNSCC-tumour-xenograft models. *Radiother Oncol*. 2017;124(3):496-503.
27. Yamatodani T, Ekblad L, Kjellén E, Johnsson A, Mineta H, Wennerberg J. Epidermal growth factor receptor status and persistent activation of Akt and p44/42 MAPK pathways correlate with the effect of cetuximab in head and neck and colon cancer cell lines. *J Cancer Res Clin Oncol*. 2009;135(3):395.
28. Erjala K, Sundvall M, Junttila TT, et al. Signaling via ErbB2 and ErbB3 associates with resistance and epidermal growth factor receptor (EGFR) amplification with sensitivity to EGFR inhibitor gefitinib in head and neck squamous cell carcinoma cells. *Clin Cancer Res*. 2006;12(13):4103-4111. doi:10.1158/1078-0432.CCR-05-2404
29. Stein AP, Swick AD, Smith MA, et al. Xenograft assessment of predictive biomarkers for standard head and neck cancer therapies. *Cancer Med*. 2015;4(5):699-712.
30. Barnea I, Haif S, Keshet R, et al. Targeting ErbB-1 and ErbB-4 in irradiated head and neck cancer: Results of in vitro and in vivo studies. *Head Neck*. 2013;35(3):399-407.
31. Kriegs M, Clauditz TS, Hoffer K, et al. Analyzing expression and phosphorylation of the EGF receptor in HNSCC. *Sci Rep*. 2019;9(1):1-8. doi:10.1038/s41598-019-49885-5
32. Fountzilas G, Kalogeta-Fountzila A, Lambaki S, et al. MMP9 but Not EGFR, MET, ERCC1, P16, and P-53 is associated with response to concomitant radiotherapy, cetuximab, and weekly cisplatin in patients with locally advanced head and neck cancer. *J Oncol*. 2009;2009. doi:10.1155/2009/305908

33. Licitra L, Mesia R, Rivera F, et al. Evaluation of EGFR gene copy number as a predictive biomarker for the efficacy of cetuximab in combination with chemotherapy in the first-line treatment of recurrent and/or metastatic squamous cell carcinoma of the head and neck: EXTREME study. *Ann Oncol*. 2011;22(5):1078-1087. doi:10.1093/annonc/mdq588
34. Licitra L, Störkel S, Kerr KM, et al. Predictive value of epidermal growth factor receptor expression for first-line chemotherapy plus cetuximab in patients with head and neck and colorectal cancer: analysis of data from the EXTREME and CRYSTAL studies. *Eur J Cancer*. 2013;49(6):1161-1168.
35. Tinhofer I, Klinghammer K, Weichert W, et al. Expression of amphiregulin and EGFRvIII affect outcome of patients with squamous cell carcinoma of the head and neck receiving cetuximab–docetaxel treatment. *Clin Cancer Res*. 2011;17(15):5197-5204.
36. da Costa AABA, D'Almeida Costa F, Ribeiro AR, et al. Low PTEN expression is associated with worse overall survival in head and neck squamous cell carcinoma patients treated with chemotherapy and cetuximab. *Int J Clin Oncol*. 2015;20(2):282-289. doi:10.1007/s10147-014-0707-1
37. Leblanc O, Vacher S, Lecerf C, et al. Biomarkers of cetuximab resistance in patients with head and neck squamous cell carcinoma. *Cancer Biol Med*. 2020;17(1):208-217. doi:10.20892/j.issn.2095-3941.2019.0153
38. Kondo N, Tsukuda M, Sakakibara A, et al. Combined molecular targeted drug therapy for EGFR and HER-2 in head and neck squamous cell carcinoma cell lines. *Int J Oncol*. 2012;40(6):1805-1812.
39. Jedlinski A, Ansell A, Johansson AC, Roberg K. EGFR status and EGFR ligand expression influence the treatment response of head and neck cancer cell lines. *J Oral Pathol Med*. 2013;42(1):26-36. doi:10.1111/j.1600-0714.2012.01177.x
40. Stegeman H, Kaanders JH, Van Der Kogel AJ, et al. Predictive value of hypoxia, proliferation and tyrosine kinase receptors for EGFR-inhibition and radiotherapy sensitivity in head and neck cancer models. *Radiother Oncol*. 2013;106(3):383-389. doi:10.1016/j.radonc.2013.02.001
41. Driehuis E, Kolders S, Spelier S, et al. Oral mucosal organoids as a potential platform for personalized cancer therapy. *Cancer Discov*. 2019;9(7):852-871. doi:10.1158/2159-8290.CD-18-1522
42. Wheeler DL, Huang S, Kruser TJ, et al. Mechanisms of acquired resistance to cetuximab: Role of HER (ErbB) family members. *Oncogene*. 2008;27(28):3944-3956. doi:10.1038/onc.2008.19
43. Oliveras-Ferraro C, Cufi S, Queralt B, et al. Cross-suppression of EGFR ligands amphiregulin and epiregulin and de-repression of FGFR3 signalling contribute to cetuximab resistance in wild-type KRAS tumour cells. *Br J Cancer*. 2012;106(8):1406-1414. doi:10.1038/bjc.2012.103
44. Jerhammar F, Johansson A-C, Ceder R, et al. YAP1 is a potential biomarker for cetuximab resistance in head and neck cancer. *Oral Oncol*. 2014;50(9):832-839.
45. Ansell A, Jedlinski A, Johansson A, Roberg K. Epidermal growth factor is a potential biomarker for poor cetuximab response in tongue cancer cells. *J Oral Pathol Med*. 2016;45(1):9-16.
46. Kogashiwa Y, Inoue H, Kuba K, et al. Prognostic role of epiregulin/amphiregulin expression in recurrent/metastatic head and neck cancer treated with cetuximab. *Head Neck*. 2018;40(11):2424-2431. doi:10.1002/hed.25353
47. Hatakeyama H, Cheng H, Wirth P, et al. Regulation of heparin-binding EGF-like growth factor by miR-212 and acquired cetuximab-resistance in head and neck squamous cell carcinoma. *PLoS One*. 2010;5(9):e12702.
48. Boeckx C, Blockx L, de Beeck KO, et al. Establishment and characterization of cetuximab resistant head and neck squamous cell carcinoma cell lines: focus on the contribution of the AP-1 transcription factor. *Am J Cancer Res*. 2015;5(6):1921.
49. Guarino M. Epithelial-mesenchymal transition and tumour invasion. *Int J Biochem Cell Biol*. 2007;39(12):2153-2160. doi:10.1016/j.biocel.2007.07.011

50. Klinghammer K, Otto R, Raguse JD, et al. Basal subtype is predictive for response to cetuximab treatment in patient-derived xenografts of squamous cell head and neck cancer. *Int J Cancer*. 2017;141(6):1215-1221. doi:10.1002/ijc.30808
51. Keck MK, Zuo Z, Khattri A, et al. Integrative analysis of head and neck cancer identifies two biologically distinct HPV and three non-HPV subtypes. *Clin Cancer Res*. 2015;21(4):870-881. doi:10.1158/1078-0432.CCR-14-2481
52. Bossi P, Bergamini C, Siano M, et al. Functional genomics uncover the biology behind the responsiveness of head and neck squamous cell cancer patients to cetuximab. *Clin Cancer Res*. 2016;22(15):3961-3970.
53. Zuo JH, Zhu W, Li MY, et al. Activation of EGFR promotes squamous carcinoma SCC10A cell migration and invasion via inducing EMT-like phenotype change and MMP-9-mediated degradation of E-cadherin. *J Cell Biochem*. 2011;112(9):2508-2517. doi:10.1002/jcb.23175
54. Kamel HFM, Al-Amadi HSAB. Exploitation of Gene Expression and Cancer Biomarkers in Paving the Path to Era of Personalized Medicine. *Genomics, Proteomics Bioinforma*. 2017;15(4):220-235. doi:10.1016/j.gpb.2016.11.005
55. Tian S, Roepman P, van't Veer LJ, Bernards R, de Snoo F, Glas AM. Biological functions of the genes in the mammaprint breast cancer profile reflect the hallmarks of cancer. *Biomark Insights*. 2010;2010(5):129-138. doi:10.4137/BMI.S6184
56. De Cecco L, Giannoccaro M, Marchesi E, et al. Integrative miRNA-gene expression analysis enables refinement of associated biology and prediction of response to cetuximab in head and neck squamous cell cancer. *Genes (Basel)*. 2017;8(1):35.
57. Braig F, Voigtlaender M, Schieferdecker A, et al. Liquid biopsy monitoring uncovers acquired RAS-mediated resistance to cetuximab in a substantial proportion of patients with head and neck squamous cell carcinoma. *Oncotarget*. 2016;7(28):42988.
58. Braig F, Kriegs M, Voigtlaender M, et al. Cetuximab resistance in head and neck cancer is mediated by EGFR-K521 polymorphism. *Cancer Res*. 2017;77(5):1188-1199.
59. da Costa AABA, Costa FD, Araújo DV, et al. The roles of PTEN, cMET, and p16 in resistance to cetuximab in head and neck squamous cell carcinoma. *Med Oncol*. 2019;36(1):1-9. doi:10.1007/s12032-018-1234-0
60. Kondo T, Ozawa S, Ikoma T, et al. Expression of the chemokine CXCL14 and cetuximab-dependent tumour suppression in head and neck squamous cell carcinoma. *Oncogenesis*. 2016;5(7):e240.
61. Brand TM, Iida M, Stein AP, et al. AXL mediates resistance to cetuximab therapy. *Cancer Res*. 2014;74(18):5152-5164. doi:10.1158/0008-5472.CAN-14-0294
62. Rebucci M, Peixoto P, Dewitte A, et al. Mechanisms underlying resistance to cetuximab in the HNSCC cell line: role of AKT inhibition in bypassing this resistance. *Int J Oncol*. 2011;38(1):189-200.
63. Weidhaas JB, Harris J, Schae D, et al. The KRAS-variant and cetuximab response in head and neck squamous cell cancer a secondary analysis of a randomized clinical trial. *JAMA Oncol*. 2017;3(4):483-491. doi:10.1001/jamaoncol.2016.5478
64. Eze N, Lee JW, Yang DH, et al. PTEN loss is associated with resistance to cetuximab in patients with head and neck squamous cell carcinoma. *Oral Oncol*. 2019;91(February):69-78. doi:10.1016/j.oraloncology.2019.02.026
65. Izumi H, Wang Z, Goto Y, et al. Pathway-Specific Genome Editing of PI3K/mTOR Tumor Suppressor Genes Reveals that PTEN Loss Contributes to Cetuximab Resistance in Head and Neck Cancer. *Mol Cancer Ther*. 2020;19(7):1562-1571. doi:10.1158/1535-7163.MCT-19-1036
66. Mriouah J, Boura C, Pinel S, et al. Cellular response to cetuximab in PTEN-silenced head and neck squamous cell carcinoma cell line. *Int J Oncol*. 2010;37(6):1555-1563.

67. Argiris A, Lee SC, Feinstein T, et al. Serum biomarkers as potential predictors of antitumor activity of cetuximab-containing therapy for locally advanced head and neck cancer. *Oral Oncol.* 2011;47(10):961-966.
68. Espinosa-Cotton M, Fertig EJ, Stabile LP, et al. A preliminary analysis of interleukin-1 ligands as potential predictive biomarkers of response to cetuximab. *Biomark Res.* 2019;7(1):1-11. doi:10.1186/s40364-019-0164-0
69. Lyu J, Song H, Tian Z, Miao Y, Ren G, Guo W. Predictive value of pAKT/PTEN expression in oral squamous cell carcinoma treated with cetuximab-based chemotherapy. *Oral Surg Oral Med Oral Pathol Oral Radiol.* 2016;121(1):67-72.
70. Bossi P, Siano M, Bergamini C, et al. Are Fusion Transcripts in Relapsed/Metastatic Head and Neck Cancer Patients Predictive of Response to Anti-EGFR Therapies? *Dis Markers.* 2017;2017.
71. Kiaris H, Spandidos DA, Jones AS, Vaughan ED, Field JK. Mutations, expression and genomic instability of the H-ras proto-oncogene in squamous cell carcinomas of the head and neck. *Br J Cancer.* 1995;72(1):123-128. doi:10.1038/bjc.1995.287
72. Lea IA, Jackson MA, Li X, Bailey S, Peddada SD, Dunnick JK. Genetic pathways and mutation profiles of human cancers: Site- and exposure-specific patterns. *Carcinogenesis.* 2007;28(9):1851-1858. doi:10.1093/carcin/bgm176
73. Vermorken JB, Stöhlmacher-Williams J, Davidenko I, et al. Cisplatin and fluorouracil with or without panitumumab in patients with recurrent or metastatic squamous-cell carcinoma of the head and neck (SPECTRUM): An open-label phase 3 randomised trial. *Lancet Oncol.* 2013;14(8):697-710. doi:10.1016/S1470-2045(13)70181-5
74. Lurje G, Lenz HJ. EGFR signaling and drug discovery. *Oncology.* 2010;77(6):400-410. doi:10.1159/000279388
75. Dickinson DM, Marshall GB, Beran GJ, et al. Identification of biomarkers in human head and neck tumor cell lines that predict for in vitro sensitivity to gefitinib. *Clin Transl Sci.* 2009;2(3):183-192. doi:10.1111/j.1752-8062.2009.00099.x
76. Rogers SJ, Box C, Chambers P, et al. Determinants of response to epidermal growth factor receptor tyrosine kinase inhibition in squamous cell carcinoma of the head and neck. *J Pathol A J Pathol Soc Gt Britain Irel.* 2009;218(1):122-130.
77. Nichols AC, Black M, Yoo J, et al. Exploiting high-throughput cell line drug screening studies to identify candidate therapeutic agents in head and neck cancer. *BMC Pharmacol Toxicol.* 2014;15(1):66.
78. Tepper SR, Zuo Z, Khattri A, Heß J, Seiwert TY. Growth factor expression mediates resistance to EGFR inhibitors in head and neck squamous cell carcinomas. *Oral Oncol.* 2016;56:62-70.
79. Tan EH, Goh C, Lim WT, et al. Gefitinib, cisplatin, and concurrent radiotherapy for locally advanced head and neck cancer: EGFR FISH, protein expression, and mutational status are not predictive biomarkers. *Ann Oncol.* 2012;23(4):1010-1016. doi:10.1093/annonc/mdr327
80. Cohen EEW, Lingen MW, Martin LE, et al. Response of some head and neck cancers to epidermal growth factor receptor tyrosine kinase inhibitors may be linked to mutation of ERBB2 rather than EGFR. *Clin Cancer Res.* 2005;11(22):8105-8108. doi:10.1158/1078-0432.CCR-05-0926
81. Bill A, Gutierrez A, Kulkarni S, et al. ANO1/TMEM16A interacts with EGFR and correlates with sensitivity to EGFR-targeting therapy in head and neck cancer. *Oncotarget.* 2015;6(11):9173.
82. Weisheit S, Liebmann C. Allosteric modulation by protein kinase C ϵ leads to modified responses of EGF receptor towards tyrosine kinase inhibitors. *Cell Signal.* 2012;24(2):422-434. doi:10.1016/j.cellsig.2011.09.010

83. Thariat J, Bensadoun RJ, Etienne-Grimaldi MC, et al. Contrasted outcomes to gefitinib on tumoral IGF1R expression in head and neck cancer patients receiving postoperative chemoradiation (GORTEC trial 2004-02). *Clin Cancer Res*. 2012;18(18):5123-5133. doi:10.1158/1078-0432.CCR-12-1518
84. Frederick BA, Helfrich BA, Coldren CD, et al. Epithelial to mesenchymal transition predicts gefitinib resistance in cell lines of head and neck squamous cell carcinoma and non-small cell lung carcinoma. *Mol Cancer Ther*. 2007;6(6):1683-1691.
85. Timpson P, Wilson AS, Lehrbach GM, Sutherland RL, Musgrove EA, Daly RJ. Aberrant expression of cortactin in head and neck squamous cell carcinoma cells is associated with enhanced cell proliferation and resistance to the epidermal growth factor receptor inhibitor gefitinib. *Cancer Res*. 2007;67(19):9304-9314. doi:10.1158/0008-5472.CAN-07-0798
86. Box C, Mendiola M, Gowan S, et al. A novel serum protein signature associated with resistance to epidermal growth factor receptor tyrosine kinase inhibitors in head and neck squamous cell carcinoma. *Eur J Cancer*. 2013;49(11):2512-2521.
87. Tan DSW, Chong FT, Leong HS, et al. Long noncoding RNA EGFR-AS1 mediates epidermal growth factor receptor addiction and modulates treatment response in squamous cell carcinoma. *Nat Med*. 2017;23(10):1167.
88. Ngan HL, Poon PHY, Su YX, et al. Erlotinib sensitivity of MAPK1p.D321N mutation in head and neck squamous cell carcinoma. *npj Genomic Med*. 2020;5(1):1-5. doi:10.1038/s41525-020-0124-5
89. Van Allen EM, Lui VWY, Egloff AM, et al. Genomic correlate of exceptional erlotinib response in head and neck squamous cell carcinoma. *JAMA Oncol*. 2015;1(2):238-244. doi:10.1001/jamaoncol.2015.34
90. Liu S, Wang Y, Han Y, et al. EREG-driven oncogenesis of Head and Neck Squamous Cell Carcinoma exhibits higher sensitivity to Erlotinib therapy. *Theranostics*. 2020;10(23):10589-10605. doi:10.7150/thno.47176
91. Dennis M, Wang G, Luo J, et al. Snail controls the mesenchymal phenotype and drives erlotinib resistance in Oral epithelial and HNSCC cells. *Otolaryngol Head Neck Surg*. 2014;147(4):726-732. doi:10.1177/0194599812446407.Snail
92. Muller S, Su L, Tighiouart M, et al. Distinctive E-cadherin and epidermal growth factor receptor expression in metastatic and nonmetastatic head and neck squamous cell carcinoma: Predictive and prognostic correlation. *Cancer*. 2008;113(1):97-107. doi:10.1002/cncr.23557
93. Haddad Y, Choi W. The transcriptional repressor Delta EF1 controls the EMT phenotype and resistance to the EGFR inhibitor erlotinib in human head & neck squamous cell. *Clin Cancer Res*. 2009;15(2):532-542. doi:10.1158/1078-0432.CCR-08-1733.The
94. Chan CY, Chang CM, Chen YH, Sheu JJC, Lin TY, Huang CY. Regulatory role of transcription factor HBP1 in anticancer efficacy of EGFR inhibitor erlotinib in HNSCC. *Head Neck*. 2020;42(10):2958-2967. doi:10.1002/hed.26346
95. Chau NG, Perez-Ordóñez B, Zhang K, et al. The association between EGFR variant III, HPV, p16, c-MET, EGFR gene copy number and response to EGFR inhibitors in patients with recurrent or metastatic squamous cell carcinoma of the head and neck. *Head Neck Oncol*. 2011;3(1):11.
96. Thomas F, Delmar P, Vergez S, et al. Gene expression profiling on pre- and post-erlotinib tumors from patients with head and neck squamous cell carcinoma. *Head Neck*. 2013;35(6):809-818.
97. Machiels JP, Bossi P, Menis J, et al. Activity and safety of afatinib in a window preoperative EORTC study in patients with squamous cell carcinoma of the head and neck (SCCHN). *Ann Oncol*. 2018;29(4):985-991. doi:10.1093/annonc/mdy013
98. Silva-Oliveira RJ, Melendez M, Martinho O, et al. AKT can modulate the in vitro response of HNSCC cells to irreversible EGFR inhibitors. *Oncotarget*. 2017;8(32):53288.

99. Young NR, Soneru C, Liu J, et al. Afatinib efficacy against squamous cell carcinoma of the head and neck cell lines in vitro and in vivo. *Target Oncol.* 2015;10(4):501-508.
100. Cohen EEW, Licitra LF, Burtneß B, et al. Biomarkers predict enhanced clinical outcomes with afatinib versus methotrexate in patients with second-line recurrent and/or metastatic head and neck cancer. *Ann Oncol.* 2017;28(10):2526-2532. doi:10.1093/annonc/mdx344
101. Greshock J, Cheng J, Rusnak D, et al. Genome-wide DNA copy number predictors of lapatinib sensitivity in tumor-derived cell lines. *Mol Cancer Ther.* 2008;7(4):935-943.
102. Beizaei K, Gleißner L, Hoffer K, et al. Receptor tyrosine kinase MET as potential target of multi-kinase inhibitor and radiosensitizer sorafenib in HNSCC. *Head Neck.* 2019;41(1):208-215.
103. Huang KK, Jang KW, Kim S, et al. Exome sequencing reveals recurrent REV3L mutations in cisplatin-resistant squamous cell carcinoma of head and neck. *Sci Rep.* 2016;6:19552.
104. Silva-Oliveira RJ, Silva VAO, Martinho O, et al. Cytotoxicity of allitinib, an irreversible anti-EGFR agent, in a large panel of human cancer-derived cell lines: KRAS mutation status as a predictive biomarker. *Cell Oncol.* 2016;39(3):253-263.
105. Ruicci KM, Meens J, Sun RX, et al. A controlled trial of HNSCC patient-derived xenografts reveals broad efficacy of PI3K α inhibition in controlling tumor growth. *Int J Cancer.* 2018:1-7. doi:10.1002/ijc.32009
106. Mazumdar T, Byers LA, Ng PKS, et al. A comprehensive evaluation of biomarkers predictive of response to PI3K inhibitors and of resistance mechanisms in head and neck squamous cell carcinoma. *Mol Cancer Ther.* 2014;13(11):2738-2750. doi:10.1158/1535-7163.MCT-13-1090
107. Sambandam V, Frederick MJ, Shen L, et al. PDK1 mediates Notch1-mutated head and neck squamous carcinoma vulnerability to therapeutic PI3K/mTOR inhibition. *Clin Cancer Res.* 2019;25(11):3329-3340. doi:10.1158/1078-0432.CCR-18-3276
108. Klinghammer K, Politz O, Eder T, et al. Combination of copanlisib with cetuximab improves tumor response in cetuximab-resistant patient-derived xenografts of head and neck cancer. *Oncotarget.* 2020;11(41):3688-3697. doi:10.18632/oncotarget.27763
109. Soulieres D, Licitra L, Mesía R, et al. Molecular alterations and buparlisib efficacy in patients with squamous cell carcinoma of the head and neck: Biomarker analysis from BERIL-1. *Clin Cancer Res.* 2018;24(11):2505-2516. doi:10.1158/1078-0432.CCR-17-2644
110. Yamaguchi K, Iglesias-Bartolomé R, Wang Z, et al. A synthetic-lethality RNAi screen reveals an ERK-mTOR co-targeting pro-apoptotic switch in PIK3CA⁺ oral cancers. *Oncotarget.* 2016;7(10):10696.
111. Niehr F, Weichert W, Stenzinger A, Budach V, Tinhofer I. CCI-779 (Temozolimus) exhibits increased anti-tumor activity in low EGFR expressing HNSCC cell lines and is effective in cells with acquired resistance to cisplatin or cetuximab. *J Transl Med.* 2015;13(1):106.
112. Klinghammer K, Raguse JD, Plath T, et al. A comprehensively characterized large panel of head and neck cancer patient-derived xenografts identifies the mTOR inhibitor everolimus as potential new treatment option. *Int J Cancer.* 2015;136(12):2940-2948. doi:10.1002/ijc.29344
113. John K, Rösner I, Keilholz U, Gauler T, Bantel H, Grünwald V. Baseline caspase activity predicts progression free survival of temsirolimus-treated head neck cancer patients. *Eur J Cancer.* 2015;51(12):1596-1602.
114. Grünwald V, Keilholz U, Boehm A, et al. TEMHEAD: A single-arm multicentre phase II study of temsirolimus in platin- and cetuximab refractory recurrent and/or metastatic squamous cell carcinoma of the head and neck (SCCHN) of the German SCCHN Group (AIO). *Ann Oncol.* 2015;26(3):561-567. doi:10.1093/annonc/mdl571

115. Vilorio-Petit A, Kerbel RS, Jothy S, et al. Acquired resistance to the antitumor effect of epidermal growth factor receptor-blocking antibodies in vivo: A role for altered tumor angiogenesis. *Cancer Res.* 2001;61(13):5090-5101.
116. Brand TM, Iida M, Wheeler DL. Molecular mechanisms of resistance to the EGFR monoclonal antibody cetuximab. *Cancer Biol Ther.* 2011;11(9):777-792. doi:10.4161/cbt.11.9.15050
117. Huang L, Fu L. Mechanisms of resistance to EGFR tyrosine kinase inhibitors. *Acta Pharm Sin B.* 2015;5(5):390-401. doi:10.1016/j.apsb.2015.07.001
118. Economopoulou P, Agelaki S, Perisanidis C, Giotakis EI, Psyrri A. The promise of immunotherapy in head and neck squamous cell carcinoma. *Ann Oncol.* 2016;27(9):1675-1685. doi:10.1093/annonc/mdw226
119. Biankin A V., Piantadosi S, Hollingsworth SJ. Patient-centric trials for therapeutic development in precision oncology. *Nature.* 2015;526(7573):361-370. doi:10.1038/nature15819
120. Roepman P, Wessels LFA, Kettelarij N, et al. An expression profile for diagnosis of lymph node metastases from primary head and neck squamous cell carcinomas. *Nat Genet.* 2005;37(2):182-186. doi:10.1038/ng1502
121. Gao D, Vela I, Sboner A, et al. Organoid cultures derived from patients with advanced prostate cancer. *Cell.* 2014;159(1):176-187. doi:10.1016/j.cell.2014.08.016
122. Van De Wetering M, Francies HE, Francis JM, et al. Prospective derivation of a living organoid biobank of colorectal cancer patients. *Cell.* 2015;161(4):933-945. doi:10.1016/j.cell.2015.03.053
123. Fujii M, Shimokawa M, Date S, et al. A Colorectal Tumor Organoid Library Demonstrates Progressive Loss of Niche Factor Requirements during Tumorigenesis. *Cell Stem Cell.* 2016;18(6):827-838. doi:10.1016/j.stem.2016.04.003
124. Vlachogiannis G, Hedayat S, Vatsiou A, et al. Patient-derived organoids model treatment response of metastatic gastrointestinal cancers. *Science (80-).* 2018;359(6378):920-926. doi:10.1126/science.aao2774

APPENDIX

PubMed syntax

```
((((((((((cancer[Title/Abstract]) OR carcinoma[Title/Abstract]) OR neoplasm[Title/Abstract])
OR "squamous cell carcinoma"[Title/Abstract]) OR ("squamous cell carcinoma of head and
neck"[MeSH Terms]))) AND (((((((((((("head and neck"[Title/Abstract]) OR "hnscc"[Title/
Abstract]) OR oral[Title/Abstract]) OR pharynx[Title/Abstract]) OR pharyngeal[Title/Abstract])
OR larynx[Title/Abstract]) OR laryngeal[Title/Abstract]) OR "hypopharynx"[Title/Abstract]) OR
"hypopharyngeal"[Title/Abstract]) OR "oropharynx"[Title/Abstract]) OR "oropharyngeal"[Title/
Abstract]))) AND (((("biomarkers"[Title/Abstract]) OR "biomarker"[Title/Abstract]) OR
biomarkers[MeSH Terms]) OR "biomarkers, tumor"[MeSH Terms]))) AND (((((((("targeted
therapy"[Title/Abstract]) OR "prediction"[Title/Abstract]) OR "predictive"[Title/Abstract])
OR "predicting"[Title/Abstract]) OR "drug therapy"[Title/Abstract]) OR "molecular targeted
therapy"[MeSH Terms]))
```

Embase syntax

```
((('malignant neoplasm':ab,ti OR 'carcinoma':ab,ti OR 'cancer':ab,ti OR 'squamous cell
carcinoma':ab,ti OR ('head'/exp AND 'neck squamous cell carcinoma')) AND ('pharynx'/exp
OR 'pharynx':ab,ti OR 'pharyngeal':ab,ti OR 'hypopharynx'/exp OR 'hypopharynx':ab,ti OR
'hypopharyngeal':ab,ti OR 'larynx'/exp OR 'larynx':ab,ti OR 'laryngeal':ab,ti OR 'oropharynx'/exp
OR 'oropharynx':ab,ti OR 'oropharyngeal':ab,ti OR 'mouth'/exp OR 'mouth':ab,ti OR 'hnscc':ab,ti
OR ('head':ab,ti AND 'neck':ab,ti))) AND ('biological marker'/exp OR 'tumor marker'/exp OR
'biomarker':ab,ti OR 'biomarkers':ab,ti OR 'tumor marker':ab,ti OR 'tumor markers':ab,ti))
AND ('molecularly targeted therapy'/exp OR 'targeted therapy':ab,ti OR 'prediction'/exp OR
'prediction':ab,ti OR 'predictive':ab,ti OR 'predicting':ab,ti OR 'drug therapy'/exp OR 'drug
therapy':ab,ti)
```

SUPPLEMENTAL TABLES CHAPTER 2

Supplemental table 1A monoclonal antibodies **pre-clinical**

Biomarker	Technique	Correlation with response (+) or resistance (-)	Sample Size	Additional treatment	Reference
Cetuximab					
Epigenetic level					
CXCL14 methylation, CXCL14 expression	qPCR, KI study	-	6		60
DNA level					
EGFR amplification	FISH; FISH & IHC; sequencing	+	10; 10; 2	RT	26-28
Epithelial marker expression (KRT13 + KRT14 + KRT16 + KRTDAP)	Microarray	+	3		48
HB-EGF expression, EMT marker expression (PLAU + TAGLN + ADAM19 + TSP-1)	Microarray	-	3		48
EGFR-K SNP polymorphism	Sequencing	-	33		58
PTEN-loss	KO	-	1		65
RNA level					
RNA expression profile	Microarray	+	10	RT	26
Basal subtype	Microarray	+	28		50
EREG expression	qPCR	+	25		39
YAP1 expression	qPCR	-	32		44
Genes controlled by AP-1 transcription	qPCR	-	3		48
EGFR,HER,HER3,HER4 expression	qPCR	No	16	Trastuzumab	38
EGFR expression	qPCR	No	12; 25		39,41
Protein level					
EGFR expression	WB; IHC	+	10; 6		28,29
pEGFR expression	WB	+	8		31
EGFR, HER4 expression	WB	+	3		30
(AREG+EREG) expression	KO study	+	1		43
AXL expression	IHC	-	6		61
FGFR3 activity	KO study	-	1		43
HB-EGF expression	KO study	-	3		47
EGF expression	KO study	-	3		45
pAKT expression	IHC	-	6		29

Supplemental table 1A monoclonal antibodies **pre-clinical** (continued)

Biomarker	Technique	Correlation with response (+) or resistance (-)	Sample Size	Additional treatment	Reference
Absence of EGFR internalization, persistent AKT activation	WB	-	1		62
HER3, Met expression	WB	-	4	RT	40
HER2, HER3 and cMET activation	WB	-	1		42
AKT expression	WB	No	8		98
AREG, EREG expression	KO study	No	3		45
PTEN expression	KO study	No	1		66
pEGFR, pERK expression	IHC	No	6		29
pEGFR, E-cadherin, Vimentin expression	WB	No	4	RT	40
pEGFR, pHER2, HER3 expression	WB	No	10		38
EGFR expression	ELISA	No	25		39
Other					
EMT characteristics	Migration assay, invasion assay	-	3		48

Supplemental table 1B: RTK-inhibitors pre-clinical

Biomarker	Technique	Correlation with response (+) or resistance (-)	Sample size	Reference
Gefitinib				
DNA level				
EGFR expression	FISH; FISH & FCM	+	20; 18	75,76
EGFR expression	CNV analysis	No	42	77
PI3K3CA mutations	Sequencing	No	42	77
RNA level				
EGFR expression	Sequencing	+	10	28
mRNA signature (E-cadherin + TGF- α + AREG + EGFR + FLJ22662 + PAK6 + GSTP1 + ABCC5)	Microarray	+	20	75
Protein level				
MET-expression	WB	+	18	76
AREG expression	ELISA	+	18	76
ANO-1 expression	KO study	+	10	81
PKCe expression	WB	+	1	82
HER3, pHER2 expression	WB	-	10	28
Protein signature (GM-CSF + IL-8 + TIMP-1 + VEGF)	Immunoassay	-	2	86
Protein signature (Vimentin expression + E-cadherin loss + claudin 4 loss + claudin 7 loss)	Immunoassay, microarray	-	9	84
AREG, HGF, IGF1, FGF1, FGF2 expression	Viability screen	-	4	78
IGFR, EGFR, MET expression	Sequencing	-	4	78
Cortactin levels	KI study	-	5	85
E-cadherin, HER2, HER3, pMAPK, pAKT expression	WB	No	18	76
Erlotinib				
DNA level				
MAPK1p.D321N Mutation	KI study	+	8	88
MAPK1 E322K Mutation	KI study	+	1	89
Snail overexpression (inhibitor E-cadherin)	KI study	-	1	91
PTEN-loss	KO study	-	2	65
EGFR amplification, PIK3CA mutations	CNV analysis	No	42	77
EGFR-K SNP polymorphism	Sequencing	No	12	58

Supplemental table 1B: RTK-inhibitors pre-clinical (continued)

Biomarker	Technique	Correlation with response (+) or resistance (-)	Sample size	Reference
RNA level				
EREg expression	KO study	+	2	90
Protein level				
ANO 1 expression	WB	+	10	81
pEGFR expression	WB	+	8	31
EREg expression	WB	+	6	90
HBPI KO	KO study	-	1	94
Protein signature (GM-CSF + IL-8 + TIMP-1 + VEGF)	Immunoassay	-	2	86
(Low EGFR expression + negative E-cadherin expression)	IHC	-	5	92
Other				
EMT characteristics	Wound healing, migration assay, WB	-	6	93
pEGFR	WB	No	6	93
Afatinib				
DNA expression level				
AKT expression	KO study	+	8	98
EGFR amplification	FISH, qPCR	+	10	99
Protein level				
Protein signature (GM-CSF + IL-8 + TIMP-1 + VEGF)	Immunoassay	-	2	86
PTEN expression	WB	No	10	99
Lapatinib				
DNA level				
Gene expression profile (gain HER2, EGFR, loss of CDKN2A)	Sequencing	+	24	101
Protein level				
ANO-1 expression	WB	+	10	81
PKCe expression	WB, KI study	-	1	82
Allitinib				
DNA level				
AKT expression	KO study	+	8	98
KRAS mutation	Sequencing	-	7	104
Sorafenib				
Protein level				
MET expression	WB	No	32	102

Supplemental table 1C: PI3K-inhibitors pre-clinical

Biomarker	Technique	Correlation with response (+) or resistance (-)	Sample Size	Reference
PI3K-inhibitors				
DNA level				
EGFR amplification, AKT1 amplification, CSMD1 deletion	Sequencing	+	28	105
PIK3CA mutations	Sequencing	+	151; 64; 42; 9	9,77,106,107
Notch1 mutation	Sequencing	+	9	107
PIK3CA mutations	Sequencing	No	28; 9	105,108
PIK3CA amplification, PTEN-loss	Sequencing	No	64	106
EGFR amplification	CNV analysis	No	42	77

Supplemental table 1D: mTOR-inhibitors pre-clinical

Biomarker	Technique	Correlation with response (+) or resistance (-)	Sample Size	Reference
mTOR-inhibitors				
DNA level				
PIK3CA mutations	Sequencing	+	64; 9	106,107
PIK3CA mutations	KI study	+	3	110
Notch1 mutation	Sequencing	+	9	107
PIK3CA amplification, PTEN-loss	Sequencing	No	64	106
TP53 mutations	Sequencing	No	10	111
RNA level				
Akt1, mTOR, RPS6KB1, FKBP1B, TSC1 expression	qPCR	No	29	112
Protein level				
EGFR expression	WB	-	10	111
Activation of the mTOR or MAPK-pathway, P53	WB	No	10	111
Other				
Cisplatin resistance	Viability screen	+	10	111
Cetuximab resistance	Viability screen	-	10	111

Supplemental table 2A: monoclonal antibodies clinical

Biomarker	Technique	Correlation with response (+)or resistance (-)	Sample Size	Additional treatment	Reference
Cetuximab					
DNA level					
KRAS mutation	Sequencing	+	413	Cisplatin + RT	63
RAS mutations	Sequencing	-	46; 3	Cisplatin/carboplatin/5FU; -	37,57
PI3KCA mutations	HRM analysis	-	6	-	37
EGFR-K SNP polymorphism	Sequencing	-	59	Cisplatin/carboplatin + RT	58
EGFR copy number	FISH	No	37;312	Cisplatin + RT; 5FU	32,33
RAS mutations	HRM analysis	No	3	RT	37
PI3KCA mutations	HRM analysis	No	6	RT	37
RNA level					
mi-RNA expression profile	miRNA/RNA sequencing	+	40	Cisplatin/carboplatin	56
Basal subtype	Microarray	+	40	Cisplatin/carboplatin	52
MMP9 expression	qPCR	+	37	Cisplatin, RT	32
EREG, AREG expression	qPCR	+	37	(Cisplatin + 5FU) or Paclitaxel	46
IL-1 ligands (IL1a and IL1β)	RNA sequencing	+	164	Cisplatin, RT	68
LNC RNA transcript fusions (CD274-PDCD1LG2)	RNA sequencing	-	40	Cisplatin/carboplatin	70
EGFR, MET, ERCC1, P16, P-53 expression	qPCR	No	37	Cisplatin, RT	32

Supplemental table 2A: monoclonal antibodies clinical (continued)

Biomarker	Technique	Correlation with response (+) or resistance (-)	Sample Size	Additional treatment	Reference
Protein level					
PTEN expression	IHC	+	61; 112; 37	5FU & Cis/Carboplatin; Sorafenib	36,59,64
VEGF, IL6 expression	Luminex, ELISA	+	31	Cisplatin, docetaxel + RT	67
pAKT expression	IHC	-	50	Cisplatin/carboplatin	69
AREG expression	IHC	-	47	Docetaxel	35
EGFRvIII expression	IHC	-	46	Docetaxel	35
EGFR expression	IHC	No	1075; 33; 61; 18	Cisplatin/carboplatin + 5FU; Docetaxel; 5FU & Cis/Carboplatin; RT	34-37
cMET expression	IHC	No	112	5FU & Cis/Carboplatin	59
p16 expression	IHC	No	112	5FU & Cis/Carboplatin	59
PTEN expression	IHC	No	50; 7	Cisplatin/carboplatin; RT	37,69
Panitumumab					
RNA level					
Gene signature Cluster3	Microarray	+	25		15
RAS onco-signature, tumor microenvironment signature	Microarray	No	25		15
miRNA expression profile	qPCR	+	25		15
Protein level					
P16 negative	IHC	+	657	Cisplatin + 5FU	73

Supplemental table 2B: RTK-inhibitors clinical

Biomarker	Technique	Correlation with response (+) or resistance (-)	Sample Size	Additional treatment	Reference
Gefitinib					
DNA level					
EGFR amplification, EGFR kinase-domain mutations	Sequencing	No	16		80
EGFR mutations	Sequencing	No	31		79
RNA level					
EGFR-AS1 long noncoding RNA	Sequencing, RNAscope	-	6		87
Protein level					
IGF1R expression	IHC	+	52	Cisplatin	83
MMP11 expression	FISH, IHC	+	31	Cisplatin	79
EGFR expression	FISH	No	31		79
Protein signature (GM-CSF + IL-8 + TIMP-1 + VEGF)	Immunoassay	No	25		86
Erlotinib					
DNA level					
EGFRvIII mutation	qPCR	No	53		95
EGFR amplification	FISH	No	45		95
EGFR amplification, EGFR kinase-domain mutations	Sequencing	No	1		80
HPV status	ISH	No	53		95
RNA level					
Gene expression profile	Microarray	No	39		96

Supplemental table 2B: RTK-inhibitors clinical (continued)

Biomarker	Technique	Correlation with response (+) or resistance (-)	Sample Size	Additional treatment	Reference
Protein level					
p16 expression	IHC	No	53		95
C-met expression	IHC	No	49		95
Afatinib					
DNA level					
TP53 wildtype	Sequencing	+	27		97
RNA level					
Gene signature Cluster3	Sequencing	+	23		97
Protein level					
PTEN expression	IHC	+	326		100
EGFR amplification	FISH	+	326		100
P16 expression	IHC	-	326		100
HER3 expression	IHC	-	326		100
PTEN, p16 expression	IHC	No	30		97
Her3, EGFR amplification	IHC	No	29		97
Dacomitinib					
DNA level					
REV3L mutations	Sequencing	+	18		103

Supplemental table 2C: PI3K-inhibitors clinical

Biomarker	Technique	Correlation with response (+) or resistance (-)	Sample Size	Additional treatment	Reference
PI3K-inhibitors					
DNA level					
TP53 mutations	Sequencing	+	158	Paclitaxel	109
PI3K3CA mutations	Sequencing	+	151		9
Protein level					
HPV negative	IHC	+	158	Paclitaxel	109
Other					
TILs, CD8-positive cells	IHC	+	158	Paclitaxel	109

Supplemental table 2D: mTOR inhibitors clinical

Biomarker	Technique	Correlation with response (+) or resistance (-)	Sample size	Ref
mTOR inhibitors				
DNA level				
PIK3CA mutations, HPV status	Sequencing	No	25	114
Other				
Caspase activity	ELISA	-	29	113

Supplemental tables

Biomarkers per EGFR inhibitor type included in this review. Correlation with outcome can be; positive (+) meaning that the biomarker correlates with improved response, Negative (-) meaning that the biomarker correlates with worse response or resistance and 'No', meaning there is no correlation between biomarker and response. Abbreviations: CNV-analysis, copy number analysis; ELISA, enzyme immuno assay; FISH, fluorescence in situ hybridization; FCM, flow cytometry; HRM, high resolution melt; IHC, immunohistochemistry; ISH, in situ hybridization; KI study, knock-In study; KO study, knock-out study; qPCR, quantitative polymerase chain reaction; WB, western blot



CHAPTER 3

Patient-derived head and neck cancer organoids allow treatment stratification and serve as a tool for biomarker validation and identification

Rosemary Millen[^], Willem W.B. De Kort[^], Mandy Koomen, Gijs J.F. van Son, Roán Gobits, Bas Penning de Vries, Harry Begthel, Maurice Zandvliet, Patricia Doornaert, Niels Raaijmakers, Maarten H. Geurts, Sjoerd Elias, Robert J.J. van Es, Remco de Bree, Lot A. Devriese, Stefan M. Willems, Onno Kranenburg, Else Driehuis, Hans Clevers

[^]These authors contributed equally to this work

ABSTRACT

Background

Organoids are in vitro three-dimensional structures that can be grown from patient tissue. Head and neck cancer (HNC) is a collective term used for multiple tumor types including squamous cell carcinomas and salivary gland adenocarcinomas.

Methods

Organoids were established from HNC patient tumor tissue and characterized using immunohistochemistry and DNA sequencing. Organoids were exposed to chemo- and radiotherapy and a panel of targeted agents. Organoid response was correlated with patient clinical response. CRISPR-Cas9-based gene editing of organoids was applied for biomarker validation.

Findings

A HNC biobank consisting of 110 models, including 65 tumor models, was generated. Organoids retained DNA alterations found in HNC. Comparison of organoid and patient response to radiotherapy (primary [n = 6] and adjuvant [n = 15]) indicated potential for guiding treatment options in the adjuvant setting. In organoids, the radio-sensitizing potential of cisplatin and carboplatin could be validated. However, cetuximab conveyed radioprotection in most models. HNC-targeted treatments were tested on 31 models, indicating possible novel treatment options with the potential for treatment stratification in the future. Activating PIK3CA mutations did not predict alpelisib response in organoids. Protein arginine methyltransferase 5 (PRMT5) inhibitors were identified as a potential treatment option for cyclin dependent kinase inhibitor 2A (CDKN2A) null HNC.

Conclusions

Organoids hold potential as a diagnostic tool in personalized medicine for HNC. In vitro organoid response to radiotherapy (RT) showed a trend that mimics clinical response, indicating the predictive potential of patient-derived organoids. Moreover, organoids could be used for biomarker discovery and validation.

INTRODUCTION

Organoids are three-dimensional structures that can be grown from patient-derived stem cells and have been shown to recapitulate *in vivo* pathology and physiology. Organoids can be maintained *in vitro* to serve as miniature disease models. Collections of tumor organoids (so-called “*living biobanks*”) derived from a range of tumor types have been shown to recapitulate the tumors from which they were derived, both genetically and phenotypically¹⁻⁹. Patient-derived organoids hold promise for personalized medicine, as multiple studies have shown correlation between organoid drug response and corresponding patient response^{8,10-13}.

To address whether organoids hold potential to stratify treatment for patients with head and neck cancer (HNC), we measured response of organoids to either radiotherapy (RT) or chemoradiotherapy (CRT) and compared to response of patients diagnosed with primary HNC. HNC is a collective term for tumors arising in the upper aerodigestive tract, including the oral cavity, larynx and pharynx, and tumors of the salivary glands. The most common HNC is head and neck squamous cell carcinomas (HNSCC). HNSCC is commonly associated with heavy smoking and drinking^{14,15}. An increasing subset of HNSCC is associated with human papillomavirus (HPV) infection^{14,15}. Treatment of HNSCC consists of surgery, RT, and/or CRT, where the chemotherapy is given as a radiosensitizer¹⁶. In 2018, RT combined with the anti-EGFR antibody Cetuximab was introduced as an alternative treatment for patients unsuitable for classic, platinum-based chemotherapy based on platinum compounds. Yet, Cetuximab has conversely been shown to act as a radioprotector in HNC *in vitro*, both in cell lines as well as in organoid models^{17,18}, and thus its usage as a chemo sensitizing agent could be questioned. Indeed, more recent clinical studies failed to reproduce the added value of Cetuximab and have even found inferior effects of Cetuximab treatment in the majority of patients¹⁹⁻²¹.

Adequate biomarkers to determine which patients would benefit from a treatment are lacking in HNC even though different therapies are available, and more targeted agents are being evaluated in clinical trials²². Preclinically identified biomarkers often fail once tested in patients. This likely relates to the fact that the pre-clinical *in vitro* models used for testing do not recapitulate the effect of that biomarker in the diverse genetic context of a real-world patient population. Therefore, validation of potential biomarkers in more accurate models that better reflect patient heterogeneity are urgently needed. This is exemplified by the above-mentioned studies on Cetuximab¹⁹⁻²¹. Human cancer-derived organoids may fill this void, potentially combined with efficient gene-editing tools such as CRISPR/Cas9 to validate a genetic biomarker effect on drug response. Gene editing using CRISPR/Cas9 technology has previously been successfully applied in organoid models²³⁻²⁷. Recently, next-generation Cas9 proteins have been developed by disabling the nuclease activity of Cas9 and fusing enzymes to Cas9 which modify individual bases in the DNA helix. These fusion proteins are termed base

editors, and induce single base changes, allowing for highly precise and efficient gene editing with very low off-target rates^{27–30}. To our knowledge, gene editing in HNC organoids has not been reported until now.^{28–31}

In 2019, we published a biobank containing 31 HNSCC-derived organoids, as well as the protocol to generate these organoid lines directly from patients' tumor tissues¹⁷. In this study, we expand this biobank by adding more organoid models including those derived from rarer forms of HNC. We furthermore explore the potential of organoids for biomarker validation and personalized medicine.

METHODS

EXPERIMENTAL MODEL AND SUBJECT DETAILS

Human subjects

Participants information on age and sex (ascribed at birth) was physician reported and is listed in Table 1 and Supplementary Table 1. Information on gender, socioeconomic status, ethnicity and race/ancestry was not collected.

Both primary and lymphonodular metastatic tumor and adjacent non-malignant tissues were obtained from head and neck cancer patients undergoing tissue biopsy or surgical resection at the University Medical Center Utrecht (UMCU) as part of their routine diagnosis and/or treatment. In addition, blood was drawn in sodium heparin on the day of tissue acquisition. Informed consent was obtained from patients before tissue acquisition, and patients could withdraw their consent at any time. The 12-093 HUB-Cancer protocol used for biobanking has been approved by The Biobank Research Ethics Committee of the University Medical Center Utrecht (TCBio).

The collection of patient tissue and data has been performed in accordance with the guidelines of the European Network of Research Ethics Committees (EUREC) following European, national, and local law. Organoids grown from patient tissue can be requested via www.huborganoids.nl. Future distribution of organoids to any third (academic or commercial) party will have to be authorised by the METC UMCU/TCBio at request of the HUB to ensure compliance with the Dutch medical research involving human subjects' act.

Table 1. Clinical parameters of participating patients

Characteristic (no. patients)	Whole Biobank (n=97)	Tumor Organoids (n=66)	Cohort Primary RT (n=6)	Cohort Adjuvant RT (n=15)
Age – yr.				
Median (range)	66 (22 – 90)	66 (22 – 90)	72 (59 – 90)	61 (29 – 76)
Sex – no. (%)				
Male	62 (64)	45 (68)	3 (50)	11 (73)
Female	35 (36)	21 (32)	3 (50)	4 (27)
Organoids – no. (%)				
Tumor	66 (60)	66 (100)	6 (100)	15 (100)
Normal	44 (40)			
Tumor organoids origin – no. (%)				
Biopsy	27 (25)	21 (32)	6 (100)	
Resection specimen	83 (75)	45 (68)		15 (100)
Location tumor organoids – no. (%)				
Oral cavity		32 (48.5)		11 (73)
Oropharynx		7 (10.6)	1 (17)	
Hypopharynx		3 (4.5)		2 (13)
Larynx		15 (22.7)	5 (83)	1 (7)
Nasal cavity		4 (6.1)		1 (7)
Salivary glands		4 (6.1)		
Unknown primary		1 (1.5)		
Type tumor organoids – no. (%)				
Squamous cell carcinoma		61 (92.4)	6 (100)	15 (100)
Adenocarcinoma		1 (1.5)		
Muco epidermoid carcinoma		1 (1.5)		
Adenoid cystic carcinoma		1 (1.5)		
Myoepithelial carcinoma		1 (1.5)		
Large cell carcinoma		1 (1.5)		
HPV status				
Positive (type 16)		4 (6.1)		
Positive (type 33)		1 (1.5)		
Negative		4 (6.1)	1 (17)	2 (13)
Not determined		57 (86.4)	5 (83)	13 (87)

Table 1. Clinical parameters of participating patients (continued)

Characteristic (no. patients)	Whole Biobank (n=97)	Tumor Organoids (n=66)	Cohort Primary RT (n=6)	Cohort Adjuvant RT (n=15)
T-stage – no. (%)				
T0		1 (1.5)		
T1		7 (10.6)		2 (13.3)
T2		26 (39.4)	3 (50)	2 (13.3)
T3		14 (21.2)	3 (50)	3 (20)
T4/T4a/T4b		18 (27.3)		8 (53.3)
N-stage – no. (%)				
N0		37 (56.1)	6 (100)	3 (20)
N+		29 (43.9)		12 (80)
M-stage – no. (%)				
M0		65 (98.5)	6 (100)	
MX		1 (1.5)		
Adjuvant treatment				
Cisplatin				4 (27)
Relapse – no. (%)				
Local			3 (50)	1 (7)
Regional			1 (17)	8 (53)
Distant			1 (17)	4 (27)
No relapse			3 (50)	6 (40)

Human specimens

For surgical resection, a small piece of tumor and adjacent non-malignant tissue were sampled after surgery from the resection specimen at the tissue facility of the pathology department. For biopsies, from patients who needed a biopsy for diagnostics an extra biopsy of suspected malignant tissue was taken for this study during the procedure. For all patients, EDTA blood pellets were stored and used for reference DNA isolation (see whole exome sequencing). In addition, blood was drawn in sodium heparin on the day of tissue acquisition.

Tissue processing for organoid establishment

HNC and normal organoids were generated as previously described^{17,52}. In short, tumor and normal surgical resections and HNC biopsies were collected in Advanced DMEM/F12 (AdDMEM/F12: Life Technologies, cat # 12634–034), supplemented with 1x GlutaMAX (Thermofisher; Gibco, cat # 35050061), Penicillin-streptomycin (Life Technologies, cat # 15140–122) and 10 mM HEPES (Life Technologies, cat # 15630–056) (+/+ medium) and 100 µg/mL Primocin (Invivogen, cat #

ant-pm1). Tissue samples were cut into small pieces (~1-3 mm²). One to three pieces were collected for DNA isolation (stored at -20 for subsequent DNA isolation), histology (placed in formalin) and tumor infiltrating T-cell (TIL) expansion (see below). The remaining tissue pieces were minced into smaller fragments and digested for 20-40 mins by incubating it at 37°C in 0.125% Trypsin (Sigma, cat # T1426) in +/+ medium supplemented with 10 µM Y-27632 (Abmole Bioscience, cat. no. M1817). Every 10 mins, mechanical force was used to aid digestion by triturating the tissue pieces with a p1000 pipette. Following incubation, tissue was triturated using a flame-sterilized pipette with a p10 tip on the end. Once pieces of tissue appeared dissociated, +/+ medium was topped up to 15 mL and this suspension was filtered through a 70 µm filter (Corning, cat # CLS431751-50EA). Tubes were centrifuged at 300g, 5 mins. After centrifugation the supernatant was aspirated and the cell pellet was resuspended in ice-cold 70% 10 mg·mL⁻¹ cold Cultrex growth factor reduced BME type 2 (Trevigen, cat # 3533-010-02) in +/+ medium. Organoids in BME were plated in 10-20 µL droplets on the bottom of a pre-heated 48-well suspension culture plate (Greiner, cat # M9312). Plates were inverted and incubated at 37°C for at least 15-30 mins for the solidification of BME. After solidification, pre-warmed culture medium supplemented with 10 µM Y-27632 and caspofungin (0.5 µg/mL, Sigma Aldrich) was added to the plates and they were incubated in a 37°C/5% CO₂ incubator. Two types of culture media were used for HNSCC organoids: HN medium as described previously² or cervical SCC medium (M7) as previously described³². For one organoid culture (T36) derived from an intestinal-type adenocarcinoma, CRC medium was used³.

Organoid culturing and biobanking

Organoids were grown from the primary material in culture media supplemented with 0.5 µg/ml caspofungin and 10 µM Y-27632 for one week. After organoids had formed and were in culture for at least one week, 0.5 µg/ml caspofungin and 10 µM Y-27632 were removed from the medium. To determine which media was optimal for each organoid line, all primary material was established on HN and M7 medium. The culture was expanded in the media that worked best for that sample. An overview of which culture is grown on which media is provided in supplementary Table 1. Medium was changed every two to three days and organoids were passaged between approximately 7 and 14 days after plating, depending on their growth rate.

For passaging, BME droplets with organoids were disrupted by resuspending the well content using a P1000 pipette and transferred to 15 mL Falcon tube, topped up to 15 mL with +/+ and centrifuged (300g, 5 min). Pellets were resuspended in 1-3 mL TrypLE Express (Life Technologies, Carlsbad, CA, USA, cat. no. 12605-010) and incubated for 3-10 mins at 37 °C. Digestion was closely monitored, by checking the tube under the microscope, and organoids were sheared mechanically using a P1000 pipette with an extra P10 tip placed on the tip, every few mins. After organoids were disrupted into single cells, tubes were topped up using +/+ to stop the TrypLE digestion, and centrifuged. Supernatant was removed and cells were resuspended in 70% BME in +/+. Organoid density was always checked under the microscope before plating, if organoids were too

dense, more 70% BME in +/+ was added. 10-20 μ L domes were plated on pre-heated suspension culture plates (Greiner, cat # M9312). Plates were inverted and incubated at 37°C for at least 15 mins for BME solidification. After solidification, pre-warmed culture medium supplemented with 10 μ M Y-27632 was added to the plates and they were incubated in a 37°C/5% CO₂ incubator. After 2 to 3 days, Y-27632 was removed from the medium and organoids were cultured in media without Y-27632 for organoids grown on HN medium, however Y-27632 was constantly in M7 media. Organoids were passaged up to passage 5, to ensure each organoid culture was capable of robust expansion. During the expansion process and prior to biobanking, a sample of the organoid culture was grown in the presence of 10 μ M Nutlin-3a. Nutlin-3a was added directly after passage and kept on the cells for two passages to determine TP53 mutational status.

Biobanking and freezing of organoids

Organoids were biobanked at various passage numbers, with an attempt to freeze multiple vials per passage. As a rule of thumb, at least 1 vial with organoids was frozen at the earliest passage where possible. For each sample at least 5 vials were frozen for biobanking. For freezing, organoids were collected from the culture plates by disrupting the BME droplets using a P1000 pipette, washing with +/+ and centrifuging at 300 g, 5 min at 4°C. Subsequently, supernatant was removed and the pellet was resuspended in Cell Banker 1 (Amsbio, cat # 11910). 1 mL Cell Banker was used per 1 well of a 12 well plate, with 100 μ L BME containing organoids. Organoids were then transferred to cryovials and stored at -80°C for 24 hours, before being transferred to liquid nitrogen for long term storage.

Thawing organoids

Organoids were removed from liquid nitrogen and placed on dry-ice. Cryovials were placed in the 37°C water bath and thawed until a small ice block remained. Organoids were transferred to 10-mL of pre-warmed +/+ medium, using a p1000 pipette in a drop-wise fashion. Tubes were centrifuged at 300 g, 5 min at 4°C. Supernatant was gently aspirated and pellet was resuspended in 70% BME in +/+. Organoid density was checked under a bright-field microscope. If density was high, more 70% BME in +/+ was added. Organoids were plated in wells of pre-warmed 48-WP, after 20-30 mins of incubation at 37°C, pre-warmed growth medium was added to wells. After 24 hours, organoid viability was checked under a bright-field microscope. If a lot of organoid death had occurred, organoids were harvested, washed (as described above) and replated in fresh BME. Organoids were expanded by passaging at least two times prior to a drug screen.

DNA isolation

DNA from tissue, organoids and whole blood was isolated using the Reliaprep gDNA Tissue Miniprep System (Promega, Catalogue # A2052) according to the manufacturer's protocol. For organoid DNA, BME droplets with organoids were disrupted by resuspending the well content using a P1000 pipette and transferred to a 15 mL Falcon tube, topped up to 15 mL with +/+ and

centrifuged (300g, 5 min). Supernatant was aspirated and the organoid pellet was frozen and stored at -20°C for subsequent DNA isolation using the Reliaprep gDNA Tissue Miniprep System (Promega, Catalogue # A2052) according to the manufacturer's protocol. DNA concentrations were measured using Invitrogen™ Qubit™ dsDNA HS Assay Kit (Invitrogen, Cat # 10616763).

SNP Fingerprinting

DNA (5ng/ μL) isolated from organoids was submitted to USeq (Utrecht Sequencing Facility) along with paired blood and/or tumor tissue from each patient for SNP fingerprinting. There, TaqMan OpenArray Barcode Panel 60, including 57 autosomal and 3 Y-chromosomal SNPs was used to identify SNPs. SNPs were checked manually by 2 independent researchers to confirm a SNP match between organoid and blood/tissue of the same patient.

Whole Exome Sequencing (WES) processing

After confirmation of a SNP match between the organoid and blood/tissue of the same patient, organoid, blood and tissue DNA samples were submitted to MacroGen Europe for WES using the Illumina platform. The SureSelectXT Target Enrichment System for the Illumina Platform v7 library preparation kit (Agilent Technologies) was used to prepare the sequencing library following the manufacturer's instructions. Libraries were sequenced on an Illumina NovaSeq 6000 system. Illumina software (bcl2fastq) was used to convert to FASTQ format for further analysis.

Whole Exome Sequencing (WES) analysis

For the WES analysis, the NF-IAP pipeline (<https://github.com/ToolsVanBox/NF-IAP>) was modified to suit exome data rather than whole genome data. Fastq files were mapped to the human genome (hg38) using bwa mapping software as described in the pipeline. Next, the pre-processing and genotyping of the samples was performed using the Genome Analysis Toolkit (GATK) HaplotypeCaller, with an adapted version of the pipeline (https://github.com/Hubrecht-Clevers/NF-IAP_exome). Per sample generated variant calls were filtered using the Somatic Mutation Rechecker and Filtering (SMuRF) pipeline (<https://github.com/ToolsVanBox/SMuRF>) to filter out likely non-pathogenic mutations and germline variants using default settings and marking the blood derived samples as germline controls. Obtained variant call files were converted to the MAF-format for further analysis using a perl script, converting only mutations with a mean variant allele frequency of above 0.1 and allele depth of >10 (https://github.com/Hubrecht-Clevers/Convert_maf). Variants were further characterised using the R package Maftools. Genome wide copy number changes were assessed using an adapted version of the Freec software described in the NF-IAP pipeline (https://github.com/Hubrecht-Clevers/Freec_exome). Copy number ratios were normalised to either a matched normal control, or, when no matched germline was available, to a technical control of a known germline sample. Data is stored at EGA under study ID: EGAS00001007076.

Blood Processing

Blood was collected in two 8 mL Lithium-Heparin tubes on the day of surgery/biopsy.

Circulating tumor DNA (CtDNA) was isolated within 2 hours of whole blood collection. Lithium-Heparin tubes were centrifuged at 1600xg, 10 mins, room temperature (RT) with the brake off. Plasma was taken off with a p1000 pipette and 1 mL was transferred to Eppendorf tubes. Eppendorf tubes were then centrifuged at 13, 830x g for 10 mins, RT. Plasma supernatant was collected and stored in 1 mL aliquots at -80°C.

Peripheral mononuclear blood cells (PBMCs) were processed at the same time as ctDNA plasma isolation using Lymphoprep™ (Stemcell Technologies, catalogue no. 07851) according to the manufacturer's protocol (Stemcell Technologies). PBMCs were stored using Cell Banker 1, as described above.

Histology and IHC of organoid and tissue sections

A small piece of tumor-tissue or tumor-adjacent normal tissue was fixed using 4% formalin and incubated at least 24 h on a rocker at room temperature. Subsequently, the material was dehydrated and embedded in paraffin. Organoids were collected after several passages, fixed and embedded in paraffin following the same procedure. Paraffin blocks were cut onto glass slides and subject to H&E and IHC staining, the details of primary antibodies and antigen retrieval conditions used for IHC staining are provided in Supplementary Table 2. IHC for AE1/AE3, CK13, P63, P16NK4a and CDX2 was performed by the diagnostic pathology department at the UMCU using an automated IHC staining system, all according to the manufacturer's protocol. IHC for PAS-D, α -amylase and AQP5 was performed manually. Slides were scanned and imaged using the VS120 virtual slide microscope (Olympus). For a subset of tissues, H&E sections were assessed by a pathologist to determine tumor percentage and/or epithelial cell percentage. The presence of tumor/epithelial cells was correlated with organoid outgrowth.

Organoid treatment to induce DNA damage experiments

The organoid line that was established from a patient with Fanconi anemia (T46) was cultured as described above and 5 days later exposed to either: cisplatin (5 μ M), Mitomycin-C (0.5 μ M) or left untreated for 24 hours. Organoids were harvested with the media in each well, using a pipette to break up the BME droplets and transferred to a 1.5-mL Eppendorf tube pre-coated with FBS. Organoids were left to settle by gravity, and supernatant was removed gently, after which where whole-mount immunofluorescence staining was performed as described below.

γ H2Ax Immunofluorescence staining and quantification.

Organoids were pre-permeabilized in 0.5% Triton-X in PBS for 10 mins at room temperature in a 1.5 mL Eppendorf tube. For all washes, organoids were left to sediment in the Eppendorf tube

by gravity before removing any supernatant. Organoids were fixed with 4% formalin for 1 hour at room temperature and permeabilized in PBS with 2% BSA, 0.5% Triton-X and 0.2% Tween-20 for 1 hour. Organoids were blocked in PBS with 2% BSA, 0.2% Triton-X and 0.2% Tween-20 for 30 mins at room temperature. Organoids were incubated with primary anti-mouse yH2AX antibody (Milipore, catalogue no. 05-635) diluted in a blocking buffer overnight at 4°C on a roller. Organoids were washed 4 times with PBS and a secondary goat anti-mouse AF-488 (Thermofisher, catalogue no. A28175) was added plus DAPI solution 1 mg/mL (Thermofisher, catalogue no. 62248) and incubated in the dark for 2-3 hours, at room temperature on a roller. Organoids were washed 4 times and then a mounting medium was added and this was transferred to a glass slide. A raised-coverslip was whole-mounted, using Vaseline to ensure the coverslip did not make full contact with the glass slide. Slides were imaged on the confocal SP8 (Leica) microscope using the DAPI and 488-channel at 20x and 63x objective. Quantification of the collected images was performed using ImageJ. Images were converted in a RGB stack, threshold was adjusted to 75-225. Images were converted to a mask with watershed. To perform analysis, we used the analyze particles option and counted objects.

HPV ddPCR

PCR mixture was generated containing 1x ddPCR Supermix for Probes without dUTP (Bio-Rad, cat. no #1863023) containing 18 pM of previously described HPV primers56 and 0.25 µM HPV16 FAM-probe, 1 µl human ESR1 primer (Bio-rad , assay ID dHsaCP1000403) in a total of 18 µL. 4 µl of DNA was added (DNA input concentration ranging from 20 to 100 ng/µl). PCR mixture was mixed and droplets were subsequently generated using the µl DX200 Droplet generator (Biorad, cat. No. #186-4002). PCR program used was 10 min at 95 °C followed by 40 cycles of 30 seconds at 94 °C and one minute at 57 °C. After 40 cycli, the sample was incubated for 10 mins at 98 °C, and stored at 4 °C until readout. Readout was performed using the QX200 Droplet Reader. Analysis was performed using Bio-rads QuantaSoft Software.

Drug screening: Preparation and plating

Organoids that were biobanked were thawed and expanded using the methods described above for organoid culture. Two days (D-2) prior to dispensing organoids for drug screening, organoids were passaged and cultured in HNC medium or cervical SCC medium depending on the line and were supplemented with 10 µM Y-27632. Organoids growing on HNC medium that were expanded for Cetuximab drug screening were cultured from this point onwards in medium without EGF. On the day 0 (D0) of the drug screen, 1 mg/mL dispase II (Sigma-Aldrich, catalogue no. D4693) was added to each well containing organoids and their growth medium and incubated for 30 mins at 37°C. Following incubation, BME domes were disrupted by resuspending the contents of the wells. Material was collected and transferred to 15 mL Falcon tubes. Dispace was diluted by topping up with +/-/- and centrifuged at 300g, 5 mins, 4°C. After removal of the supernatant, pellets were suspended in 10 mL +/-/- and centrifuged at 300g, 5 mins, 4°C.

Organoid suspensions were subsequently filtered through 70 μm nylon cell strainers (BD Falcon). The number of organoids in the flow through was counted using a KOVA™ Glasstic™ Slide 10 with Grids (Fisher-Scientific, catalogue no. 22-270141). Organoids were resuspended at a density of 25,000 organoids/mL in 5% BME/ ice-cold growth medium. Organoids were dispensed in 384-well plates (Corning, catalogue no. 4588) using the Multi-drop Combi Reagent Dispenser (Thermo Scientific, catalogue no. 5840300). Drugs were added using a Tecan D300e Digital Dispenser (see below). Plates were sealed with BreathEasy stickers (Merck, catalogue no. Z380059) and placed in a 37°C/5% CO₂ incubator that was kept shut until drug screen readout on day 5 (D5).

On Day 0, a CellTiter-Glo 3D (CTG) assay was performed, as described below, for each condition dispensed to determine organoid viability and calculate the Growth Rate metrics over the course of the drug screen^{3,12}.

Drug screening: Chemotherapy dispense

On D0, following organoid dispense into 384 well plate, chemotherapy was dispensed using the Tecan 300e digital dispenser. The chemotherapy agents used were: cisplatin 1 mg/mL (Accord healthcare limited), carboplatin 10 mg/mL (Accord healthcare limited) and Cetuximab (Erbix) 5 mg/mL (Merck). As these solutions were aqueous, for accurate dispensing with the Tecan 300e digital dispenser, these solutions required the addition of 0.3% Tween-20 (Merck, catalogue no. P1379) in PBS (Thermofisher, catalogue no. 10010023) prior to dispensing. Four technical replicates of cisplatin at 3 μM and 5 μM , carboplatin at 5 μM and 15 μM and 5 technical replicates of Cetuximab at 5 $\mu\text{g/mL}$ and 30 $\mu\text{g/mL}$ were dispensed. The rationale behind these dosages was to treat with a dose that has an effect, but does not kill all the cells, thereby allowing sufficient test window to study the effect of radiotherapy. Using these criteria, we reviewed drug sensitivity of our previously published panel of organoids treated with these drugs to define the above mentioned concentrations. Staurosporine 1 mM (Merck, catalogue no. 19-123MG) was dispensed at 0.1 μM , as a positive control for cell death. All other wells received 0.3% Tween-20 in sterile PBS (solvent-only) as RT-only and negative controls.

For targeted therapy screening, the following drugs were added following organoid dispense:

Nutlin-3a (Cayman Chemical, catalogue no. 10004372), Everolimus (LC Laboratories, catalogue no. E4040), Niraparib (Selleckchem, catalogue no. S2741), Alpelisib (LC Laboratories, catalogue no. A4477), AZD4547 (ApeXbio, catalogue no. A8250), EZP01556 (Sigma, catalogue no. SML1421) and Tipifarnib (Sigma, cat no. SML1668). All drugs were dissolved in DMSO and dispensed from stock concentrations of 10 mM and dispensed in a log-concentration gradient using the Tecan d300e dispenser. All wells were normalized for solvent used. DMSO percentage never exceeded 1%. Drug exposure was performed in triplicate for each concentration shown.

Radiotherapy screening

On D1 of the screen, RT plates were irradiated using a linear accelerator (Elekta Precise Linear Accelerator 11F49, Elekta). During irradiation, plates were submerged in water at room temperature with the water level reaching just below the surface of the plate. For each dose, a separate plate was used. Plates were irradiated with a single dose of 1, 2, 4, 6, 8 and 10 Gy, in order to generate a dose-response curve. Dose values were determined according to standard clinical dosimetry procedures. An unirradiated plate (0 Gy) was used as a negative control. To calculate percentage viability, in Microsoft Excel, the CTG signal was normalized against the unirradiated plate as a percentage.

Drug and radiotherapy screen read-out and data analysis

For all organoid screens, organoid viability was assessed using the CellTiter-glo 3D assay® measuring ATP as the signal of organoid viability.

After 5 days of initial drug exposure or 4 days of irradiation exposure, organoid viability was measured using the CellTiter-Glo 3-D assay (Promega, catalogue no. G9681) according to the manufacturer's protocol. For this, 20 µl of CTG was added to each well. Luminescence was measured using a Spark microplate reader (Tecan) with an integration time of 500 ms. Data was normalized using a positive control for cell death (Staurosporine 1 µM, with organoids in 5% BME in culture medium for 0% viability) and a negative control (solvent without drugs, with organoids in 5% BME in culture medium) for 100% viability. Quality of drug screens were assessed using Z' factor scores⁵⁷, in which Z' scores higher than 0.3 indicate a drug screen of good quality. To calculate Z' score:

$$Z' \text{ score} = 1 - \frac{3 * SD(neg. \text{ control}) + 3 * SD(pos. \text{ control})}{average(neg. \text{ control}) - average(pos. \text{ control})}$$

As a further measure of quality control, intensity and variation of luminescence signal between wells treated with RT was evaluated by 2 independent researchers. If Z' score was <0.3, there was a lot of variation between wells and a low luminescence signal was observed; the experiment required an additional repeat. The GR metric was used to calculate GR50 scores. Analysis was calculated in Microsoft Excel and graphs were generated in GraphPad Prism software (version 9.3.1). T tests were performed using GraphPad prism.

Clinical correlation

Organoids of patients that received RT and/or chemotherapy were suitable for clinical correlation. Relapse data was assessed for each patient treated with RT and CRT. Patients that were only treated with surgery were not suitable for clinical correlation. The following parameters from the patients were collected: Age, gender, cancer type, tumor location, tumor sublocation, TNM-stage,

HPV-status, treatment including dates and dosages, surgery dates and relapse data with dates. Clinical outcome was defined as relapse: yes or no. The date of relapse was defined at the first sign of clinical relapse confirmed radiologically or pathologically. When there were no clinical signs of relapse, the radiological or pathological confirmation date was taken as the relapse date. February 17th 2023 was the last day relapse status was recorded for all cases.

Kaplan Meier analysis

The parameters generated from the organoid RT screens included: AUC, IC50, GR50 and the viability of the organoids after 2 Gy of RT and were correlated with clinical outcome. Viability after 2 Gy was used as an organoid parameter to compare with clinical response, as 2 Gy is the fraction dose of RT used to treat HNC patients. For every RT-parameter, the group was divided by the median (\leq median vs. $>$ median). These two groups were compared in the context of relapse status (Kaplan meier curves Figure 3). Differences between groups were calculated with a Log-rank (mantel-cox) test, if $p \leq 0.05$ the differences were deemed statistically significant. Follow-up stopped at February 2023. In the analysis the minimum follow-up time of a patient who did not relapse was 502 days.

Cox regression

For the parameters AUC, IC50, GR50 and viability of organoids at 2 Gy a cox proportional-hazards regression with Firth's penalised (partial) likelihood maximisation was executed. Outcomes were Hazard Ratios on relapse.

Calculation of synergistic and additive effect of radio- and chemotherapy

All tested organoid cultures were exposed to a radiation dose of 1, 2, 4, 6, 8 and 10 Gy as described above. This was done in presence of 3 and 5 μ M cisplatin, 5 and 15 μ M carboplatin and 5 and 30 μ g/mL Cetuximab, or in the absence of any chemotherapy. Assay was performed in technical quadruplicate for cisplatin and carboplatin and quintuplicate for Cetuximab conditions. These concentrations were chosen based on sensitivities observed during optimisation of the assay in a panel of patient-derived organoids. For each donor, one dosage of chemotherapy was chosen, following the following criteria:

1. Viability without RT exposure should be $>70\%$ (to assure the effect of RT in the presence of the drug can be observed).
2. If both doses of chemotherapy showed $>70\%$ viability in the no RT condition, the concentration was chosen that was closest to 70% viability.
3. If both doses of chemotherapy showed $<70\%$ viability in the no RT condition, the lowest concentration was included if viability was $>55\%$ in the no RT condition. If the lowest concentration showed $<55\%$ viability, the culture was excluded for the analysis described in Figure 4.

Readout and viability calculations were further performed as above. Only drug screens with Z' scores >0.3 were included in further analysis. To assess additive effects of chemotherapy and RT, viability was normalised to untreated controls. To assess the synergistic effect of chemotherapy and RT, viability was normalised to the chemotherapy only conditions. This way, the viability represented the effect of RT, in the presence of, but corrected for, the effect of the chemotherapy. This allowed for a systematic assessment of whether the chemotherapy had a radioprotective effect. AUC of each condition was calculated using GraphPad prism v9. Paired t-tests were performed using GraphPad prism v9 to assess whether the effect of RT was significantly different when given in the presence of chemotherapeutics.

sgRNA cloning and design

The sgRNA to introduce the E545K mutation in PIK3CA was designed using Benchling and subsequently ordered as lyophilised oligos (Integrated DNA Technologies, IDT). The E545K sgRNA was cloned into an AmpR-U6-gRNA expression vector (a kind gift from Keith Joung, Addgene, #47511) using a PCR based protocol described by Hu et al⁶⁰. In short, the sgRNA expression vector was constructed by one-piece blunt-end ligation (T4 ligase) of a PCR product (Q5, NEB) containing the 20-nucleotide sequence corresponding to the sgRNA designed for PIK3CA E545K induction. Plasmids for sgRNA expression were constructed using one-piece blunt-end ligation of a PCR product containing a variable 20-nucleotide sequence corresponding to the desired sgRNA targeted site.

Electroporation of organoids for DNA delivery

Organoids were disrupted into single cells using TrypLE. Subsequently, cells were resuspended in 90 µL of Opti-MEM medium (Gibco, cat. # 31985062). 10 µg of the PiggyBac transposon system (2.8 µg transposase + 7.2 µg hygromycin resistance containing transposon), 7.5 µg of a plasmid containing the C>T base editor (pCMV_AncBE4max_P2A_GFP (A kind gift from David Liu, Addgene, #11210035) and 2.5 µg of the target sgRNA plasmid was added in a total of 10 µL Opti-MEM. Cells and DNA were incubated at RT for 10 min and subsequently electroporated in a electroporation cuvette (BTX, cat. # 45-0125) on the NEPA21 with settings described by Fujii et al²⁷. After electroporation, 400 µL of Opti-MEM was added and cells were left to recover in the cuvette for 30 mins at RT. Subsequently material was collected and centrifuged. Cell pellet was plated as normal, in ~20 µL drops of 70% BME. After solidification of the BME, a pre-warmed culture medium containing 10 µM RKI Y-27632 was added after 30 mins. The plate was placed in an incubator at 37°C and 5% CO₂ and medium was refreshed every 2-3 days.

Selection of edited organoids

At least five days after electroporation, and when organoids had reached an average diameter of >80 µm, 0.1 mg/µL Hygromycin B-gold solution (InvivoGen, cat. no. ant-hg-1) was added to the culture medium. A control well (electroporated with sgRNA but no Cas9) was taken

along and selection was continued until all organoids of the control condition had died. On average, this took 10-14 days. The hygromycin-resistant organoids were manually picked from the domes using a brightfield microscope and p20 pipette, and transferred to separate 1.5 mL Eppendorf tubes (Eppendorf, cat. no. 0030120086). Addition of 100 μ L TrypLE allowed passaging of the individual organoids that were sheared, pelleted and resuspended in 50 μ L 70% BME in +/+/. Of the 50 μ L cell suspension, 40 μ L was plated for expansion. the remaining 10 μ L was stored at -20°C for gDNA isolation (see below). Clones were subsequently expanded using routine passaging conditions until biomass was expanded sufficiently for genotyping, drug screening and biobanking.

Genotyping of individually picked clones

DNA was collected from the remaining biomass in the tubes used for the first passage of organoids (see above). Tubes were thawed, and DNA was isolated using a Quick-DNA microprep kit (Zymo Research, cat. no. D3021), by adding the lysis buffer directly to the cell pellet. The target regions were amplified with PCR using a GoTaq G2 Flexi DNA polymerase kit (Promega, cat. no. M7805) using 5'-ATCATCTGTGAATCCAGAGGGG-3' (FW) and 5'-AGTGTCTGTGTGGGAGAAACAA-3' (RV). Upon completion of the PCR, the amplified target region was isolated using a PureLink PCR Purification Kit (Invitrogen, cat. no. K3100-02) and sent for EZ-Seq Sanger sequencing (Macrogen) with sequencing primer 5'-CCGTATCACCAACAGCAGGGTA-3'. Sanger sequencing analysis was performed using B Benchling alignment software.

QUANTIFICATION AND STATISTICAL ANALYSIS

Kaplan Meier analysis

The parameters generated from the organoid RT screens included: AUC, IC50, GR50 and the viability of the organoids after 2 Gy of RT and were correlated with clinical outcome. Viability after 2 Gy was used as an organoid parameter to compare with clinical response, as 2 Gy is the fraction dose of RT used to treat HNC patients. For every RT-parameter, the group was divided by the median (\leq median vs. $>$ median). These two groups were compared in the context of relapse status (Kaplan meier curves Figure 3). Differences between groups were calculated with a Log-rank (mantel-cox) test, if $p \leq 0.05$ the differences were deemed statistically significant. Analysis were executed in IBM SPSS version 26.0. Follow-up stopped at February 2023. In the analysis the minimum follow-up time of a patient who did not relapse was 502 days.

Cox regression

For the parameters AUC, IC50, GR50 and viability of organoids at 2 Gy a cox proportional-hazards regression with Firth's penalised (partial) likelihood maximisation was executed. Outcomes were Hazard Ratios on relapse. Analysis were executed in R version 4.2.2

Drug and radiotherapy screen read-out and data analysis

Quality of drug screens were assessed using Z' factor scores⁵⁷, in which Z' scores higher than 0.3 indicate a drug screen of good quality. To calculate Z' score:

$$Z' \text{ score} = 1 - \frac{3 * SD(neg. \text{ control}) + 3 * SD(pos. \text{ control})}{average(neg. \text{ control}) - average(pos. \text{ control})}$$

As a further measure of quality control, intensity and variation of luminescence signal between wells treated with RT was evaluated by 2 independent researchers. If Z' score was <0.3, there was a lot of variation between wells and a low luminescence signal was observed; the experiment required an additional repeat. The GR metric was used to calculate GR50 scores. Analysis was calculated in Microsoft Excel and graphs were generated in GraphPad Prism software (version 9.3.1). T tests were performed using GraphPad prism.

Calculation of synergistic and additive effect of radio- and chemotherapy

To systematically assess whether the chemotherapy has a radioprotective effect. AUC was calculated using GraphPad prism v9. Paired t-tests were performed using GraphPad prism v9 to assess whether the effect of RT was significantly different when given in the presence of chemotherapeutics.

RESULTS**Organoid biobank composition**

From 2019 to 2022, 354 tissue samples were collected from 228 patients during routine surgical resection or biopsy procedures. Tissues were subsequently processed for organoid generation. This consisted of 194 tumor samples, 138 normal (tumor-adjacent) samples and 22 metastatic tumor samples. Organoid establishment rates for these different tissue samples were 28.4%, 32.6% and 4.5%, respectively (Figure S1A). A subset of tumor tissue samples received in the lab were evaluated by a pathologist using Haematoxylin & Eosin (H&E) staining to determine if epithelial (tumor) cells were present in the same tissue that was used to generate organoids. If epithelial cells were present, the success rate of organoid establishment increased from 33.3% to 85.5% (n=77, Fishers exact test, proportion 0.522, p<0.001).

The resulting biobank consist of 100 newly generated organoids, including 10 tumor organoids that were previously established (n=110)¹⁷. These models are derived from 97 HNC patients of various anatomical locations and histological cancer subtypes (Figure 1A, Tables 1 and S1).

Organoid establishment and cryopreservation

After sufficient expansion, organoid models were cryopreserved 2-3 days after passaging. 70.9% of the organoid biobank could be successfully recovered and expanded from cryopreservation (Table S1). Single Nucleotide Polymorphisms sequencing was used to exclude sample swaps where reference material was available (Table S1). Primary cultures were expanded on both previously published HN medium¹⁷ and on more recently published cervical SCC organoid medium (M7)³². Of the cultures started on both media types (n=43), 60.5% and 11.6% showed better growth on M7 or HN medium, respectively (Figure 1B). For 27.9% the media choice showed no difference. Cultures established on M7 medium typically had an increase in organoid number and size and resulted in faster biobanking (Figure S1B), but did not show an apparent different morphology (Figure S1C).

Established organoid models retain histopathological and molecular features of primary HNC.

To assess if histopathological features of HNC were retained in the established organoid models, immunohistochemical staining for HNC markers was performed. Organoid T41, derived from a HPV+ tumor tissue, recapitulated the original tissue's expression of pan-cytokeratin AE1/AE3 (epithelial cell marker), cytokeratin 13 (CK13, differentiated squamous cell marker), p63 (basal cell marker) and p16 (surrogate marker for HPV infection) (Figure 1C). Molecular HPV testing using HPV-specific digital droplet PCR confirmed HPV positivity (Figure 1D). In total, 8/9 (88.9%) organoid models established from HPV+ tissue, could be biobanked.

As HNC is characterised by a high frequency of TP53 mutations³³, TP53 status of organoids was assessed by *in vitro* treatment with Nutlin-3a. Nutlin-3a is a MDM2 antagonist which ceases growth of TP53 wildtype cells but leaves TP53 mutant cells unaffected³⁴. 63% of tested organoid cultures were insensitive to 10 μ M Nutlin-3a (Figure S2), a percentage in line with reported TP53 mutation frequencies in HNC³³.

Organoid models of rare HNCs

In addition to organoids derived from HNSCC, organoids models were successfully established from less common HNCs. These included salivary gland tumors, intestinal-type adenocarcinoma (ITAC) and Fanconi Anemia-induced HNSCC, described in more detail below.

Four salivary gland tumor organoid models (derived from mucoepidermoid carcinoma, large cell carcinoma, adenoid cystic carcinoma and myoepithelial carcinoma, respectively) and five non-cancer salivary gland models (from tumor-adjacent normal gland tissue) were established and biobanked (Table S1). Immunohistochemical staining for salivary gland markers on N19 and T73 confirms that salivary gland-derived organoids retain salivary gland tissue characteristics including production of mucin (PAS-D), α -amylase (a key component

of saliva) and expression of aquaporin-5 (AQP5), which are not present in HNSCC-derived organoid model T1 (Figure 1E).

Organoid T36 was established from a sinonasal ITAC, a tumor that histologically resembles intestinal adenocarcinoma³⁵. T36 showed a mixed phenotype, with cystic structures similar to intestinal organoids and dense structures resembling squamous epithelium-derived organoids. (Figure S3). Cystic structures express intestinal epithelial marker CDX2 whereas the dense organoids do not (Figure 1F). Therefore, we conclude culture T36 is a mixture of both ITAC cells and nasal cavity squamous epithelium.

Lastly, organoid T46 was derived from a HNC of a Fanconi Anemia patient³⁶. Fanconi Anemia is caused by genetic defects resulting in Fanconi Anemia pathway inactivation, a pathway important for the repair of DNA double stranded breaks³⁶. When organoids were exposed to mitomycin-C (MMC), a compound that induces double stranded DNA breaks, indeed T46 showed increased sensitivity to MMC compared to non-Fanconi Anemia organoid T13 (Figure 1G and H).

Taken together, organoids can successfully be derived from a range of HNC tumor types. Resulting organoid models retain key characteristics of these distinct tumor types.

Genetic landscape of HNC organoids

Organoids were subjected to DNA sequencing to confirm whether the generated organoids were indeed derived from tumor cells, and not from tumor-adjacent non-cancerous epithelium, which is a previously described concern^{37,38}. Thirty-five organoid cultures were sequenced, either using targeted next generation sequencing (NGS, n=5) or whole exome sequencing (WES, n=30). Only organoids carrying mutations in known tumor suppressors or oncogenes (see Figure 2A, 27 of 35 sequenced models) were considered tumor organoids and were taken along in downstream genetic and drug-screening analyses.

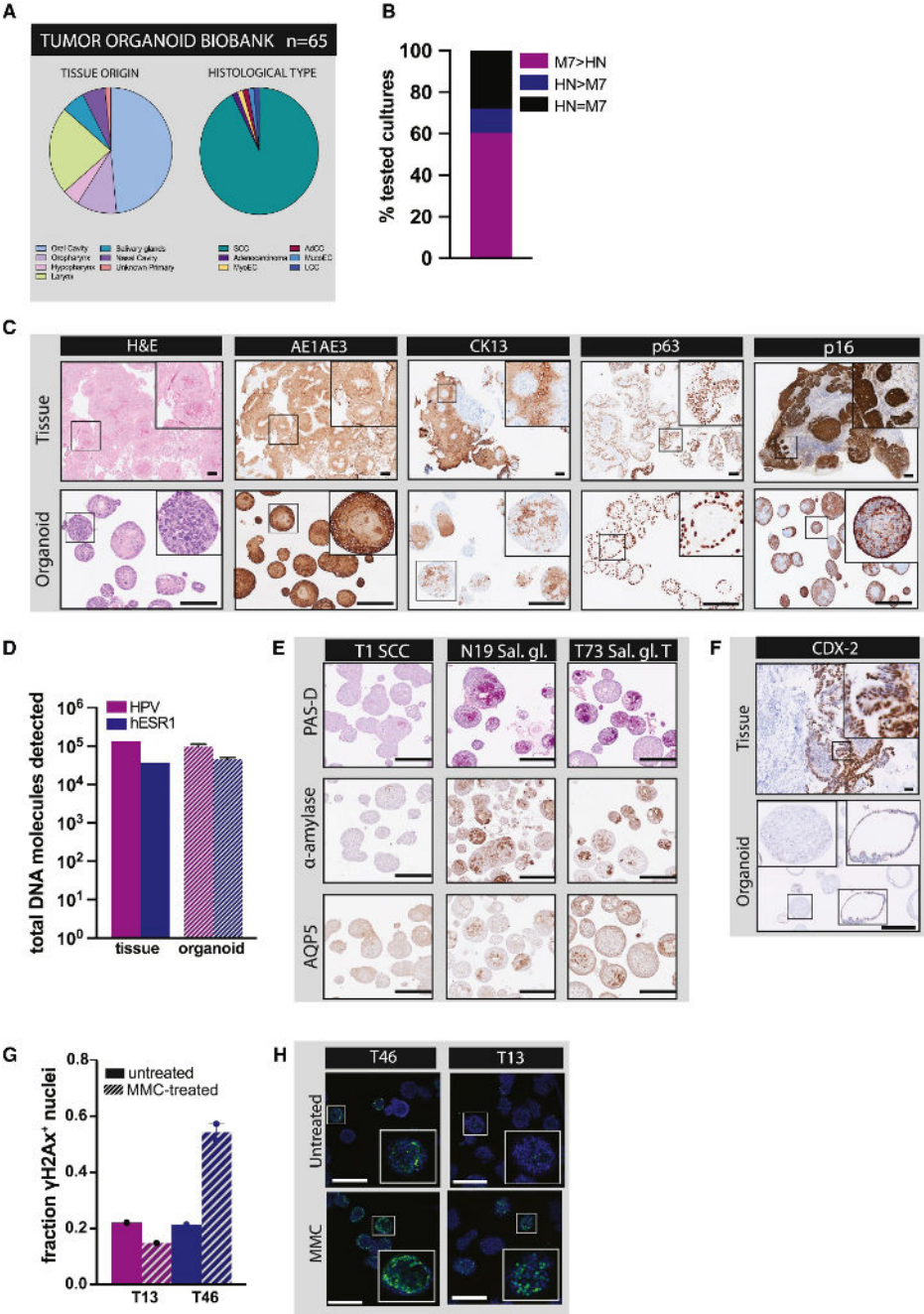


Figure 1. Generation and characterization of a large and diverse organoid biobank derived from patient head and neck tumors and tumor-adjacent non-malignant epithelium

A. Composition of the generated HNC organoid biobank. Left pie chart depicts the anatomical location of primary tissue from which tumor organoids were established. Second pie chart indicates the histological

type of the tumor organoids established (n=65) including squamous cell carcinoma (SCC) (n=60), adenocarcinoma (AC) (n=1) and other types. Part chart displays other histological types: large cell carcinoma (LCC), Mucoepidermoid (MucoEC), Adenoid Cystic Carcinoma (AdCC) and Myoepithelial Carcinoma (MyoEC), n=1 for each.

B. Bar-graph displays percentage of organoid models established on both media tested (n=43) which grow superior growth in either M7 medium (purple, M7>HN) or HN medium (blue, HN>M7) or show comparable growth in both media (black, HN=M7).

C. Histological and immunohistochemical evaluation of: Hematoxylin & Eosin (H&E), carcinoma cell marker AE1/AE3, squamous cell carcinoma marker cytokeratin 13 (CK13), basal cell marker tumor protein 63 (p63) and HPV detection protein 16 (p16) in tumor tissue and matching tumor organoid T41. Scale bar =50 μ m (top) and 200 μ m (bottom).

D. Total HPV type 16 (HPV16, purple) and human ESR1 (hESR1, dark blue) DNA molecules detected in the tissue (solid-bars) and organoid (striped-bars) by digital droplet PCR (ddPCR) in tumor organoid T41.

E. Immunohistochemical evaluation of periodic-acid schiff (PAS) with dispase (PAS-D) (magenta), α -amylase (dark brown) and aquaporin-5 (AQP5) (dark brown) in organoids established from 2 patients with salivary-gland cancer (N19 and T73) and squamous cell-derived tumor organoid (T1) as negative control. Scale bar = 200 μ m.

F. Immunohistochemical evaluation of CDX2 in T36, established from a patient with a rare intestinal-type adenocarcinoma (ITAC) derived from the nasal cavity. Scale bar =200 μ m.

G. Fraction of γ -H2AX-positive nuclei per organoid in untreated (solid bars) versus mitomycin-C treated (striped-bars) in T13 and T46 organoids.

H. Immunofluorescent staining of anti γ -H2AX positive nuclei (green) counterstained with DAPI (blue) in FA-derived T46 and non- FA T13. Scale bar =100 μ m.

Detected DNA alterations included a high frequency of mutation in known cancer-associated genes TP53, NOTCH1, PIK3CA, FAT1 and APOB (Figure 2A). These mutations are indeed described in HNC³³. Also detected copy number variations (CNVs) are comparable to those described by independent studies of primary HNSCC samples^{39,40}. CNV profiles of the organoids are characterised by loss of chromosome 3p, 8p and 17q and a gain of chromosome 3q, 8q and 20 (Figure 2B). Gains of oncogenes including PIK3CA, FGF3 and FGF4 and loss of tumor suppressor CDKN2A in the HNC organoid biobank are detected (Figure 2C)^{39,40}. Single nucleotide variants (SNVs) and CNVs present in patient-derived organoids were comparable to those observed in the tumor tissue from which they were derived (Figure 2D, 2E and Figure S4). An enrichment of CNVs in organoids can be observed when compared to tissue DNA (Figure 2E), which is expected as cancer organoids consist entirely of tumor cells, whereas the primary tissue still contains tumor microenvironment cells including stromal and immune cells. Taken together, the genetic landscape of the HNC tumor organoids reflects DNA alterations observed in the tissue of which they are derived, and corresponds to alterations described in HNC tumor databases.

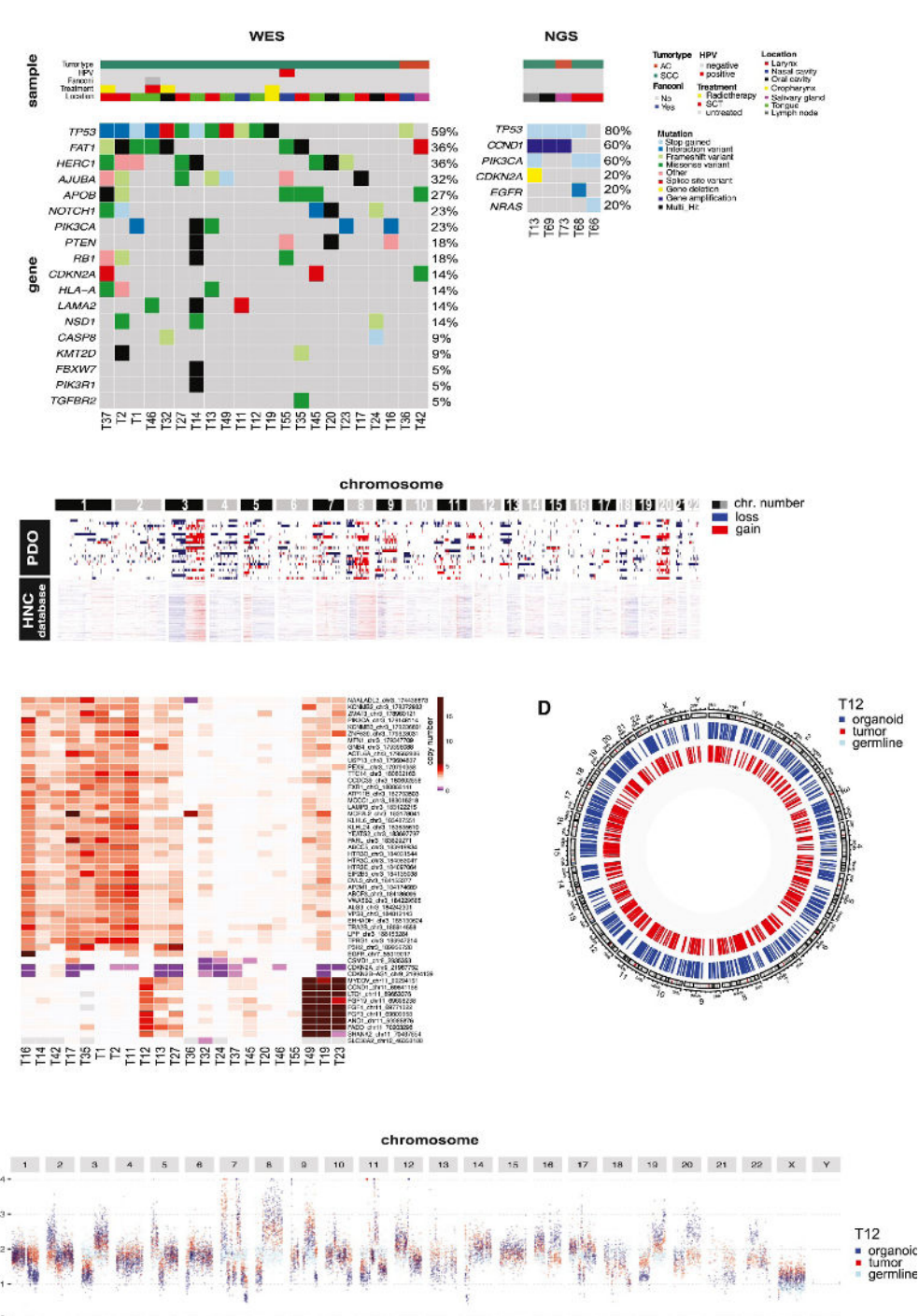


Figure 2. Patient-derived HNC organoids recapitulate genetic alterations found in HNC.

A. Oncoplot of mutations detected by DNA sequencing of organoid models. Left panel: alterations detected

in 30 organoid cultures that underwent whole exome sequencing (WES). Right panel: alterations detected in 5 organoid cultures that were sequencing using a targeted hotspot DNA sequencing panel.

B. High-level copy number variations (CNVs) detected in HNC organoids (top panel) compared to CNVs described in reference HNC datasets generated by sequencing primary patient tumors^{26,27}. Red indicates a chromosomal amplification, blue a chromosomal deletion.

C. Gene-level CNVs detected in HNC organoids. Gene copy number is indicated by color where red and purple indicate gene gain and blue indicates gene loss.

D. Circosplot describing SNVs detected in PBMC (germline, light blue, inner track), primary tumor tissue (red, middle track) and organoid culture (dark blue, outer track) of T12.

E. CNV scatter plot of alterations detected in germline (light blue), primary tumor tissue (red) and organoid culture (dark blue). Each dot represents a genomic region of 5 MB. copy number is indicated on the y-axis. Autosomal and sex chromosomes are ordered from left to right.

Correlation between HNSCC organoid treatment and clinical response

To evaluate organoid sensitivity to RT, organoids were exposed to increasing radiation doses of radiation (1-10 Gy (Figure 3A). For all organoid screens, organoid viability was assessed using the CellTiter-glo 3D assay® measuring ATP as the signal of organoid viability. Differences in RT sensitivities were observed between models derived from different patients (Figure 3B, showing eight representative models). In total, 41 tumor organoids were successfully thawed, expanded, and screened in biological duplicate for RT sensitivity (Figure S2A and S2B). Correlation was observed between area under the curve (AUC) values obtained from biological duplicates ($r^2 = 0.61$, Figure S2C).

Of the 41 screened organoids models, 21 were derived from patients who received primary (n=6) or postoperative RT (n=15). For these models, *in vitro* organoid response was correlated to clinical patient response.

Correlation of organoid and patient response in patients treated with adjuvant RT

Organoid models derived from patients receiving adjuvant RT were divided in sensitive and resistant based on the medium values of 'viability at 2Gy' and 'GR50' in the 15 screened organoids. Organoids $\leq 84.2\%$ viable at 2Gy were marked sensitive, and organoids that were $>84.2\%$ viable at 2Gy were marked resistant. For GR50, the median of 9.1 was applied as a cutoff (Figure 3C). Classification was also performed using AUC and IC50 as parameters of response (Figure S2D) as others have previously used these metrics. Patients corresponding to sensitive organoids showed longer relapse-free survival (Figure 3D). These results indicated a correlation between *in vitro* organoid and patient clinical response, which is statistically significant when categorised with GR50 ($p=0.01$, Log-rank test, Table 2), but not for viability at 2 Gy ($p=0.08$, Log-rank test, Table 2). Cox regression indicated that patients whose organoids were resistant based on GR50 score had a hazard ratio of 1.24 ($p=0.05$, Table 2), indicating increased risk of relapse. Patients with a nodal status N0/N1 relapsed later compared with patients with nodal status N2/N3 (Figure S2E). Patients with a pathology-confirmed radical resection relapsed later compared with patients with an irradiated resection (Figure 2SF).

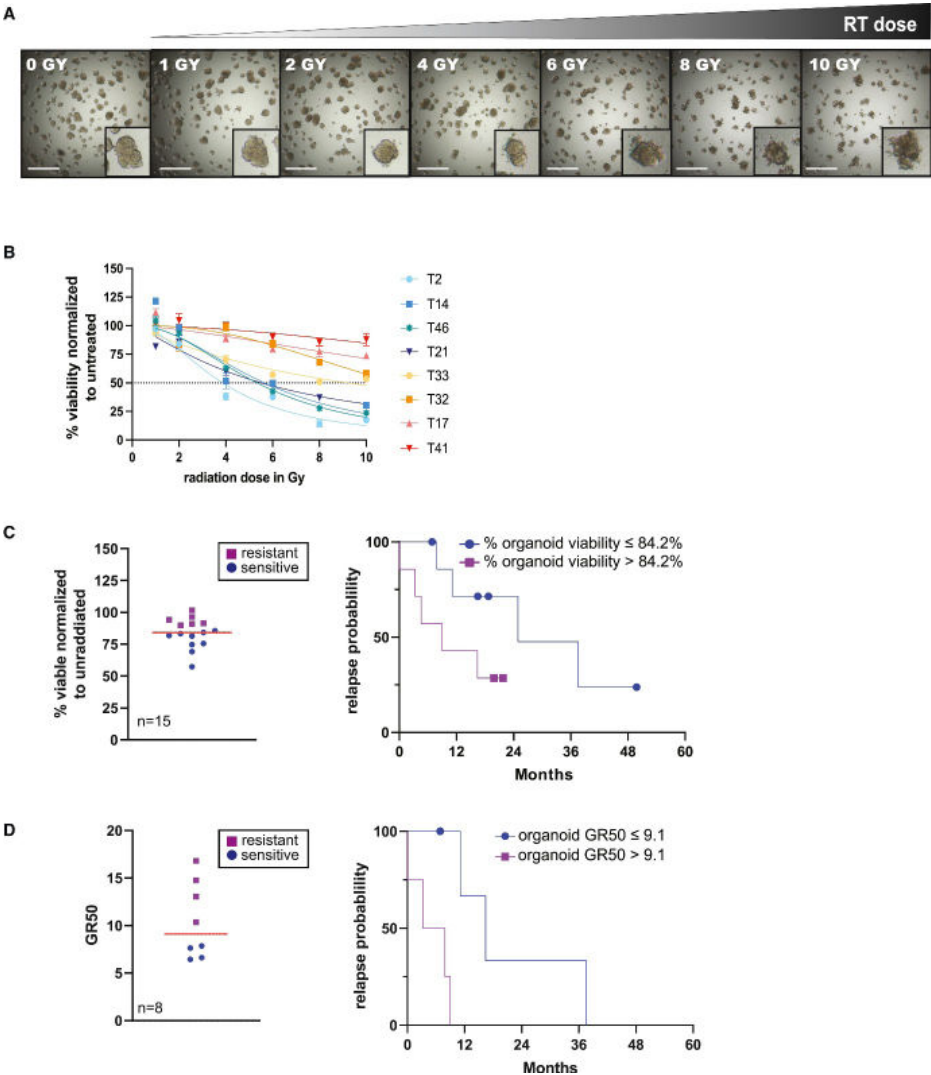


Figure 3. Radio- and chemoradio-therapy drug screening of patient-derived organoid models compared to clinical response

A. Brightfield images of HNC organoids exposed to increasing radiation dosage (0, 1, 2, 4, 6, 8 and 10 Gray), scale bar= 100 μ m.

B. Organoid viability in percentage, relative to untreated controls, of eight 8 HNC organoid cultures exposed to increasing dosage of irradiation. Light-blue to navy colors depict sensitive cultures, yellow to red colors depict more resistant cultures. Error bars indicate standard error of the mean (SEM) of 12 technical replicates. Each curve depicts the average of two biological replicates, each with technical triplicates.

C. left panel: scatter dot-plot of organoid viability at 2 Gy. Purple squares indicate models classified as resistant (above median), blue circles indicate models classified as sensitive (below median) response evaluated by: % viability 2 Gy (n=13). Each point represents the mean of 2 biological replicate experiments. Median is indicated by solid red line. Right panel: Kaplan-Meier plot with probability of relapse (in months) of patients treated with adjuvant RT stratified by organoid response

D. left panel: scatter dot-plot of organoid GR50. Purple squares indicate models classified as resistant (above median), blue circles indicate models classified as sensitive (below median) response evaluated by: % viability 2 Gy (n=8). Each point represents the mean of 2 biological replicate experiments. Median is indicated by solid red line. Right panel: Kaplan-Meier plot with probability of relapse (in months) of patients treated with adjuvant RT stratified by organoid response.

Table 2.

Specification of sensitive/resistance organoid groups \leqmedian vs. $>$median based on RT response (Log-Rank test)			
Variable	Median	p-value	Interpretation
GR50	≤ 9.1 vs. > 9.1	P=0.01	GR50 ≤ 9.1 correlates to later relapse GR50 > 9.1 correlates to earlier relapse
2Gy	$\leq 84.2\%$ vs. $> 84.2\%$	P=0.08	$\leq 84.2\%$ viability at 2Gy correlate to later relapse $> 84.2\%$ viability at 2Gy correlate to earlier relapse Differences of groups not statistical significant
AUC	≤ 540.8 vs. > 540.8	P=0.44	AUC ≤ 540.8 and > 540.8 does not correlate to earlier or later relapse
IC50	≤ 7.7 vs. > 7.7	P=0.53	IC50 ≤ 7.7 and > 7.7 does not correlate to earlier or later relapse
Proportional hazards of GR50, 2Gy, AUC and IC50 on relapse risk (Cox proportional hazard regression)			
Variable	HR (95%CI)	p-value	Interpretation
GR50	1.24 (1.00-1.59)	P=0.05	Higher GR50 correlates to a higher relapse risk
2Gy	1.5 (0.99-1.12)	P=0.11	Higher viability at 2Gy correlates to a higher relapse risk
AUC	1.00 (1.00-1.01)	P=0.58	No direction of correlation of AUC and relapse risk
IC50	1.08 (0.93-1.23)	P=0.30	Higher IC50 correlates to a higher relapse risk

Correlation of organoid and patient response in patients treated with primary RT

For the six organoid models derived from patients receiving primary RT, the same analysis was performed as described above. Here median viability was 79.5% at 2 Gy. No significant differences in patient clinical response were observed between sensitive and resistant organoids (Figure S2G), although sample size is small. Patient who got RT on the neck relapsed later compared with patients without neck RT (Figure S2H).

Combination therapy vs. monotherapy in vitro shows differential responses

Five organoid models were generated from patients receiving CRT. One patient received RT + Cetuximab and 4 patients received RT + cisplatin. Organoids were treated with RT alone, chemotherapy alone or CRT (Figures S3A-S3C)³⁶. Of the tested models, T12 was the most

sensitive to CRT (Figure S3B). T12 therapy response was compared in both a RT only and a CRT setting (Figure 4A). For CRT conditions, two types of normalisations were applied, allowing assessment of synergistic and additive effects of cisplatin and RT (see STAR Methods for more details). In the case of T12- the superior effect of CRT compared to RT alone was due to additive effects, rather than the radio sensitizing effect of cisplatin (Figure 4A). These data highlights the complexity of screening organoids for multimodal treatments and underscores the importance and of assessing treatment components in combination. Indeed, no clear correlation between organoid and patient response was observed, with 2/4 CRT (cisplatin) patients relapsing, but only one of the corresponding organoid models showing resistance, while the other model showed sensitivity (Figure S3C).

Chemotherapeutics as radiosensitizers HNSCC organoids

The radio-sensitising potential of Cisplatin, Carboplatin and Cetuximab was assessed in patient-derived organoids¹⁷. Organoids were exposed to increasing dosages of RT either in the presence or absence of sublethal doses of the chemotherapeutics. The fixed sublethal concentrations of cisplatin, carboplatin and Cetuximab were chosen based on data from our previous study¹⁷ (see START Methods for more details).

A comparison of the effect of RT in the presence of cisplatin or carboplatin with the effect of RT as a single agent, suggested that –overall- the presence of these agents enhanced the effect of RT (synergistic effect, Figure 4B and 4C, left panels). In line with what is observed in the clinic¹⁶, both cisplatin and carboplatin served as radiosensitizers. Perhaps unsurprisingly, when compared to untreated organoids, the CRT combination was more toxic to cells than RT alone (additive effects, Figure 4B and 4C, right panels). The added value of these agents differs between cultures derived from different patients. In contrast to the platinum compounds, the presence of EGFR-inhibitor Cetuximab reduced the effect of RT instead of enhancing the RT effect (first panel, Figure 4D). The effect of RT in the presence of chemo is different (statistically significantly) for all three tested chemotherapeutics (Figure 4E). Although both cisplatin and carboplatin enhance the effect of RT ($AUC_{RT[chemo]} - AUC_{RT} < 0$), Cetuximab protects against RT ($AUC_{RT[chemo]} - AUC_{RT} > 0$). These data fit the observed inferior survival of patients treated with Cetuximab + RT and highlight the value of organoid models to evaluate combination treatments before implementation in the clinic.

It is important to note that, even though Cetuximab serves as a radioprotector, the *in vitro* additive effect of RT and Cetuximab was still more toxic than that of RT alone for most patient-derived organoid models (additive effect, Figure 4D, right panel). For all three tested chemotherapeutics, CRT showed more killing than RT alone (Figure 4F).

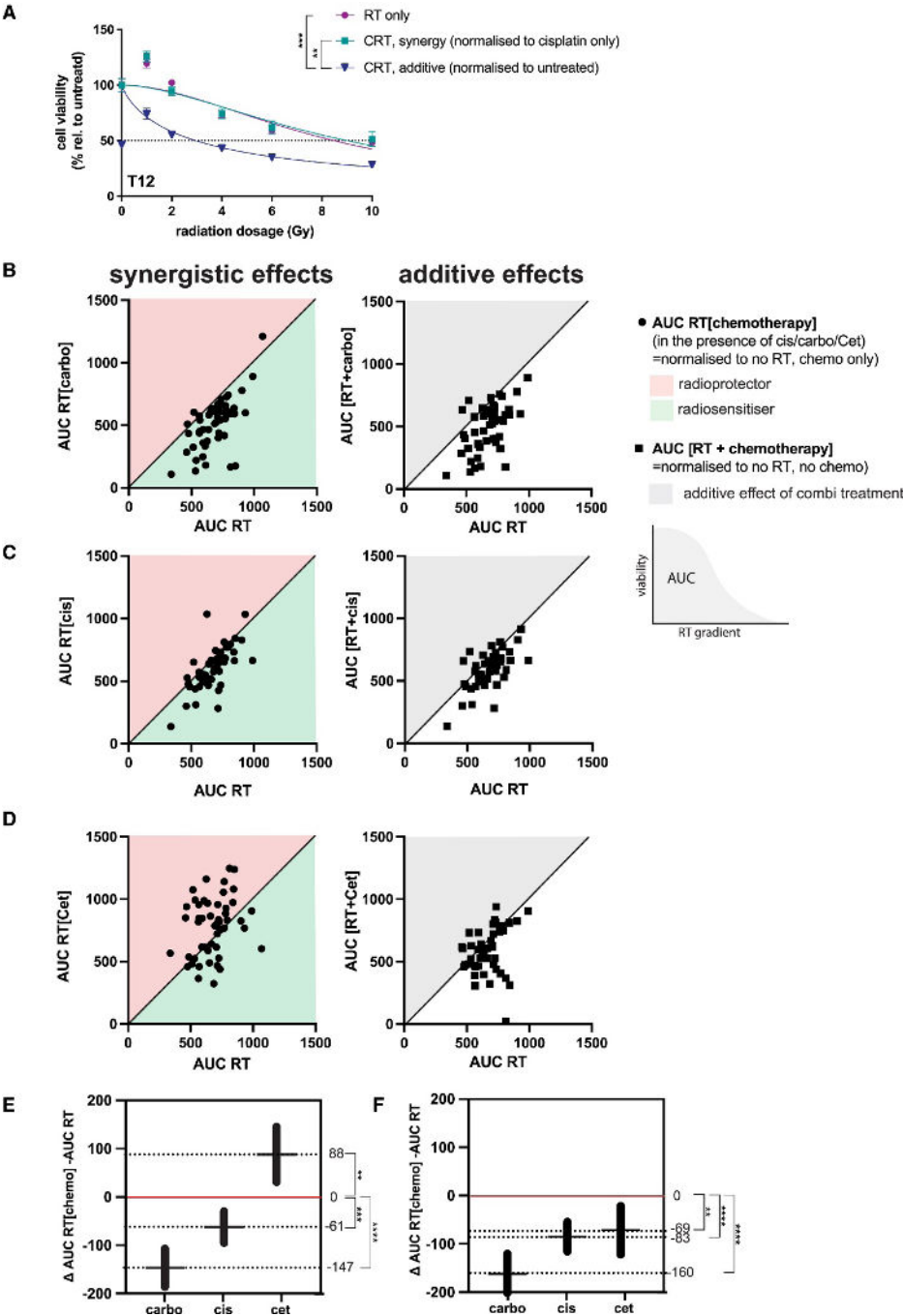


Figure 4. Synergistic versus additive effects of chemo- and radiotherapy in patient-derived organoids

A. Relative viability of organoid culture T12 exposed to increasing dosage of radiation (1-10 Gy) alone or in

combination with cisplatin. Error-bars represent standard error of the mean (SEM). Technical replicates: $n=4$ for cisplatin-treated and $n=6$ for RT only. Each curve is representative of 2 biological replicate experiments. One-way ANOVA Tukey's multiple comparison test was used to compare RT only vs. RT + cisplatin (synergistic) RT + cisplatin (additive), $**=p<0.01$ $***=p<0.001$. The effect of RT on organoid viability was assessed when given alone or together with chemotherapy. Left panels: AUC RT expressed relative to AUC [RT + chemo], which expresses the effect of RT on viability in the presence of, but corrected for, a fixed dose of chemotherapy. Green indicates the chemotherapy serves as a radiosensitizer, enhancing the effect of RT. Red indicates the chemotherapy acts as a radioprotector, decreasing the effect of RT. Right panels: AUC RT expressed relative to AUC [RT + chemo], where viability shows the result of the combinatorial treatment of RT and a fixed dose of chemo. Each dot indicates one organoid line where AUC was calculated by exposing the organoids to 6 dosages of RT in technical triplicate.

B. Effect of carboplatin on RT sensitivity of patient-derived organoids.

C. Effect of cisplatin on RT sensitivity of patient-derived organoids.

D. Effect of Cetuximab on RT sensitivity of patient-derived organoids.

E. 95% confidence intervals showing AUC RT[chemo] – AUC [RT], thereby indicating the effect the presence of the chemo has on RT sensitivity, where the effect of chemotherapy alone is corrected for. The x-axis shows the effect for carboplatin (carbo), cisplatin (cis) and Cetuximab (cet), respectively. The outcome of paired t-tests are depicted on the right side of the graph. $**=p<0.01$, $***=p<0.001$, $****=p<0.0001$.

F. Identical to E, except now the y-axis indicates AUC [RT+chemo] - AUC [RT], thereby reflecting the effect of RT+chemo, without correcting for the effect of the chemo itself. The outcome of paired t-tests are depicted on the right side of the graph. $**=p<0.01$, $***=p<0.001$, $****=p<0.0001$.

Exploring targeted therapies for HNC using organoid models

In HNSCC targeted therapy implementation has been limited. Beyond Cetuximab (and more recently immunotherapy), no targeted agents have been approved by the European Medicines Agency (EMA)²². However, genetic alterations detected in HNSCC partly overlap with other tumor types for which targeted agents have been approved. For example, the use of PIK3CA-inhibitor Alpelisib has been approved for use in PIK3CA mutant metastatic breast cancer⁴¹, but not in HNSCC. To assess the potential of such agents in HNSCC, 31 patient-derived organoid cultures were exposed to drugs targeting molecular pathways known to be affected in HNSCC (Figure 5A). Only organoids for which tumor identity was confirmed by sequencing were screened. The compounds tested were PIK3CA-inhibitor Alpelisib, FGFR-inhibitor AZD4547, PARP-inhibitor Niraparib, NRAS-inhibitor Tipifarnib, protein arginine methyltransferase 5 (PRMT5) inhibitor EZP015666 and mTOR-inhibitor Everolimus. Organoids derived from different donors showed variable responses to these agents *in vitro*. For four organoid cultures (T23, T24, T33 and T37) the assay was repeated, showing correlation between biological repeats (R^2 average= 0.66, Figure S4A and S4B).

TP53 mutation status correlated with *in vitro* Nutlin-3a sensitivity (Figure 5B),³⁴ validating our *in vitro* drug screening platform. This screening response to Nutlin-3a also correlated to the observed effect of a fixed dosage of 10 μ M Nutlin-3 in culture (see Figure S1D).

Pre-clinical studies have previously identified PIK3CA mutation as a biomarker for Alpelisib response⁴². In clinical trials, a more heterogeneous response to Alpelisib treatment was

observed. Consequently, the power of this biomarker for HNSCC patients response to alpelisib was questioned⁴³. Considering these clinical findings, we ranked organoids for response to Alpelisib based on AUC. PIK3CA mutant models were not significantly more sensitive to Alpelisib than PIK3CA wild-type models (Figure 5C, Figure S4C). This discrepancy between the value of a biomarker when studied either in pre-clinical studies or clinical trials is most likely explained by the (genetic) background of the tumors that can affect drug response. Therefore, we sought to introduce the most common activating PIK3CA mutation (E545K) into HNSCC organoids, thereby generating isogenic cancer organoid pairs, differing only by one specific mutation. We introduced single base changes in two patient-derived organoid models using CRISPR base-editing technology. These organoid models (T2 and T3) were chosen as both showed different baseline sensitivity to Alpelisib (Figure 5C). Post-editing, clonal organoid cultures were genotyped (Figure S4D) and clones carrying the desired PIK3CA mutation were expanded and subsequently tested for Alpelisib sensitivity. Compared with their isogenic wildtype counterparts, models carrying PIK3CA mutations showed increased sensitivity to Alpelisib (Figure 5D). However, the difference in response between cultures derived from different patients was larger than the difference observed between isogenic pairs (Figure 5E). Indeed, the Alpelisib response between both isogenic pairs was not statistically significantly different; however, in contrast there was a statistically significant difference in sensitivity between T2 and T3 (Figure 5E). These results underscore the potential of organoids to validate the value of a particular biomarker for drug sensitivity in the context of relevant patient heterogeneity. Moreover, organoid cohorts might be useful to identify those patients more likely to respond, thereby providing a “second chance” for agents that show positive effects, but only in a subset of patients.

Treatment with EZP01556, a PRMT5 inhibitor⁴⁴, showed differential responses in the panel of organoids screened (Figure 5E). Homozygous loss of methylthioadenosine phosphorylase (MTAP), often co-deleted with CDKN2A has been proposed to serve as a biomarker for response to PRMT5 inhibitors^{45–47}. Indeed, when correlating EZP01556 sensitivity with CDKN2A status in HNSCC organoids, CDKN2A null models showed increased sensitivity to this agent (Figure 5E). In line with our earlier observation in pancreatic cancer cells⁴⁸, a subset of the CDKN2A proficient models also showed sensitivity to EZP01556.

Taken together, these results revealed a potential treatment option for HSNCC patients, where over 50% of cases are characterised by loss of CDKN2A. Moreover, these findings again underscored the importance of personalised approaches to identify the best drug for each patient. Biomarkers such as CDKN2A status may guide treatments in patient cohorts by identifying those likely to respond, but do not hold the power to do this at the individual patient level, as illustrated by the CDKN2A proficient models that also respond to this agent. Functional testing of patient-derived models such as organoids might be better suited to identify such sensitivities for each individual patient.

A. Response of 31 patient-derived organoid models for seven targeted therapeutic agents. Sensitivity is depicted as the Z score calculated for each individual drug, to allow comparison of sensitivities between different drugs. Biological replicates are performed for T23, 24, 33 and 37, which are therefore depicted twice. Red indicates relative resistance, blue indicates relative sensitivity, grey indicates absence of data.

86

C. Alpelisib sensitivity of organoid models relative to their PIK3CA mutation status. Top row indicates the presence or absence of a PIK3CA mutation. Red indicates a PIK3CA mutation was detected, where the specific mutation is indicated by amino acid coding in text. Blue indicates absence of a PIK3CA mutation, grey indicates absence of sequencing data. Bottom row: sensitivity to Alpelisib depicted as Z score. Color coding: red indicates relative resistance, blue indicates relative sensitivity.

D. Alpelisib sensitivity of isogenic E545K PIK3CA organoid models, depicted as relative viability to DMSO-treated organoids. Viability is depicted as the average of 3 technical replicates for each concentration of alpelisib tested. Isogenic pairs are indicated by the same color, but a different color shade.

E. Alpelisib sensitivity of isogenic E545K PIK3CA organoid models depicted by IC50 value. Each IC50 is calculated from a screen with technical triplicate for 9 concentrations of Alpelisib. IC50 was determined in biological triplicate, where each dots represents the result of one experiment. Isogenic pairs are indicated by the same color, but a different color shade.

F. PRMT5-inhibitor sensitivity of organoid models relative to their CDKN2A mutation status. Top row indicates the presence or absence of a CDKN2A deletion. Red indicates a loss was detected, Blue indicates absence of a CDKN2A loss, grey indicates absence of sequencing data. Bottom row: sensitivity to PRMT-5 inhibitor EZP0001556, depicted as Z score. Color coding: red indicates relative resistance, blue indicates relative sensitivity.

DISCUSSION

Molecular diagnostics, where genetic alterations are used to guide patient diagnosis and treatment decisions is gaining prominence. Novel therapies with selective kinase inhibitors are generally indicated based on the presence of a particular genetic biomarker in the tumor DNA^{49,50}. Although associations between biomarker and drug response are detected at the population level, the presence of the applicable biomarker does not guarantee a response for the individual patient. For example, in patients affected by HER2-amplified metastatic colorectal cancer, only 30-50% respond to anti-HER2 antibodies^{49,51}. This underscores the importance of better biomarkers to guide patient treatment, ideally on the individual patient level. Here, we explored if patient-derived organoids can be used to better guide patient treatments by serving as a diagnostic tool, using organoid response as the biomarker. Moreover, we explored the value of organoids as a pre-clinical model to test and characterise already proposed biomarkers before they enter the clinic.

The potential of organoid models to guide treatment in a personalised manner has been explored before^{8,10-12}. Multiple reviews have described these studies and analysed their similarities and differences^{13,52}. Overall, correlation between patient and organoid response is observed. Regardless, these studies investigate different tumor types, disease stages, treatments and furthermore vary in applied methodology to determine organoid sensitivity. As such, it is challenging to answer the question whether organoids can help guide therapy decisions for all cancer patients. This is emphasised by a study of Ooft et al. that showed in patients with colorectal cancer, organoids can predict patient response to irinotecan-based therapies, but not to oxaliplatin and 5-FU response¹².

Correlation of organoid response and patient response

Here we have investigated the predictive potential of organoid response to RT and/or CRT in patients with primary HNSCC. In the adjuvant treatment setting, organoid viability at 2 Gy was the organoid parameter that best correlated with clinical response (n=15, Figure 3C), although the correlation was not statistically significant. For patients that received primary RT, we did not observe a statistically significant correlation between organoid response and clinical relapse (n=6, see Figure S6A). This could potentially be due to the small sample size. Taken together, larger studies are needed to confirm if organoids hold predictive potential.

There are multiple factors that could confound or weaken potential correlation. The first one, applicable in the context of adjuvant RT, is surgery. Even a resistant tumor will not relapse when completely and successfully removed by surgery. Second, the absence of the tumor microenvironment in organoid models should be considered¹². RT treatment induces immunogenicity through neoantigen presentation in the tumor microenvironment⁵³. Therefore, the presence of immune cells might be required in a model to assess the full effect of RT^{54,55}. The effect of immune cells on tumor cell killing post-RT or the effects of immunotherapy on regional lymph nodes cannot be assessed in the current screening assay. Indeed, administration of immune-checkpoint inhibitor Durvalumab following CRT has been associated with an improved overall survival in patients with stage III non-small cell lung cancer^{54,55}. For HNC, a similar strategy of combined immuno- and chemoradiotherapy has not yet shown benefit⁵⁵.

Measuring organoid response in vitro

Organoid viability was assessed at RT dosage ranging from 1 to 10 Gy. This allowed for calculations of metrics such as IC50, AUC and GR50. Similar to an approach previously used by Yao et al¹¹, organoid viability at a fixed RT dose of 2 Gy was also included as a metric, as 2 Gy is the fraction dose used clinically for patients with HNC. Of assessed metrics, viability at 2 Gy correlated best with clinical response and allowed us to use all organoid models in our analysis (as GR-metrics could not be calculated for all organoids, due to never reaching 50% viability). Importantly, using a single dose for readout as opposed to a gradient of dosages¹¹ requires less organoids and therefore, could decrease time to screening if testing would be applied in a diagnostic setting.

It remains to be determined which parameter is the best predictor of response. In a pooled analysis of 17 oncology organoid studies that assessed organoid response to clinical outcome, the most common parameter of organoid response used was the AUC¹³. Most informative parameters may depend on treatment type (e.g., RT vs. chemotherapy vs. targeted therapies) as well as the disease type. As more studies evaluating organoid response and clinical response in various oncology indications are reported, this will help to clarify the most optimal

parameter per treatment and disease type. For transparency, we have reported IC50, AUC, GR50 and viability at 2 Gy here.

Biomarker validation using patient-derived organoid models

Organoids were used to study the correlation between response to PIK3CA-inhibitor Alpelisib and the presence of activation PIK3CA mutations. When tested in a cohort of organoid models, no association between PIK3CA mutation status and Alpelisib response could be found. We hypothesised that the tumor's genetic background may overrule response to a drug, even if the relevant biomarker is present. To test this, E545K mutations were introduced in organoids derived from two different patients using CRISPR/Cas9 base-editing technology. Absolute sensitivity to Alpelisib increased upon introduction of the mutation in both cases, and the difference between the two patients remained bigger than the difference between the isogenic pairs. Indeed, in preclinical studies, PIK3CA mutation seemed a promising biomarker in HNSCC tumors, but clinical trials yielded disappointing results when selecting patients for Alpelisib treatment based on the presence of this biomarker⁴³. These results illustrate how organoid biobanks may be used to validate or characterise biomarkers before they are explored in the clinic to enhance chance of success of a drug candidate before it enters clinical trials.

Lastly, we used organoids to show that genetic loss of CDKN2A seems to be predictive for a good response to PRMT5 inhibitors. Although it has been shown both pre-clinically and clinically for other tumor types^{45–47}, to our knowledge, we are the first to show this correlation in HNSCC. These results therefore indicate a new therapy option for HNSCC, which can potentially aid many patients, as > 50% of HNSCC show a loss of CDKN2A³³.

LIMITATIONS OF THE STUDY

The sample sizes for clinical correlation, primary RT (n = 6) and adjuvant RT (n = 15), are small, and therefore results should be interpreted with caution. In the adjuvant RT group, patients' surgery may confound outcome. For clinical analysis, patients' age and sex (ascribed at birth) were collected, but ethnicity and socioeconomic status of patients were not collected. Age and sex distribution of patients included in correlation analysis was comparable to the entire HNC biobank, which is a representative cohort of patients with HNC, as worldwide, the median age for diagnosis is 66 years, and men have a 2- to 4-fold higher risk to develop HNSCC.⁵⁶ The study inclusion criteria were patients with HNC with a tumor of minimum 1 cm and a planned intervention with possible tissue collection. Tumors smaller than 1 cm were not suitable for inclusion.

CONCLUSION

Here we present a diverse biobank of organoids derived from patients with HNC that phenotypically and genetically recapitulate the original tissue they are derived from. Organoid response to RT correlates with clinical relapse status in the adjuvant setting but not in the primary setting. Finally, we demonstrate how organoids can be utilized to explore biomarker potential in the setting of targeted therapies, and we identify PRMT5 inhibition as a potential therapy option that can be explored for HNSCC.

REFERENCES

1. Drost, J., and Clevers, H. (2018). Organoids in cancer research. *Nat Rev Cancer* 18, 407–418. 10.1038/s41568-018-0007-6.
2. Tuveson, D., and Clevers, H. (2019). Cancer modeling meets human organoid technology. *Science* (1979) 364, 952–955. 10.1126/science.aaw6985.
3. van de Wetering, M., Francies, H.E., Francis, J.M., Bounova, G., Iorio, F., Pronk, A., van Houdt, W., van Gorp, J., Taylor-Weiner, A., Kester, L., et al. (2015). Prospective derivation of a living organoid biobank of colorectal cancer patients. *Cell* 161, 933–945. 10.1016/j.cell.2015.03.053.
4. Hou, S., Tiriach, H., Sridharan, B.P., Scampavia, L., Madoux, F., Seldin, J., Souza, G.R., Watson, D., Tuveson, D., and Spicer, T.P. (2018). Advanced Development of Primary Pancreatic Organoid Tumor Models for High-Throughput Phenotypic Drug Screening. *SLAS Discov* 23, 574–584. 10.1177/2472555218766842.
5. Hill, S.J., Decker, B., Roberts, E.A., Horowitz, N.S., Muto, M.G., Worley, M.J., Feltmate, C.M., Nucci, M.R., Swisher, E.M., Nguyen, H., et al. (2018). Prediction of DNA repair inhibitor response in short-term patient-derived ovarian cancer organoids. *Cancer Discov* 8, 1404–1421. 10.1158/2159-8290.CD-18-0474.
6. Sachs, N., de Ligt, J., Kopper, O., Gogola, E., Bounova, G., Weeber, F., Balgobind, A.V., Wind, K., Gracanin, A., Begthel, H., et al. (2018). A living biobank of breast cancer organoids captures disease heterogeneity. *Cell* 172, 373–386. 10.1016/j.cell.2017.11.010.
7. Yan, H.H.N., Siu, H.C., Law, S., Ho, S.L., Yue, S.S.K., Tsui, W.Y., Chan, D., Chan, A.S., Ma, S., Lam, K.O., et al. (2018). A comprehensive human gastric cancer organoid biobank captures tumor subtype heterogeneity and enables therapeutic screening. *Cell Stem Cell* 23, 882–897. 10.1016/j.stem.2018.09.016.
8. Tiriach, H., Belleau, P., Engle, D.D., Plenker, D., Deschênes, A., Somerville, T., Froeling, F.E.M., Burkhart, R.A., Denroche, R.E., Jang, G.-H., et al. (2018). Organoid profiling identifies common responders to chemotherapy in pancreatic cancer. *Cancer Discov* 8, 1112–1129. 10.1158/2159-8290.CD-18-0349.
9. Kim, M., Mun, H., Sung, C.O., Cho, E.J., Jeon, H.J., Chun, S.M., Jung, D.J., Shin, T.H., Jeong, G.S., Kim, D.K., et al. (2019). Patient-derived lung cancer organoids as in vitro cancer models for therapeutic screening. *Nat Commun* 10. 10.1038/s41467-019-11867-6.
10. Vlachogiannis, G., Hedayat, S., Vatsiou, A., Jamin, Y., Fernández-Mateos, J., Khan, K., Lampis, A., Eason, K., Huntingford, I., Burke, R., et al. (2018). Patient-derived organoids model treatment response of metastatic gastrointestinal cancers. *Science* (1979) 360, 920–926. 10.1126/science.aao2774.
11. Yao, Y., Xu, X., Yang, L., Zhu, J., Wan, J., Shen, L., Xia, F., Fu, G., Deng, Y., Pan, M., et al. (2020). Patient-Derived Organoids Predict Chemoradiation Responses of Locally Advanced Rectal Cancer. *Cell Stem Cell* 26, 17–26.e6. 10.1016/j.stem.2019.10.010.
12. Ooft, S.N., Weeber, F., Dijkstra, K.K., McLean, C.M., Kaing, S., van Werkhoven, E., Schipper, L., Hoes, L., Vis, D.J., van de Haar, J., et al. (2019). Patient-derived organoids can predict response to chemotherapy in metastatic colorectal cancer patients. *Sci Transl Med* 11, eaay2574. 10.1126/scitranslmed.aay2574.
13. Wensink, G.E., Elias, S.G., Mullenders, J., Koopman, M., Boj, S.F., Kranenburg, O.W., and Roodhart, J.M.L. (2021). Patient-derived organoids as a predictive biomarker for treatment response in cancer patients. *NPJ Precis Oncol* 5, 30. 10.1038/s41698-021-00168-1.

14. Bray, F., Ferlay, J., Soerjomataram, I., Siegel, R.L., Torre, L.A., and Jemal, A. (2018). Global cancer statistics 2018: GLOBOCAN estimates of incidence and mortality worldwide for 36 cancers in 185 countries. *CA Cancer J Clin* 68, 394–424. 10.3322/caac.21492.
15. Leemans, C.R., Snijders, P.J.F., and Brakenhoff, R.H. (2018). The molecular landscape of head and neck cancer. *Nat Rev Cancer* 18, 269–282. 10.1038/nrc.2018.11.
16. Mody, M.D., Rocco, J.W., Yom, S.S., Haddad, R.I., and Saba, N.F. (2021). Head and neck cancer. *The Lancet* 398, 2289–2299. 10.1016/S0140-6736(21)01550-6.
17. Driehuis, E., Kolders, S., Spelier, S., Löhmußaar, K., Willems, S.M., Devriese, L.A., de Bree, R., de Ruiter, E.J., Korving, J., Begthel, H., et al. (2019). Oral mucosal organoids as a potential platform for personalized cancer therapy. *Cancer Discov* 9, 852–871. 10.1158/2159-8290.cd-18-1522.
18. Nestor, M., Sundström, M., Anniko, M., and Tolmachev, V. (2011). Effect of cetuximab in combination with alpha-radioimmunotherapy in cultured squamous cell carcinomas. *Nucl Med Biol* 38, 103–112. 10.1016/J.NUCMEDBIO.2010.06.014.
19. Gebre-Medhin, M., Brun, E., Engström, P., Cange, H.H., Hammarstedt-Nordenvall, L., Reizenstein, J., Nyman, J., Abel, E., Friesland, S., Sjödin, H., et al. (2021). ARTSCAN III: A Randomized Phase III Study Comparing Chemoradiotherapy With Cisplatin Versus Cetuximab in Patients With Locoregionally Advanced Head and Neck Squamous Cell Cancer. *J Clin Oncol* 39, 38–47. 10.1200/JCO.20.02072.
20. Rischin, D., King, M., Kenny, L., Porceddu, S., Wratten, C., Macann, A., Jackson, J.E., Bressel, M., Herschtal, A., Fisher, R., et al. (2021). Randomized Trial of Radiation Therapy With Weekly Cisplatin or Cetuximab in Low-Risk HPV-Associated Oropharyngeal Cancer (TROG 12.01) - A Trans-Tasman Radiation Oncology Group Study. *Int J Radiat Oncol Biol Phys* 111, 876–886. 10.1016/J.IJROBP.2021.04.015.
21. Maddalo, M., Borghetti, P., Tomasini, D., Corvò, R., Bonomo, P., Petrucci, A., Paiar, F., Lastrucci, L., Bonù, M.L., Greco, D., et al. (2020). Cetuximab and Radiation Therapy Versus Cisplatin and Radiation Therapy for Locally Advanced Head and Neck Cancer: Long-Term Survival and Toxicity Outcomes of a Randomized Phase 2 Trial. *Int J Radiat Oncol Biol Phys* 107, 469–477. 10.1016/J.IJROBP.2020.02.637.
22. Li, Q., Tie, Y., Alu, A., Ma, X., and Shi, H. (2023). Targeted therapy for head and neck cancer: signaling pathways and clinical studies. *Signal Transduct Target Ther* 8, 31. 10.1038/s41392-022-01297-0.
23. Geurts, M.H., de Poel, E., Pleguezuelos-Manzano, C., Oka, R., Carrillo, L., Andersson-Rolf, A., Boretto, M., Brunsveld, J.E., van Boxtel, R., Beekman, J.M., et al. (2021). Evaluating CRISPR-based prime editing for cancer modeling and CFTR repair in organoids. *Life Sci Alliance* 4. 10.26508/LSA.202000940.
24. Beumer, J., Geurts, M.H., Lamers, M.M., Puschhof, J., Zhang, J., van der Vaart, J., Mykytyn, A.Z., Breugem, T.I., Riesebosch, S., Schipper, D., et al. (2021). A CRISPR/Cas9 genetically engineered organoid biobank reveals essential host factors for coronaviruses. *Nature Communications* 2021 12:1 12, 1–12. 10.1038/s41467-021-25729-7.
25. Schwank, G., Koo, B.K., Sasselli, V., Dekkers, J.F., Heo, I., Demircan, T., Sasaki, N., Boymans, S., Cuppen, E., van der Ent, C.K., et al. (2013). Functional repair of CFTR by CRISPR/Cas9 in intestinal stem cell organoids of cystic fibrosis patients. *Cell Stem Cell* 13, 653–658. 10.1016/j.stem.2013.11.002.
26. Drost, J., van Jaarsveld, R.H., Ponsioen, B., Zimberlin, C., van Boxtel, R., Buijs, A., Sachs, N., Overmeer, R.M., Offerhaus, G.J., Begthel, H., et al. (2015). Sequential cancer mutations in cultured human intestinal stem cells. *Nature* 521, 43–47. 10.1038/nature14415.
27. Fujii, M., Matano, M., Nanki, K., and Sato, T. (2015). Efficient genetic engineering of human intestinal organoids using electroporation. *Nat Protoc* 10, 1474–1485. 10.1038/nprot.2015.088.
28. Koblan, L.W., Doman, J.L., Wilson, C., Levy, J.M., Tay, T., Newby, G.A., Maianti, J.P., Raguram, A., and Liu, D.R. (2018). Improving cytidine and adenine base editors by expression optimization and ancestral reconstruction. *Nat Biotechnol* 36, 843–846. 10.1038/nbt.4172.

29. Gaudelli, N.M., Komor, A.C., Rees, H.A., Packer, M.S., Badran, A.H., Bryson, D.I., and Liu, D.R. (2017). Programmable base editing of A•T to G•C in genomic DNA without DNA cleavage. *Nature* 551, 464–471. 10.1038/nature24644.
30. Zafra, M.P., Schatoff, E.M., Katti, A., Foronda, M., Breinig, M., Schweitzer, A.Y., Simon, A., Han, T., Goswami, S., Montgomery, E., et al. (2018). Optimized base editors enable efficient editing in cells, organoids and mice. *Nat Biotechnol* 36, 888–893. 10.1038/nbt.4194.
31. Komor, A.C., Kim, Y.B., Packer, M.S., Zuris, J.A., and Liu, D.R. (2016). Programmable editing of a target base in genomic DNA without double-stranded DNA cleavage. *Nature* 533, 420–424. 10.1038/nature17946.
32. Löhmußaar, K., Oka, R., Espejo Valle-Inclán, J., Smits, M.H.H., Wardak, H., Korving, J., Begthel, H., Proost, N., van de Ven, M., Kranenburg, O.W., et al. (2021). Patient-derived organoids model cervical tissue dynamics and viral oncogenesis in cervical cancer. *Cell Stem Cell* 28, 1380–1396.e6. 10.1016/j.stem.2021.03.012.
33. The Cancer Genome Atlas Network (2015). Comprehensive genomic characterization of head and neck squamous cell carcinomas. *Nature* 517, 576–582. 10.1038/nature14129.
34. Vassilev, L.T., Vu, B.T., Graves, B., Carvajal, D., Podlaski, F., Filipovic, Z., Kong, N., Kammlott, U., Lukacs, C., Klein, C., et al. (2004). In vivo activation of the p53 pathway by small-molecule antagonists of MDM2. *Science* (1979) 303, 844–848. 10.1126/science.1092472.
35. Llorente, J.L., López, F., Suárez, C., and Hermesen, M.A. (2014). Sinonasal carcinoma: Clinical, pathological, genetic and therapeutic advances. *Nat Rev Clin Oncol* 11, 460–472. 10.1038/nrclinonc.2014.97.
36. Nalepa, G., and Clapp, D.W. (2018). Fanconi anaemia and cancer: an intricate relationship. *Nat Rev Cancer* 18, 168–185. 10.1038/nrc.2017.116.
37. Sachs, N., Papaspyropoulos, A., Zomer-van Ommen, D.D., Heo, I., Böttlinger, L., Klay, D., Weeber, F., Huelsz-Prince, G., Jakobachvili, N., Amatngalim, G.D., et al. (2019). Long-term expanding human airway organoids for disease modeling. *EMBO J* 38. 10.15252/embj.2018100300.
38. Karthaus, W.R., Iaquinta, P.J., Drost, J., Gracanin, A., van Boxtel, R., Wongvipat, J., Dowling, C.M., Gao, D., Begthel, H., Sachs, N., et al. (2014). Identification of multipotent luminal progenitor cells in human prostate organoid cultures. *Cell* 159, 163–175. 10.1016/j.cell.2014.08.017.
39. Stransky, N., Egloff, A.M., Tward, A.D., Kostic, A.D., Cibulskis, K., Sivachenko, A., Kryukov, G. v., Lawrence, M.S., Sougnez, C., McKenna, A., et al. (2011). The mutational landscape of head and neck squamous cell carcinoma. *Science* (1979) 333, 1157–1160. 10.1126/science.1208130.
40. Agrawal, N., Frederick, M.J., Pickering, C.R., Bettegowda, C., Chang, K., Li, R.J., Fakhry, C., Xie, T.X., Zhang, J., Wang, J., et al. (2011). Exome sequencing of head and neck squamous cell carcinoma reveals inactivating mutations in NOTCH1. *Science* (1979) 333, 1154–1157. 10.1126/science.1206923.
41. André, F., Ciruelos, E., Rubovszky, G., Campone, M., Loibl, S., Rugo, H.S., Iwata, H., Conte, P., Mayer, I.A., Kaufman, B., et al. (2019). Alpelisib for PIK3CA-Mutated, Hormone Receptor-Positive Advanced Breast Cancer. *New England Journal of Medicine* 380, 1929–1940. 10.1056/nejmoa1813904.
42. Fritsch, C., Huang, A., Chatenay-Rivauday, C., Schnell, C., Reddy, A., Liu, M., Kauffmann, A., Guthy, D., Erdmann, D., De Pover, A., et al. (2014). Characterization of the Novel and Specific PI3K Inhibitor NVP-BYL719 and Development of the Patient Stratification Strategy for Clinical Trials. *Mol Cancer Ther* 13, 1117–1129. 10.1158/1535-7163.MCT-13-0865.
43. Juric, D., Rodon, J., Tabernero, J., Janku, F., Burris, H.A., Schellens, J.H.M., Middleton, M.R., Berlin, J., Schuler, M., Gil-Martin, M., et al. (2018). Phosphatidylinositol 3-Kinase α -Selective Inhibition With Alpelisib (BYL719) in PIK3CA-Altered Solid Tumors: Results From the First-in-Human Study. *Journal of Clinical Oncology* 36, 1291–1299. 10.1200/JCO.2017.72.7107.

44. Chan-Penebre, E., Kuplast, K.G., Majer, C.R., Boriack-Sjodin, P.A., Wigle, T.J., Johnston, L.D., Rioux, N., Munchhof, M.J., Jin, L., Jacques, S.L., et al. (2015). A selective inhibitor of PRMT5 with in vivo and in vitro potency in MCL models. *Nat Chem Biol.* 10.1038/nchembio.1810.
45. Marjon, K., Cameron, M.J., Quang, P., Clasquin, M.F., Mandley, E., Kunii, K., McVay, M., Choe, S., Kernysky, A., Gross, S., et al. (2016). MTAP Deletions in Cancer Create Vulnerability to Targeting of the MAT2A/PRMT5/RIOK1 Axis. *Cell Rep.* 10.1016/j.celrep.2016.03.043.
46. Kryukov, G. v, Wilson, F.H., Ruth, J.R., Paulk, J., Tsherniak, A., Marlow, S.E., Vazquez, F., Weir, B.A., Fitzgerald, M.E., Tanaka, M., et al. (2016). MTAP deletion confers enhanced dependency on the PRMT5 arginine methyltransferase in cancer cells. *Science* 351, 1214–1218. 10.1126/science.aad5214.
47. Mavrakis, K.J., McDonald, E.R. 3rd, Schlabach, M.R., Billy, E., Hoffman, G.R., deWeck, A., Ruddy, D.A., Venkatesan, K., Yu, J., McAllister, G., et al. (2016). Disordered methionine metabolism in MTAP/CDKN2A-deleted cancers leads to dependence on PRMT5. *Science* 351, 1208–1213. 10.1126/science.aad5944.
48. Driehuis, E., van Hoeck, A., Moore, K., Kolders, S., Francies, H.E., Gulersonmez, M.C., Stigter, E.C.A., Burgering, B., Geurts, V., Gracanin, A., et al. (2019). Pancreatic cancer organoids recapitulate disease and allow personalized drug screening. *Proc Natl Acad Sci U S A* 116, 26580–26590. 10.1073/pnas.1911273116.
49. Meric-Bernstam, F., Hurwitz, H., Raghav, K.P.S., McWilliams, R.R., Fakih, M., VanderWalde, A., Swanton, C., Kurzrock, R., Burris, H., Sweeney, C., et al. (2019). Pertuzumab and trastuzumab for HER2-amplified metastatic colorectal cancer: an updated report from MyPathway, a multicentre, open-label, phase 2a multiple basket study. *Lancet Oncol* 20, 518. 10.1016/S1470-2045(18)30904-5.
50. Mosele, F., Remon, J., Mateo, J., Westphalen, C.B., Barlesi, F., Lolkema, M.P., Normanno, N., Scarpa, A., Robson, M., Meric-Bernstam, F., et al. (2020). Recommendations for the use of next-generation sequencing (NGS) for patients with metastatic cancers: a report from the ESMO Precision Medicine Working Group. *Annals of Oncology.* 10.1016/j.annonc.2020.07.014.
51. Gupta, R., Garrett-Mayer, E., Halabi, S., Mangat, P.K., D'Andre, S.D., Meiri, E., Shrestha, S., Warren, S.L., Ranasinghe, S., and Schilsky, R.L. (2020). Pertuzumab plus trastuzumab (P+T) in patients (Pts) with colorectal cancer (CRC) with ERBB2 amplification or overexpression: Results from the TAPUR Study. https://doi.org/10.1200/JCO.2020.38.4_suppl.132 38, 132–132. 10.1200/JCO.2020.38.4_SUPPL.132.
52. Driehuis, E., Kretzschmar, K., and Clevers, H. (2020). Establishment of patient-derived cancer organoids for drug-screening applications. *Nat Protoc* 15, 3380–3409. 10.1038/s41596-020-0379-4.
53. Formenti, S.C., Rudqvist, N.P., Golden, E., Cooper, B., Wennerberg, E., Lhuillier, C., Vanpouille-Box, C., Friedman, K., Ferrari de Andrade, L., Wucherpfennig, K.W., et al. (2018). Radiotherapy induces responses of lung cancer to CTLA-4 blockade. *Nat Med* 24, 1845–1851. 10.1038/s41591-018-0232-2.
54. Antonia, S.J., Villegas, A., Daniel, D., Vicente, D., Murakami, S., Hui, R., Kurata, T., Chiappori, A., Lee, K.H., de Wit, M., et al. (2018). Overall Survival with Durvalumab after Chemoradiotherapy in Stage III NSCLC. *New England Journal of Medicine* 379, 2342–2350. 10.1056/nejmoa1809697.
55. Lee, N.Y., Ferris, R.L., Psyrris, A., Haddad, R.I., Tahara, M., Bourhis, J., Harrington, K., Mu-Hsin Chang, P., Lin, J.-C., Abdul Razaq, M., et al. (2021). Avelumab plus standard-of-care chemoradiotherapy versus chemoradiotherapy alone in patients with locally advanced squamous cell carcinoma of the head and neck: a randomised, double-blind, placebo-controlled, multicentre, phase 3 trial.
56. Johnson, D.E., Burtneess, B., Leemans, C.R., Lui, V.W.Y., Bauman, J.E., and Grandis, J.R. (2020). Head and neck squamous cell carcinoma. *Nat. Rev. Dis. Primers* 6, 92. <https://doi.org/10.1038/s41572-020-00224-3>.
57. Gupta, S.M., and Mania-Pramanik, J. (2019). Molecular mechanisms in progression of HPV-associated cervical carcinogenesis. *J Biomed Sci* 26. 10.1186/s12929-019-0520-2.

58. Zhang, J.-H., and Oldenburg, K.R. (2009). Z-Factor. In *Encyclopedia of Cancer*, M. Schwab, ed. (Springer Berlin Heidelberg), pp. 3227–3228. 10.1007/978-3-540-47648-1_6298.
59. Hu, J.H., Miller, S.M., Geurts, M.H., Tang, W., Chen, L., Sun, N., Zeina, C.M., Gao, X., Rees, H.A., Lin, Z., et al. (2018). Evolved Cas9 variants with broad PAM compatibility and high DNA specificity. *Nature* 556, 57–63. <https://doi.org/10.1038/nature26155>.
60. Andersson-Rolf, A., Mustata, R.C., Merenda, A., Kim, J., Perera, S., Grego, T., Andrews, K., Tremble, K., Silva, J.C.R., Fink, J., et al. (2017). One-step generation of conditional and reversible gene knockouts. *Nat Methods* 14, 287–289. 10.1038/NMETH.4156.

SUPPLEMENTAL MATERIAL

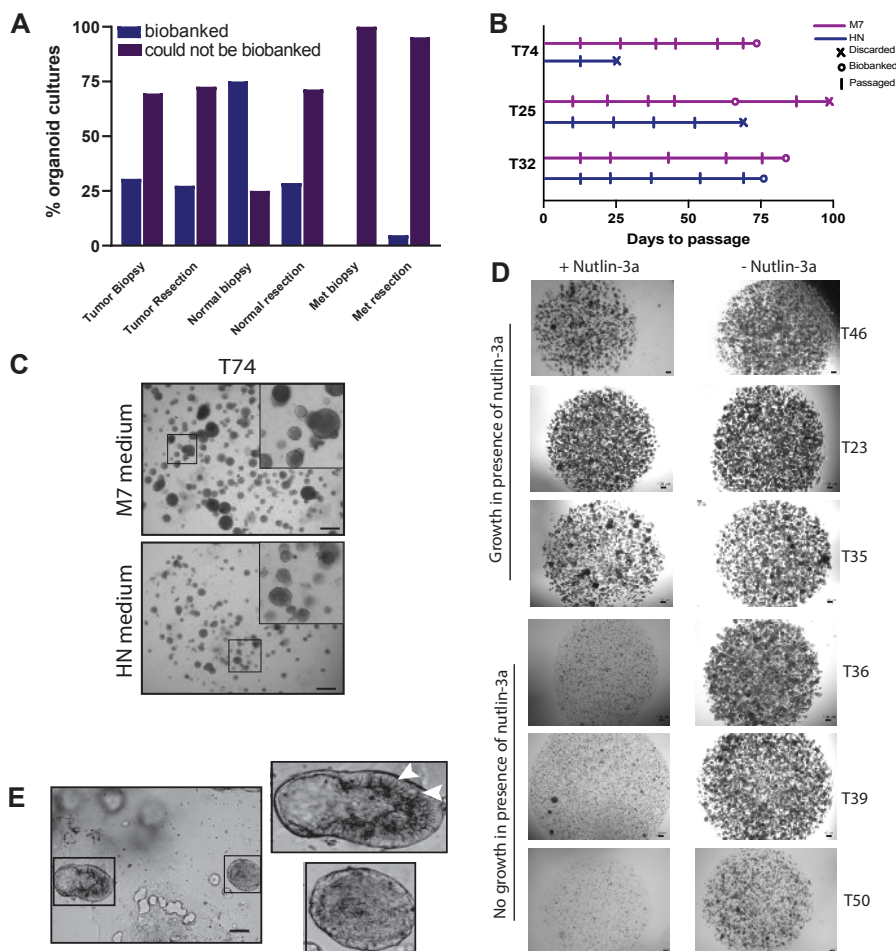


Figure S1 Organoid outgrowth and phenotypic characterization, related to Figure 1.

A. Bar-graph indicating percentage of successful (blue) or unsuccessful (purple) biobanking of organoids isolated from tumor, normal or metastatic (met) tissues, either from a biopsy or resection procedure. B. Comparison of organoid outgrowth from three primary tumors (T74, T25 and T32) on M7 (purple) and HN (navy) media. Cross shape indicates when organoid was discarded due to lack of growth, circle shape indicates when organoid was biobanked and vertical line indicates an organoid passage. C. Brightfield microscopy images of tumor organoid T74 grown from isolation on M7 or HN media. Scale bars=100 μ m. D. Brightfield images display 6 tumor organoid cultures that are insensitive (T46, T23 and T35) or sensitive (T36, T39 and T50) to Nutlin-3a (7-10 days) following passage. Scale bars=100 μ m. E. Brightfield images of ITAC organoid T36, highlighting the phenotypic difference of the cystic adenocarcinoma organoid with columnar cells (white arrows) compared to the solid squamous organoid phenotype. Scale bars=100 μ m.

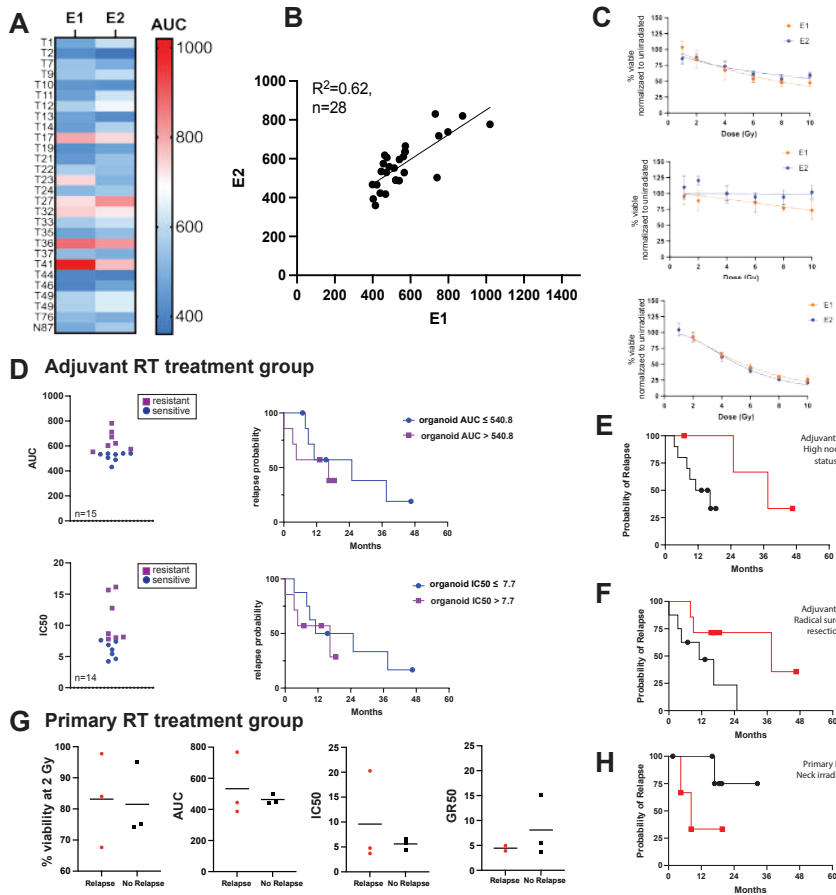


Figure S2. Radiotherapy screening in organoids and clinical correlation in primary and adjuvant setting, related to Figure 3.

A. Heatmap of AUC from 28 organoids that were used to evaluate reproducibility from 2 biological replicate experiments (E): 1 and 2. B. Correlation between AUC obtained in RT screening: E1, x-axis and E2, y-axis. Each dot represents an organoid model, $n=28$. Pearson correlation was used to determine the R squared value. C. Examples of kill curves obtained during E1 (yellow) and E2 (blue) of RT screens in organoids T33, T41 and T46 (top to bottom). D. Scatter dot plots and Kaplan-Meier curves corresponding to organoid models derived from patients that received adjuvant RT. E. Kaplan-Meier curve showing the probability of relapse (in months) in patients who received adjuvant RT, stratified by patients with high nodal status: no (N0/1 nodal status, black line, $n=4$) or yes (N2/N3 nodal status, red line, $n=11$) at the time of irradiation. F. Kaplan-Meier curve showing the probability of relapse (in months) in patients who received adjuvant RT, stratified by patients who had a radical surgical resection: No (black line, $n=8$) or yes (red line, $n=7$). G. Response of organoid cultures corresponding to patients receiving primary RT, categorised based on patient relapse status. Red indicates a relapse, black indicates no relapse. Different plots show response of organoids depicted for different response parameters: % viability at 2 Gy, AUC, IC50 and GR50 (left to right). H. Kaplan-Meier curve depicts the probability of relapse (in months) in patients who received primary RT, stratified by yes (black line, $n=3$) or no (red line, $n=6$) receiving irradiation to the neck. Drop in line indicates relapse; Dot indicates censored data point.

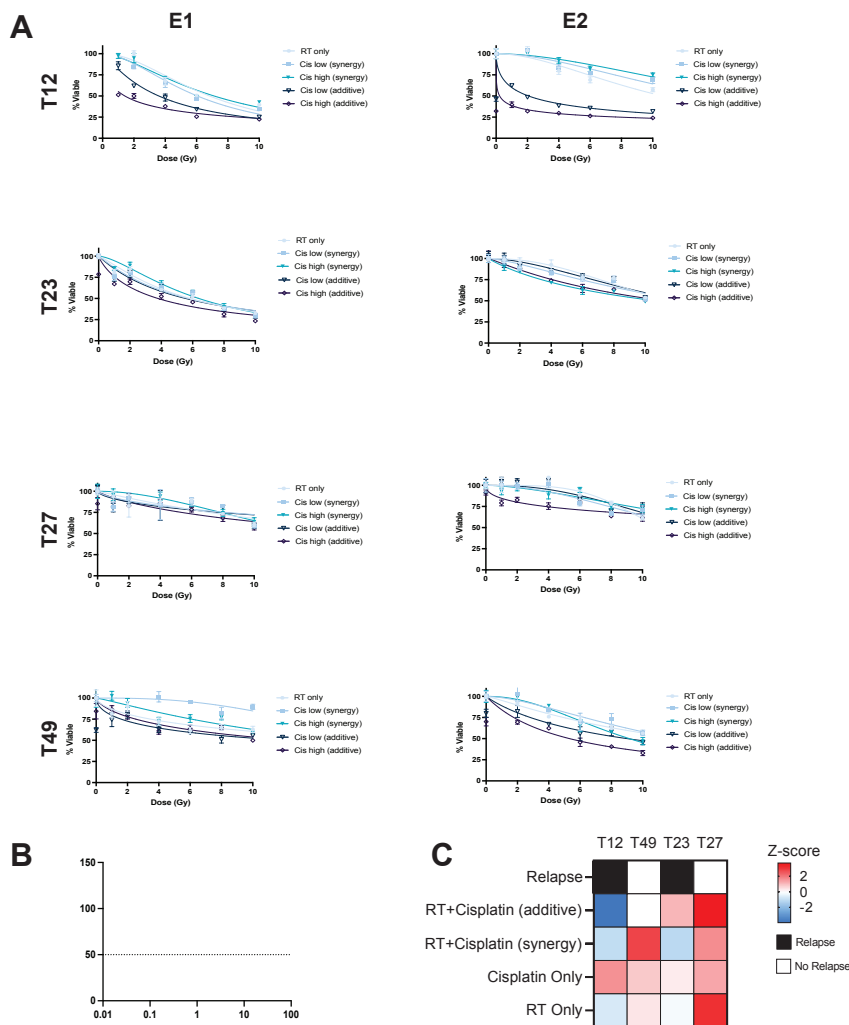


Figure S3. Chemo-radiotherapy screening in organoids derived from patients who received chemoradiotherapy in the clinic, related to Figure 4A.

A. Dose-response curves show percentage of viable organoids (T12, T23, T27 and T49) following exposure to increasing dosage of irradiation (1-10 Gy) alone or in combination with cisplatin at a low (3 μ M) and high (5 μ M) concentration, E1 (Experiment 1) on the left and E2 on the right. Error-bars represent standard error of the mean (SEM) of 4 technical replicates in the cisplatin- treated conditions and 6 technical replicates in the RT only conditions, each curve is representative of 2 biological replicates. B. Dose-response curves of organoids T12, T23, T27, T49 and T46 exposed to a titration of cisplatin monotherapy. The percentage of viability is calculated per concentration of cisplatin, normalized to solvent-only (untreated), error bars are SEM of 4 technical replicates, each curve is representative of 2 biological replicates. C. Heatmap represents the Z-score AUC taken from 4 HNC organoids exposed to: RT only, cisplatin + RT and cisplatin only from patients that received cisplatin + RT in the clinic. Z-score AUC depicts the range of more sensitive (blue) to least sensitive (red). Organoid sensitivity has been ranked from most to least sensitive to cisplatin + RT (additive), clinical relapse (black) is indicated at the top.

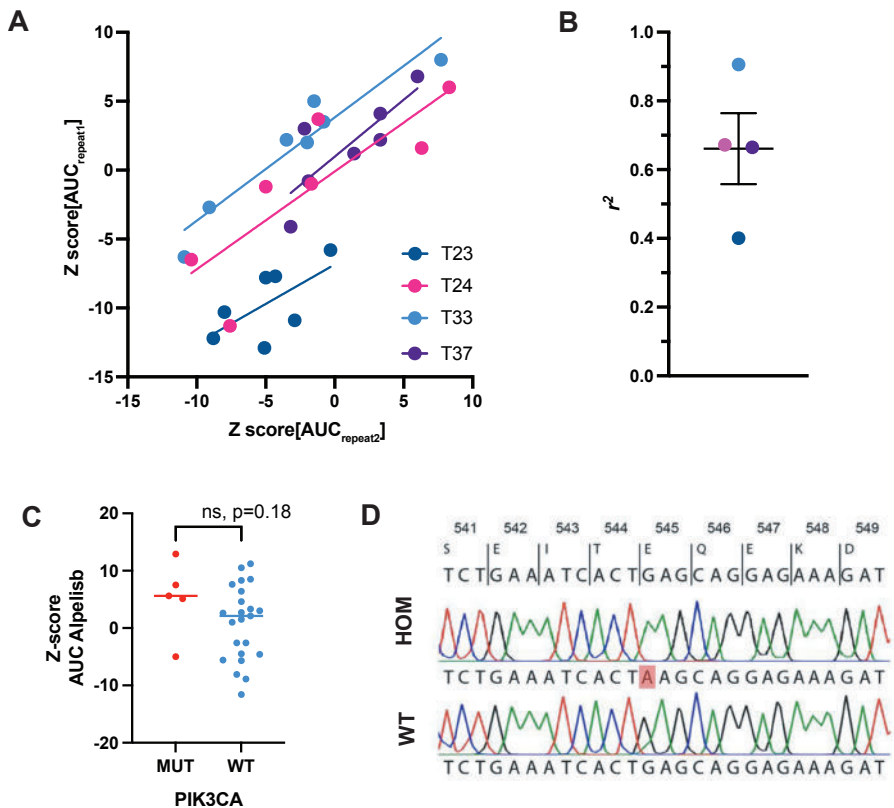


Figure S4. Targeted therapy in organoids, related to Figure 5.

A. correlation between Z-score normalised AUC values for the seven drugs depicted in Figure 5A. Each color indicates a different organoid culture. B. r^2 for the correlation depicted in panel A. color coding is identical to A. C. Alpelisib sensitivity of organoids carrying a PIK3CA activating mutation (red) versus organoids without PIK3CA activating mutation (blue). T-test, ns, $p=0.1811$. D. Sanger sequencing results of generated from one PIK3CA E545K mutant and a wildtype control. The G<A mutation induced is indicated in a red triangle. Top row indicates the sequencing results of one of generated mutants. Bottom row indicates sequencing results of the wildtype parent culture.

Supplementary table 2. Antibody Specifications, related to STAR METHODS

Primary							
Antibody	Supplier	Catalogue number	Host Species	Clone	Lot number	Dilution	Pretreatment/ Antigen Retrieval
AE1AE3	Roche	5267145001	Mouse	AE1/AE3/PCK2 6	J12362	RTU	CC1 '16/'8 Ab/ '4 post Prot 3
CK13	Invitrogen	MA1-5764	Rabbit	AE8	76403269	1 in 1000	CC1 24/'32'ab
P63	Ventana	790-4509	Mouse	4A4	J14838	RTU	CC1 '24/Ab '32/AMP
P16NK4a	Roche	6695256001	Mouse	E6H4	J19683	RTU	48 CC1/ '12 Ab
CDX2	Cellmarque	760-4380	Rabbit	EPR2764Y	V0002431	RTU	CC1 32/'16'Ab
α -amylase	Sigma	A8273-1VL	Rabbit	Polyclonal		1 in 1000 O/N RT	Citrate buffer
Aquaporin 5 (AQP5)	Origene	TA321387	Rabbit	Polyclonal		1 in 800 O/N RT	Citrate buffer
yH2AX	Milipore	MA1-2022	Mouse	3F2		1 in 500 O/N 4C	
Secondary							
Goat anti-mouse AF-488	Thermofisher	A28175	Goat			1 in 500	



CHAPTER 4

p-mTOR, p-ERK and PTEN expression in tumor biopsies and organoids as predictive biomarkers for patients with HPV negative head and neck cancer.

W.W.B. de Kort, E.J. de Ruiter, W.E. Haakma, E. Driehuis,
L.A. Devriese, R.J.J. van Es, S.M. Willems

ABSTRACT

Background

Survival rates of head and neck squamous cell carcinoma (HNSCC) have only marginally improved in the last decades. Hence there is a need for predictive biomarkers for long-time survival that can help to guide treatment decisions and might lead to the development of new therapies. The phosphatidylinositol 3-kinase (PI3K)/AKT/mTOR signaling pathway is the most frequently altered pathway in HNSCC, genes are often mutated, amplified and overexpressed causing aberrant signaling affecting cell growth and differentiation. Numerous genetic alterations of upstream and downstream factors have currently been clarified. However, their predictive value has yet to be established. Therefore we assess the predictive value of p-mTOR, p-ERK and PTEN expression

Methods

Tissue microarrays(TMA's) of HPV-negative patients with oropharyngeal (n=48), hypopharyngeal (n=16) or laryngeal (n=13) SCC, treated with primary chemoradiation (cisplatin/carboplatin/cetuximab and radiotherapy), were histologically stained for p-mTOR, PTEN and p-ERK. Expression was correlated to overall survival (OS), disease free survival (DFS) and locoregional control (LRC). Also p-mTOR was histologically stained in a separate cohort of HNSCC organoids (n=8) and correlated to mTOR-inhibitor everolimus response.

Results

High p-mTOR expression correlated significantly with worse OS in multivariate analysis in the whole patient cohort (Hazar Ratio(HR)1.06, 95%CI 1.01–1.11, p=0.03) and in the cisplatin/carboplatin group with both worse OS (HR1.09, 95%CI1.02–1.16, p=0.02) and DFS (HR1.06, 95%CI 1.00–1.12, p=0.04). p-ERK expression correlated significantly with DFS in univariate analysis in the whole patient cohort (HR1.03, 95%CI 1.00–1.05, p=0.04) and cisplatin/carboplatin group (HR1.03, 95%CI1.00–1.07, p=0.04). PTEN-expression did not correlate with OS/DFS/LRC. Better organoid response to everolimus correlated significantly to higher p-mTOR expression (Rs = -0.731, p=0.04).

Conclusion

High p-mTOR expression predicts and high p-ERK expression tends to predict worse treatment outcome in HPV negative HNSCC patients treated with chemoradiation, providing additional evidence that these markers are candidate prognostic biomarkers for survival in this patient population. Also this study shows that the use of HNSCC organoids for biomarker research has potential. The role of PTEN expression as prognostic biomarker remains unclear, as consistent evidence on its prognostic and predictive value is lacking.

INTRODUCTION

Head and neck cancer is the 7th most common type of cancer worldwide with approximately 1.000.000 new cases in 2020¹. Over 95% of these cancers are squamous cell carcinoma (SCC)²⁻⁴. In current practice, therapy for head and neck squamous cell carcinoma (HNSCC) generally depends on the anatomical location. For oral SCC, the standard treatment is primary surgery, whereas pharyngeal and laryngeal SCC often undergo primary (chemo)radiation. At the time of diagnosis, HNSCC has frequently spread to regional lymph nodes. Despite advances in surgical techniques and adjuvant therapies, survival rates have only marginally improved over the last two decades⁵. Therefore, there is a need for biomarkers predicting long-time survival that can help to guide treatment decisions and might lead to the development of new therapies^{6,7}.

The phosphatidylinositol 3-kinase (PI3K)/AKT/mTOR signaling pathway is the most frequently altered pathway in HNSCC⁸. Normal activation of this signaling pathway fosters cell growth, survival, development and differentiation⁹. In HNSCC, genes in the PI3K-pathway are often mutated, amplified and overexpressed causing aberrant signaling¹⁰. This affects normal cell growth, survival and differentiation contributing to development and maintenance of cancer. Numerous genetic alterations of upstream and downstream factors have currently been clarified. However, their predictive value has yet to be established.

The 'mammalian target of rapamycin'(mTOR) is part of the PI3K/AKT/mTOR-pathway and is a serine/threonine kinase which mediates cellular homeostasis and growth^{11,12}. mTOR is activated by phosphorylation (p-mTOR). Aberrant mTOR signaling is commonly observed in cancer, making it an interesting therapeutic target. mTOR-inhibition as therapy for HNSCC was reviewed in several clinical trials. Tumor response improved after treatment with mTOR-inhibition in combination with other agents¹³. Increased activation of mTOR is associated with worse survival in several types of cancer¹⁴⁻¹⁹. Also for oral, tongue and esophageal SCC, mTOR-expression is associated with worse survival^{20,21}.

Phosphatase and tensin homolog (PTEN) is a protein encoded by the PTEN tumor suppressor gene²². PTEN is a natural inhibitor of the PI3K pathway and thereby a tumor suppressor gene. Loss of PTEN results in PI3K/AKT/mTOR pathway overactivity. PTEN mutations have been described in several tumor types²³⁻²⁶. Loss of PTEN on protein level correlates with a worse prognosis in breast, prostate and lung cancers²⁷⁻²⁹. In HNSCC, PTEN mutations are present in 5-10% of the patients³⁰⁻³². Also for tongue cancer, loss of PTEN on protein level is associated with worse survival^{33,34}.

Apart from the PI3K/AKT/mTOR pathway, the Ras/Raf/MEK/ERK pathway also contributes to cell cycle proliferation. Phosphorylated ERK (p-ERK) phosphorylates cytoskeletal proteins, kinases

and several transcriptional factors³⁵, leading to cellular survival, proliferation, differentiation and angiogenesis³⁶. ERK expression correlated with worse survival in several types of cancer^{37–41}. In nasopharyngeal carcinoma, high p-ERK expression correlates with worse survival⁴².

In this study, we assess the predictive value of p-mTOR, p-ERK and PTEN expression in a cohort of patients with HPV-negative oropharyngeal, hypopharyngeal and laryngeal SCC who were treated with primary chemoradiotherapy. Moreover, we assess the p-mTOR expression and mTOR inhibition response by everolimus in a cohort of HNSCC organoids.

MATERIALS AND METHODS

Patients and clinical data

This study uses a retrospective cohort of patients with HNSCC, treated at the University Medical Center (UMC) Utrecht described previously by de Ruiter et al. in 2020⁴³. Inclusion criteria were: HPV-negative oropharyngeal, hypopharyngeal and laryngeal SCC (1), treated with radiotherapy and concomitant cisplatin, carboplatin or cetuximab with curative aim (2) whereof both clinical response data and tumor tissue was available (3). Exclusion criteria were: previous radiotherapy in the head and neck region, complete surgical resection of tumor, presence of distant metastases, presence of a prognosis-affecting double or prior malignancy. The following clinical data were collected: age, sex, tumor site, T and N stage.

All patients were treated with primary chemoradiotherapy. Standard treatment consisted of 35 fractions of 2 Gy (total 70 Gy) on both the primary tumor and positive lymph nodes. An elective total dose of 46–57.75 Gy on other lymph nodes, combined with 3 cycles of cisplatin or carboplatin administered intravenously every three weeks, or weekly cetuximab intravenously.

Tissue microarray construction and immunohistochemistry

Pre-treatment biopsies were collected from every patient and were formalin fixed and paraffin embedded (FFPE). To determine representative tumor regions, sections of the FFPE blocks were stained with hematoxylin and eosin and assessed by a head and neck pathologist (SW). From these tumor regions, three tissue cores of 0.6mm were obtained from the FFPE blocks and collected in a tissue microarray (TMA). The TMA was constructed using an automated tissue microarray instrument as described before⁴⁴. TMA tissue sections (4 µm) were immunohistochemically stained with antibodies for the following antigens: phospho-mTOR (Ser2448; 49F9; 1:300; Cell Signaling), phospho-MAPK (ERK1/2) (p42/44; D13.14.4E; 1:400; Cell Signaling), PTEN (138G6; 1:100; Cell signaling). All antibodies were visualized with 3,3'-diaminobenzidine (DAB) chromagen and hematoxylin was used for counterstaining. Like TMA's, organoids were FFPE and stained for phosphor-mTOR as described above.

HPV detection

All patients in this study had a HPV-negative tumor. Tumors were stained for p16 INK4a by immunohistochemistry (JC8, 1:1200, Immunologic) and considered HPV-negative if less than 70% of tumor cells stained positive. Presence of HPV-DNA was tested in p16 positive tumors by PCR. These tumors were excluded if high-risk HPV-DNA was detected⁴⁵.

Immunohistochemical analysis

The staining assessment was performed by a head and neck researcher (EDR) and a dedicated head and neck pathologist (SW), who were blinded for clinical outcome. Discrepancies were resolved by consensus. For each marker, staining intensity (0-3) and the percentage of stained tumor cells (0-100%) were scored. Cells were considered positive for p-mTOR and PTEN if expression was observed in the cytoplasm. Scoring of p-ERK was based on expression in the cytoplasm and in the nucleus. For organoids, expression of p-mTOR was scored in the same way as described above.

Organoids and Everolimus

HNSCC organoids from oral cavity and larynx were cultured as described earlier by Driehuis et al.⁴⁶ and Millen et al.⁴⁷ Organoids were treated with everolimus (LC Laboratories, catalog no. E4040) an mTOR inhibitor. This drugscreen was described in detail by Driehuis et al. previously⁴⁶. The Biobank Research Ethics Committee of the University Medical Center Utrecht (TCBio) approved the biobanking protocol: 12-093 HUB-Cancer according to the University Medical Center Utrecht (UMCU) Biobanking Regulation. All donors participating in this study signed informed-consent forms and can withdraw their consent at any time.

Statistical analysis

For each TMA core, a H-score was calculated by multiplying the intensity with the percentage of positive cells resulting in scores ranging from 0-300⁴⁸. The H-score for each tumor was calculated by averaging their corresponding TMA cores. Tumors were excluded from analysis if less than two TMA cores were assessable. Of patients where three TMA cores were available, intraclass correlation coefficients (ICCs) were calculated. A model with two-way mixed-effects was used⁴⁹.

The expression p-mTOR, p-ERK and PTEN was correlated to overall survival (OS), disease-free survival (DFS) and locoregional control (LRC). OS was defined as the number of days between the date of inclusion (first hospital visit before start of treatment) and date of death. DFS and LRC were defined as the number of days between the last day of radiotherapy and recurrence of the disease or date of death. Patients were censored at the date of last visit in case of absence of an event.

Expression of biomarkers was correlated with clinical variables. The correlation between tumor site and biomarker expression was assessed using a Kruskal-Wallis test. For dichotomous variables and biomarker expression Mann-Whitney U tests were used. Correlation of age and biomarker expression was assessed with a Spearman's rank correlation coefficient. Univariate and multivariate cox proportional hazard regressions were used to assess the correlation of biomarker expression with OS, DFS and LRC. The multivariate model contained: biomarker as predictor corrected for age, gender, T-stage and N-stage. Statistical analysis was performed with SPSS Statistics (IBM Corp. Released 2020. IBM SPSS Statistics for Windows, Version 27.0. Armonk, NY: IBM Corp). The prognostic value of p-mTOR, p-ERK and PTEN expression was visualized by Kaplan–Meier curves comparing tumors with high and low biomarker expression stratified by the median value (Figure 2, Supplemental Figure 2, Supplemental figure 3). A spearman's rank-order correlation was run to assess the Correlation between p-mTOR and PTEN.

For organoids a H-score of p-mTOR was calculated as described above. Response to everolimus was extracted using the Area Under the Curve(AUC) in the dose-response curve (Figure 3). A spearman's rank-order correlation was run to assess the relationship between H-score of p-mTOR expression and AUC of everolimus response in all HNSCC organoids.

RESULTS

Patient characteristics

A total of 77 patients with a mean age of 61.4 years were included for analysis: 48 with oropharyngeal, 16 with hypopharyngeal and 13 with laryngeal cancer. The 3- and 5-year OS of the patient cohort was 46% and 31%, respectively. The patient characteristics are described in Table 1.

All patients were treated with radiotherapy in combination with cisplatin (n=53), carboplatin (n=3) or cetuximab (n=21). A total of 8 HNSCC organoids were established including oral cavity (n=6), larynx (n=2).

Immunohistochemistry

Of each tumor, three tissue cores were included in the TMA. However, some tissue cores were lost during processing or didn't contain sufficient tumor cells. Cases were excluded if there were less than 2 out of 3 cores assessable. Consequently, for p-mTOR, 75 cases were eligible for inclusion, for p-ERK 69 cases, and for PTEN 72 cases.

Representative images of TMA cores containing low and high expression of each marker are displayed in Figure 1. Boxplots were generated to represent the distribution of the scoring

data of each marker (supplemental Figure 1). The median H-scores per marker of the patient cohort and organoids with corresponding interquartile ranges are displayed in supplementary Table 1.

Table 1: Characteristics study population.

Characteristic		n	% of total n
Sex	Female	31	(40.3%)
	Male	46	(59.7%)
Tumor site	Oropharynx	48	(62.3%)
	Hypopharynx	16	(20.8%)
	Larynx	13	(16.9%)
T-stage	T1	1	(1.3%)
	T2	4	(5.2%)
	T3	27	(35.1%)
	T4a	38	(49.4%)
	T4b	7	(9.1%)
N-stage	N0	9	(11.7%)
	N1	6	(7.8%)
	N2a	2	(2.6%)
	N2b	23	(29.9%)
	N2c	37	(48.1%)
Immunohistochemistry	p-mTOR	75	(97.4%)
	p-ERK	69	(89.6%)
	PTEN	72	(93.5%)

Correlation clinicopathologic parameters

No significant correlations between clinicopathologic parameters and immunohistochemical expression of p-mTOR, p-ERK and PTEN were observed. The results of all correlations are displayed in supplementary Table 2. None of the clinical variables showed a correlation with OS, DFS and LRC (Table 2).

p-mTOR expression

A 10-point p-mTOR H-score increase correlated significantly with a worse OS in univariate analysis (HR 1.06, 95%CI 1.01 – 1.11, $p=0.03$)(Table 2), sub analysis of the Cisplatin/Carboplatin group showed this worse OS likewise (HR 1.08, 95%CI 1.01 – 1.15, $p=0.02$)(Table 3). In multivariate analysis a 10-point p-mTOR H-score increase remained independently correlated with worse OS in the whole patient cohort (HR 1.06, 95%CI 1.01 – 1.11, $p=0.03$)(Table 2) as well as in the cisplatin/carboplatin group (HR 1.09, 95%CI 1.02 – 1.16, $p=0.02$)(Table 3).

10-point p-mTOR H-score increase did not correlate with DFS and LRC in univariate and multivariate analysis in the patient cohort (Table 2). However, sub analysis of the cisplatin/ carboplatin group showed a significant correlation with worse DFS in multivariate analysis (HR 1.06, 95%CI 1.00 – 1.12, p=0.04)(Table 3). The prognostic value of p-mTOR in a Kaplan-Meier curve is displayed in Figure 2. Sub analysis per subsite is displayed in supplemental Table 3.

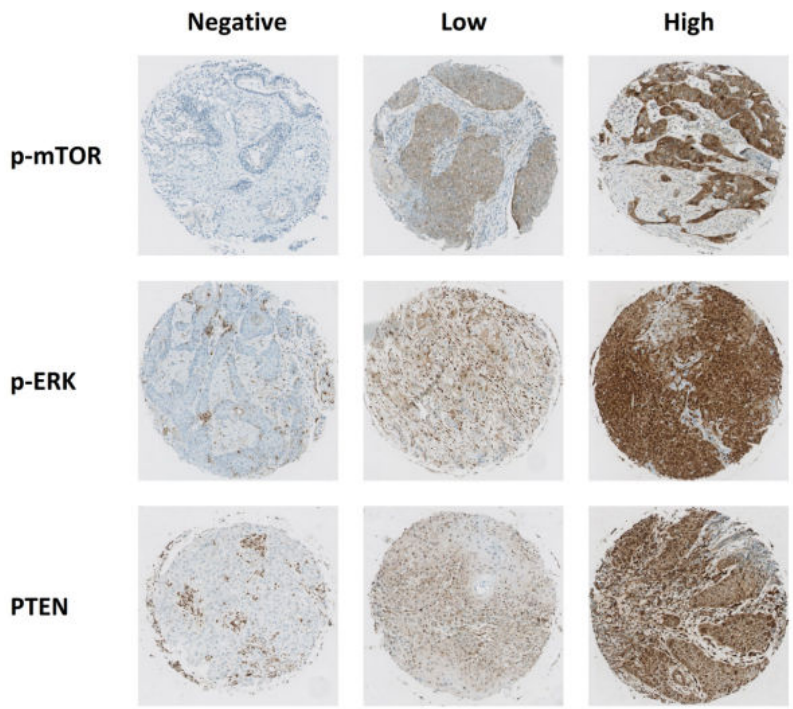


Figure 1: Representative images of TMA cores with negative, low and high scores for p-mTOR, p-ERK and PTEN expression.

ICCs were calculated for three TMA cores from the same patients. Three TMA cores were available for p-mTOR (n=57, 76%), p-ERK (n=48, 70%) and PTEN (n=51, 71%). ICC for p-mTOR cases was 0.83 (95%CI 0.73 – 0.89), for p-ERK cases 0.78 (95%CI 0.65 – 0.87) and for PTEN cases 0.88 (95%CI 0.81 – 0.93). ICCs for all three markers are therefore considered good⁴⁹.

Table 2: Univariate/Multivariate analysis between markers and OS,DFS and LRC in whole study population.

Univariate analysis			OS		DFS		LRC	
Marker	Comparison	n	HR (95%CI)	p	HR (95%CI)	p	HR (95%CI)	p
p-mTOR	Per 10 H-score increase	75	1.06 (1.01 – 1.11)	0.03	1.04 (0.99 – 1.08)	0.11	1.00 (0.94 – 1.07)	0.98
p-ERK	Per 10 H-score increase	69	1.02 (0.99 – 1.05)	0.17	1.03 (1.00 – 1.05)	0.04	1.03 (1.00 – 1.06)	0.08
PTEN	Per 10 H-score increase	72	1.06 (0.99 – 1.15)	0.11	1.02 (0.95 – 1.10)	0.58	0.97 (0.88 – 1.07)	0.53
T stage	T1-3 vs T4	77	0.71 (0.38 – 1.32)	0.28	0.89 (0.50 – 1.57)	0.69	0.97 (0.46 – 2.05)	0.93
N stage	N0-1 vs N2-3	77	0.94 (0.44 – 2.03)	0.88	0.71 (0.33 – 1.51)	0.37	0.61 (0.21 – 1.75)	0.35
Age	Per 1 increase (year)	77	1.00 (0.95 – 1.05)	1.00	0.98 (0.93 – 1.02)	0.31	1.00 (0.94 – 1.06)	0.91
Sex	Male vs Female	77	1.43 (0.78 – 2.63)	0.25	1.55 (0.86 – 2.78)	0.14	2.07 (0.91 – 4.70)	0.08
Multivariate analysis			OS		DFS		LRC	
Marker	Comparison	n	HR (95%CI)	p	HR (95%CI)	p	HR (95%CI)	p
p-mTOR	Per 10 H-score increase	75	1.06 (1.01 – 1.11)	0.03	1.04 (0.99 – 1.09)	0.11	1.00 (0.94 – 1.07)	0.96
p-ERK	Per 10 H-score increase	69	1.02 (0.99 – 1.05)	0.19	1.02 (0.99 – 1.05)	0.07	1.03 (0.99 – 1.06)	0.13
PTEN	Per 10 H-score increase	72	1.07 (0.99 – 1.15)	0.09	1.02 (0.95 – 1.10)	0.54	0.98 (0.88 – 1.08)	0.62

Univariate/Multivariate Cox proportional hazards regression of markers/clinicopathological parameters and overall survival (OS), Disease free survival (DFS) and Locoregional control (LRC). The prognostic values are displayed in Hazard Ratios (HR). 95%CI, 95% Confidence interval. Significant p-values (p < 0.05) are shown in bold. Multivariate: Model contains biomarker as predictor corrected for age, gender, T-stage and N-stage.

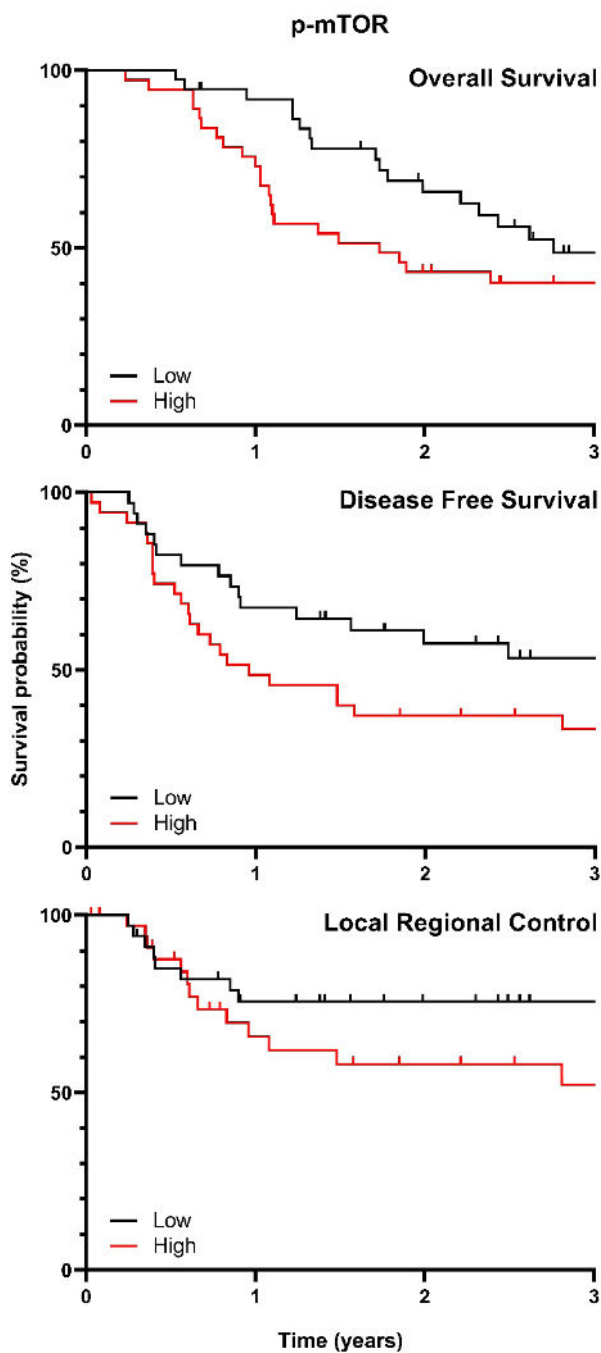


Figure 2: Kaplan-Meier curves visualizing the association between p-mTOR expression and OS, DFS and LRC. The median score of expression was used as cutoff for the survival analysis.

p-ERK expression

10-point p-ERK H-score increase correlated significantly with worse DFS in univariate analysis in the patient cohort (HR 1.03, 95%CI 1.00 – 1.05, $p=0.04$)(Table 2) and in the cisplatin/carboplatin group (HR 1.03, 95%CI 1.00 – 1.07, $p=0.04$)(Table 3). In multivariate analysis 10-point p-ERK H-score increase did not remain independently correlated with DFS, although trends were observed: whole patient cohort (HR 1.02, 95%CI 0.99 – 1.05, $p=0.07$)(Table 2) and cisplatin/carboplatin group (HR 1.03, 95%CI 1.00 – 1.06, $p=0.08$)(Table 3).

10 point p-ERK H-score increase did not correlate with OS and LRC in uni – and multivariate analysis. However trends were observed for worse LRC in univariate analysis; whole patient cohort (HR 1.03, 95%CI 1.00 – 1.06, $p=0.08$)(Table 2) and cisplatin/carboplatin group (HR 1.03 95%CI 1.00 – 1.08, $p=0.08$)(Table 3). The prognostic value of p-ERK in a Kaplan-Meier curve is displayed in Supplemental Figure 2. Sub analysis per subsite is displayed in supplemental Table 3.

PTEN-expression

10 point PTEN H-score increase did not correlate with OS, DFS and LRC. Though, a trend was observed in the cisplatin/carboplatin group for worse OS in univariate (HR 1.09, 95%CI 0.99 – 1.20, $p=0.07$)(Table 3) and in multivariate analysis (HR 1.10, 95%CI 1.00 – 1.21, $p=0.06$)(Table 3). The prognostic value of PTEN in a Kaplan-Meier curve is displayed in Supplemental Figure 3. Sub analysis per subsite is displayed in supplemental Table 3.

Everolimus organoid response

The mean AUC of the organoids was 177.2 (95%CI 120.9 – 233.4). The mean H-score of p-mTOR expression in the organoids was 90.6 (95%CI 51.5 – 129.7). There was a statistically significant negative correlation between H-score and AUC $R_s = -0.731$, $p=0.04$ (Spearman's rank order correlation), indicating a lower AUC (less organoid viability interpreted as better response to everolimus) correlates with a higher expression of p-mTOR measured as H-score (Figure 3).

Table 3: Univariate/Multivariate sub-analysis between markers and OS,DFS and LRC in HPV negative patients treated with cisplatin/carboplatin.

Univariate analysis			OS		DFS		LRC	
Marker	Comparison	n	HR (95%CI)	p	HR (95%CI)	p	HR (95%CI)	p
p-mTOR	Per 10 H-score increase	54	1.08 (1.01 – 1.15)	0.02	1.06 (1.00 – 1.12)	0.06	1.02 (0.95 – 1.10)	0.55
p-ERK	Per 10 H-score increase	50	1.03 (0.99 – 1.06)	0.16	1.03 (1.00 – 1.07)	0.04	1.03 (1.00 – 1.08)	0.08
PTEN	Per 10 H-score increase	53	1.09 (0.99 – 1.20)	0.07	1.03 (0.94 – 1.13)	0.52	0.96 (0.85 – 1.10)	0.57
T stage	T1-3 vs T4	56	0.82 (0.39 – 1.72)	0.59	0.94 (0.47 – 1.86)	0.85	0.78 (0.32 – 1.93)	0.59
N stage	N0-1 vs N2-3	56	0.78 (0.27 – 2.24)	0.64	0.54 (0.19 – 1.53)	0.24	0.23 (0.03 – 1.69)	0.15
Age	Per 1 increase (year)	56	0.97 (0.91 – 1.02)	0.23	0.95 (0.90 – 1.00)	0.06	0.96 (0.89 – 1.03)	0.22
Sex	Male vs Female	56	1.10 (0.53 – 2.29)	0.80	1.22 (0.61 – 2.46)	0.57	1.47 (0.58 – 3.73)	0.42
Multivariate analysis			OS		DFS		LRC	
Marker	Comparison	n	HR (95%CI)	p	HR (95%CI)	p	HR (95%CI)	p
p-mTOR	Per 10 H-score increase	54	1.09 (1.02 – 1.16)	0.02	1.06 (1.00 – 1.12)	0.04	1.02 (0.95 – 1.10)	0.54
p-ERK	Per 10 H-score increase	50	1.03 (0.99 – 1.07)	0.17	1.03 (1.00 – 1.06)	0.08	1.02 (0.98 – 1.06)	0.31
PTEN	Per 10 H-score increase	53	1.10 (1.00 – 1.21)	0.06	1.04 (0.94 – 1.14)	0.47	0.97 (0.86 – 1.10)	0.68

Univariate/Multivariate Cox proportional hazards regression of markers/clinicopathological parameters and overall survival (OS), Disease free survival (DFS) and Locoregional control (LRC). The prognostic values are displayed in Hazard Ratios (HR). 95%CI, 95% Confidence interval. Significant p-values (p < 0.05) are shown in bold. Multivariate: Model contains biomarker as predictor corrected for age, gender, T-stage and N-stage.

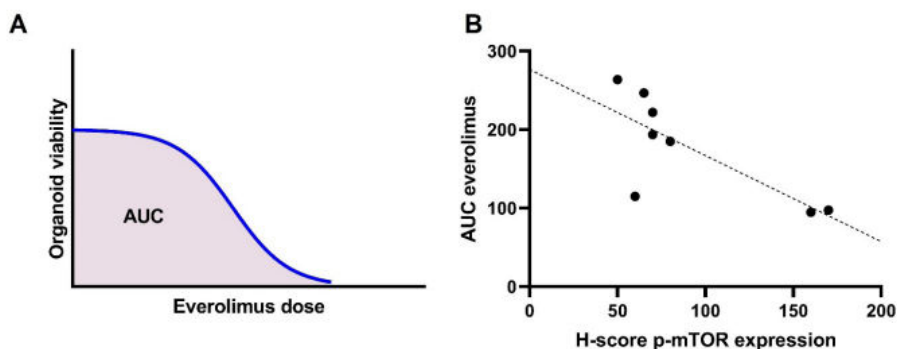


Figure 3. A: Example of an everolimus dose-response curve depicted in blue with corresponding Area Under the Curve (AUC) shown in red. Everolimus dose increases on x-axis to the right. Organoid viability decreases if value on Y-axis is lower. B: correlation of organoid response to everolimus (Y-axis) to H-score p-mTOR expression (X-axis)

DISCUSSION

HNSCC-survival only marginally improved over the last decades⁵. Therefore, there is a need for prognostic and predictive biomarkers for long-time survival that can help to guide treatment decisions and might lead to the development of new therapies^{6,7}. In this study we determined p-mTOR, PTEN and p-ERK expression and correlated it with survival in patients with HPV-negative oropharyngeal, hypopharyngeal and laryngeal SCC, treated with primary chemoradiotherapy and assessed p-mTOR expression and everolimus response in a subset of HNSCC organoids.

In solid tumors, mTOR is often activated⁵⁰. The prognostic value of mTOR expression is still unclear. This study demonstrates in multivariate analysis that higher p-mTOR expression correlates with worse OS in a homogeneous cohort of 75 HNSCC patients. Several other studies also investigated the prognostic value of mTOR in HNSCC. For oral SCC, high p-mTOR expression correlated with poor survival in two studies^{51,52}. Li et al. investigated p-mTOR expression in patients with tongue SCC and found a worse overall survival with higher p-mTOR expression⁵³. For laryngeal SCC, one study showed that high p-S6 expression, a surrogate marker of mTORC1 activation, correlated with improved survival⁵⁴. This is not in line with the studies mentioned above, however, the investigated marker was different from p-mTOR. Although several subsites of HNSCC were examined, results are inconclusive.

Our study only included HPV-negative patients. HPV-positive patients are considered a separate group of HNCC and appear to have an increased survival^{55,56}. Wilson et al. assessed

the prognostic value of mTOR in both HPV-negative and HPV-positive patients and found that high mTOR expression correlated with worse outcome in HPV-negative patients, which is in line with our findings. For HPV-positive patients they were not able to correlate mTOR expression with outcome⁵⁷. This could be because HPV-positive patients harbor significantly less p53 mutations compared to HPV-negative patients⁵⁸ and, once activated, p53 is known to inhibit the activity of mTOR⁵⁹. There are several studies that assessed the prognostic value of mTOR. Most of the studies included patients receiving postoperative chemotherapy and/or radiotherapy, which is different from our study that only included patients treated with primary chemoradiotherapy. The results of this study are in line with aforementioned studies⁵¹⁻⁵³, indicating that mTOR expression correlates with worse overall survival.

In addition to p-mTOR expression in patients, we investigated p-mTOR expression in a panel of HNSCC organoids. Here we show that HNSCC organoids express p-mTOR on protein level and that the expression, depicted in H-score, is comparable with p-mTOR expression in our patient cohort (Supplemental Figure 1). As mTOR is a potential target for targeted therapy we assessed everolimus response in 8 HNSCC organoids and investigated if p-mTOR expression correlated with everolimus response. Despite the small sample size we demonstrated a correlation of p-mTOR expression and everolimus response. This finding underscores that organoid-platforms are suitable to perform biomarker research, validation and assessment of targeted therapies in HNSCC^{46,47}.

As PTEN loss is more often seen in an aggressive tumor-type⁶⁰ it could explain the worse survival in HNSCC^{33,34}. Malfunctioning leads to overactivity of the AKT/mTOR signaling pathway, and a correlation between loss of PTEN and worse survival seems logical. However, the results of this study do not support this hypothesis. Patients with lower PTEN tumor expression even have a tendency to improved OS ($p = 0.11$). This could be explained by ignition of negative feedback loops by AKT/mTOR overexpression leading to higher PTEN expression in response⁶¹. In our cohort, sub analysis shows a statistically significant positive correlation between p-mTOR – and PTEN expression $R_s = 0.245$ $p=0.04$ which supports this hypothesis.

Lee et al. found worse survival in case of PTEN loss in patients with oral tongue SCCs receiving surgery³³. Compared to this study, they investigated a different treatment modality and a different subsite. Additionally, PTEN expression can differ per subsite⁶². Also scoring systems of PTEN expression differ. Lee et al. compare PTEN expression in tumor and normal tissue to assess PTEN-loss³³. Zhao et al. use four percentage categories of PTEN expressing cells combined with staining intensity³⁴ and our study uses a continuous scale for assessing the percentage of PTEN expressing cells multiplied by the staining intensity ranging from 0-3. These different scoring systems indicate a lack of standard approach. Furthermore, in literature, the terms 'PTEN-expression' and 'PTEN-loss' are used interchangeably and both arguments

make it hard to compare results not supporting generalizability. In other tumor types, loss of PTEN expression has been linked to advanced stage disease^{27–29} which in our study was not assessable as we only included advanced stage HNSCC. Overall, studies investigating PTEN expression report different findings for HNSCC.

The Ras/Raf/MEK/ERK pathway also contributes to cell cycle proliferation³⁵. Activation results in cellular survival, proliferation, differentiation and angiogenesis³⁶. P-ERK is one of the last steps in the pathway making it an interesting therapeutic target. ERK expression correlates with worse overall survival in several types of cancer^{37–41}.

For HNSCC, this study demonstrates that high p-ERK expression correlates with a worse DFS only in univariate analysis and not in the multivariate model ($p=0.07$). The value of p-ERK as prognostic biomarker was analyzed in a few other studies. p-ERK expression correlated with a worse overall survival in nasopharyngeal carcinoma⁴², esophageal SCC⁶³ and oral tongue SCC⁶⁴. In contrast, the study of Psyrri et al. showed an improved overall survival with high ERK expression in patients with oral cavity, oropharyngeal, hypopharyngeal and laryngeal SCC⁶⁵. Although this finding indicates the opposite, this correlation applies for the unphosphorylated ERK expression. Computational biology studies indicate that ERK is inversely correlated with p-ERK⁶⁶, meaning low levels of ERK correspond with high levels of p-ERK. With this in mind, the findings of Psyrri et al.⁶⁵ are in line with the aforementioned studies^{42,63,64}. Since this study is partially in line with literature, p-ERK may be considered a possible prognostic biomarker for HNSCC.

A limitation of this study is the application of TMA's that only partially represent the whole character of the tumor, which is inevitable in daily clinical practice after obtaining tissue biopsies. To overcome this issue, three TMA cores were taken per patient whereby the heterogeneity within the tumor biopsy is taken into account⁶⁷.

CONCLUSION

This study shows that high p-mTOR expression predicts and p-ERK expression tends to predict worse treatment outcome in a cohort of advanced stage, HPV negative HNSCC patients treated with chemoradiation, providing additional evidence that these markers are candidate prognostic biomarkers for survival in this patient population. Also this study shows that the use of HNSCC organoids for biomarker research has potential. The role of PTEN expression as prognostic biomarker remains unclear, as consistent evidence on its prognostic and predictive value is lacking.

REFERENCES

1. Sung H, Ferlay J, Siegel RL, et al. Global Cancer Statistics 2020: GLOBOCAN Estimates of Incidence and Mortality Worldwide for 36 Cancers in 185 Countries. *CA Cancer J Clin.* 2021;71(3):209-249. doi:10.3322/CAAC.21660
2. Chen J, Eisenberg E, Krutchkoff DJ, Katz R V. Changing trends in oral cancer in the United States, 1935 to 1985: A Connecticut study. *J Oral Maxillofac Surg.* 1991;49(11):1152-1158. doi:10.1016/0278-2391(91)90406-C
3. Ostman J, Anneroth G, Gustafsson H, Tavelin B. Malignant oral tumours in Sweden 1960-1989--an epidemiological study. *Eur J Cancer B Oral Oncol.* 1995;31B(2):106-112. doi:10.1016/0964-1955(94)00018-y
4. Muir C, Weiland L. Upper aerodigestive tract cancers. *Cancer.* 1995;75(1 S):147-153. doi:10.1002/1097-0142(19950101)75:1+<147::AID-CNCR2820751304>3.0.CO;2-U
5. Haddad RI, Shin DM. Recent advances in head and neck cancer. *N Engl J Med.* 2008;359(11):1143. doi:10.1056/NEJMra0707975
6. Weber RS, Lewis CM, Eastman SD, et al. Quality and performance indicators in an academic department of head and neck surgery. *Arch Otolaryngol Head Neck Surg.* 2010;136(12):1212-1218. doi:10.1001/archoto.2010.215
7. Hessel AC, Moreno MA, Hanna EY, et al. Compliance with quality assurance measures in patients treated for early oral tongue cancer. *Cancer.* 2010;116(14):3408-3416. doi:10.1002/cncr.25031
8. Lui VWY, Hedberg ML, Li H, et al. Frequent mutation of the PI3K pathway in head and neck cancer defines predictive biomarkers. *Cancer Discov.* 2013;3(7):761-769. doi:10.1158/2159-8290.CD-13-0103
9. Cantley LC. The phosphoinositide 3-kinase pathway. *Science (80-).* 2002;296(5573):1655-1657. doi:10.1126/science.296.5573.1655
10. Cai Y, Dodhia S, Su GH. Dysregulations in the PI3K pathway and targeted therapies for head and neck squamous cell carcinoma. *Oncotarget.* 2017;8(13):22203-22217. doi:10.18632/oncotarget.14729
11. Wullschlegel S, Loewith R, Hall MN. TOR signaling in growth and metabolism. *Cell.* 2006;124(3):471-484. doi:10.1016/j.cell.2006.01.016
12. Shaw RJ, Cantley LC. Ras, PI(3)K and mTOR signalling controls tumour cell growth. *Nature.* 2006;441(7092):424-430. doi:10.1038/nature04869
13. Patel J, Nguyen SA, Ogretmen B, Gutkind JS, Nathan C, Day T. mTOR inhibitor use in head and neck squamous cell carcinoma: A meta-analysis on survival, tumor response, and toxicity. *Laryngoscope Investig Otolaryngol.* 2020;5(2):243-255. doi:10.1002/lto2.370
14. Zhou L, Huang Y, Li J, Wang Z. The mTOR pathway is associated with the poor prognosis of human hepatocellular carcinoma. *Med Oncol.* 2010;27(2):255-261. doi:10.1007/s12032-009-9201-4
15. Bakarakos P, Theohari I, Nomikos A, et al. Immunohistochemical study of PTEN and phosphorylated mTOR proteins in familial and sporadic invasive breast carcinomas. *Histopathology.* 2010;56(7):876-882. doi:10.1111/j.1365-2559.2010.03570.x
16. Sun CH, Chang YH, Pan CC. Activation of the PI3K/Akt/mTOR pathway correlates with tumour progression and reduced survival in patients with urothelial carcinoma of the urinary bladder. *Histopathology.* 2011;58(7):1054-1063. doi:10.1111/j.1365-2559.2011.03856.x
17. Xu D zhi, Geng Q rong, Tian Y, et al. Activated mammalian target of rapamycin is a potential therapeutic target in gastric cancer. *BMC Cancer.* 2010;10(1):1-10. doi:10.1186/1471-2407-10-536

18. Herberger B, Puhalla H, Lehnert M, et al. Activated mammalian target of rapamycin is an adverse prognostic factor in patients with biliary tract adenocarcinoma. *Clin Cancer Res.* 2007;13(16):4795-4799. doi:10.1158/1078-0432.CCR-07-0738
19. Liu D, Huang Y, Chen B, et al. Activation of mammalian target of rapamycin pathway confers adverse outcome in nonsmall cell lung carcinoma. *Cancer.* 2011;117(16):3763-3773. doi:10.1002/cncr.25959
20. Hirashima K, Baba Y, Watanabe M, et al. Phosphorylated mTOR expression is associated with poor prognosis for patients with esophageal squamous cell carcinoma. *Ann Surg Oncol.* 2010;17(9):2486-2493. doi:10.1245/s10434-010-1040-1
21. Li S-H, Chien C-Y, Huang W-T, et al. Prognostic significance and function of mammalian target of rapamycin in tongue squamous cell carcinoma OPEN. doi:10.1038/s41598-017-08345-8
22. Steck PA, Pershouse MA, Jasser SA, et al. Identification of a candidate tumour suppressor gene, MMAC1, at chromosome 10q23.3 that is mutated in multiple advanced cancers. *Nat Genet.* 1997;15(4):356-362. doi:10.1038/ng0497-356
23. Cairns P, Okami K, Halachmi S, et al. Frequent inactivation of PTEN/MMAC1 in primary prostate cancer. *Cancer Res.* 1997;57(22):4997-5000.
24. Tsao H, Zhang X, Benoit E, Haluska FG. Identification of PTEN/MMAC1 alterations in uncultured melanomas and melanoma cell lines. *Oncogene.* 1998;16(26):3397-3402. doi:10.1038/sj.onc.1201881
25. Duerr EM, Rollbrocker B, Hayashi Y, et al. PTEN mutations in gliomas and glioneuronal tumors. *Oncogene.* 1998;16(17):2259-2264. doi:10.1038/sj.onc.1201756
26. Perren A, Weng LP, Boag AH, et al. Immunohistochemical evidence of loss of PTEN expression in primary ductal adenocarcinomas of the breast. *Am J Pathol.* 1999;155(4):1253-1260. doi:10.1016/S0002-9440(10)65227-3
27. Depowski PL, Rosenthal SI, Ross JS. Loss of expression of the PTEN gene protein product is associated with poor outcome in breast cancer. *Mod Pathol.* 2001;14(7):672-676. doi:10.1038/modpathol.3880371
28. McMenamin ME, Soung P, Perera S, Kaplan I, Loda M, Sellers WR. Loss of PTEN expression in paraffin-embedded primary prostate cancer correlates with high Gleason score and advanced stage. *Cancer Res.* 1999;59(17):4291-4296.
29. Tang JM, He QY, Guo RX, Chang XJ. Phosphorylated Akt overexpression and loss of PTEN expression in non-small cell lung cancer confers poor prognosis. *Lung Cancer.* 2006;51(2):181-191. doi:10.1016/j.lungcan.2005.10.003
30. Stransky N, Egloff AM, Tward AD, et al. The Mutational Landscape of Head and Neck Squamous Cell Carcinoma. *Source Sci New Ser.* 2011;333(6046):1157-1160. doi:10.1126/science.1206923
31. Poetsch M, Lorenz G, Kleist B. Detection of new PTEN/MMAC1 mutations in head and neck squamous cell carcinomas with loss of chromosome 10. *Cancer Genet Cytogenet.* 2002;132(1):20-24. doi:10.1016/S0165-4608(01)00509-X
32. Shao X, Tandon R, Samara G, et al. Mutational analysis of the PTEN gene in head and neck squamous cell carcinoma. *Int J Cancer.* 1998;77(5):684-688. doi:10.1002/(SICI)1097-0215(19980831)77:5<684::AID-IJC4>3.0.CO;2-R
33. Lee JI, Soria JC, Hassan KA, et al. Loss of PTEN expression as a prognostic marker for tongue cancer. *Arch Otolaryngol - Head Neck Surg.* 2001;127(12):1441-1445. doi:10.1001/archotol.127.12.1441
34. Zhao J, Chi J, Gao M, Zhi J, Li Y, Zheng X. Loss of PTEN Expression Is Associated With High MicroRNA 24 Level and Poor Prognosis in Patients With Tongue Squamous Cell Carcinoma. *J Oral Maxillofac Surg.* 2017;75(7):1449.e1-1449.e8. doi:10.1016/j.joms.2017.03.025
35. Wortzel I, Seger R. The ERK cascade: Distinct functions within various subcellular organelles. *Genes and Cancer.* 2011;2(3):195-209. doi:10.1177/1947601911407328

36. Gough NR. MAPK signaling focus issue: Recruiting players for a game of ERK. *Sci Signal*. 2011;4(196):eg9. doi:10.1126/scisignal.2002601
37. Bartholomeusz C, Gonzalez-Angulo AM, Liu P, et al. High ERK Protein Expression Levels Correlate with Shorter Survival in Triple-Negative Breast Cancer Patients. *Oncologist*. 2012;17(6):766-774. doi:10.1634/theoncologist.2011-0377
38. Schmitz KJ, Wohlschlaeger J, Lang H, et al. Activation of the ERK and AKT signalling pathway predicts poor prognosis in hepatocellular carcinoma and ERK activation in cancer tissue is associated with hepatitis C virus infection. *J Hepatol*. 2008;48(1):83-90. doi:10.1016/j.jhep.2007.08.018
39. Oba J, Nakahara T, Abe T, Hagihara A, Moroi Y, Furue M. Expression of c-Kit, p-ERK and cyclin D1 in malignant melanoma: An immunohistochemical study and analysis of prognostic value. *J Dermatol Sci*. 2011;62(2):116-123. doi:10.1016/j.jdermsci.2011.02.011
40. Fujimori Y, Inokuchi M, Takagi Y, Kato K, Kojima K, Sugihara K. *Prognostic Value of RKIP and P-ERK in Gastric Cancer*; 2012. doi:10.1186/1756-9966-31-30
41. Chadha KS, Khoury T, Yu J, et al. Activated Akt and Erk expression and survival after surgery in pancreatic carcinoma. *Ann Surg Oncol*. 2006;13(7):933-939. doi:10.1245/ASO.2006.07.011
42. Wang S sen, Guan Z zhen, Xiang Y qun, et al. Significance of EGFR and p-ERK expression in nasopharyngeal carcinoma. *Zhonghua Zhong Liu Za Zhi*. 2006;28(1):28-31.
43. de Ruiter EJ, de Roest RH, Brakenhoff RH, et al. Digital pathology-aided assessment of tumor-infiltrating T lymphocytes in advanced stage, HPV-negative head and neck tumors. *Cancer Immunol Immunother*. 2020;69(4):581-591. doi:10.1007/s00262-020-02481-3
44. van Kempen PMW, van Bockel L, Braunius WW, et al. HPV-positive oropharyngeal squamous cell carcinoma is associated with TIMP3 and CADM1 promoter hypermethylation. *Cancer Med*. 2014;3(5):1185-1196. doi:10.1002/cam4.313
45. Smeets SJ, Hesselink AT, Speel EJM, et al. A novel algorithm for reliable detection of human papillomavirus in paraffin embedded head and neck cancer specimen. *Int J Cancer*. 2007;121(11):2465-2472. doi:10.1002/ijc.22980
46. Driehuis E, Kolders S, Spelier S, et al. Oral mucosal organoids as a potential platform for personalized cancer therapy. *Cancer Discov*. 2019;9(7):852-871. doi:10.1158/2159-8290.CD-18-1522
47. Millen R, De Kort WWB, Koomen M, et al. Patient-derived head and neck cancer organoids allow treatment stratification and serve as a tool for biomarker validation and identification. *Med*. 2023;4(5):290-310.e12. doi:10.1016/j.medj.2023.04.003
48. McCarty KS, Miller LS, Cox EB, Konrath J, McCarty KS. Estrogen receptor analyses. Correlation of biochemical and immunohistochemical methods using monoclonal antireceptor antibodies. *Arch Pathol Lab Med*. 1985;109(8):716-721. <http://www.ncbi.nlm.nih.gov/pubmed/3893381>.
49. Koo TK, Li MY. A Guideline of Selecting and Reporting Intraclass Correlation Coefficients for Reliability Research. *J Chiropr Med*. 2016;15(2):155-163. doi:10.1016/j.jcm.2016.02.012
50. Sabatini DM. mTOR and cancer: Insights into a complex relationship. *Nat Rev Cancer*. 2006;6(9):729-734. doi:10.1038/nrc1974
51. Monteiro LS, Delgado ML, Ricardo S, et al. Phosphorylated mammalian target of rapamycin is associated with an adverse outcome in oral squamous cell carcinoma. *Oral Surg Oral Med Oral Pathol Oral Radiol*. 2013;115(5):638-645. doi:10.1016/j.oooo.2013.01.022
52. Naruse T, Yanamoto S, Yamada S ichi, et al. Anti-Tumor Effect of the Mammalian Target of Rapamycin Inhibitor Everolimus in Oral Squamous Cell Carcinoma. *Pathol Oncol Res*. 2015;21(3):765-773. doi:10.1007/s12253-014-9888-1
53. Li SH, Chien CY, Huang WT, et al. Prognostic significance and function of mammalian target of rapamycin in tongue squamous cell carcinoma. *Sci Rep*. 2017;7(1). doi:10.1038/s41598-017-08345-8

54. García-Carracedo D, Ángeles Villaronga M, Álvarez-Teijeiro S, et al. Impact of PI3K/AKT/mTOR pathway activation on the prognosis of patients with head and neck squamous cell carcinomas. *Oncotarget*. 2016;7(20):29780-29793. doi:10.18632/oncotarget.8957
55. Ang KK, Harris J, Wheeler R, et al. Human Papillomavirus and Survival of Patients with Oropharyngeal Cancer. *N Engl J Med*. 2010;363(1):24-35. doi:10.1056/NEJMoa0912217
56. Fakhry C, Westra WH, Li S, et al. Improved survival of patients with human papillomavirus-positive head and neck squamous cell carcinoma in a prospective clinical trial. *J Natl Cancer Inst*. 2008;100(4):261-269. doi:10.1093/jnci/djn011
57. Wilson TG, Hanna A, Recknagel J, Pruetz BL, Baschnagel AM, Wilson GD. Prognostic significance of MTOR expression in HPV positive and negative head and neck cancers treated by chemoradiation. *Head Neck*. 2020;42(2):153-162. doi:10.1002/hed.25983
58. Hong A, Zhang X, Jones D, et al. Relationships between p53 mutation, HPV status and outcome in oropharyngeal squamous cell carcinoma. *Radiother Oncol*. 2016;118(2):342-349. doi:10.1016/j.radonc.2016.02.009
59. Feng Z, Zhang H, Levine AJ, Jin S. The coordinate regulation of the p53 and mTOR pathways in cells. *Proc Natl Acad Sci U S A*. 2005;102(23):8204. doi:10.1073/PNAS.0502857102
60. Mastronikolis NS, Tsiambas E, Papadas TA, et al. Deregulation of PTEN expression in laryngeal squamous cell carcinoma based on tissue microarray digital analysis. *Anticancer Res*. 2017;37(10):5521-5524. doi:10.21873/anticancer.11983
61. Rozengurt E, Soares HP, Sinnet-Smith J. Suppression of feedback loops mediated by pi3k/mtor induces multiple overactivation of compensatory pathways: An unintended consequence leading to drug resistance. *Mol Cancer Ther*. 2014;13(11):2477-2488. doi:10.1158/1535-7163.MCT-14-0330
62. Guney K, Ozbilim G, Derin AT, Cetin S. Expression of PTEN protein in patients with laryngeal squamous cell carcinoma. *Auris Nasus Larynx*. 2007;34(4):481-486. doi:10.1016/j.anl.2007.03.014
63. Wang H, Zhang Y, Yun H, Chen S, Chen Y, Liu Z. ERK expression and its correlation with STAT1 in esophageal squamous cell carcinoma. *Oncotarget*. 2017;8(28):45249-45258. doi:10.18632/oncotarget.16902
64. Theocharis S, Kotta-Loizou I, Klijanienko J, et al. Extracellular signal-regulated kinase (ERK) expression and activation in mobile tongue squamous cell carcinoma: Associations with clinicopathological parameters and patients survival. *Tumor Biol*. 2014;35(7):6455-6465. doi:10.1007/s13277-014-1853-9
65. Psyrri A, Lee JW, Pectasides E, et al. Prognostic biomarkers in phase II trial of cetuximab-containing induction and chemoradiation in resectable HNSCC: Eastern Cooperative Oncology Group E2303. *Clin Cancer Res*. 2014;20(11):3023-3032. doi:10.1158/1078-0432.CCR-14-0113
66. Schoeberl B, Eichler-Jonsson C, Gilles ED, Müller G. Computational modeling of the dynamics of the MAP kinase cascade activated by surface and internalized EGF receptors. *Nat Biotechnol*. 2002;20(4):370-375. doi:10.1038/nbt0402-370
67. Goethals L, Perneel C, Debucquoy A, et al. A new approach to the validation of tissue microarrays. *J Pathol*. 2006;208(5):607-614. doi:10.1002/path.1934

SUPPLEMENTAL MATERIAL

Supplemental Table 1

	Markers	Median score	Interquartile range
Patient cohort	p-mTOR	95	63 – 140
	p-ERK	143	77 – 253
	PTEN	60	41 – 85
Organoids	p-MTOR	70	38 – 103

Median values of scoring per marker with corresponding interquartile ranges of patient cohort and organoids.

Supplemental Table 2: Correlations between immunohistochemical markers and clinical variables

		p-mTOR	p	p-ERK	p	PTEN	p
Age		R=0.04	0.97	R=0.07	0.59	R=0.05	0.71
Sex	Male	103 [63 – 147]	0.51	137 [83 – 268]	0.51	153 [90 – 280]	0.44
	Female	83 [63 – 120]		148 [77 – 227]		157 [77 – 227]	
Tumor site	Oropharynx	103 [69 – 160]	0.41	120 [57 – 270]	0.58	130 [63 – 270]	0.67
	Hypopharynx	80 [53 – 113]		190 [82 – 310]		195 [83 – 320]	
	Larynx	98 [62 – 132]		168 [127 – 220]		167 [110 – 213]	
T stage	T1-3	100 [65 – 125]	0.96	193 [93 – 258]	0.09	203 [85 – 280]	0.59
	T4	91 [57 – 150]		117 [58 – 208]		120 [67 – 208]	
N stage	N0-1	117 [53 – 163]	0.52	110 [50 – 208]	0.24	112 [50 – 220]	0.46
	N2-3	87 [67 – 140]		167 [83 – 258]		167 [85 – 260]	

The correlation between markers and age was performed using Spearman Rho correlation. The correlation between markers and tumor site was performed using Kruskal-Wallis test. The other correlations were performed using Mann-Whitney U tests. Numbers displayed in table are as follows: Median, 25th quartile, 75th quartile and p-value.

Supplemental Table 3: Univariate/Multivariate sub-analysis between markers and OS,DFS and LRC split by subsite

Oropharynx treated with Cetuximab/Cisplatin/Carboplatin									
Univariate analysis		OS		DFS		LRC			
Marker	Comparison	n	HR (95%CI)	p	HR (95%CI)	p	HR (95%CI)	p	
p-mTOR	Per 10 H-score increase	48	1.04 (0.98 – 1.09)	0.22	1.02 (0.97 – 1.02)	0.53	0.97 (0.90 – 1.04)	0.39	
p-ERK	Per 10 H-score increase	44	1.01 (0.98 – 1.05)	0.57	1.01 (0.98 – 1.04)	0.40	1.02 (0.98 – 1.05)	0.42	
PTEN	Per 10 H-score increase	43	1.08 (0.98 – 1.18)	0.13	1.05 (0.96 – 1.14)	0.34	0.98 (0.86 – 1.11)	0.75	
T stage	T1-3 vs T4	48	0.54 (0.21 – 1.41)	0.21	0.66 (0.29 – 1.53)	0.34	0.70 (0.23 – 2.10)	0.52	
N stage	N0-1 vs N2-3	48	1.22 (0.52 – 2.86)	0.64	0.29 (0.68 – 3.62)	0.29	2.17 (0.63 – 7.46)	0.22	
Age	Per 1 increase (year)	48	1.00 (0.93 – 1.07)	0.94	0.99 (0.93 – 1.05)	0.72	1.01 (0.93 – 1.09)	0.85	
Sex	Male vs Female	48	1.73 (0.83 – 3.63)	0.14	0.57 (0.28 – 1.18)	0.13	0.43 (0.16 – 1.20)	0.11	
Multivariate analysis									
		OS		DFS		LRC			
Marker	Comparison	n	HR (95%CI)	p	HR (95%CI)	p	HR (95%CI)	p	
p-mTOR	Per 10 H-score increase	48	1.04 (0.98 – 1.10)	0.16	1.02 (0.96 – 1.07)	0.55	0.97 (0.89 – 1.05)	0.39	
p-ERK	Per 10 H-score increase	44	1.01 (0.98 – 1.05)	0.59	1.01 (0.98 – 1.04)	0.54	1.01 (0.97 – 1.05)	0.67	
PTEN	Per 10 H-score increase	43	1.10 (0.99 – 1.22)	0.08	1.06 (0.96 – 1.16)	0.28	0.99 (0.86 – 1.13)	0.88	
Larynx treated with Cetuximab/Cisplatin/Carboplatin									
Univariate analysis		OS		DFS		LRC			
Marker	Comparison	n	HR (95%CI)	p	HR (95%CI)	p	HR (95%CI)	p	
p-mTOR	Per 10 H-score increase	12	1.21 (0.97 – 1.52)	0.10	1.20 (0.98 – 1.46)	0.07	1.19 (0.91 – 1.56)	0.21	
p-ERK	Per 10 H-score increase	12	1.19 (0.98 – 1.46)	0.08	1.21 (0.98 – 1.50)	0.07	1.36 (0.93 – 2.01)	0.12	
PTEN	Per 10 H-score increase	13	2.16 (1.00 – 4.67)	0.05	1.15 (0.78 – 1.68)	0.48	0.88 (0.59 – 1.31)	0.52	

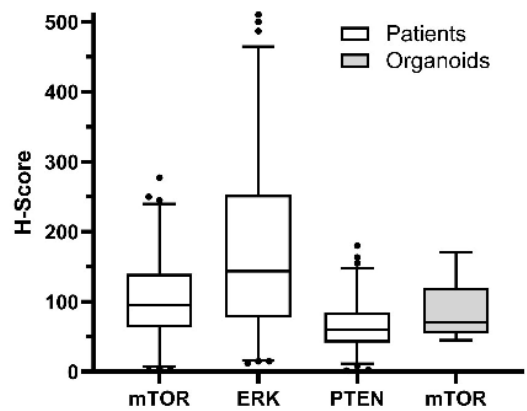
Supplemental Table 3: Univariate/Multivariate sub-analysis between markers and OS,DFS and LRC split by subsite (continued)

Larynx treated with Cetuximab/Cisplatin/Carboplatin						
Univariate analysis		OS		DFS		LRC
Marker	Comparison	HR (95%CI)	p	HR (95%CI)	p	HR (95%CI)
T stage	T1-3 vs T4	13	40.1 (0.01 - >999)	0.37	40.6 (0.03 - >999)	0.32
						33.1 (0.01 - >999)
N stage	N0-1 vs N2-3	13	0.04 (0.00 - >999)	0.59	0.04 (0.00 - >999)	0.56
						0.04 (0.00 - >999)
Age	Per 1 increase (year)	13	1.04 (0.89 - 1.22)	0.61	0.97 (0.86 - 1.11)	0.69
						0.97 (0.83 - 1.13)
Sex	Male vs Female	13	2.35 (0.39 - 14.3)	0.35	1.26 (0.25 - 6.29)	0.78
						0.71 (0.06 - 7.86)
Multivariate analysis		OS		DFS		LRC
Marker	Comparison	HR (95%CI)	p	HR (95%CI)	p	HR (95%CI)
p-mTOR	Per 10 H-score increase	12	1.14 (0.88 - 1.48)	0.31	1.18 (0.93 - 1.49)	0.17
						1.17 (0.85 - 1.61)
p-ERK	Per 10 H-score increase	12	1.10 (0.85 - 1.44)	0.46	1.19 (0.89 - 1.58)	0.24
						>999 (0.00 - >999)
PTEN	Per 10 H-score increase	13	1.73 (0.91 - 3.28)	0.09	1.10 (0.73 - 1.66)	0.65
						0.86 (0.47 - 1.57)
Hypopharynx treated with Cetuximab/Cisplatin/Carboplatin						
Univariate analysis		OS		DFS		LRC
Marker	Comparison	HR (95%CI)	p	HR (95%CI)	p	HR (95%CI)
p-mTOR	Per 10 H-score increase	15	1.03 (0.87 - 1.20)	0.76	1.03 (0.90 - 1.18)	0.69
						1.07 (0.91 - 1.25)
p-ERK	Per 10 H-score increase	13	1.03 (0.97 - 1.09)	0.39	1.05 (0.99 - 1.12)	0.10
						1.06 (0.99 - 1.14)
PTEN	Per 10 H-score increase	16	0.94 (0.79 - 1.13)	0.54	0.95 (0.81 - 1.10)	0.48
						0.95 (0.80 - 1.14)
T stage	T1-3 vs T4	16	3.35 (0.39 - 28.9)	0.27	4.48 (0.55 - 36.6)	0.16
						3.11 (0.36 - 26.9)
N stage	N0-1 vs N2-3	16	1.62 (0.19 - 14.0)	0.66	1.30 (0.16 - 10.7)	0.81
						1.78 (0.21 - 15.4)
Age	Per 1 increase (year)	16	0.96 (0.86 - 1.06)	0.40	0.94 (0.86 - 1.03)	0.21
						1.00 (0.88 - 1.15)
Sex	Male vs Female	16	0.45 (0.09 - 2.34)	0.34	1.90 (0.47 - 7.61)	0.37
						1.85 (0.34 - 10.1)

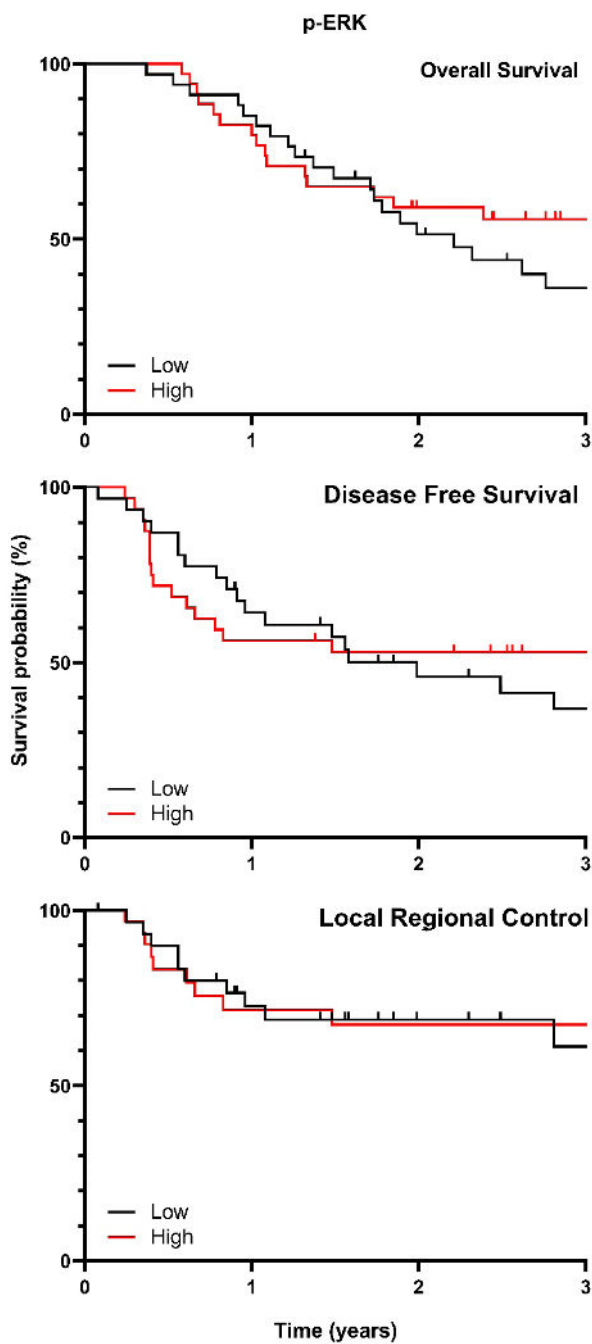
Supplemental Table 3: Univariate/Multivariate sub-analysis between markers and OS,DFS and LRC split by subsite (continued)

Multivariate analysis		OS		DFS		LRC	
Marker	Comparison	HR (95%CI)	p	HR (95%CI)	p	HR (95%CI)	p
p-mTOR	Per 10 H-score increase	15	0.94 (0.76 – 1.17)	0.57	0.95 (0.79 – 1.15)	0.61	0.99 (0.80 – 1.22)
p-ERK	Per 10 H-score increase	13	1.03 (0.93 – 1.13)	0.62	1.04 (0.96 – 1.14)	0.33	1.05 (0.94 – 1.17)
PTEN	Per 10 H-score increase	16	0.72 (0.46 – 1.13)	0.15	0.70 (0.46 – 1.06)	0.09	0.72 (0.46 – 1.15)

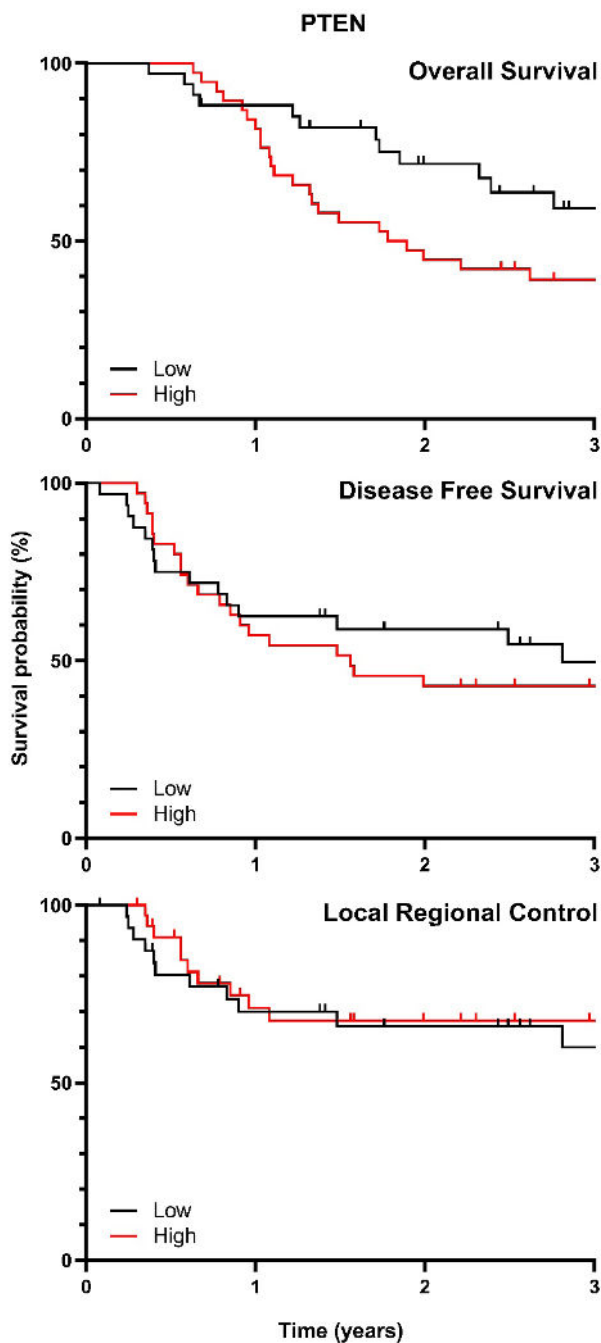
Supplemental Table 3: Univariate/Multivariate Cox proportional hazards regression of markers/clinicopathological parameters and overall survival (OS), Disease free survival (DFS) and Locoregional control (LRC). The prognostic values are displayed in Hazard Ratios (HR), 95%CI, 95% Confidence interval. Significant p-values (p < 0.05) are shown in bold. Multivariate: Model contains biomarker as predictor corrected for age, gender, T-stage and N-stage.



Supplemental Figure 1: Boxplot of H-score per marker (5-95%CI).



Supplemental Figure 2: Kaplan-Meier curves visualizing the association between p-ERK expression and OS, DFS and LRC. The median score of expression was used as cutoff for the survival analysis.



Supplemental Figure 3: Kaplan-Meier curves visualizing the association between PTEN expression and OS, DFS and LRC. The median score of expression was used as cutoff for the survival analysis.



CHAPTER 5

Jaw bone invasion of oral squamous cell carcinoma is associated with osteoclast count and expression of its regulating proteins in patients and organoids

Willem W. B. de Kort, Wisse E. Haakma, Robert J. J. van Es, Debby Gawlitta, Else Driehuis, Merel Gansevoort, Stefan M. Willems

ABSTRACT

Aims

Oral squamous cell carcinoma (OSCC) frequently invades the jaw. The exact mechanism of bone invasion remains unclear. This study investigates (premature) osteoclasts and the expression of differentiation regulating proteins RANKL, OPG and RANK in patients with OSCC.

Methods

Resection specimens from OSCC patients were divided into NI group (No Invasion), E group (Erosion) or I group (bone Invasion). Tissue sections were stained with Cathepsin K (osteoclast-counting), RANKL, OPG and RANK. The staining intensity was scored on different regions of the tumor: front, center, back and normal mucosa. Immunohistochemistry and qPCR for RANKL/OPG/RANK were performed on five head and neck squamous cell carcinoma (HNSCC) organoids.

Results

The mean number of osteoclasts (I group) and premature osteoclasts (E group) was significantly higher compared to the NI group ($p = 0.003$, $p = 0.036$). RANKL expression was significantly higher in the tumor front and tumor center compared to normal mucosa (all groups). In the I group, RANKL and RANK expression was significantly higher in the tumor front compared to the tumor back and there was a trend of higher RANKL expression in the tumor front compared to the E group and NI group. qPCR showed a 20–43 times higher RANKL mRNA expression in three out of five tumor organoids compared to a normal squamous cell organoid line. There was no correlation between protein and mRNA expression in the HNSCC organoids.

Conclusions

These findings suggest that OSCCs induce bone invasion by stimulating osteoclast activation by regulating the production of RANKL and RANK proteins.

INTRODUCTION

Over 90% of all oral cancers are squamous cell carcinoma (OSCC)¹. If in contact with bone, OSCC frequently invades the jaw. Cancers of the floor-of-mouth, tongue or retromolar regions invade the jaw in 62%, 42% and 48% of the cases, respectively². In the case of bone invasion, the tumor TNM classification for malignant tumors is staged to the highest T stage of T4³. OSCC is primarily treated with surgery⁴. Patients with bone invasion have worse disease-free survival and overall survival rates⁵. Moreover, the presence of bone invasion is clinically relevant as it often requires a partial resection of the mandible, which has a major impact on quality of life, aesthetics and function^{6,7}.

Two patterns of mandibular destruction by tumor tissue are recognized: an invasive and an erosive pattern. In the invasive pattern, the tumor breaks through cortical bone and islands of tumor grow into cancellous spaces without an intervening layer of connective tissue. The erosive pattern is characterized by cohesive tumor growth which separates from the bone by an intervening connective tissue layer⁸. Bone invasion starts with bone destruction, which then allows the access of malignant cells. In OSCC, this requires osteoclast differentiation and activation rather than direct growth of tumor cells into the bone⁹. Osteoclasts are multinucleated cells that are differentiated from mononuclear pre-fusion osteoclasts due to expression of a Receptor Activator of Nuclear factor Kappa-B Ligand (RANKL)^{10,11}. RANKL binds its receptor RANK, expressed on hematopoietic osteoclast progenitors and osteoclasts, which induces the differentiation of osteoclasts⁹. Osteoprotegerin (OPG) is the decoy receptor of RANKL. OPG is also known as 'osteoclastogenesis inhibitory factor'. OPG that binds RANKL prevents RANKL binding RANK thus blocking osteoclast differentiation¹². RANK and RANKL signaling is also known to contribute to bone invasion or bone metastasis in other types of cancer that are not OSCC¹³⁻²¹.

To further elucidate the mechanisms of bone invasion in OSCC, this study assesses the number of osteoclasts and expression of RANK, RANKL and OPG in a panel of both OSCC patient tissues and head and neck squamous cell carcinoma (HNSCC) organoids, with bone invasion of either the invasive or the erosive pattern. These parameters are compared with a panel of OSCC patients without bone invasion.

MATERIALS AND METHODS

Selection of Patients and Clinical Data

This is a retrospective cohort study of patients treated at the University Medical Center Utrecht between January 2016 and December 2018. Inclusion criteria were: (1) patients with OSCC of the upper/lower gum, cheek or mandible, (2) patients treated with primary resection, (3) enough tissue was available for tissue sections and (4) tissue sections were deemed suitable by a dedicated head and neck pathologist (SMW) for assessing the front of the tumor to the bone. As all included tissues were primary resections, the tissues did not receive radiotherapy and/or chemotherapy before surgery. All tissues and data were handled according to the General Data Protection Regulation (GDPR). For all included patients, representative formalin-fixed, paraffin-embedded (FFPE) resection blocks were collected. Then, 4 μ m tissue sections of the FFPE blocks were stained with 1:3 diluted hematoxylin for 4 min and with eosin for 1 min (H&E). These stained H&E sections were classified by a head and neck pathologist (SMW) into three categories: No bone Invasion (NI group, tumor did not damage the bone), bone Erosion (E group, tumor eroded the bony cortex but did not grow into the bone) and bone Invasion (I group, tumor did grow into the bone marrow, strands and islands of tumor were identified between the bone trabeculae).

In addition, available tumor tissue of five HNSCCs was cultured as organoids described by Millen et al.²². Organoids are three-dimensional tissue cultures derived from stem cells of the tumor. The 5 HNSCC organoid lines originated from the oral cavity ($n = 1$), oropharynx ($n = 1$), nasal cavity ($n = 1$) and the larynx ($n = 2$). The oral cavity organoid was derived from a tumor with bone invasion. One normal mucosa organoid was included as control; this normal mucosa organoid originated from a SCC resection specimen of the oral tongue, from which normal mucosa was used for organoid isolation. The oropharynx organoid was HPV type 16 positive; all the other organoids were HPV negative.

Immunohistochemistry

To recognize and count the number of osteoclasts, tissue sections were stained for Cathepsin K. Alongside, tissue sections and organoids were stained for RANKL, RANK and OPG according to the details displayed in Table 1. All antibody incubation was carried out at room temperature for 1 h. After washing off secondary antibodies, sections were stained with 3,3'-Diaminobenzidine (DAB) for 15 min and counterstained with 1:3 diluted hematoxylin for 30 s.

Counting Osteoclasts and Pre-Osteoclasts

The average number of osteoclasts and mononuclear primary osteoclasts (pre-osteoclasts) were counted in the Cathepsin K stained sections by counting them in five, randomly picked, 500 micrometer wide, areas on the front of the bone close to the tumor. The 500 micrometer-

wide compartments were chosen because this allowed the presence of multiple osteoclasts while retaining the possibility to differentiate osteoclasts and pre-osteoclasts (Figure 1). An osteoclast was recognized as a large multinucleated cell. Mononuclear primary osteoclasts and mature osteoclasts were differentiated. Two trained observers (WdK, MG) and a dedicated head and neck pathologist (SMW) manually counted the number of osteoclasts independently. If there was discordance in osteoclast counting between the three observers, that specific case was assessed together and recounted to reach consensus.

Table 1. Antibody stains and dilutions.

Antibody	Manufacturer	Ordering Number	Antigen Retrieval	Primary Antibody Dilution	Secondary Antibody
Cathepsin K	Abcam, Cambridge, UK	ab19027	pH6 Citrate	1:500	Goat anti-rabbit HRP
RANKL	Abcam, Cambridge, UK	ab13918	pH6 citrate	1:100	Goat anti-rabbit HRP
RANK	Abcam, Cambridge, UK	ab9957	pH9 EDTA	1:100	Goat anti-mouse HRP
OPG	Abcam, Cambridge, UK	ab183910	pH9 EDTA	1:200	Goat anti-rabbit HRP

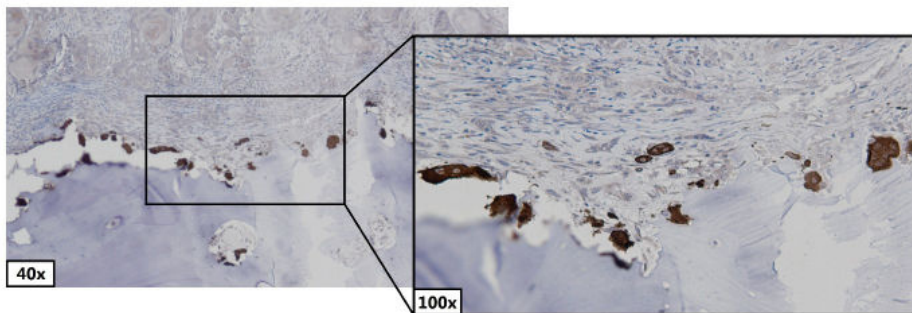


Figure 1. Cathepsin K staining. Multinucleated brown cells depicted are recognized as osteoclasts. Blue depicted area in the bottom half is bone.

Scoring RANKL, RANK and OPG Intensity Staining

Cytoplasmic RANKL, OPG and RANK expression in tumor (tumor front, tumor center and tumor back) were compared with expression in normal mucosa to see if there were differences in expression between tumor and normal squamous cell mucosa and if there were differences in expression within the tumor towards the bone.

Each staining was scored in three tumor areas: tumor front, tumor center and tumor back. "Tumor front" was defined as the area closest to or invading the bone, "tumor center" as

the central part of the tumor and “tumor back” as the area opposite to the tumor front. RANKL staining was scored using a 4-stage intensity scale; 0 negative, 1 light, 2 medium and 3 strong (Figure 2A–C). OPG- and RANK staining both were scored using a 3-stage intensity scale; 0 negative, 1 light, 2 strong (Figure 2D–I). RANKL was scored using a 4-stage intensity scale because the RANKL staining was more discriminative compared to the RANK and OPG stainings. Per staining, every tumor area was scored separately. Three observers scored tissue sections independently (WdK, WH, SMW). In line with the osteoclast counting, if there was discordance between the three observers, expression of that specific case was reassessed together to reach consensus.

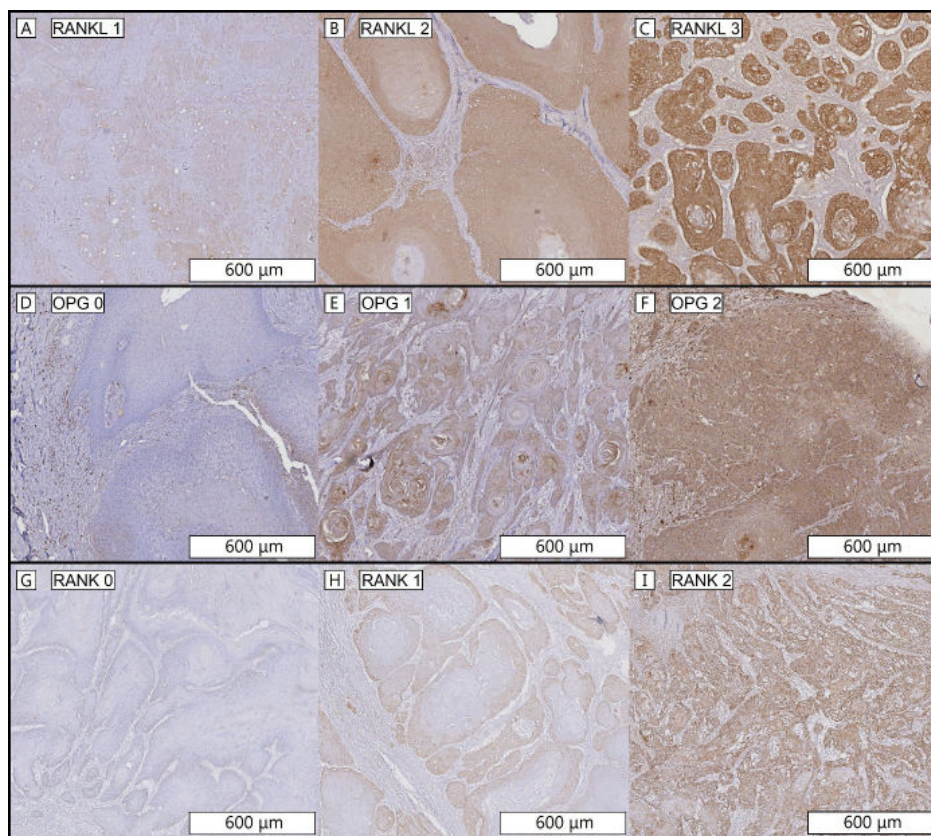


Figure 2. Representative staining intensity score, magnification 6×. RANKL staining intensity **A** = 1, **B** = 2, **C** = 3. OPG staining intensity **D** = 0, **E** = 1, **F** = 2. RANK staining intensity **G** = 0, **H** = 1, **I** = 2. Important note. RANKL is scored on a scale from 0–3 (score 0 for RANKL not shown), OPG and RANK are scored on a scale from 0–2.

Organoid Culture and RNA Isolation

Organoids were cultured as described by Millen et al.²². In short, sampled pieces of HNSCC tissue obtained during resections were mechanically disrupted by cutting them into small pieces and were digested enzymatically (0.125% Trypsin, catalog no. T1426, Sigma-Aldrich, Saint Louis, Missouri, USA). Once tissues were macro and microscopically dissociated, cell suspension was filtered through a 70 µm filter (catalog no. CLS431751-50EA, Corning, Glendale, Arizona, USA), resuspended in Cultrex (catalog no. 3533-010-02, Trevigen, Gaithersburg, Maryland, USA) and plated in droplets of culture medium on 48-well suspension culture plates (catalog no. M9312, Greiner, Kremsmünster, Austria). During the first week of culture, Caspofugin (0.5 mg/mL, Sigma-Aldrich, Saint Louis, Missouri, USA), an antimycotic, was present and was removed after one week. Medium was changed every two to three days and organoids were passaged between approximately 7 and 14 days after plating, depending on their growth rate. For more details regarding organoid medium see Millen et al.²².

The Biobank Research Ethics Committee of the University Medical Center Utrecht (TCBio) approved the biobanking protocol: 12-093 HUB-Cancer according to the University Medical Center Utrecht (UMCU) Biobanking Regulation. All donors participating in this study signed informed-consent forms and can withdraw their consent at any time.

RANKL, OPG and RANK immunohistochemistry was performed as described above. For protein scoring the staining intensity of RANKL, OPG and RANK, we used a 3-stage intensity scale; 0 (negative), 1 (light) and 2 (strong). To investigate the mRNA expression levels of RANKL, OPG and RANK in the HNSCC organoids, a quantitative polymerase chain reaction (qPCR) was executed.

Organoids were cultured for twelve days, and RNA was collected after passaging. For RNA collection, organoids were collected from the culture plates by disrupting the basement membrane extract using a p1000 pipette, centrifuged at 300× *g*, 5 min at 4 °C and washed twice in 10 mL medium. RNA was isolated according to protocol using RNeasy Mini Kit of Qiagen. In short, the organoid pellet was lysed in 350 µL RLT buffer, and subsequently incubated 5 min at room temperature. The lysate was stored at –80 °C until further use. On the day of processing, lysate was thawed on ice and 350 µL 70% ethanol was added. Suspension was loaded on columns provided, washed once using 700 µL RW1 buffer and twice using 500 µL RPE buffer. Membranes were spun dry to remove residual buffer, after which the RNA was eluted in 30 µL RNA-free water. RNA concentration was measured using a nanodrop and stored at –80 °C until further use. Only RNA samples with 260/280 ratios ranging from 1.95–2.05 and a concentration > 10 µg/µL were used for subsequent analysis.

cDNA Synthesis and Quantitative PCR

For cDNA synthesis, RNA eluate was thawed on ice, and a volume equal to 500 ng was incubated with 50 µg/mL Oligo (dT) 15 Primer (catalog no. C1101, Promega, Madison, Wisconsin, USA) in water for 5 min at 70 °C. To generate cDNA, GoScript Reverse Transcriptase (Promega, catalog no. A5003) was used according to protocol. qPCR reactions were performed in 384-well format using IQ SYBR green (catalog no. 1708880, Bio-Rad, Veenendaal, The Netherlands) in the presence of 0.67 µmol/L forward and reverse primer (Table S1) and 20 ng of cDNA. For qPCR, samples were incubated for 2 min at 95 °C (initial denaturation) and for 40 cycles at: 15 s at 98 °C (denaturation), 15 s at 58 °C (annealing), and 15 s at 72 °C (extension). Results were calculated by using the delta–delta Ct method, also known as the $2^{-\Delta\Delta Ct}$ method. Expression was expressed relative to expression of the housekeeping gene actin and to RNA isolated from a wildtype tongue epithelium. Melt peak analysis was performed to assure primers used generated only one product. RANKL, OPG and RANK expression on mRNA level was compared to RANKL, OPG and RANK expression on protein level (Figure S2).

Statistics

To assess if there were differences in mean number of (pre)osteoclasts between three patient groups, a one-way ANOVA was used. There were no outliers as assessed by boxplot, data was normally distributed as assessed by Shapiro–Wilk’s test ($p > 0.05$). For osteoclasts there was homogeneity of variances as assessed by Levene’s test ($p > 0.05$) and Tukey–Kramer post hoc testing was used. For premature osteoclasts there was no homogeneity of variances as assessed by Levene’s test ($p = 0.003$), therefore the Welch ANOVA was used with Games–Howell post hoc testing.

As RANKL, OPG and RANK expression is ordinal data, differences in expression were analyzed with non-parametric tests. To compare expression in the tumor front, tumor center, tumor back and normal mucosa the Friedman test was used as expression is compared within the same patient. Pairwise comparisons were performed with a Bonferroni correction for multiple comparisons. To compare expression between patient groups per tumor area, the Kruskal–Wallis H test was used as expression is compared between different patients. Post hoc testing was not performed as the Kruskal–Wallis H tests did not yield significant values.

A p -value of <0.05 was interpreted as statistically significant. Statistical analysis was performed with SPSS Statistics (IBM Corp. Released 2017. IBM SPSS Statistics for Windows, Version 26.0. Armonk, NY, USA: IBM Corp).

RESULTS

Patients

In total 29 patients were included: 7 in the NI group, 12 in the E group and 10 in the I group. Patient characteristics are described in Table 2.

Table 2. Patient characteristics

		No Invasion (n = 7)	Erosion (n = 12)	Invasion (n = 10)
Age	Median (range)	67 (43–88)	72 (60–79)	63 (40–79)
Gender	Male:Female	1:6	8:4	5:5
Tumor site	Lower gum	4	9	6
	Upper gum	2	3	3
	Cheek	1		
	Mandible *			1
Growth Pattern	Cohesive	5	5	4
	Non-cohesive	2	7	6
Peri-neural invasion	No	7	3	4
	Yes	0	9	6
Angioinvasion	No	7	12	9
	Yes	0	0	1

* Primary intraosseous carcinoma (PIOC)

Number of Osteoclasts

The mean number of osteoclasts in the Cathepsin K stained sections were 3.09 ± 2.13 (NI group), 6.15 ± 3.13 (E group) and 10.58 ± 5.70 (I group) (Figure 3). These differences in means were statistically significant ($p = 0.004$ one-way ANOVA). Tukey post hoc tests revealed a significant difference in the mean of the I group versus the NI group (7.49 , $95\%CI$ 2.42 – 12.56 , $p = 0.003$) and a trend comparing the I group with the E group (4.43 , $95\%CI$ -0.13 – 8.98 , $p = 0.058$). The difference in mean of the E group versus the NI group was not statistically significant. The mean number of premature osteoclasts was 1.06 ± 0.91 (NI group), 3.05 ± 2.10 (E group) and 6.03 ± 5.72 (I group) (Figure 3). These differences in means were also statistically significant ($p = 0.015$ Welch's ANOVA). Games–Howell post hoc tests revealed a significant difference in the mean number of premature osteoclasts of the E group versus the NI group (2.00 , $95\%CI$ 0.12 – 3.87 , $p = 0.036$). Other group differences were not statistically significant (I group versus NI group $p = 0.10$, I group versus E group $p = 0.38$).

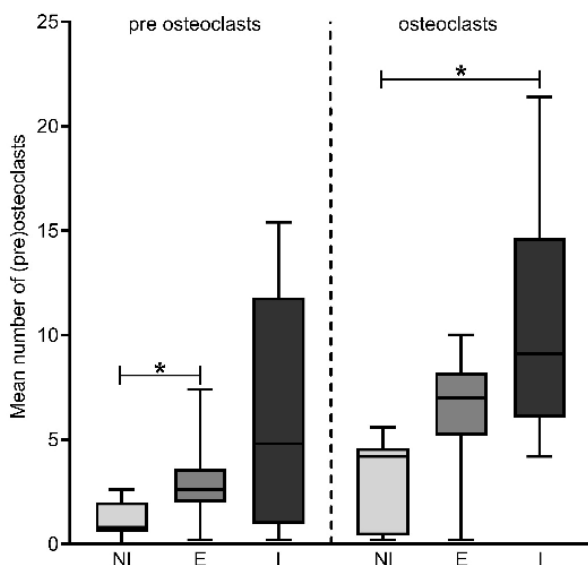


Figure 3. Boxplots mean number of counted osteoclasts with Cathepsin K staining. NI, No Invasion; E, Erosion; I, Invasion. Differences in means between three groups are statistically significant; left Welch's ANOVA ($p = 0.015$), right one-way ANOVA ($p = 0.004$); * indicates significant difference in group means assessed with post hoc testing.

RANKL, OPG and RANK Stainings

Tissue sections of all 29 patients were stained with RANKL, OPG and RANK. OPG staining failed due to technical issues for 2 patients resulting in an OPG intensity score for 27 patients. Immunohistochemical scores are displayed in Table 3.

Expression in Tumor versus Normal Mucosa

Cytoplasmic RANKL, OPG and RANK expression in tumors (tumor front, tumor center and tumor back) was compared with expression in normal mucosa (Figure 4, Table S2). RANKL expression, assessed by Friedman's test, was significantly different in all patient groups comparing normal mucosa, tumor back, tumor center and tumor front; NI group ($\chi^2(3) = 12.60$, $p = 0.006$), E group ($\chi^2(3) = 17.855$, $p < 0.001$) and I group ($\chi^2(3) = 17.468$, $p = 0.001$). Post hoc analysis revealed statistically significant differences in RANKL expression between tumor front and normal mucosa in all three groups; NI group (mean rank 3.50 versus 1.00, $p = 0.013$), E group (mean rank 3.25 versus 1.0, $p = 0.004$) and I group (mean rank 3.57 versus 1.14, $p = 0.003$). Also, post hoc analysis revealed statistically significant differences in RANKL expression between tumor center and normal mucosa in all three groups; NI group (mean rank 3.20 versus 1.00, $p = 0.042$), E group (mean rank 2.94 versus 1.06, $p = 0.022$) and I group (mean rank 3.21 versus 1.14, $p = 0.016$) (Figure 4, Table S2).

Table 3. Immunohistochemical scores RANKL/RANK/OPG per patient group. Each number indicates number of patients with the corresponding expression score.

RANKL Score	No Invasion (n = 7)				Erosion (n = 12)				Invasion (n = 10)			
	0	1	2	3	0	1	2	3	0	1	2	3
<i>Normal mucosa *</i>	5*	0	0	0	7	1	0	0	6	1	0	0
<i>Back of tumor</i>	0	3	3	1	0	5	7	0	1	3	5	1
<i>Center of tumor</i>	0	1	5	1	0	3	8	1	0	1	5	4
<i>Front of tumor</i>	0	1	4	2	0	3	8	1	0	0	6	4

OPG Score	No Invasion (n = 6)			Erosion (n = 11)			Invasion (n = 10)		
	0	1	2	0	1	2	0	1	2
<i>Normal mucosa **</i>	3	2	1	4	3	3	4	1	1
<i>Back of tumor ***</i>	1	4	2	0	4	7	0	4	5
<i>Center of tumor</i>	0	3	3	0	4	7	0	2	8
<i>Front of tumor</i>	0	2	4	0	6	5	1	4	5

RANK Score	No Invasion (n = 7)			Erosion (n = 12)			Invasion (n = 10)		
	0	1	2	0	1	2	0	1	2
<i>Normal mucosa ****</i>	5	1	1	10	0	0	2	1	0
<i>Back of tumor</i>	6	1	0	9	3	0	9	1	0
<i>Center of tumor</i>	2	5	0	3	8	1	2	7	1
<i>Front of tumor</i>	2	4	1	2	7	3	1	7	2

* Expression of RANKL in normal mucosa could not be assessed for 2 patients without invasion, 4 patients with erosion and 3 patients with invasion. ** Expression of OPG in normal mucosa could not be assessed for 1 patient with erosion and 4 patients with invasion. *** Expression of OPG in the back of the tumor could not be assessed for 1 patient with invasion. **** Expression of RANK in normal mucosa could not be assessed for 2 patients with erosion and 7 patients with invasion.

OPG expression was assessed by Friedman's test, and was not significantly different in the NI group and the E group comparing normal mucosa, tumor back, tumor center and tumor front. Although, the I group did significantly differ ($\chi^2(3) = 10.705, p = 0.013$), post hoc testing revealed no statistically significant differences in OPG expression (Figure 4, Table S2).

RANK expression, assessed by Friedman's test, was not significantly different in the NI group and I group comparing normal mucosa, tumor back, tumor center and tumor front, but the E group did significantly differ; $\chi^2(3) = 19.857, p < 0.001$. Post hoc analysis revealed a statistically significant difference in RANK expression between the tumor front (mean rank 3.40) and normal mucosa (mean rank 1.65) ($p = 0.015$) (Figure 4, Table S2).

Expression within the Tumor

RANKL expression, assessed by Friedman's test, was not significantly different in the NI group and E group comparing tumor front, tumor center and tumor back, but the I group did significantly differ; $\chi^2(2) = 10.571, p = 0.005$. Post hoc analysis revealed a statistically significant difference in RANKL expression between the tumor front (mean rank 2.40) and tumor back (mean rank 1.30) ($p = 0.042$) (Figure 4, Table S3).

OPG expression, assessed by Friedman's test, was not significantly different in all patient groups comparing the tumor front, tumor center and tumor back (Figure 4, Table S3).

RANK expression, assessed by Friedman's test, was significantly different in all patient groups comparing the tumor front, tumor center and tumor back; NI group ($\chi^2(2) = 7.538, p = 0.023$), E group ($\chi^2(2) = 13.923, p = 0.001$) and I group ($\chi^2(2) = 14.000, p = 0.001$). Post hoc analysis revealed a statistically significant difference in RANK expression between the tumor front (mean rank 2.46) and tumor back (mean rank 1.38) ($p = 0.024$) in the E group and a statistically significant difference in RANK expression between the tumor front (mean rank 2.50) and tumor back (1.25) ($p = 0.016$) in the I group. For the NI group, post hoc testing revealed no statistically significant differences in RANK expression (Figure 4, Table S3).

Expression between Invasion Categories

RANKL, OPG and RANK expression were not statistically significantly different when comparing the patient groups; no invasion, erosion and invasion, per tumor side (tumor front, tumor center and tumor back) (Kruskal–Wallis H test). However, there was a trend of higher RANKL expression in the tumor front in patients with bone invasion compared to patients with erosion and without invasion ($p = 0.10$) (Figures 4 and S3, Table S4).

Organoid Staining and qPCR

Immunohistochemically, all organoids scored medium intensity for RANKL, OPG and RANK. There was no difference in RANKL, OPG and RANK expression between organoids with and without bone invasion. Quantitative PCR showed a 20–43 times higher expression of RANKL in three out of five HNSCC organoids compared to expression in the normal mucosa organoid (Figures 5 and S1). For OPG and RANK, qPCR did not show higher mRNA expression compared to expression in a normal mucosa organoid. There was no correlation between RANKL/OPG/RANK protein and RANKL/OPG/RANK mRNA expression in the HNSCC organoids (Figure S2).

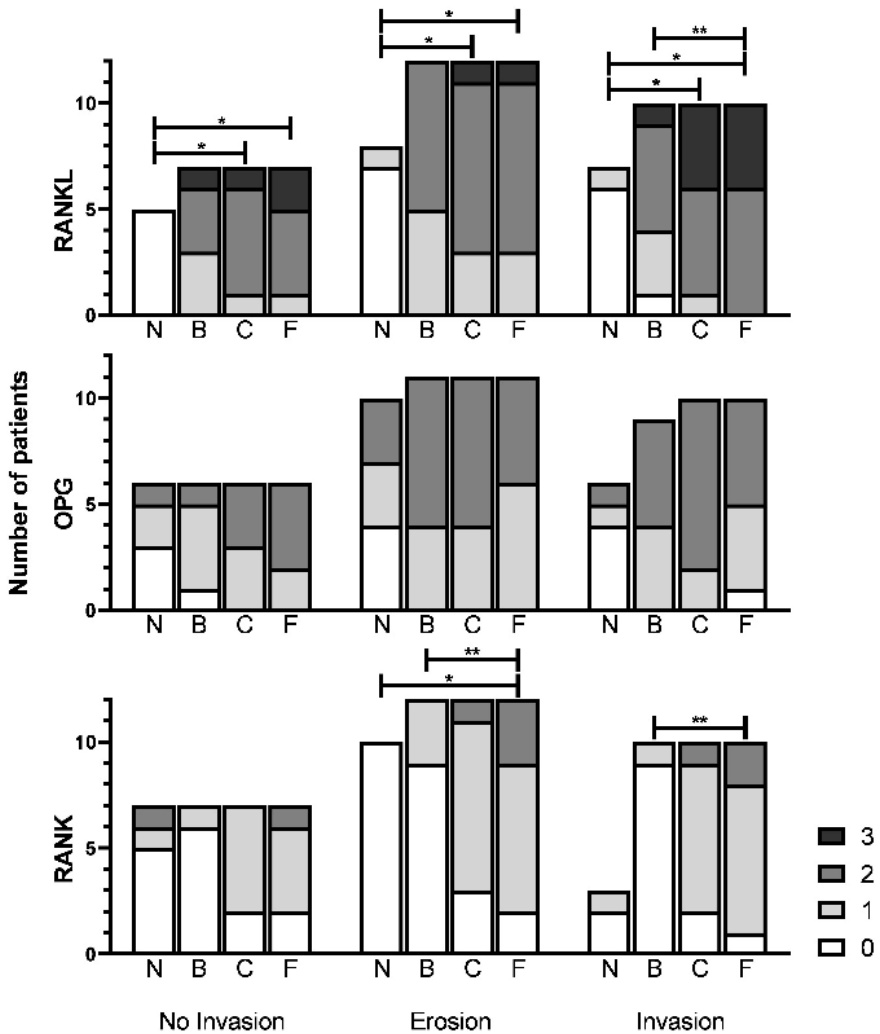


Figure 4. Stacked bar charts of RANKL/OPG/RANK staining intensity score. Legend at the right displays color per staining intensity. X-axis displays three patient groups with subdivision per subsite; N: Normal mucosa, B: Back of tumor, C: Center of tumor, F: Front of tumor. Y-axis displays number of patients. * Displays significant difference in comparison of N, B, C and F in Friedman's test with multiple comparisons and Bonferroni correction. ** Displays significant difference in comparison of B, C and F in Friedman's test with multiple comparisons and Bonferroni correction. Important note: RANKL intensity scored 0–3, OPG and RANK intensity scored 0–2.

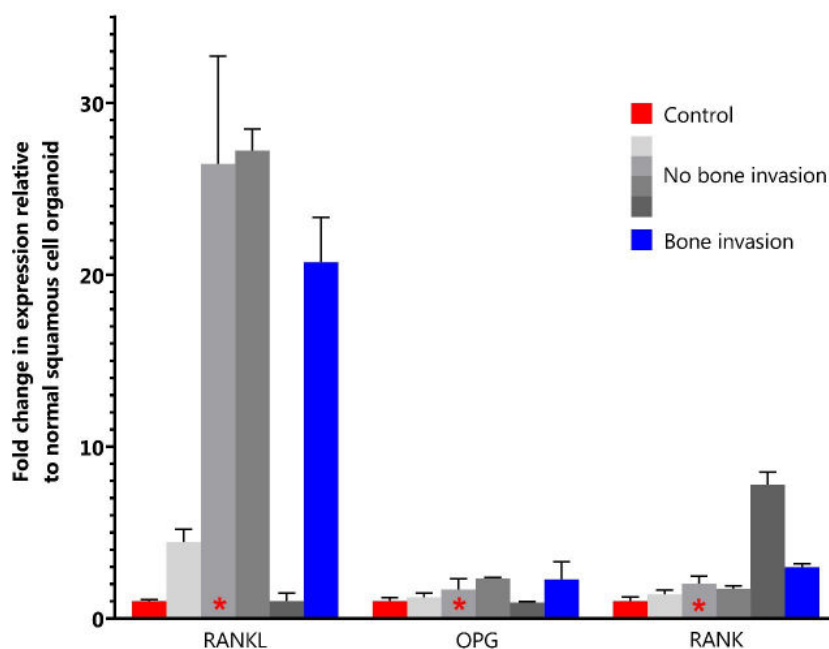


Figure 5. Results of quantitative PCR. * indicates HPV positive organoid line. Red: indicates organoid line of wildtype tongue epithelium used as control; Blue: indicates organoid line with bone invasion; Gray: indicates 4 organoid lines without bone invasion.

DISCUSSION

The presence of bone invasion in OSCC has clinical relevance because it may influence the extent of mandibular or maxillary resection. In OSCC it is known that osteoclast differentiation and activation contributes significantly to bone invasion rather than direct growth of tumors in bone⁹.

In this study we aimed to unravel some of the underlying mechanisms of bone invasion. We showed that bone invasion is associated with a higher osteoclast count compared to patients without bone invasion, and found a strong trend of higher osteoclast count comparing patients with bone invasion and erosion ($p = 0.06$). The absolute number of premature osteoclasts was significantly higher in patients with bony erosion compared to patients without invasion. A possible explanation for these findings could be that bone-erosive tumors recruit premature osteoclasts which fuse and become multinucleated active osteoclasts resulting in bone destruction whereby the tumor progresses to a bone-invading tumor. Apart from our study, two other studies report a “mixed” pattern where progression is possible from the erosive to the invasive pattern^{2,23}.

In contrast, Carter et al. showed an accumulation of osteoclasts in the erosive phase, leading to bone resorption ahead of the tumor, but a decrease in osteoclast amount in the invasive phase where the tumor destructs the bone itself²⁴. A possible explanation for these differences in results is the location where we measured the number of osteoclasts. We measured the number of osteoclasts at the location where the tumor enters the bone. The front of an invasive tumor could already have passed this 'entering' area and this front of the tumor destructs the bone itself so the osteoclast count could be low. At the 'entering' area we measured a high osteoclast count, as the tumor accumulates osteoclasts for entering the bone. Apart from head and neck squamous cell carcinoma, two studies describe the ability of human breast cancer, prostate cancer and bone metastasis to induce osteolysis by stimulating osteoclasts^{25,26}.

Apart from the absolute number of osteoclasts, we investigated RANKL, OPG and RANK that regulate osteoclast differentiation. This study showed a significantly higher RANKL expression in tumors compared to normal mucosa, indicating that tumor cells can express RANKL. These findings are in line with the study of Chuang et al. which also found increased immunohistochemical RANKL expression in tumors compared to normal mucosa²⁷. This indication is confirmed in our q-PCR, where HNSCC organoids from different subsites, and HPV status, express higher RANKL compared to a non-malignant squamous cell organoid line.

Additionally, we showed there was significantly higher RANKL expression in the tumor front versus the tumor back in the invasion group. For the other groups, a visible trend is present of increasing RANKL staining towards the tumor front. When comparing patient groups, a trend was visible of high RANKL expression in the tumor front in the I group compared to the E group and NI group ($p = 0.10$). Cui et al. also found higher RANKL expression in patients with bone invasion compared to patients without bone invasion²⁸. A possible hypothesis of this could be that the tumor encounters bone and increases RANKL expression to induce osteoclastogenesis for osteolysis and hereby becomes an invasive tumor. A higher RANK expression in the tumor front compared to the tumor back supports this hypothesis. In addition to this, Elmusrati et al. 2017 describe that RANKL is expressed in tumors proximal to bone and plays an important role in bone invasion in OSCC²⁹. As previously described, RANKL expression in the tumor front was highest in patients with bone invasion. However, these differences were not statistically significant which may have been caused by the limited sample size of our study. Nevertheless, there was a visible trend.

Apart from OSCC, RANK and RANKL signaling is also known to contribute to bone invasion or bone metastasis in myeloma, breast, hepatocellular, lung and prostate cancer¹³⁻²¹. It is known that osteoclastogenesis can be induced by squamous cell carcinoma, myeloma and promyelocytic leukemia cells expressing RANKL^{10,11}. We found no significant differences in OPG expression related to bone invasion. However, in one study a higher OPG expression correlated with infiltrative bone invasion³⁰.

It is interesting to consider RANKL as a potential ‘bone-invasion-inhibiting-target’, as OSCC is capable of producing RANKL. Denosumab is a monoclonal RANKL inhibitor and is clinically administered in patients with metastatic bone lesions^{31–34}. In patients that received Denosumab, bone metastasis and/or skeletal-related events occurred significantly later compared to patients receiving zoledronic acid. Despite bone invasion in OSCC affecting a different anatomical subsite compared to patients with osteolytic metastasis, the mechanism of bone invasion is comparable. Good et al. investigated RANKL expression in several osteolytic bone tumors and metastasis and concluded that tumor tissue is capable of expressing RANKL³⁵, which is in line with our study. In palliative treatment of a local recurrence or bone metastasis, suppressing bone invasion by RANKL inhibition could be interesting as bone-invading tumors prefer nutrient-rich bone, which may lead to more tumor growth⁹. Inhibiting bone invasion could constrain tumor growth. Implementing Denosumab as a treatment in primary OSCC is difficult as in some cases the tumor has already invaded the jawbone at the time of diagnosis. However, understanding the mechanism of bone invasion, which this study explored, is crucial to investigate new options for implementing Denosumab. The role of Denosumab in head and neck cancer has yet to be elucidated as, to our knowledge, no studies have investigated this issue.

To investigate whether the protein expression of RANKL, OPG and RANK correlated with mRNA expression, we compared these two groups. There appeared no correlation between protein and mRNA expression in the HNSCC organoids, meaning that RANKL, OPG and RANK could be regulated post-transcriptionally (Figure S2). However, with only five included organoids it is hard to draw such firm conclusions. The limited sample size affects the power of the study. Moreover, the five organoid lines originated from different locations in the head and neck area and one organoid was HPV positive. On the other hand, they are all HNSCC organoids and therefore basically comparable.

This study has several limitations. First, the limited sample size of the tissue slides hampers drawing firm conclusions, which is due to the fact that the number of cases encountered per year is limited. Secondly, the sample size of the organoids is small as described above, and thirdly the way of analyzing the tissue slides with many parameters could introduce statistically significant findings by chance that are not clinically relevant. In conclusion, this study shows that bone-invasive and erosive OSCCs have more osteoclasts (invasion) and premature osteoclasts (erosion) at the tumor front compared to OSCCs without invasion and that OSCCs can express RANKL regardless of bone invasion. Also, in patients with bone invasion, RANKL and RANK expression in the tumor front is significantly higher compared to the tumor back and there is a trend of higher RANKL expression in the tumor front compared to patients with erosion and without invasion. Apart from this, this study describes the capability of HNSCC organoids to express RANKL on protein and mRNA levels. These findings suggest that OSCCs induce bone invasion by stimulating osteoclast activation by regulating the production of RANKL and RANK proteins.

REFERENCES

1. Speight PM, Farthing PM. The pathology of oral cancer. *Br Dent J*. 2018;225(9):841-847. doi:10.1038/sj.bdj.2018.926
2. Brown JS, Lowe D, Kalavrezos N, D'Souza J, Magennis P, Woolgar J. Patterns of invasion and routes of tumor entry into the mandible by oral squamous cell carcinoma. *Head Neck*. 2002;24(4):370-383. doi:10.1002/hed.10062
3. Huang SH, O'Sullivan B. Overview of the 8th Edition TNM Classification for Head and Neck Cancer. *Curr Treat Options Oncol*. 2017;18(7). doi:10.1007/s11864-017-0484-y
4. Johnson DE, Burtneis B, Leemans CR, Lui VWY, Bauman JE, Grandis JR. Head and neck squamous cell carcinoma. *Nat Rev Dis Prim*. 2020;6(1). doi:10.1038/s41572-020-00224-3
5. Vaassen LAA, Speel EJM, Kessler PAWH. Bone invasion by oral squamous cell carcinoma: Molecular alterations leading to osteoclastogenesis – a review of literature. *J Cranio-Maxillofacial Surg*. 2017;45(9):1464-1471. doi:10.1016/j.jcms.2017.04.012
6. Van Cann EM, Dom M, Koole R, Merks MAW, Stoeltinga PJW. Health related quality of life after mandibular resection for oral and oropharyngeal squamous cell carcinoma. *Oral Oncol*. 2005;41(7):687-693. doi:10.1016/j.oraloncology.2005.03.001
7. Van Gemert J, Holtslag I, Van Der Bilt A, Merks M, Koole R, Van Cann E. Health-related quality of life after segmental resection of the lateral mandible: Free fibula flap versus plate reconstruction. *J Cranio-Maxillofacial Surg*. 2015;43(5):658-662. doi:10.1016/j.jcms.2015.03.018
8. Jimi E, Shin M, Furuta H, Tada Y, Kusukawa J. The RANKL/RANK system as a therapeutic target for bone invasion by oral squamous cell carcinoma (Review). *Int J Oncol*. 2013;42(3):803-809. doi:10.3892/ijo.2013.1794
9. Jimi E, Furuta H, Matsuo K, Tominaga K, Takahashi T, Nakanishi O. The cellular and molecular mechanisms of bone invasion by oral squamous cell carcinoma. *Oral Dis*. 2011;17(5):462-468. doi:10.1111/j.1601-0825.2010.01781.x
10. Nagai M, Kyakumoto S, Sato N. Cancer cells responsible for humoral hypercalcemia express mRNA encoding a secreted form of ODF/TRANCE that induces osteoclast formation. *Biochem Biophys Res Commun*. 2000;269(2):532-536. doi:10.1006/bbrc.2000.2314
11. Farrugia AN, Atkins GJ, To LB, et al. Receptor activator of nuclear factor- κ B ligand expression by human myeloma cells mediates osteoclast formation in vitro and correlates with bone destruction in vivo. *Cancer Res*. 2003;63(17):5438-5445. <https://pubmed.ncbi.nlm.nih.gov/14500379/>. Accessed March 31, 2021.
12. Boyle WJ, Simonet WS, Lacey DL. Osteoclast differentiation and activation. *Nature*. 2003;423(6937):337-342. doi:10.1038/nature01658
13. Sezer O, Heider U, Zavrski I, Kühne CA, Hofbauer LC. RANK ligand and osteoprotegerin in myeloma bone disease. *Blood*. 2003;101(6):2094-2098. doi:10.1182/blood-2002-09-2684
14. Santini D, Schiavon G, Vincenzi B, et al. Receptor activator of NF- κ B (rank) expression in primary tumors associates with bone metastasis occurrence in breast cancer patients. *PLoS One*. 2011;6(4). doi:10.1371/journal.pone.0019234
15. Jones DH, Nakashima T, Sanchez OH, et al. Regulation of cancer cell migration and bone metastasis by RANKL. *Nature*. 2006;440(7084):692-696. doi:10.1038/nature04524
16. Owen S, Ye L, Sanders AJ, Mason MD, Jiang WG. Expression profile of receptor activator of nuclear- κ B (rank), rank ligand (rankl) and osteoprotegerin (OPG) in breast cancer. *Anticancer Res*. 2013;33(1):199-206.

17. Sasaki A, Ishikawa K, Haraguchi N, et al. Receptor activator of nuclear factor- κ B ligand (RANKL) expression in hepatocellular carcinoma with bone metastasis. *Ann Surg Oncol*. 2007;14(3):1191-1199. doi:10.1245/s10434-006-9277-4
18. Peng X, Guo W, Ren T, et al. Differential Expression of the RANKL/RANK/OPG System Is Associated with Bone Metastasis in Human Non-Small Cell Lung Cancer. *PLoS One*. 2013;8(3). doi:10.1371/journal.pone.0058361
19. Roux S, Meignin V, Quillard J, et al. RANK (receptor activator of nuclear factor- κ B) and RANKL expression in multiple myeloma. *Br J Haematol*. 2002;117(1):86-92. doi:10.1046/j.1365-2141.2002.03417.x
20. Chen G, Sircar K, Aprikian A, Potti A, Goltzman D, Rabbani SA. Expression of RANKL/RANK/OPG in primary and metastatic human prostate cancer as markers of disease stage and functional regulation. *Cancer*. 2006;107(2):289-298. doi:10.1002/cncr.21978
21. Santini D, Perrone G, Roato I, et al. Expression pattern of receptor activator of NF κ B (RANK) in a series of primary solid tumors and related bone metastases. *J Cell Physiol*. 2011;226(3):780-784. doi:10.1002/jcp.22402
22. Millen R, De Kort WWB, Koomen M, et al. Patient-derived head and neck cancer organoids allow treatment stratification and serve as a tool for biomarker validation and identification. *Med*. 2023;4(5):290-310.e12. doi:10.1016/j.medj.2023.04.003
23. Brown JS, Browne RM. Factors influencing the patterns of invasion of the mandible by oral squamous cell carcinoma. *Int J Oral Maxillofac Surg*. 1995;24(6):417-426. doi:10.1016/S0901-5027(05)80471-0
24. Carter RL, Tsao SW, Burman JF, Pittam MR, Clifford P, Shaw HJ. Patterns and mechanisms of bone invasion by squamous carcinomas of the head and neck. *Am J Surg*. 1983;146(4):451-455. doi:10.1016/0002-9610(83)90229-5
25. Clohisy DR, Palkert D, Ramnaraine MLR, Pekurovsky I, Oursler MJ. Human breast cancer induces osteoclast activation and increases the number of osteoclasts at sites of tumor osteolysis. *J Orthop Res*. 1996;14(3):396-402. doi:10.1002/JOR.1100140309
26. Maurizi A, Rucci N. The Osteoclast in Bone Metastasis: Player and Target. *Cancers (Basel)*. 2018;10(7):218. doi:10.3390/CANCERS10070218
27. Chuang FH, Hsue SS, Wu CW, Chen YK. Immunohistochemical expression of RANKL, RANK, and OPG in human oral squamous cell carcinoma. *J Oral Pathol Med*. 2009;38(10):753-758. doi:10.1111/j.1600-0714.2009.00793.x
28. Cui N, Nomura T, Takano N, et al. Osteoclast-related cytokines from biopsy specimens predict mandibular invasion by oral squamous cell carcinoma. *Exp Ther Med*. 2010;1(5):755-760. doi:10.3892/etm.2010.128
29. Elmusrati AA, Pilborough AE, Khurram SA, Lambert DW. Cancer-associated fibroblasts promote bone invasion in oral squamous cell carcinoma. *Br J Cancer*. 2017;117(6):867-875. doi:10.1038/bjc.2017.239
30. Gibo T, Yamada S ichi, Kawamoto M, Uehara T, Kurita H. Immunohistochemical Investigation of Predictive Biomarkers for Mandibular Bone Invasion in Oral Squamous Cell Carcinoma. *Pathol Oncol Res*. 2020;26(4):2381-2389. doi:10.1007/s12253-020-00826-y
31. Stopeck AT, Lipton A, Body JJ, et al. Denosumab compared with zoledronic acid for the treatment of bone metastases in patients with advanced breast cancer: A randomized, double-blind study. *J Clin Oncol*. 2010;28(35):5132-5139. doi:10.1200/JCO.2010.29.7101
32. Smith MR, Saad F, Coleman R, et al. Denosumab and bone-metastasis-free survival in men with castration-resistant prostate cancer: results of a phase 3, randomised, placebo-controlled trial. *Lancet*. 2012;379(9810):39-46. doi:10.1016/S0140-6736(11)61226-9

33. Henry DH, Costa L, Goldwasser F, et al. Randomized, double-blind study of denosumab versus zoledronic acid in the treatment of bone metastases in patients with advanced cancer (excluding breast and prostate cancer) or multiple myeloma. *J Clin Oncol*. 2011;29(9):1125-1132. doi:10.1200/JCO.2010.31.3304
34. Fizazi K, Carducci M, Smith M, et al. Denosumab versus zoledronic acid for treatment of bone metastases in men with castration-resistant prostate cancer: A randomised, double-blind study. *Lancet*. 2011;377(9768):813-822. doi:10.1016/S0140-6736(10)62344-6
35. Good CR, O'Keefe RJ, Edward Puzas J, Schwarz EM, Rosier RN. Immunohistochemical study of receptor activator of nuclear factor kappa-B ligand (RANK-L) in human osteolytic bone tumors. *J Surg Oncol*. 2002;79(3):174-179. doi:10.1002/jso.10067

SUPPLEMENTAL MATERIAL

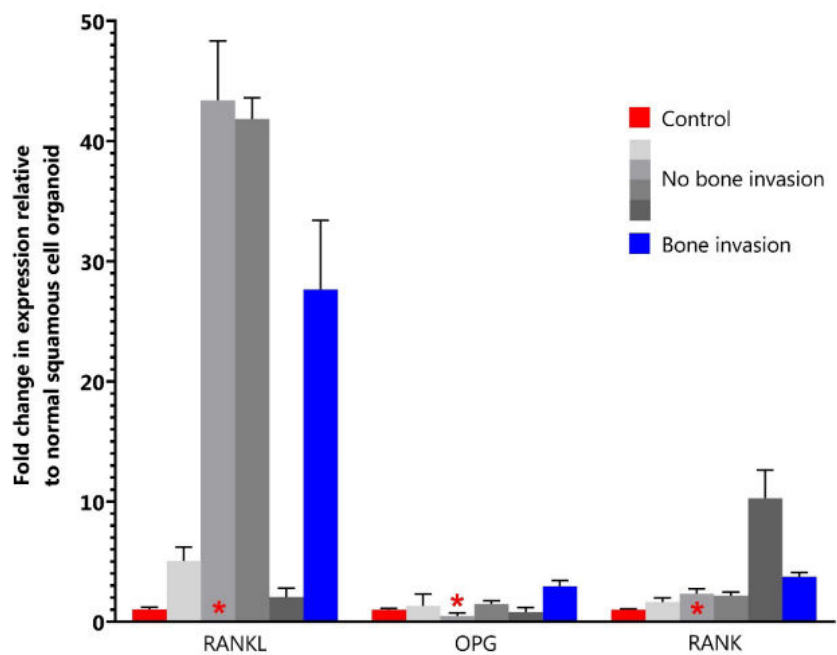


Figure S1. Results of 2nd quantitative PCR, *indicates HPV positive organoid line. Red: indicates organoid line of wildtype tongue epithelium used as control; Blue: indicates organoid line with bone invasion; Grey: indicates 4 organoid lines without bone invasion

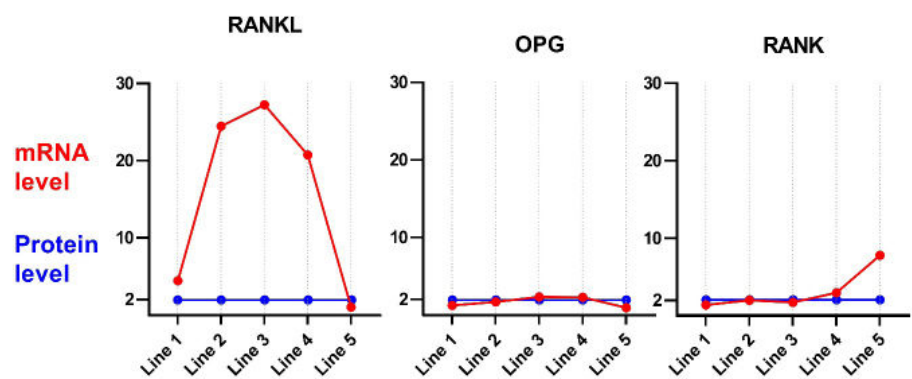


Figure S2. Protein versus mRNA expression, Immunohistochemical protein expression of RANKL, OPG and RANK was compared with mRNA expression assessed with qPCR.

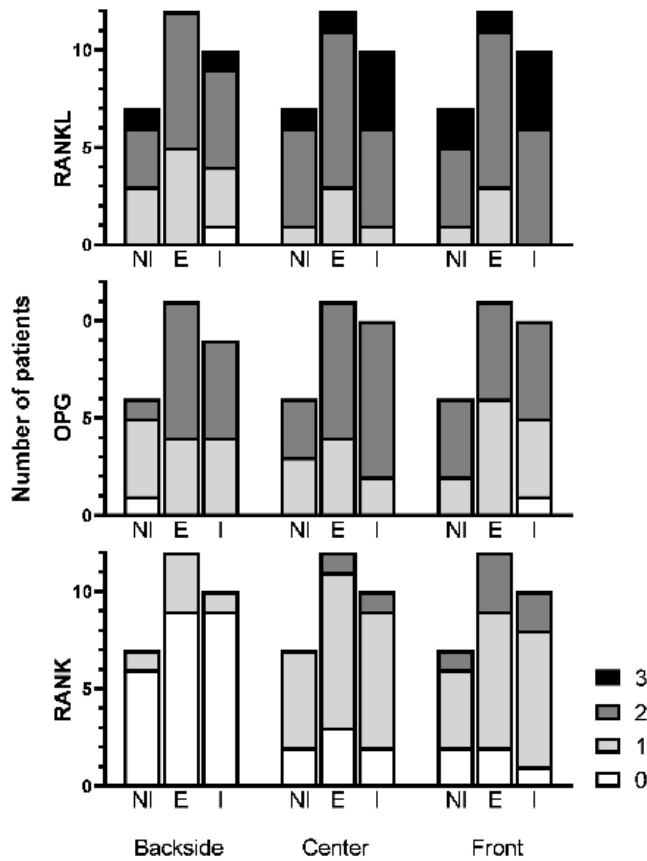


Figure S3. Differences in expression between patient groups per tumor side. Stacked bar charts of RANKL/OPG/RANK staining intensity score. Legend at the right displays color per staining intensity. X-axis displays three tumor sides with subdivision per patient group; NI: No Invasion, E: Erosion, I: Invasion. Y-axis displays number of patients. Groups were analyzed using Kruskal-Wallis H test, differences between groups were not statistically significant. Important note: RANKL intensity scored 0-3, OPG and RANK intensity scored 0-2.

Table S1. Primers for qPCR

primer name		primer sequence	length of product
Human RANKL(TNFSF11)	Forward 1	CAACATATCGTTGGATCACAGCA	161
Human RANKL(TNFSF11)	Reverse 1	GACAGACTCACTTTATGGGAACC	
Human RANKL(TNFSF11)	Forward 2	CCCATAAAGTGAGTCTGTCC	256
Human RANKL(TNFSF11)	Reverse 2	CAATACTGGTGCTTCTCTCC	
Human OPG(TNFRSF11B)	Forward 1	CACAAATTGCAGTGTCTTTGGTC	216
Human OPG(TNFRSF11B)	Reverse 1	TCTGCGTTTACTTTGGTGCCA	
Human OPG(TNFRSF11B)	Forward 2	GAAGGGCGCTACCTTGAGAT	102
Human OPG(TNFRSF11B)	Reverse 2	GCAAACGTATTTTCGCTCTGG	
Human RANK(TNFRSF11A)	Forward 1	TCCTCCACGGACAAATGCAG	92
Human RANK(TNFRSF11A)	Reverse 1	CAAACCGCATCGGATTTCTCT	
Human RANK(TNFRSF11A)	Forward 2	CACCAAATGAACCCCATGTTTAC	182
Human RANK(TNFRSF11A)	Reverse 2	GGACTCCTTATCTCCACTTAGGC	

Table S2: Differences in expression in tumor compared to expression in normal mucosa

	Friedman test		Multiple comparison with Bonferroni correction		
	Test statistic	p-value test statistic	Tumor front versus Normal mucosa	Tumor center versus Normal mucosa	Tumor backside versus Normal mucosa
RANKL					
No invasion	$\chi^2(3) = 12.60$	0.006	0.013	0.042	0.668
Erosion	$\chi^2(3) = 17.855$	<0.001	0.004	0.022	0.054
Invasion	$\chi^2(3) = 17.468$	0.001	0.003	0.016	1.000
OPG					
No invasion	$\chi^2(3) = 6.480$	0.09	*	*	*
Erosion	$\chi^2(3) = 3.766$	0.288	*	*	*
Invasions	$\chi^2(3) = 10.705$	0.013	0.877	0.061	0.152
RANK					
No invasion	$\chi^2(3) = 7.235$	0.065	*	*	*
Erosion	$\chi^2(3) = 19.857$	<0.001	0.015	0.116	1.000
Invasion	$\chi^2(3) = 7.174$	0.067	*	*	*

Table S2: Statistical testing of RANKL/OPG/RANK expression comparing tumor front, tumor center and tumor backside with expression in normal mucosa. As the expression score is ordinal data and expression is compared within a patient, the non-parametric Friedman's test was used. If the Friedman's test was statistically significant, multiple comparison with Bonferroni correction was executed. A p-value of ≤ 0.05 was interpreted as statistical significant and is displayed in bold.

Table S3: Differences in expression within tumor

	Friedman test		Multiple comparison with Bonferroni correction		
	Test statistic	p-value test statistic	Tumor front versus Tumor backside	Tumor center versus Tumor backside	Tumor front versus Tumor center
RANKL					
No invasion	$\chi^2(2) = 2.333$	0.311	*	*	*
Erosion	$\chi^2(2) = 2.571$	0.276	*	*	*
Invasion	$\chi^2(2) = 10.571$	0.005	0.042	0.076	1.000
OPG					
No invasion	$\chi^2(2) = 2.947$	0.229	*	*	*
Erosion	$\chi^2(2) = 4.000$	0.135	*	*	*
Invasions	$\chi^2(2) = 2.273$	0.321	*	*	*
RANK					
No invasion	$\chi^2(2) = 7.538$	0.023	0.247	0.425	1.000
Erosion	$\chi^2(2) = 13.923$	0.001	0.024	0.157	1.000
Invasion	$\chi^2(2) = 14.000$	0.001	0.016	0.076	1.000

Table S3: Statistical testing of RANKL/OPG/RANK expression comparing tumor front, tumor center and tumor backside. As the expression score is ordinal data and expression is compared within a patient, the non-parametric Friedman's test was used. If the Friedman's test was statistically significant, multiple comparison with Bonferroni correction was executed. A p-value of ≤ 0.05 was interpreted as statistical significant and is displayed in bold.

Table S4: Differences in expression between patient groups per tumor side

	Mean Rank			Kruskal Wallis Test	
	No invasion	Erosion	Invasion	Test statistic	p-value
RANKL	n=7	n=12	n=10		
Tumor-front	15.50	11.79	18.50	4.587	0.101
Tumor-center	14.57	12.63	18.15	3.102	0.212
Tumor-Backside	15.64	14.58	15.05	0.085	0.958
OPG	n=6	n=11	n=10		
Tumor-front	16.17	13.41	13.35	0.743	0.690
Tumor-center	11.75	13.59	15.80	1.536	0.464
Tumor-backside	8.50	15.45	14.44	4.397	0.111
RANK	n=7	n=12	n=10		
Tumor-front	12.93	15.58	15.75	0.733	0.693
Tumor-center	13.64	15.04	15.90	0.440	0.802
Tumor-backside	14.57	16.13	13.95	0.885	0.642

Table S4: Statistical testing of RANKL/OPG/RANK expression comparing patient groups; no invasion, erosion and invasion per tumor side (tumor front, tumor center and tumor backside). As the expression score is ordinal data and expression is compared from different patients, the non-parametric Kruskal-Wallis H test was used. As none of these tests were statistically significant, post-hoc testing was not executed. A p-value of ≤ 0.05 was interpreted as statistical significant and is displayed in bold.



CHAPTER 6

Clinicopathological factors as predictors for establishment of patient derived head and neck squamous cell carcinoma organoids

W.W.B. de Kort, R. Millen, E. Driehuis, L.A. Devriese, R.J.J. van Es, S.M. Willems

ABSTRACT

Introduction

Patient derived organoids (PDOs) are 3D *in vitro* models and have shown to better reflect patient and tumor heterogeneity than conventional 2D cell lines. To utilize PDOs in clinical settings and trials for biomarker discovery or drug response evaluation, it is valuable to determine the best way to optimize sample selection for maximum PDO establishment. In this study, we assess patient, tumor and tissue sampling factors and correlate them with successful PDO establishment in a well-documented cohort of patients with head and neck squamous cell carcinoma (HNSCC).

Methods

Tumor and non-tumorous adjacent tissue samples were obtained from HNSCC patients during routine biopsy or resection procedures at the University Medical Center Utrecht. The tissue was subsequently processed to establish PDOs. The sample purity was determined as the presence of epithelial cells in the culture on the day of organoid isolation as visualized microscopically by the researcher. PDO establishment was recorded for all samples. Clinical data was obtained from the medical records and was correlated to PDO establishment and presence of epithelial cells.

Results

Organoids could be established in 133/250 (53.2%) primary tumor site tissues. HNSCC organoid establishment was significantly more successful if patients were younger than the median age of 68 years (74/123 (60.2%) vs. 59/127 (46.5%), $p=0.03$). For a subset of samples, the presence of epithelial cells in the organoid culture on the day of organoid isolation was recorded in 112/149 (75.2%) of these samples. When cultures were selected for presence of epithelial cells, organoid establishment increased to 76.8% (86/112 samples).

Conclusion

This study found a trend between age and successful organoid outgrowth in patients with HNSCC younger than 68 years and emphasizes the value of efficient sampling regarding PDO establishment.

INTRODUCTION

The 5-year survival rates of head and neck squamous cell carcinoma (HNSCC) have only modestly improved over the past three decades from 55 to 66%¹. Numerous predictive and prognostic biomarkers have been investigated to predict survival and guide treatment decisions²⁻⁴. However many of these biomarkers have been investigated using traditional 2D cell line models, which do not harbor the complex genetic and phenotypic heterogeneity that exists in these tumors *in vivo*. Therefore, there is a need to improve *in vitro* models to validate biomarkers that better reflect patient and tumor heterogeneity more accurately. Patient derived organoids (PDO) may fill this gap.

Organoids are microscopic 3D structures that can be grown from patient derived stem cells of healthy or tumor tissues⁵. Organoids were first established from intestinal epithelium, and replicated the morphology of the crypt-villus structures present *in vivo*, demonstrating the ability to recapitulate the native tissue pathophysiology *in vitro*⁶⁻⁸. For several tumor types, living biobanks of PDO's have been established⁹⁻¹⁴ and correlations between patient- and PDO drug response have been reported^{6,15-19}.

Although PDOs have promising potential for personalized medicine, establishing PDOs can be laborious and costly. PDO establishment is more time-consuming compared to conventional 2D cell lines, and technically more difficult, requiring trained personnel^{20,21}. To utilize PDOs in clinical trials, it is important to know the success rates of establishing PDOs and if this correlates to clinical factors associated with the patient they are derived from. The reported pooled success rates for PDO establishment from multiple tissue and tumor types varies from 56.5-78.5%¹⁶. Herein, we assessed the correlation of patient tissue sampling and tumor-factors to PDO establishment in a previously published cohort of HNSCC patients^{6,15}.

MATERIALS AND METHODS

Patients and clinical data

This study analyzed organoids derived from a prospective cohort of patients with cancers of the head and neck area in the University Medical Center Utrecht (UMCU) as described in previously^{6,15}. The study protocol was approved by the Biobank Research Ethics Committee of the University Medical Center Utrecht (12-093 HUB-Cancer). All donors participating in this study signed informed-consent forms and could withdraw their consent at any time. Informed consent was obtained before tissue acquisition, patients were given a minimum of 24 hours to consider participation.

Patients were eligible for inclusion if 1) patients gave consent for the 12-093 HUB-cancer protocol, 2) patients had a type of HNSCC, 3) tissue acquisition was successful during biopsy for diagnostic histopathology or resection, 4) the laboratory of the Hubrecht institute tried to establish organoids for the sampled tissues.

Tissue acquisition

Primary tumor and/or lymph node metastatic tissue and tumor adjacent non-malignant tissue was obtained from HNSCC patients during either biopsy or resection procedures as part of their routine diagnostic or treatment regimen. For tissue acquisition during diagnostic biopsies, an extra biopsy of suspected malignant tissue was taken for this study during the procedure. For resection specimens, a small piece of tissue was sampled from the resected specimen at the tissue facility in the department of pathology. Tissue samples were immediately collected in +/+ organoid medium which consisted of advanced DMEM/F12 (AdDMEM/F12: Life Technologies, cat # 12634-034), supplemented with: 1x GlutaMAX (Thermofisher; Gibco, cat # 35050061), Penicillin-streptomycin (Life Technologies, cat # 15630-056), 10 mM HEPES (Life Technologies, cat # 15630-056) (+/+ medium) and 100 mg/mL Primocin (Invivogen, cat # ant-pm1). After transportation to the laboratory, organoid isolation was mostly performed on the same day as the tissue sampling, however in some cases isolation was performed within 3 days with an outlier of 10 days

Organoid isolation

The PDO culturing in this study has been described previously^{6,15}. In short, tissue samples were mechanically cut into pieces (1-3 mm²) and digested for 20-40 mins in 0.125% Trypsin (Sigma, cat # T1426) in +/+ medium supplemented with 10 μ M Y-27632 (Abmole Bioscience, cat. no. M1817) at 37°C. During incubation, mechanical force was used every 10 minutes to aid digestion by triturating the tissue pieces with a p1000 pipette. Tissue was subsequently triturated using a flame-sterilized pipette with a p10 tip on the end. Once pieces of tissue appeared macro- and microscopically dissociated, +/+ medium was topped up to 15 mL and the suspension was

filtered through a 70 mM filter (Corning, cat # CLS431751-50EA). Tubes were centrifuged at 300g, 5 mins and the supernatant was aspirated. Using ice-cold 70% 10 mg/mL-1 cold Cultrex growth factor reduced basement membrane extract (BME) type 2 (Trevigen, cat # 3533-010-02) in +/+ medium, the pellet was resuspended. BME/organoid suspension was plated in 10-20 mL droplets on the base of a preheated 48-well suspension culture plate (Greiner, cat # M9312). Plates were inverted and incubated at 37°C for at least 15-30 mins to allow solidification of BME. After solidification, pre-warmed culture medium supplemented with 10 μ M Y-27632 and caspofungin (0.5 mg/mL, Sigma Aldrich) was added to the plates and they were incubated in a 37C/5% CO₂ incubator. Two types of culture media were used for HNSCC organoids: A head neck(HN) cancer medium⁶ or cervical squamous cell medium(M7) as previously described²².

Organoid culturing

Organoids were subsequently grown from the primary material in culture media. All primary material was established on both HN and M7 medium to determine which medium was optimal for each organoid line. If an organoid line had an improved growth on a particular medium, this medium was subsequently used. HN and M7 medium were both supplemented with 0.5 mg/mL caspofungin for the first week of organoid culture and then removed. HN medium was also supplemented with 10 μ M of Y-27632 for the first week of organoid culture and was then removed. However M7 medium was constantly supplemented with 10 μ M of Y-27632. Medium was changed every two to three days and organoids were passaged between approximately 7 and 14 days after plating, depending on their growth rate.

To passage organoids, BME droplets were disrupted by resuspending the entire well content using a P1000 pipette. This was transferred to 15 mL Falcon tube, where up to 15 mL of +/+ was added and then centrifuged (300g, 5 min). After centrifugation, the organoid pellet was resuspended in 1-3 mL TrypLE Express (Life Technologies, Carlsbad, CA, USA, cat. no. 12605-010) and incubated for 3-10 mins at 37°C. The digestion was constantly monitored by checking the tube under the microscope. Organoids were sheared mechanically using a P1000 pipette with an extra P10 tip placed on the tip. After organoids were disrupted into single cells, tubes were topped up to 15 mL of +/+ to inhibit the TrypLE digestion, and centrifuged. Supernatant was removed down to the pellet and cells were resuspended in 70% BME in +/+/. The density of organoids were checked under the microscope before plating, if organoids were too dense, more 70% BME in +/+ was added. Multiple domes of 10-20 mL were plated on pre-heated suspension culture plates (Greiner, cat # M9312). Plates were inverted and incubated at 37C for at least 15 mins for BME solidification. After solidification, pre-warmed HN or M7 media supplemented with 10 μ M Y-27632 was added to the plates and they were incubated in a 37C/5% CO₂ incubator. For cultures growing on HN media, Y-27632 was removed from the medium after 2-3 days and organoids were subsequently cultured in media without Y-27623.

For M7 medium, Y-27632 was constantly in the media, and was therefore not removed after passaging.

To show that organoids contain tumor cells, the organoid cultures are exposed to nutlin-3a as described in Millen et al.¹⁵ Nutlin-3a is an MDM2 antagonist that ceases growth of TP53 wildtype cells (non-tumor epithelial cells) but leaves TP53 mutant cells (tumor epithelial cells) unaffected. Cultures are exposed to nutlin-3a for a period of 7-10 days and it is determined to be a tumor-derived organoid if growth continues in the presence of nutlin-3a and normal-derived organoid if it dies in the presence of nutlin-3a.

Clinical data

Clinical data was extracted from the medical records. The following clinical parameters were collected: Sex, age, prior cancer treatment status (defined as chemo- and/or radio-therapy). For tissue sampling details: type of sampling (biopsy or resection), date of sampling (i.e. time in days between sampling and organoid isolation), and for tumor details: tumor type, tumor location, TNM-stage²³ (if available pTNM otherwise cTNM), tumor diameter in centimeters, HPV-status, histopathological grade (Grade 1 well, Grade 2 moderately and Grade 3 poorly differentiated), presence of bone invasion, presence of angio-invasion, presence of perineural growth and growth pattern (cohesive vs. non-cohesive). HPV status was positive if it was pathologically confirmed. Bone invasion was positive if it was stated positive in the pathological report.

Analysis

For the analysis, each organoid line was analyzed as a separate case. For 15 patients, more than one HNSCC tissue specimen was collected. For example: a biopsy was initially collected for diagnosis, a resection of the primary or recurrent tumor was subsequently performed. The primary outcome was organoid establishment (yes/no) and was defined as 'successful' (or 'yes') if organoids reached Passage 1 (P1) and as 'no' if they did not grow and could not be passaged. P1 was defined as organoids that grew from isolation (P0) of primary tissue and were large enough to passage. Group differences were assessed for organoid establishment regarding the collected clinical variables on patient data, sampling data and tumor data.

The presence of epithelial cells in the organoid culture at P0 was available from the samples of 2019 onwards. After tissue processing, and upon plating the organoids (P0), the researcher recorded presence of epithelial cells with microscopic examination and presence was defined as 'yes' if either single cells or clumps of epithelial cells were present in the culture. If these were not observed, these were defined as "no epithelial cells present".

Statistics

The outcome variables are reported dichotomously. The continuous variables, age at surgery and tumor diameter, were split into two groups based on the median. The continuous variable 'number of days between sampling and isolation' was split into two groups (day 0 versus day 1 onwards). All of the other variables were nominal. Group differences per variable regarding organoid establishment and epithelial cell presence were assessed using the test of two proportions with a chi-square test of homogeneity. Bonferroni correction for multiple comparisons was executed. Statistical significance was considered if $p < 0.0167$ for patient factors (three comparisons), if $p < 0.025$ for sampling factors (two comparisons) and if $p < 0.0083$ for tumor factors (six comparisons). In case of an insufficient sample size, Fisher's exact test was used. Statistical analysis was performed with SPSS Statistics (IBM Corp. Released 2020. IBM SPSS Statistics for Windows, Version 27.0. Armonk, NY: IBM Corp).

RESULTS

521 collected tissue samples for which organoid establishment was attempted were included in this study. Tissues that were not derived from squamous cell carcinoma were excluded from this analysis ($n=24$) and organoid cultures that had a microscopically visible fungal or bacterial infection between isolation (P0) and P1 ($n=12$). Tissues from 250 samples originated from primary tumor site (primary tumor $n=200$, recurrent $n=17$, second primary $n=26$, third primary $n=6$ and fifth primary $n=1$), 27 originated from SCC-containing metastatic lymph nodes and 208 originated from normal mucosa adjacent to the HNSCC tumor. Patient characteristics are displayed in Table 1.

HNSCC organoid establishment and sample purity

Organoids could be established in 133/250 (53.2%) primary tumor site tissues (Table 1). For the samples from 2019 onwards ($n=149$) data about the presence of epithelial cells was confirmed. This was done on the day of isolation where epithelial cells were observed in the culture by bright-field microscopy in 112/149 (75.2%) of these samples. If there were epithelial cells present at P0, organoid establishment success rate increased to 76.8% (86/112 samples).

Table 1: Patient and tumor characteristics for corresponding organoid cultures. Values are numbers with (%) unless otherwise stated.

Characteristics		SCC tumor lines N=250	Normal mucosa lines N=208
Organoids	Established	133 (53.2)	141 (67.8)
Organoids	Established if epithelial cells present (n=112)	86/112 (76.8)	
Tumor nature	Primary	200 (80.0)	
	2 nd primary onwards	33 (13.2)	
	Recurrent	17 (6.8)	
Age (year)	Median (range)	68 (22 – 92)	69 (22 – 92)
Sex	Males	170 (68.0)	135 (64.9)
	Females	80 (32.0)	73 (35.1)
Pre treatment	No	208 (83.2)	168 (80.8)
	Yes		
	▪ Chemotherapy	1 (0.4)	2 (1.0)
	▪ Radiotherapy	27 (10.8)	27 (13.0)
	▪ Radiotherapy + Chemo	12 (4.8)	10 (4.8)
	▪ Radiotherapy + Cetuximab	2 (0.8)	1 (0.5)
	▪ Total	42 (16.8)	40 (19.2)
Sampling	Biopsy	75 (30.0)	12 (5.8)
	Resection	175 (70.0)	196 (94.2)
Organoid isolation day after surgery	Day 0	169 (75.8)	127 (70.9)
	Day 1	47 (21.1)	47 (26.3)
	Day 2 - 10	7 (3.1)	5 (2.8)
Tumor location	Oral cavity	151 (60.4)	
	Oropharynx	22 (8.8)	
	Hypopharynx	22 (8.8)	
	Larynx	48 (19.2)	
	Other*	7 (2.8)	
HPV status	Positive	12 (4.8)	
	Negative / not determined	238 (95.2)	
T-stage	T1	26 (10.4)	
	T2	88 (35.2)	
	T3	56 (22.4)	
	T4	80 (32.0)	
N-stage	N0	132 (52.8)	
	N1	28 (11.2)	
	N2	49 (19.6)	
	N3	41 (16.4)	

Table 1: Patient and tumor characteristics for corresponding organoid cultures. Values are numbers with (%) unless otherwise stated. (continued)

Characteristics		SCC tumor lines N=250	Normal mucosa lines N=208
Bone invasion	No / Not reported	195 (78.0)	
	Yes	55 (22.0)	
Peri neural invasion	No	102 (53.1)	
	Yes	90 (46.9)	
Angio invasion	No	152 (85.4)	
	Yes	26 (14.6)	
Tumor differentiation	Well	11 (10.8)	
	Moderately	74 (72.5)	
	Poor	17 (16.7)	
Growth Pattern	Cohesive	63 (36.4)	
	Non-Cohesive	110 (63.6)	
Tumor Diameter	Median (range cm)	3.0 (0.7 – 9.50)	

*Other comprises: Parotis (n=1), Nasopharynx (n=1), Nasal cavity (n=5). Pathological TNM-status was used if possible otherwise the clinical TNM-stage was used.

HNSCC organoid establishment correlation factors

Patient factors

PDO establishment tended to be more successful in patients who were younger than the median age of 68 years (74/123 (60.2%) vs. 59/127 (46.5%), $p=0.03$) Table 2 and Figure 1. There was no difference in successful establishment of organoids between males and females (93/170 (54.7%) vs. 40/80 (50.0%), $p=0.49$) nor for patients that received previous anti-cancer treatment compared to patients without prior treatment (11/208 (52.9%) vs. 23/42 (54.8%), $p=0.82$).

Tissue sampling factors

The majority of resection tumor specimens originated from the oral cavity, while the biopsy specimens were mostly derived from oropharyngeal, hypopharyngeal and laryngeal samples. There were no significant differences in PDO establishment between biopsy- and resection-specimens: 42/75 (56.0%) vs. 91/175 (52.0%), $p=0.56$ nor between the organoids isolated at the day of surgery or later: 96/169 (56.8%) vs. 29/54 (53.7%), $p=0.69$ (Table 2, Figure 1).

Table 2. HNSCCC group: Analysis of organoid establishment per clinical factor. Tests of proportions used were the chi-square tests of homogeneity. Statistical significance after Bonferroni correction was considered if $p < 0.0167$ for patient factors (three comparisons), if $p < 0.025$ for sampling factors (two comparisons) and if $p < 0.0083$ for tumor factors (six comparisons) NA: Not applicable as there are several proportion differences between more than two groups.

Factor with total number of cases available	Number of organoid lines established				Total (%)	Proportion Difference	p	
	Groups (% of total within group)							
Patient Factors								
Sex n=250	Males 93 (54.7)	Females 40 (50.0)			133 (53.2)	0.047	0.49	
Age (split median) n=250	< 68 years 74 (60.2)	≥ 68 years 59 (46.5)			133 (53.2)	0.137	0.03	
Pretreatment n=250	No 110 (52.9)	Yes 23 (54.8)			133 (53.2)	0.019	0.82	
Sampling factors								
Method n=250	Biopsy 42 (56.0)	Resection 91 (52.0)			133 (53.2)	0.04	0.56	
Days to org isolation n=223	0 96 (56.8)	1-5 29 (53.7)			125 (56.0)	0.031	0.69	
Tumor factors								
Tumor location* n=243	Oral Cavity 80 (53.0)	Oropharynx 14 (63.6)	Hypopharynx 9 (40.9)	Larynx 27 (56.3)	130 (53.5)	NA	0.48	
HPV status n=250	Negative 126 (52.9)	Positive 7 (58.3)			133 (53.2)	0.054	0.72	
T stage n=250	T1 12 (46.2)	T2 53 (60.2)	T3 28 (50.0)	T4 40 (50.0)	133 (53.2)	NA	0.42	
N stage n=250	N0 66 (50.0)	N1 16 (57.1)	N2 28 (57.1)	N3 23 (56.1)	133 (53.2)	NA	0.76	
Bone invasion n=250	No 108 (55.4)	Yes 25 (45.5)			133 (53.2)	0.099	0.19	
Peri neural invasion n=192	No 52 (51.0)	Yes 48 (53.3)			100 (52.0)	0.023	0.74	
Angio invasion n=178	No 78 (51.3)	Yes 14 (53.8)			92 (51.7)	0.028	0.81	
Differentiation n=102	Grade I 6 (54.5)	Grade II 36 (48.6)	Grade III 10 (58.8)			52 (51.0)	NA	0.73
Growth pattern n=173	Cohesive 35 (55.6) 55 (50.0)		Non-Cohesive		90 (52.0)	0.056	0.48	
Tumor diameter n=184	< 3 cm 45 (50.6)	≥ 3 cm 49 (51.6)			94 (51.0)	0.016	0.89	

*Excluding location tumor 'other' (n=7)

Clinical parameters

Of the 250 SCC samples, 151/250 (60.4%) tumor tissues originated from the oral cavity, 22/250 (8.8%) from the oropharynx, 22/250 (8.8%) from the hypopharynx, 48/250 (19.2%) from the larynx, and 7/250 (2.8%) from other tumor sites documented in Table 1. There were no differences regarding PDO establishment for: Tumor location, HPV-status, T-stage, N-stage, Bone invasion, perineural invasion, angioinvasion, tumor grade, growth pattern and tumor diameter (Table 2, Figure 1).

Primary tumor site SCC vs Metastatic SCC

For SCC tissues from the primary tumor site, PDO establishment was slightly more successful compared to metastatic SCC, (133/250 (53.3%) vs. 12/27 (44.4%), $p=0.39$). However, differences in proportions were not statistically significant.

Primary tumor vs Secondary (or more) primary and recurrent

PDO establishment was not more successful for primary SCC tissues, compared to secondary (or more) or recurrent SCC, (108/200 (54%) vs. 25/50 (50%), $p=0.61$).

Normal mucosa organoid establishment

Normal mucosa organoids could be established in 141/208 (67.8%) samples of tumor-adjacent epithelium. In this cohort, there were no differences in the success rate of PDO establishment for: sex, median age, pre-treated vs. untreated tumors and isolation on day of surgery or later (Table 3). There was a strong trend towards an improved success rate of PDOs from resection samples as compared to biopsies: 136/196 (69.4%) vs. 5/12 (41.7%), $p=0.06$ (Table 3).

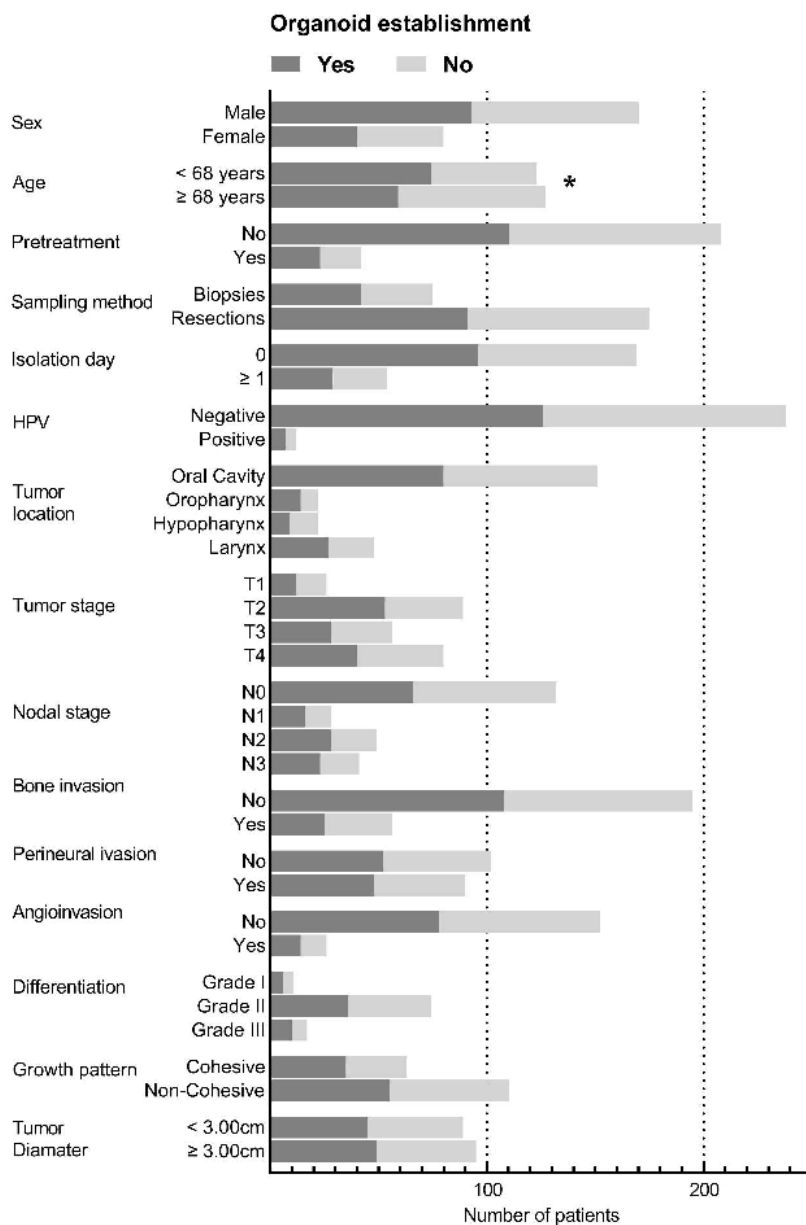


Figure 1 HNSCC group: Organoid establishment correlating to clinical-, sampling- and tumor-parameters. X-axis shows number of patients. Y-axis shows different clinical parameters. * indicates a trend towards a statistical significant difference using the test of two proportions with a chi-square test of homogeneity. Pretreatment was defined as: Patient received radiotherapy anywhere on the body and/or chemotherapy ever. Isolation day means: Days between surgery and organoid isolation. Tumor and Nodal stage according to the TNM criteria.

Table 3 Normal Mucosa: Analysis of organoid establishment per clinical factor. Tests of proportions used were the chi-square tests of homogeneity. Statistical significance after Bonferroni correction was considered if $p < 0.0167$ for patient factors (three comparisons) and if $p < 0.025$ for sampling factors (two comparisons). NA: Not applicable as there are several proportion differences between more than two groups.

Factor with total number of cases available	Number of organoid lines established		Proportion Difference	p	
	Groups (% of total within group)	Total (%)			
Patient Factors					
Sex n=208	Males 91 (67.4)	Females 50 (68.5)	141 (67.8)	0.011	0.87
Age (split median) n=208	< 69 years 73 (70.2)	≥ 69 years 68 (65.4)	141 (67.8)	0.048	0.46
Pretreatment n=208	No 118 (70.2)	Yes 23 (57.5)	141 (67.8)	0.127	0.12
Sampling factors					
Method n=208	Biopsy 5 (41.7)	Resection 136 (69.4)	141 (67.8)	0.277	0.06*
Days to org isolation** n=179	0 86 (67.7)	1-5 39 (75.0)	125 (69.8)	0.073	0.35

*fisher exact test because of low sample size biopsies. **Data of this parameters was not available for all tissues.

Tissue sample purity

In biopsies, there were significantly more epithelial cells present in the culture on the day of organoid isolation compared to resection specimens (45/52 (86.5%) vs. 67/97 (69.1%), $p=0.02$, Table S1). Likewise, in the primary/local recurrent HNSCC samples, there were significantly more epithelial cells present in the culture on the day of isolation compared to the metastatic HNSCC samples (112/149 (75.2%) vs. 15/27 (55.6%), $p=0.04$). There was a strong trend that cultures from patients below the median age of 68 years had more epithelial cells present in the culture on the day of isolation (82.6% vs 68.8%, $p=0.05$, Table S1). The other clinical factors revealed no differences in presence of epithelial cells in the culture on the day of isolation, neither for SCC tissues nor for normal mucosa tissues (Table S1+S2). Figure 2 displays H&E staining's of 4 sampled tumor tissues before the start of organoid culturing. For Figure 2A and 2B epithelial cells were present at P0, for Figure 2C and 2D epithelial cells were not present in the culture at P0.

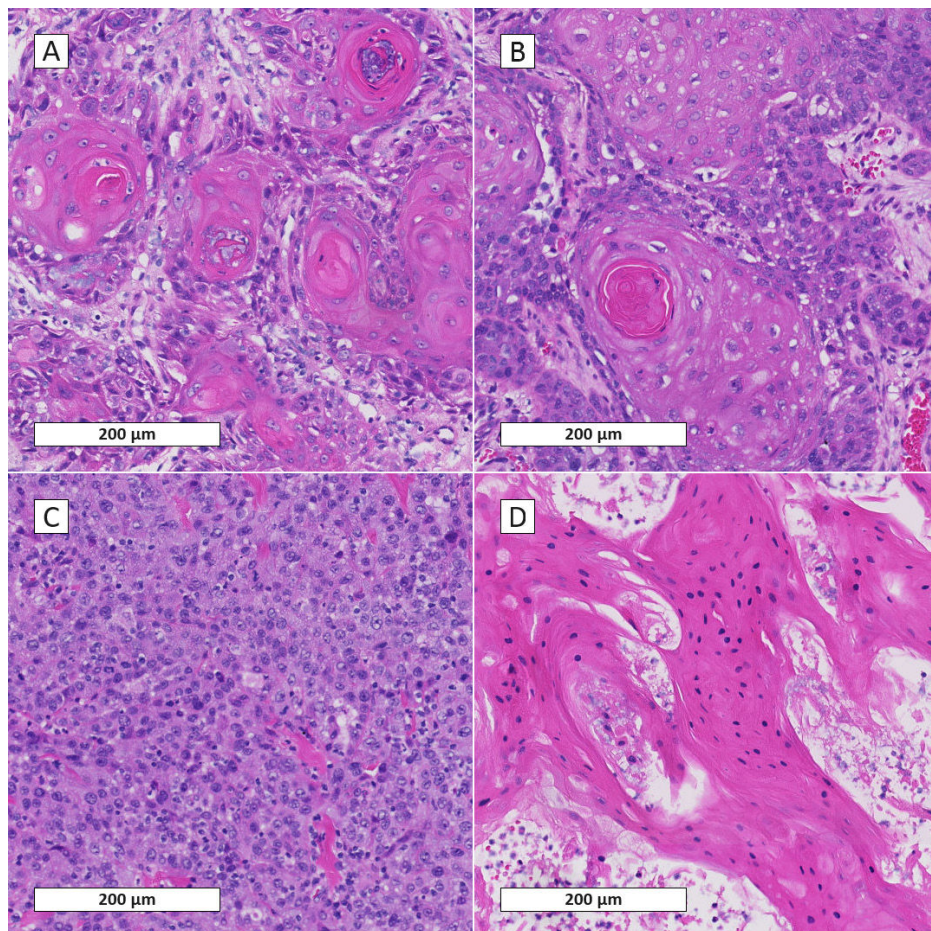


Figure 2: Hematoxylin and eosin stain of 4 tumor samples before organoid culturing; A: Tumor sample of Larynx; B: Tumor sample of oropharynx; C: Tumor sample of Lymph Node metastasis; D: Tumor sample of Oral Cavity; For 2A and 2B epithelial cells were present in the culture at P0; For 2C and 2D epithelial cells were not present in the culture at P0.

DISCUSSION

It is relevant to know if there are patient- and/or tumor-factors in tissue sampling that influence PDO establishment, as this could help future researchers navigate organoid biobanks. However, to date, there have been no studies in HNSCC to assess such factors. This study assessed clinical factors regarding PDO establishment and found a trend of PDO establishment being more successful in younger patients with HNSCC, below the median age of 68 years, although this was just not statistically significant ($p=0.03$). This could be explained

by the fact that cell division rates decrease with age²⁴. The study of Larsen et al. published their supplemental data on age of 77 HNSCC organoids of which 12 were biobankable²⁵. The mean age in deciles for the biobankable organoids was 6.67 and the mean age in deciles for the 65 non-biobankable organoids was 7.09. These findings are in line with our trend. In the whole cohort, which consisted of several organoid tumor types, age was not different for the biobankable and non-biobankable organoids²⁵. For future HNSCC organoid studies, this could be considered, as this may support successful organoid outgrowth. This seems clinically applicable as elderly patients with comorbidities are already often refrained from chemotherapy²⁶. As this cohort of patients only contained HNSCC, the median age associated with successful organoid outgrowth, may vary between other tumor types. Therefore, age as a factor for successful organoid culture should also be explored in other types of cancer.

There was no difference in PDO establishment between patients that received chemo – and/or radiotherapy compared to untreated patients. This is reassuring, as many cancer regimens include surgery as well as adjuvant systemic therapy, highlighting that the use of systemic therapy in HNSCC has no impact on organoid outgrowth. In line with this, Ooft et al. (colorectal cancer), Larsen et al. (several tumortypes) and Sharick et al. (pancreatic cancer) also did not find a correlation between previous chemotherapy and PDO outgrowth^{18,25,27}. Interestingly, another study on colorectal cancer found a reduced PDO outgrowth if patients had received neoadjuvant chemoradiotherapy prior to tissue sampling compared to non-adjuvant and chemotherapy-only groups²⁸. We did not find differences in PDO establishment between primary/locally recurrent tumors and metastatic tumors, which is in line with two other studies^{17,24}. Again, this is reassuring for future organoid studies that plan to establish organoids from metastatic tissue, as this may not affect outgrowth. Like Larsen et al. we did not find differences in PDO establishment based on tumor size²⁵.

We found a significantly higher presence of epithelial cells in biopsies compared to surgical resection specimens for HNSCC PDOs (86.5% vs 69.1%, $p=0.02$), although there was no difference in PDO establishment itself. For prostate cancer, sampling with radical prostatectomy compared to transurethral resection of the prostate resulted in an improved PDO establishment for the radical prostatectomy group²⁹. Likewise, for colorectal cancer, the rate of successful PDO culture was lower for endoscopic biopsies compared to surgical resection specimen²⁸. Similar to our findings, differentiation grade did not influence PDO establishment in prostate cancer²⁹.

The influence of efficient sampling of the tumor on organoid establishment may be bigger than the influence of the clinical factors themselves. Here we show an increase in PDO establishment from 53.2% to 76.8% if organoid cultures were found to have epithelial cells present in the culture at P0. Moreover, in a subset analysis, we previously found an increase in

the success rate of HNSCC organoids from 33.3% to 85.5% in cases where epithelial cells were present in the collected tissues, assessed by H&E staining of the tissue sample ($n = 77$, Fisher's exact test, proportion 0.522, $p < 0.001$)¹⁵. For metastatic gastro-intestinal cancer organoids Vlachochiannis et al. also describe that the establishment rate strongly correlated with tumor cellularity in the original tissue biopsy¹⁷. Likewise in prostate organoids, a significant correlation between tumor cell percentage in the original tissue sample and prostate organoid establishment was reported²⁹. This indicates that efficient sampling is important for optimizing PDO establishment. Figure 2 emphasizes the importance for efficient sampling.

Interestingly, in this analysis, we showed a statistically significant difference between biopsies and resections, with biopsy-derived organoid cultures typically having more epithelial cells present on the day of isolation compared to resections specimens. For biopsies, the sample is taken directly by the surgeon whereas for surgical resections, the tissue is removed from the body whereupon it is sampled at a later point by the pathology department. This difference in presence of epithelial cells on the day of isolation could be due to difficulty to recognize tumor versus normal tissue during sampling of the resected specimen vs. a tumor that is in situ in the body during a biopsy procedure. Additionally, we found epithelial cells more frequently in the culture at P0 for primary tumor tissues compared to metastatic tumors in lymph nodes (75.5% vs 55.6%, $p=0.03$). A tendency that the success rate of PDO establishment is better for primary tumor site samples, suggests sampling efficiency is better at the primary tumor site compared to HNSCC lymph node metastasis.

In this study, organoids were deemed successful if they reached P1, and most organoids included in the analysis were started on both HN and M7 media types to determine the optimal media for each organoid line. Therefore, the effect of the media composition on successful outgrowth is not a factor in our analysis, and it is more important if a culture has epithelial cells present on day of isolation or not. Larsen et al have investigated the effect that various growth factors have on functional growth and phenotypes in tumor organoids derived from various tumor types. They found that although EGF stimulated proliferation in most cultures, there was no significant difference in growth between the 5 various media conditions that were tested. In particular, they assessed the success rate of head and neck organoids when established on complete versus minimum media type, and found no difference.

In conclusion, this study found a positive trend between age and successful organoid outgrowth in patients with HNSCC younger than 68 years and emphasizes the value of efficiently sampling tumors to achieve successful PDO establishment. This study highlights the importance of future organoid studies to evaluate clinical factors that may influence organoid outgrowth, and investigating this in other tumor types.

REFERENCES

1. Johnson DE, Burtneß B, Leemans CR, Lui VWY, Bauman JE, Grandis JR. Head and neck squamous cell carcinoma. *Nat Rev Dis Prim.* 2020;6(1). doi:10.1038/s41572-020-00224-3
2. Gavrielatou N, Doulas S, Economopoulou P, Foukas PG, Psyrri A. Biomarkers for immunotherapy response in head and neck cancer. *Cancer Treat Rev.* 2020;84. doi:10.1016/j.ctrv.2020.101977
3. Hsieh JCH, Wang HM, Wu MH, et al. Review of emerging biomarkers in head and neck squamous cell carcinoma in the era of immunotherapy and targeted therapy. *Head Neck.* 2019;41(S1):19-45. doi:10.1002/hed.25932
4. de Kort WWB, Spelier S, Devriese LA, van Es RJJ, Willems SM. Predictive Value of EGFR-PI3K-AKT-mTOR-Pathway Inhibitor Biomarkers for Head and Neck Squamous Cell Carcinoma: A Systematic Review. *Mol Diagnosis Ther.* 2021;25(2):123-136. doi:10.1007/s40291-021-00518-6
5. Drost J, Clevers H. Organoids in cancer research. *Nat Rev Cancer.* 2018;18(7):407-418. doi:10.1038/s41568-018-0007-6
6. Driehuis E, Kolders S, Spelier S, et al. Oral mucosal organoids as a potential platform for personalized cancer therapy. *Cancer Discov.* 2019;9(7):852-871. doi:10.1158/2159-8290.CD-18-1522
7. Tuveson D, Clevers H. Cancer modeling meets human organoid technology. *Science (80-).* 2019;364(6444):952-955. doi:10.1126/science.aaw6985
8. Sato T, Vries RG, Snippert HJ, et al. Single Lgr5 stem cells build crypt-villus structures in vitro without a mesenchymal niche. *Nature.* 2009;459(7244):262-265. doi:10.1038/nature07935
9. Kim M, Mun H, Sung CO, et al. Patient-derived lung cancer organoids as in vitro cancer models for therapeutic screening. *Nat Commun.* 2019;10(1). doi:10.1038/s41467-019-11867-6
10. Yan HHN, Siu HC, Law S, et al. A Comprehensive Human Gastric Cancer Organoid Biobank Captures Tumor Subtype Heterogeneity and Enables Therapeutic Screening. *Cell Stem Cell.* 2018;23(6):882-897. e11. doi:10.1016/j.stem.2018.09.016
11. Van De Wetering M, Francies HE, Francis JM, et al. Prospective derivation of a living organoid biobank of colorectal cancer patients. *Cell.* 2015;161(4):933-945. doi:10.1016/j.cell.2015.03.053
12. Sachs N, de Ligt J, Kopper O, et al. A Living Biobank of Breast Cancer Organoids Captures Disease Heterogeneity. *Cell.* 2018;172(1-2):373-386.e10. doi:10.1016/j.cell.2017.11.010
13. Hill SJ, Decker B, Roberts EA, et al. Prediction of DNA repair inhibitor response in short-term patient-derived ovarian cancer organoids. *Cancer Discov.* 2018;8(11):1404-1421. doi:10.1158/2159-8290.CD-18-0474
14. Hou S, Tiriach H, Sridharan BP, et al. Advanced Development of Primary Pancreatic Organoid Tumor Models for High-Throughput Phenotypic Drug Screening. *SLAS Discov.* 2018;23(6):574-584. doi:10.1177/2472555218766842
15. Millen R, De Kort WWB, Koomen M, et al. Patient-derived head and neck cancer organoids allow treatment stratification and serve as a tool for biomarker validation and identification. *Med.* 2023;4(5):290-310.e12. doi:10.1016/j.medj.2023.04.003
16. Wensink GE, Elias SG, Mullenders J, et al. Patient-derived organoids as a predictive biomarker for treatment response in cancer patients. *npj Precis Oncol.* 2021;5(1). doi:10.1038/s41698-021-00168-1
17. Vlachogiannis G, Hedayat S, Vatsiou A, et al. Patient-derived organoids model treatment response of metastatic gastrointestinal cancers. *Science (80-).* 2018;359(6378):920-926. doi:10.1126/science.aao2774

18. Ooft SN, Weeber F, Dijkstra KK, et al. Patient-derived organoids can predict response to chemotherapy in metastatic colorectal cancer patients. *Sci Transl Med*. 2019;11(513). doi:10.1126/scitranslmed.aay2574
19. Yao Y, Xu X, Yang L, et al. Patient-Derived Organoids Predict Chemoradiation Responses of Locally Advanced Rectal Cancer. *Cell Stem Cell*. 2020;26(1):17-26.e6. doi:10.1016/j.stem.2019.10.010
20. Kondo J, Inoue M. Application of cancer organoid model for drug screening and personalized therapy. *Cells*. 2019;8(5). doi:10.3390/cells8050470
21. Foo MA, You M, Chan SL, et al. Clinical translation of patient-derived tumour organoids- bottlenecks and strategies. *Biomark Res*. 2022;10(1). doi:10.1186/s40364-022-00356-6
22. Löhmußaar K, Oka R, Espejo Valle-Inclán J, et al. Patient-derived organoids model cervical tissue dynamics and viral oncogenesis in cervical cancer. *Cell Stem Cell*. 2021;28(8):1380-1396.e6. doi:10.1016/j.stem.2021.03.012
23. Huang SH, O'Sullivan B. Overview of the 8th Edition TNM Classification for Head and Neck Cancer. *Curr Treat Options Oncol*. 2017;18(7). doi:10.1007/s11864-017-0484-y
24. Tomasetti C, Poling J, Roberts NJ, et al. Cell division rates decrease with age, providing a potential explanation for the age-dependent deceleration in cancer incidence. *Proc Natl Acad Sci U S A*. 2019;116(41):20482-20488. doi:10.1073/pnas.1905722116
25. Larsen BM, Kannan M, Langer LF, et al. A pan-cancer organoid platform for precision medicine. *Cell Rep*. 2021;36(4). doi:10.1016/j.celrep.2021.109429
26. Bahig H, Fortin B, Alizadeh M, et al. Predictive factors of survival and treatment tolerance in older patients treated with chemotherapy and radiotherapy for locally advanced head and neck cancer. *Oral Oncol*. 2015;51(5):521-528. doi:10.1016/j.oraloncology.2015.02.097
27. Sharick JT, Walsh CM, Sprackling CM, et al. Metabolic Heterogeneity in Patient Tumor-Derived Organoids by Primary Site and Drug Treatment. *Front Oncol*. 2020;10. doi:10.3389/fonc.2020.00553
28. Zeng YL, Wang SD, Li YR, et al. Analysis of factors influencing the success rate of organoid culture in 1231 cases of colorectal cancer. *Zhonghua Wei Chang Wai Ke Za Zhi*. 2023;26(8):780-786. doi:10.3760/cma.j.cn441530-20221128-00499
29. Servant R, Garioni M, Vlajnic T, et al. Prostate cancer patient-derived organoids: detailed outcome from a prospective cohort of 81 clinical specimens. *J Pathol*. 2021;254(5):543-555. doi:10.1002/path.5698

SUPPLEMENTAL MATERIAL

Table S1.

Factor with total number of cases available	Number of cultures with epithelial cell presence				Proportion Difference	P	
	Groups (% of total within group)			Total (%)			
Patient Factors							
Sex n=149	Males 78 (74.3)	Females 34 (77.3)		112 (75.2)	0.03	0.70	
Age n=149	< 68 years 57 (82.6)	≥ 68 years 55 (68.8)		112 (75.2)	0.138	0.05	
Pretreatment n=149	No 87 (74.4)	Yes 25 (78.1)		112 (75.2)	0.037	0.66	
Sampling factors							
Method n=149	Biopsy 45 (86.5)	Resection 67 (69.1)		112 (75.2)	0.174	0.02	
Days to org isolation n=146	Day 0 88 (77.9)	Day 1-5 23 (69.7)		111 (76.0)	0.082	0.33	
Tumor factors							
Tumor location n=142	Oral Cavity 53 (69.7)	Oropharynx 12 (85.7)	Hypopharynx 15 (88.2)	Larynx 28 (80.0)	108 (76.0)	NA	0.25
HPV status n=149	Negative 107 (74.8)	Positive 5 (83.3)		112 (75.2)	0.085	1.00*	
T stage n=149	T1 12 (92.3)	T2 37 (72.5)	T3 26 (74.3)	T4 37 (74.0)	112 (75.2)	NA	0.56*
N stage n=149	N0 58 (74.4)	N1 15 (78.9)	N2 14 (70.0)	N3 25 (78.1)	112 (75.2)	NA	0.89*
Bone invasion n=149	No 86 (78.2)	Yes 26 (66.7)		112 (75.2)	0.115	0.15	
Peri neural invasion n=110	No 37 (64.9)	Yes 40 (75.5)		77 (70.0)	0.106	0.23	
Angio invasion n=101	No 56 (69.1)	Yes 13 (65.0)		69 (68.3)	0.041	0.72	
Differentiation n=79	Grade 1 3 (42.9)	Grade 2 41 (70.7)	Grade 3 10 (71.4)		54 (68.4)	NA	0.36*
Growth pattern n=96	Cohesive 18 (66.7)		Non-Cohesive 49 (71.0)		67 (69.8)	0.043	0.68
Tumor diameter n=104	< 3.15cm 34 (65.4)	≥ 3.15 cm 37 (71.2)		71 (68.3)	0.058	0.53	

HNSCCC group: Analysis of epithelial cell presence on day of isolation per clinical factor. Tests of proportions used were the chi-square tests of homogeneity. Statistical significance after Bonferroni

correction was considered if $p < 0.0167$ for patient factors (three comparisons), if $p < 0.025$ for sampling factors (two comparisons) and if $p < 0.0083$ for tumor factors (six comparisons) NA: Not applicable as there are several proportion differences between more than two groups.

*fisher exact test because of low sample size.

Table S2.

Factor with total number of cases available	Number of cultures with epithelial cell presence		Proportion Difference	P value	
	Groups (% of total within group)	Total (%)			
Patient Factors					
Sex n=133	Males 65 (71.4)	Females 34 (81.0)	99 (74.4)	0.096	0.24
Age (split median) n=133	< 69 years 47 (74.6)	≥ 69 years 52 (74.3)	99 (74.4)	0.003	0.97
Pretreatment n=133	No 78 (76.5)	Yes 21 (67.7)	99 (74.4)	0.088	0.33
Sampling factors					
Method n=133	Biopsy 7 (63.6)	Resection 92 (75.4)	99 (74.4)	0.118	0.47*
Days to org isolation n=130	0 64 (69.6)	1-5 32 (84.2)	96 (73.8)	0.146	0.08

Normal Mucosa: Analysis of epithelial cell presence on day of isolation per clinical factor. Tests of proportions used were the chi-square tests of homogeneity. Statistical significance after Bonferroni correction was considered if $p < 0.0167$ for patient factors (three comparisons) and if $p < 0.025$ for sampling factors (two comparisons). NA: Not applicable as there are several proportion differences between more than two groups.

*fisher exact test because of low sample size.



CHAPTER 7

Summary and general discussion

SUMMARY AND GENERAL DISCUSSION

Head and neck cancer (HNC) is the 7th most common type of cancer worldwide with around 1.000.000 new cases and 465.000 deaths in 2020¹. HNC is a collective term for tumors arising from the upper aerodigestive tract, i.e. the oral cavity, pharynx, larynx, nasal cavity, paranasal sinuses and the salivary glands. Over 95% of these cancers are squamous cell carcinomas (HNSCC) that develop from the mucosal epithelium²⁻⁴. Despite the different treatment options and the advances in targeted therapy development, the 5-year HNC survival has only modestly improved over the last three decades to around 66% for all subsites and stages combined⁵. Robust biomarkers, that predict survival outcome and help with treatment decisions are lacking and only few biomarkers have been confirmed in clinical trials. Furthermore, biomarkers are difficult to test in traditional in vitro models as the in vivo tumor structure and 3D morphology is missing. Accordingly, better models mirroring a more accurate tumor heterogeneity, are needed. Organoids may fill this void. As mentioned in the introduction organoids can be used for both cancer biology research and personalized medicine.

The understanding of molecular pathogenesis of HNSCC has considerably improved in the last decades. This resulted in new strategies for treating HNSCC, especially targeted therapies e.g. targeting EGFR, which is overexpressed in the majority of HNSCCs⁶. Although primary and acquired resistance is a challenge, these targeted therapies have potential. Biomarkers are pivotal for the introduction and use of targeted therapies. As reviewed in **Chapter 2**, many biomarkers for targeted therapy in the EGFR-PI3K-AKT-mTOR pathway have been researched but only few were confirmed in clinical trials. A robust biomarker predicting treatment outcome is still lacking. Current research is hindered by small sample sizes, heterogeneous study populations, and discrepancies in treatment protocols. A more systematic approach to biomarker research, including incorporation into clinical trials and patient-centred trial designs, is needed. Overall, while several biomarkers have been investigated, their clinical validation remains limited, emphasizing the need for continued research to advance personalized medicine in HNSCC treatment. Integration of multiple biomarkers and the use of patient-derived HNC-organoids offer promising avenues for improving predictive accuracy.

Driehuis et al. described the first long-term culture of organoids derived from HNSCC and normal corresponding tissue⁷. In **Chapter 3** we describe an expansion of the previously described biobank of organoids derived from HNSCC and also add other histological types of HNC. Here we present an expansion of the earlier published biobank of HNC organoids from 31 to 110 models. In the adjuvant radiotherapy setting for HNSCC we describe a correlation where organoids which were more resistant to radiotherapy corresponded to patients who relapsed earlier compared to patients of which organoids were sensitive to radiotherapy.

Despite the small sample size (n=15) a correlation is present. We did not find a correlation between cisplatin sensitivity in organoids and relapse of patients.

We screened a subset of these organoids for response to radiotherapy with or without cisplatin, carboplatin and cetuximab. In general, both cisplatin and carboplatin increased sensitivity to radiotherapy, as corresponds to findings in clinical practice⁸. The EGFR inhibitor cetuximab however reduced the sensitivity to radiotherapy, which is in line with current literature that describes a worse survival for patients treated with cetuximab and radiotherapy compared to cisplatin and radiotherapy.^{9–11} All this confirms, that organoids reflect tumor behaviour of HNSCC in the clinical situation. However, it is important to note that even though cetuximab served as a radioprotector, the in vitro additive effect of radiotherapy and cetuximab was still more toxic than that of radiotherapy alone for most patient-derived organoid models.

In addition, in **Chapter 3** we also describe the response to multiple targeted therapies for a subset of HNC organoids. For preclinical targeted therapies, patient response to therapy is unknown as these agents are not yet introduced clinically. Exploring organoid response for new targeted therapies is helpful to acquire drug screen data that can help future screening and research towards implementation of targeted therapies. This not only applies to preclinical therapies but also for existing therapies. Moreover, we also used HNSCC organoids for biomarker research: Preclinical studies describe PIK3CA mutations as biomarker for targeted therapy alpelisib¹². We determined alpelisib response in HNSCC organoids: PI3KCA mutant organoids did not respond significantly better compared to non-mutant organoids. We introduced the most common PIK3CA mutation (E545K) in two organoid lines using CRISPR base-editing technology creating two isogenic pairs differing only by one specific mutation. The difference in alpelisib response between the two patients was bigger than the difference within the isogenic pairs. This finding underscores the potential of organoids to determine the value of a particular biomarker to drug sensitivity in the context of relevant patient heterogeneity.

In **chapter 4** we investigated protein expression of p-mTOR, p-ERK and PTEN as prognostic biomarkers in HPV negative HNSCC patients treated with primary chemoradiotherapy. We found a significant worse overall survival in patients with high p-mTOR expression which is in line with other HNC studies^{13–15}. Moreover, protein p-mTOR expression in a panel of HNSCC organoids correlated to mTOR-inhibitor everolimus response in these organoids. We show the potential of HNSCC organoids for predicting everolimus response based on p-mTOR expression.

Chapter 5 describes a retrospective cohort study that tries to clarify the mechanism of jaw bone invasion in patients with oral squamous cell carcinoma. The findings of this study suggest that oral squamous cell carcinoma induces bone invasion due to the stimulation of osteoclast activation by regulating the production of RANKL and RANK proteins. In this study

we show the ability of HNSCC organoids to express RANKL, OPG and RANK on protein level and on mRNA level as determined by qPCR. These findings are the first steps for biomarker research and targeted therapy regarding bone invasion in HNSCC. It is interesting to consider RANKL as a potential ‘bone-invasion-inhibiting-target’, as HNSCC is capable of producing RANKL. Suppressing bone invasion by denosumab (a monoclonal RANKL inhibitor) could be interesting as bone-invading tumors prefer nutrient-rich bone, which may lead to more tumor growth¹⁶. However the role of denosumab in HNC has yet to be elucidated.

In **chapter 6** we correlated clinical parameters to organoid outgrowth. Organoids of older patients tended to grow worse compared to younger patients. Furthermore we did not find other clinical factors that correlated with organoid outgrowth. Moreover, we show an increase in organoid establishment to 75.2% if cultures were selected on the presence of sufficient epithelial cells in the culture on the day of isolation. These findings imply that a significant part of our tissue samples did not have enough epithelial cells to grow organoids in advance and make it clear that there is still room for optimizing the tissue collection.

Organoids in personalized medicine

Several studies highlight the potential of organoids regarding personalized medicine. For multiple cancer types correlations are present between patient- and organoid response^{17–20} which in turn can be used in clinical practice to screen the potency of patient response to therapy. For oncology purposes this would also be advantageous to prevent unnecessary side effects of ineffective chemo-, radio-, or targeted-therapy.

For HNSCC, this thesis describes a potential correlation between organoid response to radiotherapy and clinical outcomes, particularly in the adjuvant treatment setting. However, the small sample size limits the statistical significance of these findings, highlighting the need for larger studies to confirm the predictive potential of organoids. Also we show that organoids yield the possibility to analyse the separate effects of radiotherapy and chemotherapeutics, which is not possible in patients.

Although we think the use of HNSCC organoids is promising for correlating organoid response to patient response, several challenges still exist for wide clinical implementation. Several factors may confound the correlation between organoid response and patient outcomes, including the impact of surgery and the absence of the tumor microenvironment in organoid models. Additionally, the optimal parameter for predicting response remains uncertain and may vary depending on treatment type and disease characteristics. There are several ways to calculate organoid response. For radiotherapy, we assessed organoid viability at dosages ranging from 1 – 10 Gray. From this range GR50, IC50 and AUC could be calculated. In addition we used organoid viability at 2 Gray as separate parameter similar to Yao et al.¹⁸ but it is still

unknown which is the most reliable parameter to predict organoid response. In literature, the most commonly used parameter for predicting organoid response is the Area Under the Curve (AUC)²¹ (as e.g. is depicted in chapter 3 figure 3A).

On the other hand, all parameters are somewhat comparable as they are extracted from the same experiment. For clinical implementation cut-off values for organoid response are needed but are hard to determine without big patient cohorts and generalized drug-screen protocols.

Also, although HNSCC is treated primarily with surgery and or (chemo)radiotherapy, the use of immunotherapy for recurrent metastatic HNSCC has been introduced in 2016²²⁻²⁴. HNSCC organoids consist solely of adult stem cell derived epithelial cells devoid of the presence of blood vessels, nerves, extracellular matrix, immune cells and cell interactions. For colorectal - and non-small cell lung cancer, co-cultures have been described with organoids and immune cells and serve as a tool to study the tumor microenvironment²⁵. However, for HNSCC, these co cultures have not been described yet.

To implement HNSCC organoids clinically it is needed to optimize organoid outgrowth. Hurdles in the following domains have to be overcome before an organoid can be screened for response to therapy:

- **Inclusion**
- **Sampling**
- **Culturing**
- **Screening**

Patients must want to participate in the inclusion domain. For sampling, there shouldn't be logistic errors and the sampled tissue must contain epithelial cells. During culturing the organoids have to be passaged multiple times where the right conditions are important and swapping errors are lurking with many organoid lines in a laboratory. For organoid drug screening, experiments should be standardized and shouldn't contain technical errors. Also the organoid lines should be matched to the correct patient. As such, organoid culturing is an extensive and laborious process. As described in **chapter 6** success percentages of organoid establishment range from 56.5-78.5%²¹ and in our HNSCC organoid cohort success rates are 53.2%. For screening, percentages are lower due to the hurdles that need to be taken explained above. Therefore it is desirable to optimize organoid cultures and know if there are parameters which effect organoid growth.

Organoids in cancer biology research

Apart from linking organoid response to patient response, tumor organoids can be used to improve the knowledge about the development of cancer, enhance the understanding of tumor heterogeneity, expand tissues of rare cancers, investigate mechanisms of drug resistance, contribute to drug discovery and development and support biomarker research.

Organoids yield the possibility to test numerous drugs including new targeted therapies which are not yet clinically approved. Also testing drugs on organoids is beneficial because it is fast and prevents unnecessary side effects in patients. In the end, clinical trials to test drugs in patients are still needed but organoids can possibly reduce the number of trials and can be helpful in the first phases of drug development. However, as addressed before, the microenvironment of HNSCC organoids is different and the organoids are not exact nor complete replicas of the patients' tumor and could theoretically respond differently. Also the sampled tumor tissue from biopsies or resection specimen could not reflect the tumor perfectly as it is known that HNSCCs can show intra-tumor heterogeneities²⁶. This also applies for studying cancer biology. Organoids could draw opportunities for studying the biology of different tumors but the question remains if the cancer organoid behaves as a patients' tumor as the microenvironment of the tumor is absent in organoids²⁷.

Future perspectives

Organoid research is a relatively young, promising research field. As discussed, success rates of organoid culturing are far from 100% and future research should focus on obtaining a higher success rate for organoid culturing. It is important to have a dedicated team for tissue sampling and organoid culturing as there are many hurdles to take before an organoid can be correlated to a patient. It can possibly help if sampling tissue for organoid culturing becomes a routine task for the surgical team. In this thesis, tissue from biopsies was sampled by the surgeon and tissue from resections was sampled from the resection specimen at the tissue department after the surgery. For tissue samples obtained from resection specimen it could be worthwhile to investigate if sampling tissue directly from patients, immediately at the start of the resection could increase organoid success rates. The tissue would be fresher and the recognizability of the tumor by the surgeon is maybe higher resulting in possible adequate number of epithelial cells in more tissue samples. The rise of Artificial Intelligence (AI) could support and accelerate organoid research in several domains^{28,29}. AI could optimize culture conditions with analysing datasets to determine the optimal conditions for organoid growth and real time monitor cultures for the best combinations of growth factors, nutrients, and physical conditions. AI-powered robots can automate repetitive tasks like medium changes, cell passaging and monitoring, to reduce human error, increase efficiency and adjust culturing terms based on upfront – and culture collected data.

Besides focusing on increasing success rates for organoid culturing it is also important to reach consensus on drug-screen protocols. Collaboration between biobanks of different hospitals is important and can enable bigger patient cohorts for analysing the best parameter, with corresponding cut-off values, for drug-screens which eventually could lead to generalized protocols despite the differences in ethical legislation which hampers easy collaboration.

Culturing organoids generates large amounts of data and AI can help to manage and analyse these data, extracting meaningful insights in a structured manner which could easily be shared for collaboration. AI algorithms can identify patterns and correlations in complex datasets that might be missed by human researchers, leading to new discoveries about organoid development and function.

Future organoid research should focus on improving the organoid micro environment. Co culturing organoids with different cell types e.g. immune cells could gain valuable insights in a more patient-like microenvironment.

Concluding remarks

HNC organoids yield promising possibilities for biomarker research as they phenotypically and genetically recapitulate the original tissue they are derived from. As shown, organoids can aid in biomarker and targeted therapy research and we do believe there is additive value for the use of organoids in the research and treatment of HNC. The main drawback for the use of organoids is the poor reflection of the complex tumor microenvironment yet without extracellular matrix, nerves, blood vessel, immune cells and cell interactions which is indispensable for the development and treatment of cancer.

Second, although we show correlations between patients and organoids regarding radiotherapy response, clinical implementation in the HNC field is still challenging. Robust clinical correlations in large cohorts lack due to the laborious process of organoid culturing and lack of collaboration between biobanks.

To conclude, the use of patient derived HNC organoids shows promising opportunities for cancer research and holds potential as personalized medicine tool. Ongoing research is essential to address existing challenges and optimize their applicability in guiding treatment decisions for HNC patients.

REFERENCES

1. Sung H, Ferlay J, Siegel RL, et al. Global Cancer Statistics 2020: GLOBOCAN Estimates of Incidence and Mortality Worldwide for 36 Cancers in 185 Countries. *CA Cancer J Clin*. 2021;71(3):209-249. doi:10.3322/CAAC.21660
2. Carvalho AL, Nishimoto IN, Califano JA, Kowalski LP. Trends in incidence and prognosis for head and neck cancer in the United States: A site-specific analysis of the SEER database. *Int J Cancer*. 2005;114(5):806-816. doi:10.1002/ijc.20740
3. Ostman J, Anneroth G, Gustafsson H, Tavelin B. Malignant oral tumours in Sweden 1960-1989--an epidemiological study. *Eur J Cancer B Oral Oncol*. 1995;31B(2):106-112. doi:10.1016/0964-1955(94)00018-y
4. Muir C, Weiland L. Upper aerodigestive tract cancers. *Cancer*. 1995;75(1 S):147-153. doi:10.1002/1097-0142(19950101)75:1+<147::AID-CNCR2820751304>3.0.CO;2-U
5. Pulte D, Brenner H. Changes in Survival in Head and Neck Cancers in the Late 20th and Early 21st Century: A Period Analysis. *Oncologist*. 2010;15(9):994-1001. doi:10.1634/theoncologist.2009-0289
6. Bossi P, Resteghini C, Paielli N, Licitra L, Pilotti S, Perrone F. Prognostic and predictive value of EGFR in head and neck squamous cell carcinoma. *Oncotarget*. 2016;7(45):74362-74379. doi:10.18632/oncotarget.11413
7. Driehuis E, Kolders S, Spelier S, et al. Oral mucosal organoids as a potential platform for personalized cancer therapy. *Cancer Discov*. 2019;9(7):852-871. doi:10.1158/2159-8290.CD-18-1522
8. Mody MD, Rocco JW, Yom SS, Haddad RI, Saba NF. Head and neck cancer. *Lancet*. 2021;398(10318):2289-2299. doi:10.1016/S0140-6736(21)01550-6
9. Gebre-Medhin M, Brun E, Engström P, et al. ARTSCAN III: A randomized phase III study comparing chemoradiotherapy with cisplatin versus cetuximab in patients with locoregionally advanced head and neck squamous cell cancer. *J Clin Oncol*. 2021;39(1):38-47. doi:10.1200/JCO.20.02072
10. Rischin D, King M, Kenny L, et al. Randomized Trial of Radiation Therapy With Weekly Cisplatin or Cetuximab in Low-Risk HPV-Associated Oropharyngeal Cancer (TROG 12.01) – A Trans-Tasman Radiation Oncology Group Study. *Int J Radiat Oncol Biol Phys*. 2021;111(4):876-886. doi:10.1016/j.ijrobp.2021.04.015
11. Maddalo M, Borghetti P, Tomasini D, et al. Cetuximab and Radiation Therapy Versus Cisplatin and Radiation Therapy for Locally Advanced Head and Neck Cancer: Long-Term Survival and Toxicity Outcomes of a Randomized Phase 2 Trial. *Int J Radiat Oncol Biol Phys*. 2020;107(3):469-477. doi:10.1016/j.ijrobp.2020.02.637
12. Fritsch C, Huang A, Chatenay-Rivauday C, et al. Characterization of the novel and specific PI3Ka inhibitor NVP-BYL719 and development of the patient stratification strategy for clinical trials. *Mol Cancer Ther*. 2014;13(5):1117-1129. doi:10.1158/1535-7163.MCT-13-0865
13. Li SH, Chien CY, Huang WT, et al. Prognostic significance and function of mammalian target of rapamycin in tongue squamous cell carcinoma. *Sci Rep*. 2017;7(1). doi:10.1038/s41598-017-08345-8
14. Monteiro LS, Delgado ML, Ricardo S, et al. Phosphorylated mammalian target of rapamycin is associated with an adverse outcome in oral squamous cell carcinoma. *Oral Surg Oral Med Oral Pathol Oral Radiol*. 2013;115(5):638-645. doi:10.1016/j.oooo.2013.01.022
15. Naruse T, Yanamoto S, Yamada S ichi, et al. Anti-Tumor Effect of the Mammalian Target of Rapamycin Inhibitor Everolimus in Oral Squamous Cell Carcinoma. *Pathol Oncol Res*. 2015;21(3):765-773. doi:10.1007/s12253-014-9888-1

16. Jimi E, Furuta H, Matsuo K, Tominaga K, Takahashi T, Nakanishi O. The cellular and molecular mechanisms of bone invasion by oral squamous cell carcinoma. *Oral Dis.* 2011;17(5):462-468. doi:10.1111/j.1601-0825.2010.01781.x
17. Ooft SN, Weeber F, Dijkstra KK, et al. Patient-derived organoids can predict response to chemotherapy in metastatic colorectal cancer patients. *Sci Transl Med.* 2019;11(513). doi:10.1126/scitranslmed.aay2574
18. Yao Y, Xu X, Yang L, et al. Patient-Derived Organoids Predict Chemoradiation Responses of Locally Advanced Rectal Cancer. *Cell Stem Cell.* 2020;26(1):17-26.e6. doi:10.1016/j.stem.2019.10.010
19. Ganesh K, Wu C, O'Rourke KP, et al. A rectal cancer organoid platform to study individual responses to chemoradiation. *Nat Med.* 2019;25(10):1607-1614. doi:10.1038/s41591-019-0584-2
20. Vlachogiannis G, Hedayat S, Vatsiou A, et al. Patient-derived organoids model treatment response of metastatic gastrointestinal cancers. *Science (80-).* 2018;359(6378):920-926. doi:10.1126/science.aao2774
21. Wensink GE, Elias SG, Mullenders J, et al. Patient-derived organoids as a predictive biomarker for treatment response in cancer patients. *npj Precis Oncol.* 2021;5(1). doi:10.1038/s41698-021-00168-1
22. Seiwert TY, Burtneß B, Mehra R, et al. Safety and clinical activity of pembrolizumab for treatment of recurrent or metastatic squamous cell carcinoma of the head and neck (KEYNOTE-012): an open-label, multicentre, phase 1b trial. *Lancet Oncol.* 2016;17(7):956-965. doi:10.1016/S1470-2045(16)30066-3
23. Burtneß B, Harrington KJ, Greil R, et al. Pembrolizumab alone or with chemotherapy versus cetuximab with chemotherapy for recurrent or metastatic squamous cell carcinoma of the head and neck (KEYNOTE-048): a randomised, open-label, phase 3 study. *Lancet.* 2019;394(10212):1915-1928. doi:10.1016/S0140-6736(19)32591-7
24. Ferris RL, Blumenschein G, Fayette J, et al. Nivolumab for Recurrent Squamous-Cell Carcinoma of the Head and Neck. *N Engl J Med.* 2016;375(19):1856-1867. doi:10.1056/nejmoa1602252
25. Bar-Ephraim YE, Kretzschmar K, Clevers H. Organoids in immunological research. *Nat Rev Immunol.* 2020;20(5):279-293. doi:10.1038/s41577-019-0248-y
26. Canning M, Guo G, Yu M, et al. Heterogeneity of the head and neck squamous cell carcinoma immune landscape and its impact on immunotherapy. *Front Cell Dev Biol.* 2019;7(APR). doi:10.3389/fcell.2019.00052
27. Drost J, Clevers H. Organoids in cancer research. *Nat Rev Cancer.* 2018;18(7):407-418. doi:10.1038/s41568-018-0007-6
28. Shi H, Kowalczewski A, Vu D, et al. Organoid intelligence: Integration of organoid technology and artificial intelligence in the new era of in vitro models. *Med Nov Technol Devices.* 2024;21. doi:10.1016/j.medntd.2023.100276
29. Bai L, Wu Y, Li G, Zhang W, Zhang H, Su J. AI-enabled organoids: Construction, analysis, and application. *Bioact Mater.* 2024;31:525-548. doi:10.1016/j.bioactmat.2023.09.005



CHAPTER 8

Appendices

NEDERLANDSE SAMENVATTING

Hoofdstuk 1 start met een algemene inleiding over hoofd-halskanker (HHK) en organoïden. HHK is een verzamelnaam voor tumoren die ontstaan in de mondholte, farynx, larynx, neusholte, paranasale sinussen en speekselklieren. HHK is wereldwijd de 7e meest voorkomende vorm van kanker met ongeveer 1.000.000 nieuwe gevallen en 465.000 sterfgevallen in 2020¹. Meer dan 95% van deze kankers zijn plaveiselcelcarcinomen (PCC) die zich ontwikkelen vanuit het slijmvliesepitheel²⁻⁴. Risicofactoren voor het ontwikkelen van HHK zijn roken en excessief alcoholgebruik met een synergistisch effect⁵. Naast deze risicofactoren is een infectie met hoog risico humaan papillomavirus (HPV) geassocieerd met een hoger risico op met name orofaryngeale kanker^{6,7}. HPV-positieve orofarynxcarcinomen hebben een betere prognose en komen voor bij een jongere populatie in vergelijking met HPV-negatieve orofarynxcarcinomen, die veroorzaakt worden door alcohol- en/of tabaksgebruik⁸⁻¹⁰. De incidentie van HPV-negatief HHK neemt langzaam af, mede door een afname van de prevalentie van roken¹¹. Daarentegen neemt de incidentie van HPV-positieve HHKs toe¹². Het onderscheid tussen HPV-negatieve en HPV-positieve HHK heeft geleid tot een andere aanpak voor de stadiëring en behandeling van deze tumoren¹³.

Behandeling van HHK bestaat kan bestaan uit chirurgie, radiotherapie en/of systeemtherapie. Behandeling hangt af van grootte en locatie van de tumor. Ondanks de verschillende behandelingsopties en vooruitgang in de ontwikkeling van gerichte therapie, is de 5-jaarsoverleving van HHK de afgelopen drie decennia slechts minimaal verbeterd tot ongeveer 66% voor alle locaties en stadia samen¹⁴. Daarom zijn er veel biomarkers onderzocht die de overlevingskans voorspellen en helpen bij behandelbeslissingen wat om onnodige bijwerkingen en kosten zou kunnen voorkomen¹⁵⁻¹⁷. Desondanks, ontbreken robuuste biomarkers en zijn er weinig biomarkers bevestigd in klinische studies. Bovendien zijn biomarkers moeilijk te testen in traditionele in-vitromodellen, omdat de in-vivo tumorstructuur en 3D-morfologie ontbreekt. Hierdoor zijn betere modellen nodig die een nauwkeurigere tumorheterogeniteit weerspiegelen.

Organoïden zijn driedimensionale structuren gekweekt uit pluripotente of volwassen stamcellen uit weefsel van een patient¹⁸. De driedimensionale structuur van organoïden maakt een betere nabootsing van de in vivo micro-omgeving mogelijk. Organoïden kunnen uit meerdere celtypen bestaan en een zekere mate van zelforganisatie hebben die lijken op de architectuur van het echte orgaan. Bovendien kunnen organoïden een zekere mate van orgaanspecifieke functionaliteit vertonen en de mogelijkheid hebben om in vivo functionele en structurele kenmerken van het oorspronkelijke weefsel te reproduceren¹⁹. De mogelijkheid om patiëntspecifiek weefsel in 3D te kweken, maakt organoïden geschikt voor het bestuderen van de fysiologie van organen en de pathofysiologie van gerelateerde ziekten.

Naast het kweken van organoïden uit gezond weefsel is het ook mogelijk om organoïden te kweken uit kankerweefsel. In het afgelopen decennium zijn tumororganoïden, voornamelijk afkomstig van volwassen stamcellen, ontwikkeld voor vele tumortypen²⁰. Tumororganoïden kunnen worden gebruikt voor twee belangrijke gebieden in kankeronderzoek: kankerbiologisch onderzoek en gepersonaliseerde geneeskunde. Voor onderzoek in de kankerbiologie kunnen tumororganoïden worden gebruikt verschillende doeleinden; verbeteren van het begrip van de ontwikkeling van kanker en tumorheterogeniteit, uitbreiden van weefsels van zeldzame kankers, mechanismen onderzoeken van geneesmiddelenresistentie, bijdragen aan de ontdekking en ontwikkeling van geneesmiddelen en biomarkeronderzoek. Voor gepersonaliseerde geneeskunde kunnen tumororganoïden de respons op behandelingen voorspellen en bijdragen aan gepersonaliseerde screening van geneesmiddelen voor behandelingsoptimalisatie.

Op het gebied van oncologie tonen meerdere studies correlaties aan tussen geneesmiddelen-respons in kankerorganoïden en de geneesmiddelenrespons bij de patiënten waarvan de organoïden afkomstig zijn²¹⁻²⁵. Voor HHK introduceerde Driehuis et al. de eerste biobank van plaveiselcelcarcinomen van het hoofd-halsgebied¹⁹. Deze HHK-organoïden reproduceren de moleculaire kenmerken die bekend zijn voor HHK en reageren verschillend op cisplatine, carboplatine, cetuximab en radiotherapie. Deze studie leidde tot de vervolgstudie waarin de een uitgebreidere biobank voor HHK-organoïden werd gegenereerd, die in dit proefschrift wordt beschreven. In dit proefschrift wordt de potentie van organoïden in het HHK veld verder uitgewerkt.

Het inzicht in de moleculaire pathogenese van HHK is de afgelopen decennia aanzienlijk verbeterd. Dit heeft geleid tot nieuwe strategieën voor de behandeling van HHK. Deze nieuwe therapieën zijn met name gericht op de Epidermale Groei Factor Receptor (EGFR) welke in de meeste HHKs overexpressie vertoont²⁶. Hoewel primaire en verworven resistentie een uitdaging vormen, hebben deze gerichte therapieën potentie. Biomarkers zijn cruciaal voor de introductie en het gebruik van gerichte therapieën. **Hoofdstuk 2** beschrijft een systematische review van de literatuur waar wordt besproken dat er veel biomarkers voor doelgerichte therapie in het EGFR-pad zijn onderzocht, maar slechts enkele zijn bevestigd in klinische studies. Een robuuste biomarker die de behandeluitkomst voorspelt, ontbreekt nog steeds. Huidig onderzoek wordt belemmerd door kleine steekproeven, heterogene onderzoekspopulaties en discrepanties in behandelprotocollen. Een meer systematische aanpak van biomarkeronderzoek, inclusief integratie in klinische studies en patiëntgerichte onderzoeksopzetten, is nodig. Hoewel er al verschillende biomarkers zijn onderzocht, blijft hun klinische validatie over het algemeen beperkt. **Hoofdstuk 2** benadrukt de noodzaak voor het doen van verder onderzoek om met name de al onderzochte biomarkers klinisch te valideren. Integratie van meerdere biomarkers en het gebruik van HHK organoïden bieden veelbelovende mogelijkheden voor het verbeteren van gepersonaliseerde behandeling.

Hoofdstuk 3 beschrijft een uitbreiding van de eerder beschreven biobank van HHK organoïden van 31 naar 110 modellen waarbij naast het plaveiselcelcarcinoom ook andere histologische typen van HHK organoïden werden gekweekt. In de adjuvante radiotherapiesetting voor HHK beschrijft **hoofdstuk 3** een correlatie waarbij organoïden die resistentere waren tegen radiotherapie, correspondeerden met patiënten die eerder een recidief kregen in vergelijking met patiënten waarvan de organoïden gevoelig waren voor radiotherapie. Ondanks de kleine steekproefgrootte (n=15) is er een correlatie aanwezig. Er werd geen correlatie beschreven tussen cisplatinegevoeligheid bij organoïden en recidief bij patiënten.

Een subgroep van deze HHK organoïden werd gescreend op respons op radiotherapie met of zonder cisplatine, carboplatine en cetuximab. Over het algemeen verhoogden zowel cisplatine als carboplatine de gevoeligheid voor radiotherapie, wat overeenkomt met bevindingen in de klinische praktijk²⁷. De EGFR-remmer Cetuximab verminderde echter de gevoeligheid voor radiotherapie, wat in lijn is met de huidige literatuur die een slechtere overleving beschrijft voor patiënten die behandeld worden met cetuximab en radiotherapie in vergelijking met cisplatine en radiotherapie²⁸⁻³⁰. Dit alles bevestigt dat organoïden het tumorgedrag van HHK in de klinische situatie weerspiegelen. Het is echter belangrijk om op te merken dat, hoewel cetuximab als radioprotector fungeerde, het in vitro additieve effect van radiotherapie en cetuximab samen leidde tot meer celdood dan dat van radiotherapie alleen voor de meeste organoïdemodellen.

Hiernaast beschrijft **hoofdstuk 3** ook de respons op meerdere doelgerichte therapieën voor een deel van de HHK organoïden. Voor preklinische doelgerichte therapieën is de patiëntrespons op de therapie onbekend, aangezien deze middelen nog niet klinisch zijn geïntroduceerd. Het onderzoeken van de organoïdrespons voor nieuwe doelgerichte therapieën is nuttig om data te verkrijgen die toekomstige screening en onderzoek naar de implementatie van gerichte therapieën kunnen ondersteunen. Dit geldt niet alleen voor preklinische therapieën, maar ook voor bestaande therapieën.

Tevens beschrijft **hoofdstuk 3** het gebruik van HHK-organoiden voor biomarkeronderzoek. Preklinische studies beschrijven PIK3CA-mutaties als biomarker voor de doelgerichte therapie alpelisib³¹. De respons van HHK organoïden op het geneesmiddel alpelisib (PI3K α remmer) en de PI3KCA mutatiestatus werden bepaald. Organoïden met een PI3KCA mutatie reageerden niet significant beter in vergelijking met organoïden zonder deze mutatie. Hiernaast werd de meest voorkomende PI3KCA-mutatie (E545K) in twee HHK organoïds geïntroduceerd met behulp van CRISPR-base-editing technologie, waardoor twee isogene paren ontstonden die slechts in één specifieke mutatie verschilden. Het verschil in alpelisib-respons tussen de twee patiënten was groter dan het verschil in response binnen de isogene paren. Deze bevinding onderstreept het potentieel van organoïden om de waarde van een bepaalde biomarker voor geneesmiddelgevoeligheid te bepalen.

Hoofdstuk 4 beschrijft de eiwitexpressie van p-mTOR, p-ERK en PTEN als prognostische biomarkers bij Humaan Papillomavirus (HPV) negatieve HHK-patiënten die werden behandeld met primaire chemoradiotherapie. Er werd een significant slechtere algehele overleving gevonden bij patiënten met een hoge p-mTOR-expressie. Dit is in lijn met andere HHK studies³²⁻³⁴. Bovendien correleerde de eiwitexpressie van p-mTOR in een panel van HHK-organoïden met de respons op de mTOR-remmer everolimus in deze organoïden. Dit beschrijft het potentieel van HHK-organoïden om de everolimus-respons te voorspellen op basis van p-mTOR-expressie.

Hoofdstuk 5 beschrijft een retrospectieve cohortstudie die het mechanisme van kaakbotinvasie bij patiënten met mondholte plaveiselcelcarcinoom probeert te verhelderen. De bevindingen van deze studie suggereren dat plaveiselcelcarcinoom van de mondholte botinvasie induceert door stimulatie van osteoclastactivatie door de productie van RANKL- en RANK-eiwitten te reguleren. In deze studie wordt aangetoond dat HHK-organoïden RANKL, OPG en RANK tot expressie kunnen brengen op eiwitniveau en op mRNA-niveau (bepaald met kwantitatieve PCR). Deze bevindingen vormen de eerste stappen voor biomarkeronderzoek en doelgerichte therapie met betrekking tot botinvasie bij HHK. Het onderdrukken van botinvasie met denosumab (een monoklonale RANKL-remmer) zou interessant kunnen zijn, aangezien botinvasieve tumoren de voorkeur geven aan voedingsrijk bot, wat kan leiden tot meer tumorgroei³⁵. De rol van denosumab bij HHK moet echter nog worden opgehelderd.

Hoofdstuk 6 beschrijft klinische parameters van patiënten welke gecorreleerd werden aan het succesvol uitgroeien van organoïden. Organoïden van oudere patiënten groeiden over het algemeen slechter dan die van jongere patiënten. Er werden geen andere klinische factoren gevonden die correleerden met het succesvol uitgroeien van organoïden. Ook werd er gekeken naar de aanwezigheid van epitheelcellen in het ontvangen weefsel voor het kweken van organoïden. Het succespercentage voor het kweken van organoïden steeg tot 75,2% als weefsels werden geselecteerd op basis van de aanwezigheid van voldoende epitheelcellen in de kweek op de dag van isolatie. Deze bevindingen impliceren dat een aanzienlijk deel van de verzamelde weefsels onvoldoende epitheelcellen bevatte om organoïden te laten groeien wat duidelijk maakt dat er nog ruimte is voor optimalisatie van de weefselverzameling.

In **hoofdstuk 7** is ruimte voor algemene discussie en conclusies van de voorgenoemde hoofdstukken. HHK-organoïden bieden veelbelovende mogelijkheden voor biomarkeronderzoek omdat ze het oorspronkelijke weefsel fenotypisch en genetisch nabootsen. Zoals aangetoond, kunnen organoïden helpen bij onderzoek naar biomarkers en doelgerichte therapie. Dit proefschrift beschrijft dat het gebruik van organoïden toegevoegde waarde heeft in het onderzoek naar en de behandeling van HHK. Het belangrijkste nadeel van organoïden is de slechte weerspiegeling van het complexe tumor micromilieu met het

ontbreken van extracellulaire matrix, zenuwen, bloedvaten, immuuncellen en celinteracties, die onmisbaar zijn voor de ontwikkeling en behandeling van kanker.

Ten tweede, hoewel we correlaties aantonen tussen patiënten en organoïden met betrekking tot de respons op radiotherapie, is klinische implementatie in het HHK-veld uitdagend. Robuuste klinische correlaties in grote cohorten ontbreken vanwege het moeizame proces van organoïdenkweek en het gebrek aan samenwerking tussen biobanken.

Concluderend biedt het gebruik van HHK organoïden veelbelovende mogelijkheden voor kankeronderzoek en heeft het potentieel als hulpmiddel voor gepersonaliseerde geneeskunde. Voortdurend onderzoek is essentieel om bestaande uitdagingen aan te pakken en de toepasbaarheid van HHK organoïden te optimaliseren.

Referenties

1. Sung H, Ferlay J, Siegel RL, et al. Global Cancer Statistics 2020: GLOBOCAN Estimates of Incidence and Mortality Worldwide for 36 Cancers in 185 Countries. *CA Cancer J Clin.* 2021;71(3):209-249. doi:10.3322/CAAC.21660
2. Carvalho AL, Nishimoto IN, Califano JA, Kowalski LP. Trends in incidence and prognosis for head and neck cancer in the United States: A site-specific analysis of the SEER database. *Int J Cancer.* 2005;114(5):806-816. doi:10.1002/ijc.20740
3. Ostman J, Anneroth G, Gustafsson H, Tavelin B. Malignant oral tumours in Sweden 1960-1989--an epidemiological study. *Eur J Cancer B Oral Oncol.* 1995;31B(2):106-112. doi:10.1016/0964-1955(94)00018-y
4. Muir C, Weiland L. Upper aerodigestive tract cancers. *Cancer.* 1995;75(1 S):147-153. doi:10.1002/1097-0142(19950101)75:1+<147::AID-CNCR2820751304>3.0.CO;2-U
5. Mello FW, Melo G, Pasetto JJ, Silva CAB, Warnakulasuriya S, Rivero ERC. The synergistic effect of tobacco and alcohol consumption on oral squamous cell carcinoma: a systematic review and meta-analysis. *Clin Oral Investig.* 2019;23(7):2849-2859. doi:10.1007/s00784-019-02958-1
6. Isayeva T, Li Y, Maswahu D, Brandwein-Gensler M. Human Papillomavirus in Non-Oropharyngeal Head and Neck Cancers: A Systematic Literature Review. *Head Neck Pathol.* 2012;6(SUPPL. 1):104-120. doi:10.1007/s12105-012-0368-1
7. Gillison ML, Alemany L, Snijders PJF, et al. Human papillomavirus and diseases of the upper airway: Head and neck cancer and respiratory papillomatosis. *Vaccine.* 2012;30(SUPPL.5). doi:10.1016/j.vaccine.2012.05.070
8. Ang KK, Harris J, Wheeler R, et al. Human Papillomavirus and Survival of Patients with Oropharyngeal Cancer. *N Engl J Med.* 2010;363(1):24-35. doi:10.1056/nejmoa0912217
9. Marur S, D'Souza G, Westra WH, Forastiere AA. HPV-associated head and neck cancer: A virus-related cancer epidemic. *Lancet Oncol.* 2010;11(8):781-789. doi:10.1016/S1470-2045(10)70017-6
10. Wang MB, Liu IY, Gornbein JA, Nguyen CT. HPV-Positive Oropharyngeal Carcinoma: A Systematic Review of Treatment and Prognosis. *Otolaryngol - Head Neck Surg (United States).* 2015;153(5):758-769. doi:10.1177/0194599815592157

11. Sturgis EM, Cinciripini PM. Trends in head and neck cancer incidence in relation to smoking prevalence: An emerging epidemic of human papillomavirus-associated cancers? *Cancer*. 2007;110(7):1429-1435. doi:10.1002/cncr.22963
12. Stein AP, Saha S, Kraninger JL, et al. Prevalence of human papillomavirus in oropharyngeal cancer. *Cancer J (United States)*. 2015;21(3):138-146. doi:10.1097/PPO.0000000000000115
13. Badoual C. Update from the 5th Edition of the World Health Organization Classification of Head and Neck Tumors: Oropharynx and Nasopharynx. *Head Neck Pathol*. 2022;16(1):19-30. doi:10.1007/s12105-022-01449-2
14. Pulte D, Brenner H. Changes in Survival in Head and Neck Cancers in the Late 20th and Early 21st Century: A Period Analysis. *Oncologist*. 2010;15(9):994-1001. doi:10.1634/theoncologist.2009-0289
15. Gavrielatou N, Dumas S, Economopoulou P, Foukas PG, Psyrri A. Biomarkers for immunotherapy response in head and neck cancer. *Cancer Treat Rev*. 2020;84. doi:10.1016/j.ctrv.2020.101977
16. Hsieh JCH, Wang HM, Wu MH, et al. Review of emerging biomarkers in head and neck squamous cell carcinoma in the era of immunotherapy and targeted therapy. *Head Neck*. 2019;41(S1):19-45. doi:10.1002/hed.25932
17. de Kort WWB, Spelier S, Devriese LA, van Es RJJ, Willems SM. Predictive Value of EGFR-PI3K-AKT-mTOR-Pathway Inhibitor Biomarkers for Head and Neck Squamous Cell Carcinoma: A Systematic Review. *Mol Diagnosis Ther*. 2021;25(2):123-136. doi:10.1007/s40291-021-00518-6
18. Kretschmar K, Clevers H. Organoids: Modeling Development and the Stem Cell Niche in a Dish. *Dev Cell*. 2016;38(6):590-600. doi:10.1016/j.devcel.2016.08.014
19. Driehuis E, Kolders S, Spelier S, et al. Oral mucosal organoids as a potential platform for personalized cancer therapy. *Cancer Discov*. 2019;9(7):852-871. doi:10.1158/2159-8290.CD-18-1522
20. Yang S, Hu H, Kung H, et al. Organoids: The current status and biomedical applications. *MedComm*. 2023;4(3). doi:10.1002/mco2.274
21. Tiriach H, Belleau P, Engle DD, et al. Organoid profiling identifies common responders to chemotherapy in pancreatic cancer. *Cancer Discov*. 2018;8(9):1112-1129. doi:10.1158/2159-8290.CD-18-0349
22. Vlachogiannis G, Hedayat S, Vatsiou A, et al. Patient-derived organoids model treatment response of metastatic gastrointestinal cancers. *Science (80-)*. 2018;359(6378):920-926. doi:10.1126/science.aao2774
23. Wensink GE, Elias SG, Mullenders J, et al. Patient-derived organoids as a predictive biomarker for treatment response in cancer patients. *npj Precis Oncol*. 2021;5(1). doi:10.1038/s41698-021-00168-1
24. Ooft SN, Weeber F, Dijkstra KK, et al. Patient-derived organoids can predict response to chemotherapy in metastatic colorectal cancer patients. *Sci Transl Med*. 2019;11(513). doi:10.1126/scitranslmed.aay2574
25. Yao Y, Xu X, Yang L, et al. Patient-Derived Organoids Predict Chemoradiation Responses of Locally Advanced Rectal Cancer. *Cell Stem Cell*. 2020;26(1):17-26.e6. doi:10.1016/j.stem.2019.10.010
26. Bossi P, Resteghini C, Paielli N, Licitra L, Pilotti S, Perrone F. Prognostic and predictive value of EGFR in head and neck squamous cell carcinoma. *Oncotarget*. 2016;7(45):74362-74379. doi:10.18632/oncotarget.11413
27. Mody MD, Rocco JW, Yom SS, Haddad RI, Saba NF. Head and neck cancer. *Lancet*. 2021;398(10318):2289-2299. doi:10.1016/S0140-6736(21)01550-6
28. Gebre-Medhin M, Brun E, Engström P, et al. ARTSCAN III: A randomized phase III study comparing chemoradiotherapy with cisplatin versus cetuximab in patients with locoregionally advanced head and neck squamous cell cancer. *J Clin Oncol*. 2021;39(1):38-47. doi:10.1200/JCO.20.02072

29. Rischin D, King M, Kenny L, et al. Randomized Trial of Radiation Therapy With Weekly Cisplatin or Cetuximab in Low-Risk HPV-Associated Oropharyngeal Cancer (TROG 12.01) – A Trans-Tasman Radiation Oncology Group Study. *Int J Radiat Oncol Biol Phys.* 2021;111(4):876-886. doi:10.1016/j.ijrobp.2021.04.015
30. Maddalo M, Borghetti P, Tomasini D, et al. Cetuximab and Radiation Therapy Versus Cisplatin and Radiation Therapy for Locally Advanced Head and Neck Cancer: Long-Term Survival and Toxicity Outcomes of a Randomized Phase 2 Trial. *Int J Radiat Oncol Biol Phys.* 2020;107(3):469-477. doi:10.1016/j.ijrobp.2020.02.637
31. Fritsch C, Huang A, Chatenay-Rivauday C, et al. Characterization of the novel and specific PI3Ka inhibitor NVP-BYL719 and development of the patient stratification strategy for clinical trials. *Mol Cancer Ther.* 2014;13(5):1117-1129. doi:10.1158/1535-7163.MCT-13-0865
32. Li SH, Chien CY, Huang WT, et al. Prognostic significance and function of mammalian target of rapamycin in tongue squamous cell carcinoma. *Sci Rep.* 2017;7(1). doi:10.1038/s41598-017-08345-8
33. Monteiro LS, Delgado ML, Ricardo S, et al. Phosphorylated mammalian target of rapamycin is associated with an adverse outcome in oral squamous cell carcinoma. *Oral Surg Oral Med Oral Pathol Oral Radiol.* 2013;115(5):638-645. doi:10.1016/j.oooo.2013.01.022
34. Naruse T, Yanamoto S, Yamada S ichi, et al. Anti-Tumor Effect of the Mammalian Target of Rapamycin Inhibitor Everolimus in Oral Squamous Cell Carcinoma. *Pathol Oncol Res.* 2015;21(3):765-773. doi:10.1007/s12253-014-9888-1
35. Jimi E, Furuta H, Matsuo K, Tominaga K, Takahashi T, Nakanishi O. The cellular and molecular mechanisms of bone invasion by oral squamous cell carcinoma. *Oral Dis.* 2011;17(5):462-468. doi:10.1111/j.1601-0825.2010.01781.x

DANKWOORD

Allereest wil ik alle patiënten bedanken die hebben geparticipeerd aan mijn onderzoek. Verder wil ik de volgende mensen bedanken.

Prof. Dr. Willems, beste Stefan. We leerden elkaar kennen voor een wetenschappelijke keuzestage. We schreven samen een leuke review over de ‘Nodal Yield’. Jouw enthousiasme werkte aanstekelijk en jij gaf me de kans om dit promotietraject te starten. Je hebt me weten te enthousiasmeren voor het vak pathologie, iets wat ik tijdens mijn studie geneeskunde nooit voor mogelijk had gehouden. Hartelijk dank voor de kans die je me hebt gegeven en de begeleiding tijdens mijn promotietraject.

Prof. Dr. Clevers, beste Hans. Bedankt voor de mogelijkheid om dit promotietraject in samenwerking met het Hubrecht instituut te starten. Ondanks dat we elkaar niet vaak hebben gezien wil ik je graag bedanken voor de kans om in de wereld van organoïds te duiken.

Dr. van Es, beste Robert. Ik kan me mijn eerste afspraak met jou (en Toine) nog goed herinneren. Op zoek naar een wetenschappelijke stage had jij ‘nog wel wat liggen’. Uiteindelijk heb jij mij samen met Stefan goed begeleid bij dit project. Jij wist me meteen te enthousiasmeren voor het vak Mondziekten, Kaak – en Aangezichtschirurgie waardoor ik na mijn keuzeruimte bij de MKA, zeker wist dat ik in dit vak verder wilde. Ik wil je graag bedanken voor je enthousiasme en je begeleiding tijdens mijn promotie. Je heb altijd kritische vragen paraat en vond altijd wel een gaatje om snel naar mijn artikelen te kijken, al was het om 02:00 ’s nachts. Bedankt dat je mijn copromotor wilde zijn.

Dr. Devriese, beste Lot. Dank voor je begeleiding tijdens mijn onderzoek, je inhoudelijke feedback en je enthousiasme over de projecten.

Geachte leden van de beoordelingscommissie, **Prof. dr. R.P. Coppes**, **Prof. dr. P.J. van Diest**, **Prof. dr. M. Koopman**, **Dr. M. de Ridder** en **Prof. dr. M.J.H. Witjes**, bedankt voor de tijd die u heeft genomen om mijn proefschrift te lezen en te beoordelen.

Beste **Else**, Mijn eerste dag in het Hubrecht nam je me op sleeptouw. Je gaf me een rondleiding en ik had duidelijk geen idee waar ik aan begon. Ik wil je graag bedanken voor je engelen geduld, ik kon altijd bij je terecht en jij was nooit te beroerd om mijn vragen te beantwoorden. Ik heb enorm veel van je geleerd. Ik wil je graag bedanken voor alle hulp!

Dear **Rosie**, thank you for being a great colleague. I want to thank you for the pleasant collaboration. We got along well and had some interesting discussions from time to time. I wish you all the best in your future.

Beste **Mandy en Roán**, bedankt voor de samenwerking en het kweken van heel veel organoids. Zonder jullie hulp was het project nooit zo ver gekomen.

Em. Prof. Rosenberg, beste Toine, Het eerste gesprek met jou en Robert kan ik me goed herinneren. Ik kwam voor het bespreken van een wetenschappelijke keuzestage maar jij zag je kans schoon om me meteen van alles te vragen; waar kom je vandaan? ben je handig? repareer je je fiets zelf of breng je hem naar een fietsenmaker? Ik had toen nog geen idee wat ik wilde gaan doen. Jij wist me te enthousiasmeren en ik wil je graag bedanken voor de kans die je mij hebt geboden zodat ik de opleiding Mondziekten, Kaak – en Aangezichtschirurgie kon starten in Utrecht. Gedurende mijn promotietraject ben je dan niet inhoudelijk betrokken geweest bij mijn projecten wel was je voor mij een mentor die mijn planning en de voortgang van mijn projecten in de gaten hield. Ik wil je hier graag voor bedanken!

Beste **Wybren**, We kennen elkaar ondertussen alweer meer dan 13 jaar. Ik waardeer je als goede vriend. Je bent een oprecht mens, altijd geïnteresseerd, zeer attent met goed gevoel voor humor. Ik heb goede herinneringen aan onze eurotrip waar we in Boedapest en Warschau door ons bed zijn gezakt. Je bent in je element als je dingen kan organiseren, van ceremoniemeester op onze bruiloft tot de promotieborrel vandaag, jij regelt het. Wyb, leuk dat je mijn paranimf wil zijn en bedankt voor alles!

Beste **Gert-Jan**, vanaf het eerste moment dat ik startte als AIOS hadden we een goede klik. Uiteindelijk hebben we niet eens lang samengewerkt maar was het altijd gezellig en zaten we vaak op één lijn. Bedankt dat je paranimf wil zijn en ik kijk uit naar onze verdere samenwerking.

Natuurlijk ook dank aan alle **stafleden en (oud) assistenten** van de afdeling Mondziekten, Kaak- en Aangezichtschirurgie in het UMC Utrecht.

Beste **Floris en Betzabel**, Dank voor de leuke tijd die we als kamergenoten in het UMC hebben doorgebracht samen met onze rode Nespresso. **Emma** bedankt voor de samenwerking en input voor ons mTOR project en gezelligheid. **Wisse** bedankt voor je hulp bij het botinvasie project, zonder jouw aanvullingen was het niet zo ver gekomen. Ook dank aan alle andere onderzoekers van de **PRL**. Bedankt voor een leuke start van mijn promotie, de lunches en gezellige borrels.

Beste **Gino**, in werkgroep 24 hadden we meteen een goede klik. Ik heb goede herinneringen aan onze reis door Colombia en Ecuador en natuurlijk het coschap SEH in Paramaribo. Onze vriendschap is mij dierbaar, en ik ga ervan uit dat we elkaar, al verhuis je naar Nijmegen, zullen blijven zien. Beste **Mark**, tijdens het coschap interne geneeskunde bleek jij ook te fietsen. We hebben inmiddels heel wat kilometers afgelegd op de racefiets, en hoeveel je ook traint, ik weet je altijd uit de tent te lokken. Een aantal jaar geleden kwam je zelfs bij ons in de straat wonen. Ik wil je bedanken voor je gezelligheid en interesse. Laten we afspreken weer eens op de fiets te stappen.

Beste **Shank, Anisha** en **Meeke**, bedankt voor de gezellige tijd tijdens de TOVA. We hebben elkaar in deze twee jaar goed leren kennen, ze zijn voorbij gevlogen! Ik draag hiervan goede herinneringen met me mee.

Geachte leden van **Jaarclub Ferluci**, beste **Douwe, Edward, Herm, Jonas, Martin, Ruben, Rolf, Tim** en **Wybren**. Als club alweer meer dan 13 jaar bij elkaar. Dank voor het opleuken van mijn studententijd met alle borrels, 21-diners, lustrumreizen en natuurlijk ook goede gesprekken. Van puberjongens naar volwassen mannen met volwassen gesprekken. Samen met alle aanhangsels is er een hechte groep ontstaan wat enorm waardevol is. Bedankt voor alles!

Beste (schoon)familie, **Lieve Jos, Lily, Suus, Larissa** en natuurlijk **Philip, Chris en Quinn**, jullie zijn alweer 9 jaar in mijn leven. Vanaf het begin voelde ik me bij jullie thuis. Dank voor alle interesse en betrokkenheid bij mijn onderzoek maar bovenal dank voor alle liefde. Ik had me geen betere schoonfamilie kunnen wensen.

Lieve **Freek**, je kon me als klein broertje vast af en toe achter het behang plakken maar in de basis konden we het altijd goed met elkaar vinden en hielp jij mij stiekem aan GTA en ZOO tycoon downloads. Lieve **Floor**, ik heb goede herinneringen aan onze jeugd. We sliepen zelfs een poos op dezelfde kamer in een stapelbed waar we voor het slapen eindeloos met elkaar praatten. Dank voor jouw zorgzaamheid, je bent altijd geïnteresseerd in mij en mijn onderzoek. Jullie zijn altijd een voorbeeld voor mij geweest. Ondanks onze verschillen is onze band hecht. Dank voor alle interesse en steun. Natuurlijk ook dank aan **Jeske, Tom, Marg, Aafke, Wies en Pelle**, allemaal onderdeel van onze warme familie. Het is heel fijn dat jullie zo dichtbij wonen waardoor we elkaar regelmatig zien.

Lieve **papa** en **mama**, dank voor jullie liefde en kansen die jullie me geboden hebben in het leven. Ik heb een ontzettend fijne, liefdevolle jeugd gehad en heb de vrijheid gekregen om te kunnen doen en laten wat ik wilde. Af en toe werden de teugels dan wat strakker getrokken

maar nooit op een vervelende manier en ik heb altijd het gevoel gehad dat jullie vertrouwen in me hadden.

Lieve **Bianca**, mijn liefje, alweer meer dan 9 jaar in mijn leven. Waar een simpel oogheekundig onderzoek bij coschap oogheekunde al niet toe kan leiden. Ik ben dankbaar dat je in mijn leven bent gekomen. De afgelopen jaren was het soms best druk met promoveren, verbouwen, tandheekunde en opleiding. Gelukkig vormen we samen een goed team en ondersteunen we elkaar in alles, ik wil je hier graag voor bedanken. Ik prijs mezelf enorm gelukkig met zo'n lieve vrouw en ben er van verzekerd dat we samen een mooie toekomst tegemoet gaan.

Lieve **Lora**, zo recent ben je pas in mijn leven maar wat maak je me gelukkig. Ik kijk er erg naar uit om je te zien opgroeien.

CURRICULUM VITAE

Willem de Kort werd geboren op 24 maart 1994 te Tilburg. In 2012 behaalde hij zijn Atheneum diploma aan het Odulphus Lyceum in Tilburg. In de periode van 2012 tot 2018 studeerde hij geneeskunde aan de universiteit Utrecht. In dezelfde periode was hij lid van de studentenvereniging Unitas S.R. Als onderdeel van de studie geneeskunde volgde hij in 2017 een coschap spoedeisende hulp (SEH) in het Academisch Ziekenhuis Paramaribo evenals een coschap chirurgie in het Mulago Ziekenhuis aan de Makerere Universiteit te Kampala.

Na het behalen van zijn geneeskundediploma startte Willem in januari 2019 als arts-onderzoeker aan een promotietraject naar hoofd-halskankerorganoïden. Een samenwerking tussen de afdeling Pathologie, afdeling Medische Oncologie en afdeling Mondziekten, Kaak- en Aangezichtschirurgie van het Universitair Medisch Centrum Utrecht en de Clevers onderzoeksgroep van het Hubrecht instituut.

In september 2021 startte Willem de studie Tandheelkunde aan de Radboud Universiteit (Tandheelkunde Opleiding Voor Artsen, TOVA) waar hij in februari 2025 zijn diploma van behaalde.

In januari 2024 startte Willem met de opleiding tot specialist Mondziekten, Kaak- en Aangezichtschirurgie in het Universitair Medisch Centrum Utrecht (opleider tot 11-2024 Prof. Dr. A.J.W.P. Rosenberg, opleider vanaf 11-2024 Prof. Dr. J.E. Bergsma). Als onderdeel van deze opleiding heeft hij van maart 2025 tot en met augustus 2025 een perifere stage in het Amphia ziekenhuis Breda gevolgd (opleider Drs. A.J. Kouwenberg).

LIST OF PUBLICATIONS

de Kort WWB, Millen R, Driehuis E, Devriese LA, van Es RJJ, Willems SM. Clinicopathological Factors as Predictors for Establishment of Patient Derived Head and Neck Squamous Cell Carcinoma Organoids. *Head Neck Pathol.* 2024;18(1):1-11. doi:10.1007/S12105-024-01658-X/FIGURES/2

Millen R, **de Kort WWB**, Koomen M, et al. Patient-derived head and neck cancer organoids allow treatment stratification and serve as a tool for biomarker validation and identification. *Med.* 2023;4(5):290-310.e12. doi:10.1016/j.medj.2023.04.003

de Kort WWB, Haakma WE, van Es RJJ, et al. Jaw Bone Invasion of Oral Squamous Cell Carcinoma Is Associated with Osteoclast Count and Expression of Its Regulating Proteins in Patients and Organoids. *J Clin Med.* 2023;12(18):6035. doi:10.3390/JCM12186035/S1

de Kort WWB, de Ruiter EJ, Haakma WE, et al. p-mTOR, p-ERK and PTEN Expression in Tumor Biopsies and Organoids as Predictive Biomarkers for Patients with HPV Negative Head and Neck Cancer. *Head Neck Pathol.* 2023;17(3):697-707. doi:10.1007/S12105-023-01576-4/TABLES/3

de Kort WWB, Van Hout WMMT, Ten Harkel TC, Van Cann EM, Rosenberg AJWP. A Novel Method for Quantitative Three-Dimensional Analysis of Zygomatico-Maxillary Complex Symmetry. *J Craniofac Surg.* 2022;33(5):1474-1478. doi:10.1097/SCS.00000000000008382

van Hout WMMT, **de Kort WWB**, ten Harkel TC, Van Cann EM, Rosenberg AJWP. Zygomaticomaxillary complex fracture repair with intraoperative CBCT imaging. A prospective cohort study. *J Cranio-Maxillofacial Surg.* 2022;50(1):54-60. doi:10.1016/J.JCMS.2021.09.009

de Kort WWB, Spelier S, Devriese LA, van Es RJJ, Willems SM. Predictive Value of EGFR-PI3K-AKT-mTOR-Pathway Inhibitor Biomarkers for Head and Neck Squamous Cell Carcinoma: A Systematic Review. *Mol Diagnosis Ther.* 2021;25(2):123-136. doi:10.1007/s40291-021-00518-6

de Kort WWB, Maas SLN, Van Es RJJ, Willems SM. Prognostic value of the nodal yield in head and neck squamous cell carcinoma: A systematic review. *Head Neck.* 2019;41(8). doi:10.1002/hed.25764

